A Carbon and Nitrogen Isotope Study of Chondritic Diamond and Silicon Carbide

Thesis

UNRESTRICTED

A CARBON AND NITROGEN ISOTOPE STUDY OF CHONDRITIC DIAMOND AND SILICON CARBIDE

A thesis submitted for the degree of

Doctor of Philosophy

by

Sara Russell B.A. (Cantab, 1988)

June, 1992,

Department of Earth Sciences,

The Open University.

ABSTRACT

A suite of identically prepared, acid-resistant residues from the three chondrite classes have been analysed for carbon and nitrogen by stepped combustion. Diamond and silicon carbide were found to be ubiquitous components of the residues along with some other minor carbonaceous phases. The diamond and silicon carbide were associated with isotope anomalies suggesting that they are presolar circumstellar condensates.

The diamond nitrogen content ranges from 2000 to 13000 ppm, and the $\delta^{13}C$ from -32 to -38‰. These two variables are systematically related to petrologic type, with the high petrologic types containing diamond with a heavier carbon isotopic composition and lower nitrogen content. However, the $\delta^{15}N$, at -351±8‰, was found to be indistinguishable between meteorite samples, suggesting that the variation in nitrogen content cannot be explained by metamorphic degassing of the diamond. A more likely explanation is that the more nitrogen rich crystals are more prone to metamorphic destruction that the nitrogen poor grains, perhaps implying that the grains are a mixture of nitrogen rich and nitrogen poor grains that may originate in different sources.

Silicon carbide was found to have a similar $^{12}C/^{13}C$ ratio in all the meteorites in which its abundance was >10ppm of the whole rock, with $^{12}C/^{13}C$ =36.6±0.5; this is interpreted as evidence that a similar mixture of grains were incorporated into each parent body. SiC poor, higher petrologic type meteorites have lower $\delta^{13}C$ values. The combustion dynamics of the grains differ from meteorite to meteorite, suggesting that processing since accretion has caused the SiC grains of separate meteorite classes to have different characteristics.

The enstatite chondrite Abee (EH4) appears to be free of carbonaceous phases containing isotopic anomalies but contains isotopically "normal" diamond and silicon carbide. Diamond and silicon carbide may have been stable condensates in some regions of the early solar nebula.

Overall the isotope data suggest that presolar grains, from a mixture of sources, were well mixed in the meteorite parent body region of the early solar nebula before accretion. Subsequent metamorphism has however caused the grains isolated from different meteorite classes to be distinguishable.

ACKNOWLEDGEMENTS

I would like to thank my supervisor Colin Pillinger for instigating this project, for his enthusiastic interest throughout this study, for putting up with my jaunts abroad, and for his helpful comments on the early drafts of this thesis. I am extremely grateful to John Arden, of the University of Oxford, who prepared the samples discussed in this thesis by performing chemical treatments on a seemingly endless supply of meteorites.

This work would not have been possible without the collaboration of many people who devoted much of their time to characterising the acid-resistant residues. I would like to thank Martin Lee of the University of Essex, for TEM work; Richard Greenwood, of the British Museum, for SEM characterisation; Gordon Cressey, for X-ray analyses; Kai Gilkes, of the University of Cambridge, for TEM and STEM characterisations; Uli Ott, of the Max Planck Institut für Chemie, Mainz, for the noble gas analysis of the Abee sample; Eddy Pelan of Unilever UK, for the laser scattering work; Andrew Cox and Mark Newton, of the University of Oxford, for the EPR study; Richard Becker of the University of Minnesota for the nitrogen degassing computer program; and Judith Milledge of UCL for the X-ray analyses, infra-red analyses, and donating the carbonado samples. To all of the above I am also grateful for the many discussions that helped my understanding of the samples.

All the members of the PSU have contributed much appreciated advice, drinks and/or moral support. I am particularly grateful to Jenny Gibson, for laboratory assistance; all of the Ia(i)ns for their interest and helpful comments; Judy Pillinger for sorting out the admin; Stuart "It'll never work" Boyd for his time, coffee and frank advice; Sascha Verchovsky for his interest; Jo Morris for typing many of my references; Paul "Hull City FC" Yates, whose line in lunchtime conversation was guaranteed to send me back to work; Leon, for tidying up; Dave Peate for always eating my chocolate brownies; Jez Higgins for his proof-reading and organising the coffee breaks; Andy Morse for the gin and for troubleshooting round the lab; Phil Bland for the use of his Mac and for being a buffoon; and Chris Hartmetz for the war commentary and American weather reports. I would also like to thank Naomi Williams for her help and patience while I was learning to use the SEM, and the security men at the Open University for keeping me awake on those night-time stepwises.

Most meteorite samples were donated by the Antarctic meteorite working group, NIPR, and Robert Hutchison of the British Museum; the specimens of Abee and Indarch were donated by E. Olsen, the Tieschitz sample by G. Kurat, and the Orgueil sample by P. Pellas. Some acid residues were donated by Luba Semjenova and Anatole Fisenko of the Vernadsky Instititute, Moscow, to whom I am also grateful for the useful if occasionally unintelligible discussions. Plessey of Towcester donated the CVD samples.

The Meteoritical Society and Barringer Crater Company are thanked for the travel funds and inspiration.

I would like to thank my parents, sisters and grandmother for their support and interest.

Most of all I would like to thank Richard Ash, who has been a constant source of good advice and guidance, for his seemingly endless patience, enthusiasm and support throughout the course of this study.

TABLE OF CONTENTS

LIST OF FIGURES

CHAPTER 3: METEORITIC DIAMOND ASSOCIATED WITH ISOTOPE ANOMALIES

CHAPTER 4: DIAMOND AND OTHER ACID-RESISTANT COMPONENTS IN THE ABEE METEORITE

CHAPTER 5: SYNTHETIC AND NATURAL TERRESTRIAL DIAMONDS: THE SEARCH FOR METEORITIC DIAMOND ANALOGUES

CHAPTER 6: SILICON CARBIDE AND HIGH TEMPERATURE COMPONENTS.

CHAPTER 7: OVERVIEW AND FUTURE WORK

LIST OF TABLES

CHAPTER 1
INTRODUCTION

1.1 Presolar grains in meteorites

The Solar system formed 4.55 x 10^9 years ago from a cloud of dust and gas. This material was made up of a mixture of matter which had been formed in older stars and primordial elements produced in the big bang. Although most of the original grains are believed to have been mostly reprocessed and homogenised during early Solar system processing, there is now evidence that some primitive meteorites still contain presolar grains which formed around stars, such as supernovae and red giants, that were ancestors to our own. The study of presolar grains can provide a wealth of information about the origins of the material from which the Solar system was created as well as the processes that have taken place during its evolution. Presolar grains - of which the most widely studied are silicon carbide and diamond - are most easily recognisable by their anomalous isotopic ratios, which cannot be explained by Solar system processing from an original homogenised source; these distinctive isotopic signatures however can sometimes be matched to a particular stellar environment in which the elements may have formed. The introductory chapter attempts to map out a history of presolar grains; firstly, stellar evolution, grain formation and ejection into the interstellar medium, and the incorporation of interstellar material into the Solar system will be summarised, followed by a discussion of the metamorphic processes to which they may have been subjected on their meteorite parent body. In the latter part of the chapter formation of carbon and nitrogen isotopes and their typical Solar system abundances are discussed, and finally a synopsis of the research aims of the thesis is presented.

1.2 Stellar evolution: The Early Years

To form stars a great deal of interstellar cloud material (diffuse matter) is needed (~1000$M_\odot$, where $M_\odot$ is the mass of the Sun; Cooper *et al.*, 1985). The cloud collapses under the influence of gravity, increasing in density and allowing local condensation to take place where local inhomogeneities have caused a more dense region of gas, to

form a cluster of new stars. As the collapse progresses in each of the denser regions, the temperature of the dust and gas rises; as the opacity increases, this heat cannot be lost easily and so the centre becomes increasingly hot. Temperature rises can occur extremely quickly - in more massive proto-stars they take place in only a few thousand years. When the temperature has risen to several million degrees Kelvin, hydrogen fusion begins and the star's temperature and luminosity is such that it will plot on the Main Sequence of the Hertzprung-Russell (H-R) diagram (figure 1.1). In fact, 90% of all observed stars lie on the Main Sequence, during which time they use up their complement of hydrogen by fusion to produce helium. One important way in which this occurs, in the higher mass stars, is by CNO cycling. This is a mechanism of ^{4}He production from ^{1}H, *via.* ^{13}N, ^{13}C, ^{14}N, ^{15}N, and ^{15}O intermediaries, also resulting in the increase in abundance of ^{14}N. The process changes the isotopic composition of the carbon, nitrogen and oxygen to equilibrium values and is an important cosmic production mechanism for ^{13}C.

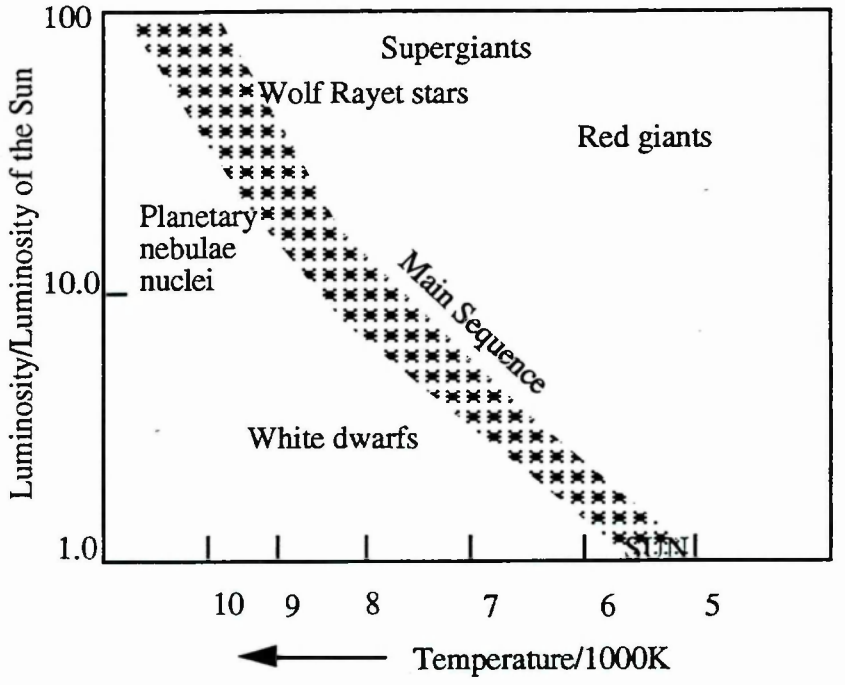

Figure 1.1. The Hertzprung-Russell diagram (after Cooper *et al.*, 1985).

1.3 Evolution of lower mass stars: Red Giants

When hydrogen in the stellar core becomes depleted, the hydrostatic pressure will no longer support the mass of the star; it begins to contract under gravity and moves off

the main sequence, figures 1.1 and 1.3. If the mass is greater than $0.5M_{\odot}$ then a red giant will form, which is typified by He burning reactions[1]. The structure and evolution of the red giant is entirely governed by its mass, but this section focuses on the more common lower mass stars. The eventual fate of high mass stars is discussed in more detail in the next section.

The new heat generated by helium burning causes the star to expand, allowing the outer layers to cool to around 3000K. The large volume occupied by the star at this stage allows a high flux of mass to escape from it (10^{-7} to 10^{-4} $M_{\odot}$ $year^{-1}$, Sackmann and Boothroyd, 1992). The most important new nuclear reaction involving He is the "triple α" reaction. This begins to occur slowly in larger mass stars but explosively in smaller ($<\sim 2.2M_{\odot}$) stars in which core degeneracy occurs before helium burning begins. Initially two helium nuclei fuse to form ^{8}Be, which has a half life of 10^{-16}s. This time is longer than the average collision time between particles and so another He nuclei is likely to collide with the ^{8}Be to form ^{12}C in an activated state. Although most of the carbon will then disintegrate back to ^{4}He, a small proportion will then decay to its stable ground state. The reaction can thus be summarised:

$$^{4}He + {}^{8}Be \rightarrow {}^{12}C^{*} \rightarrow {}^{12}C + \gamma 1 + \gamma 2$$

For stars with mass $9M_{O}>M>1M_{\odot}$, the star at this stage is in a quasi equilibrium state lying on the horizontal branch of the H-R diagram (figure 1.3) during helium burning. After the helium in the core has been depleted by 3α reactions, the core is made up of carbon and oxygen surrounded by shells of helium and hydrogen that burn alternately (figure 1.2). At this stage the star lies on the asymptotic giant branch (AGB), or secondary red giant branch, of the Hertzsprung-Russell diagram (figure 1.3).

Carbon burning reactions are now the most important source of heat in the the helium shell, *e.g.* the (α,γ) reaction:

$$^{12}C + \alpha \rightarrow {}^{16}O + \gamma$$

and the (α,n) reactions, *e.g*:

$$^{13}C + \alpha \rightarrow {}^{16}O + n.$$

The (α,n) reactions are important as they release free neutrons for the first time in the star's evolution. As the star heats up, because of nuclear reactions, to around $3x10^{9}K$,

[1] stars of $M = < 0.5M_{\odot}$ are not massive enough to undergo He burning and these stars die after the hydrogen is depleted

equilibrium reactions, in which a nuclear statistical equilibrium is achieved in the stellar core begin. Equilibrium reactions are very varied but include for example γ activated processes such as (γ,α), (γ,n) and (γ,p). In addition, nuclei fuse and release neutrons, *e.g.*:

$$^{16}O + {}^{16}O \rightarrow {}^{31}S + n$$

The equilibrium reactions increase the mass of the nuclei and also increase the neutron flux in the core. The free neutrons produced have a half life of around ten minutes but before disintegration may be absorbed by a nucleus to produce a heavier isotope of the same element. The neutron flux is low enough that the chance of an unstable nucleus absorbing another neutron before decay is minimal. The decay of the unstable nuclei is by $n \rightarrow p+e^-+\gamma$ to form an isobaric element. This is called the "neutron capture" or "s-process" and the elements thus produced have distinctive isotope abundance patterns. The "s" process is believed to be the most important mechanism for producing elements in the mass range 57-207 (Burbidge *et al.*, 1957).

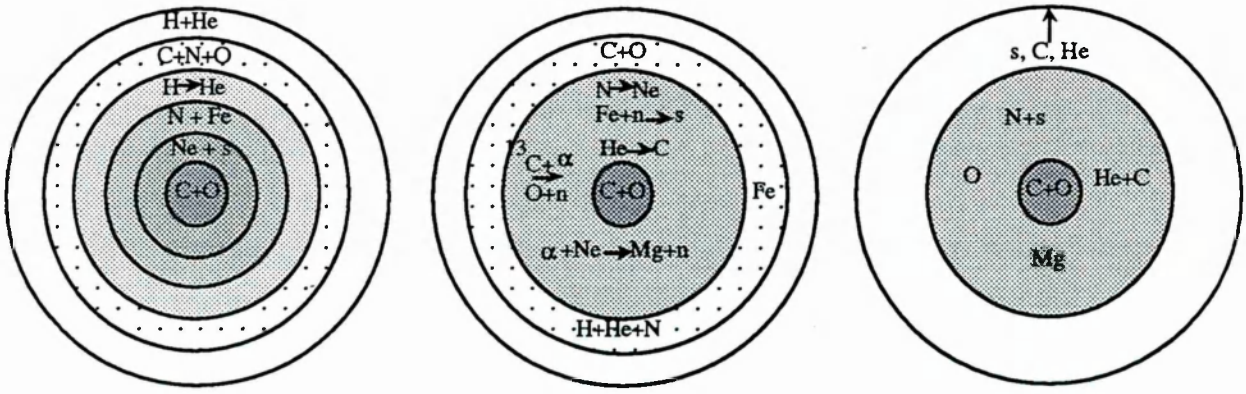

(a) "Off" (b) "On" (c) "Dredge-up"

Figure 1.2 Stages of ~1$M_\odot$ AGB star. s = "s-process" elements (from Iben, 1985)

Lower mass stars (~1$M_\odot$) evolve along the asymptotic giant branch (AGB) of the HR diagram as follows. In the H shell of the AGB star hydrogen first burns to produce helium (called the "off" stage: see figure 1.2 which is summarised from Iben, 1985). Hydrogen burning causes the star to heat up sufficiently that helium burning is triggered in the He zone (the "on" stage). Helium burning is initially thermally unstable and this stage, called the shell flashing phase or "thermal pulse", is short but dramatic. After each flash the products of α burning (^{12}C) and n capture (the "s process"

elements) are dredged up towards the surface of the star. If dredging is extensive then the abundance of carbon becomes greater than the abundance of oxygen at the star's surface and a carbon star will be formed. The first dredge up is characterised by a ^{13}C enrichment produced by mixing of ^{12}C with the hydrogen layer:

$$^{12}C + p \rightarrow {}^{13}N$$

$$^{13}N + e^{+} \rightarrow {}^{13}C + \gamma.$$

Later dredge ups are more ^{12}C rich from α burning associated with the "s" process.

The flashes cause the star to have fluctuations in luminosity that can be demonstrated by its calculated position in the H-R diagram, figure 1.3.

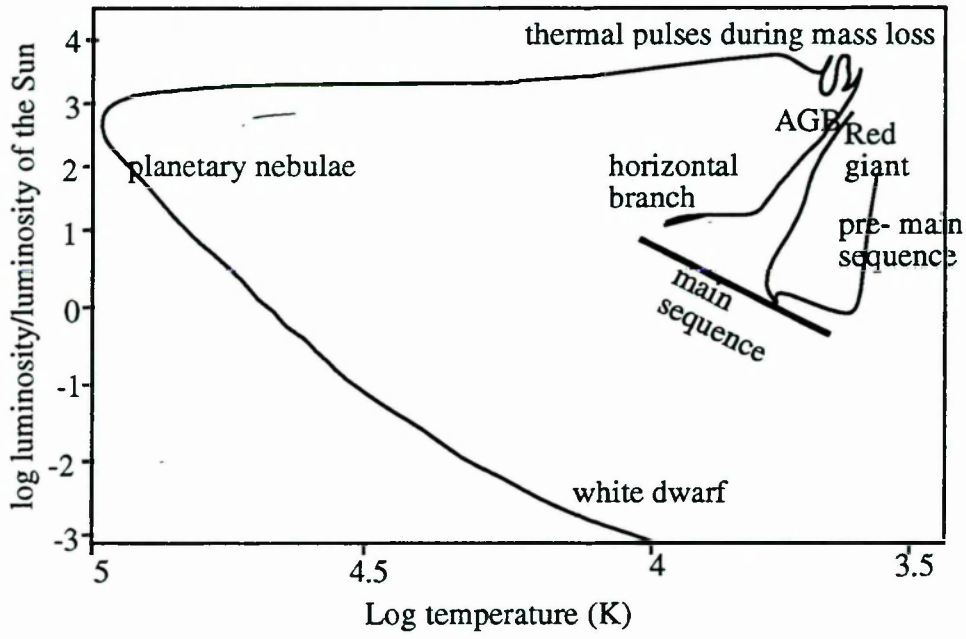

Figure 1.3 Evolution of a $1M_{\odot}$ star on the Hertzprung Russell diagram. Sketched from D'Anatona and Mazzitelli, 1992.

In the final stages of red giant evolution, the last part of the stellar envelope is blown off to become a planetary nebula, revealing a white dwarf stellar core.

1.4 Supernovae and novae

Higher mass stars (>8$M_{\odot}$) evolve much faster than low mass stars, and occasionally undergo dramatic death, as a Type II supernova. These stars are massive enough to have evolved a Fe/Ni core by exothermic nucleosynthesis (figure 1.4) from progressively burning hydrogen into helium into carbon into the higher mass elements; after the iron forming stage further fusion would require an energy input. The core begins to collapse, unsupported by the heat of fresh nuclear reactions. This causes a rise in the core temperature that leads to electron degeneracy and disintegration of the iron elements to α particles and neutrons, allowing the core to collapse quickly into a very dense mass. The collapse extends past the equilibrium density of nuclear matter which causes the core material to "bounce" back (Bethe and Brown, 1985). The shock waves of the bounce, and the interaction of the core matter with neutrinos produced during collapse, causes a highly energetic explosion that triggers a runaway nucleosynthetic event.

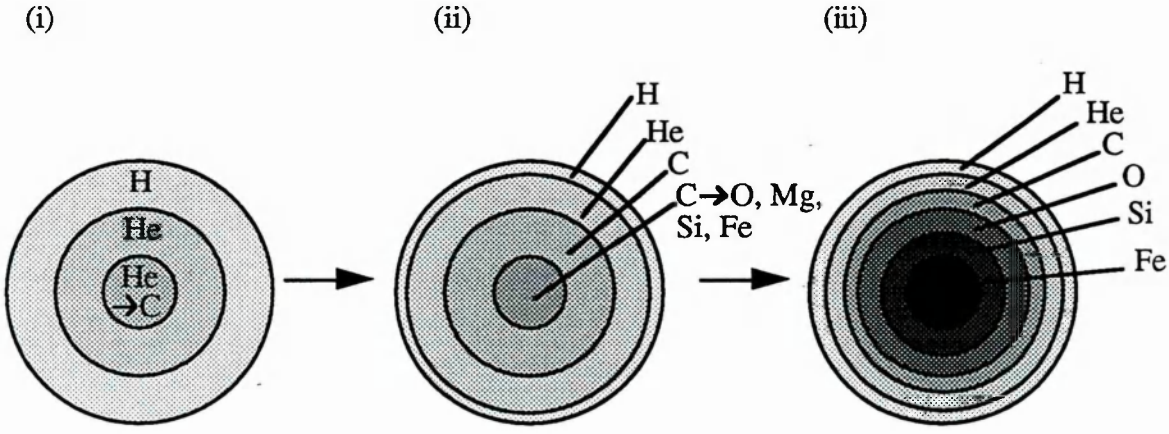

Figure 1.4 Evolution of Fe core in a 15M⊙ star: (i) The helium burns to form an carbon core, (ii) carbon in turn forms oxygen, magnesium and iron (iii) after an iron rich core has built up there are no further exothermic reactions reactions that can take place, the star collapses as in the text, triggering a supernova explosion. Figure adapted from Karttunen *et al.*, 1987.

The high flux of neutrons liberated by the core collapse in the supernova ensures that nucleosynthesis proceeds *via.* the "r" or "rapid" process. This is a major mechanism by which the heavier elements (>^{56}Fe) can be produced and the only way that massive isotopes can be synthesized. Another important nucleosynthetic process in supernovae

is the "p" process which forms the light isotopes of heavy elements (Burbidge *et al.*, 1957).

Observations of the recent supernova in the Large Magellenic Cloud (SN1987A) has led to a greater understanding of the nucleosynthetic processes that occur during these events (*e.g.* Atwood, 1990). Firstly, the presence of γ rays at energies 847 keV and 1238 keV (from ^{56}Co decay) confirms unambiguously the presence of heavy isotopes in supernovae (Matz *et al.*, 1988). Secondly, a surprising result was the observation of extremely energetic neutrinos (Burrows and Lattimer, 1987) that would be expected to collide with heavy nuclei, causing neutron emissions which would in turn be recaptured. This process would alter the nucleosynthetic products in the supernova, and especially affect the expected isotopic abundances of heavy elements (*e.g.* Clayton, 1989).

A somewhat less dramatic input into the interstellar medium is provided by novae. These occur in binary star systems in which one star has evolved to a white dwarf. The second star, when it reaches the red giant stage, will lose mass, that will fall under the influence of gravity towards the dwarf companion. The influx of mass can be large enough to trigger a hydrogen burning event resulting in an increase in luminosity in the growing star. The nova outbursts are accompanied by an ejection of matter from the star, but this does not result in its destruction.

Type I supernovae occur in less massive stars that also make up one of a binary unit. The more evolved star will accrete mass from its companion from which it will synthesize helium, carbon and oxygen during nova explosions. If the mass gain from the star's companion causes the more massive star to exceed a mass limit, called the Chandrasekhar limit, then core collapse will occur triggering a supernova explosion.

The Wolf Rayet stars (very hot, massive and apparently highly evolved stars, which have variable compositions but generally containing abundant carbon or nitrogen) are stellar sources that are also believed to eject a steady stream of material into the interstellar medium, although their evolutionary status is still controversial.

1.5 Grains in the interstellar medium (ISM)

Grains in the interstellar medium are detectable by the scattering and absorption of background starlight (Russell 1928; Trumpler, 1930). The grains - believed to make up about 1% of interstellar matter (*e.g.* Moore, 1985) - can be formed either in circumstellar environments around the outermost parts of stars, where temperatures, at

1000-2000K, are cool enough to allow newly formed elements to condense into molecules and grains (Hoyle and Wickramasinghe, 1970), or *in situ* in interstellar clouds. Grains have been detected around red giant stars by their infrared emission. For example, SiC and MgS have been detected around IRC + 10216 by Campbell *et al.* (1975), and around the red giant star ζ Ophiuchi grains of silicate, graphite, SiC, and iron are believed to have condensed (Field, 1974). The recent supernovae 1987A has provided indirect evidence that grains have formed (*e.g.* Moseley *et al.*,1989). The grains produced by this process - believed to be silicates, graphite and iron oxide - began to form 350 days after the explosion (Meikle, oral presentation to the RAS, Durham, 1992). Similarly, grains have been detected around novae (McLaughlin, 1935; Bode and Evans, 1983; Bode and Evans, 1988; Bode, 1988). The relative importance of output (of both gas and dust) into the interstellar medium from various stellar types has been estimated by Jura (1987) and these results are summarised in table 1.1. For comparison, the output from dust only estimated by Bode (1988) is also listed. Although the stellar classification of the two authors differs somewhat it is clear that the main output is believed to be from red giant stars (M giants, AGB, and C stars), with supernovae and novae also important.

Source	**Total output (a)** $M_\odot$ year $^{-1}$ x 10^{-3}	**Dust output (b)** $M_\odot$ year $^{-1}$ x 10^{-3}
AGB/ planetary nebula	300-1000	
M giants		3
C stars		0.4
Planetary nebula		0.3
Early type stars	80-500	
Supernovae	30	0.2
Novae	3	0.01

Table 1.1. Sources of interstellar matter in the Milky Way. (a) Jura, 1987; (b) Bode, 1988.

The first carbonaceous species to form as the elements cool is CO, and this is the main carbon sink for oxygen rich stars but if there is an excess of carbon then carbonaceous grains will also form once all the oxygen has been removed in the form of CO. A simplistic but quantative condensation sequence was first calculated by Gillman (1969) as a function of O/C ratio (figure 1.5). Observations of stellar environments, such as the references described above, has since demonstrated that circumstellar heterogeneities allow the condensation of both silicates and carbonaceous grains in

some stars. The grains formed are believed to be of the order of <100 nm in diameter (Jura, 1988), but it is probable that a wide range of grain sizes is formed.

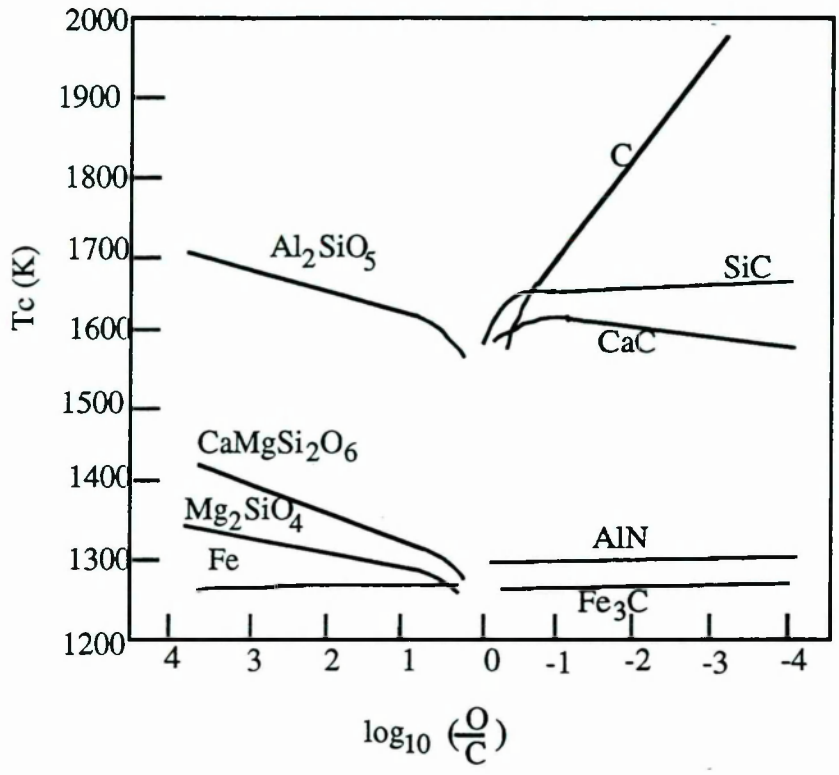

Figure 1.5. Expected circumstellar condensates as a function of O/C ratio. From Gillman, 1969.

Mass loss from stars takes place throughout the star's lifetime, but it is most important in the later stages of a star's life, discussed in sections 1.3 and 1.4. For stars that pass through the red giant stage, this mass loss occurs because the volume of the star is large compared to its mass and so escape from its gravitational field is moderately easy. A steady stream of material is expelled into the interstellar medium by the stellar wind, at a typical rate of 10^{-5} $M_\odot$ yr^{-1} (Thronson *et al.*, 1987; Sackman and Boothroyd, 1992). For larger stars, the supernova event expels much of their mass into the interstellar medium in a violent explosion. A typical supernova may have a mass of $25M_\odot$, of which $23M_\odot$ is lost during the explosion (Woosley and Weaver, 1986). In red giants and supernovae the expelled matter is believed to be in the form of both gas and dust.

More than half of all the elements heavier than He in the interstellar medium are believed by some authors to be in the form of solid grains (Spitzer, 1978). Presumably most of the refractory grains were formed in circumstellar environments where the concentration of elements is much higher than in the interstellar medium. The

cosmic abundance of O (the third most abundant element in the cosmos) is twice that of C (the fourth most abundant), but most stars of $M < 9M_{\odot}$, at the end of their lifetime, as well as massive stars, are enriched in C (the carbon stars). These tend to lose such a large amount of material (Claussen *et al.*, 1987), that up to half of all grains injected into the interstellar medium may be from this source (Zuckerman *et al.*, 1977). It follows that carbonaceous interstellar grains should be common.

Infrared spectroscopy of the interstellar medium (*e.g.* Tielens and Allamandola, 1987) suggest that the grains therein are mainly composed of silicates, ices and graphite (figure 1.5). The ices and refractory organics, which form grain mantles, are believed to be formed in the interstellar medium itself (*e.g.* Schutte and Greenberg, 1987). Of the other components, which are circumstellar in origin, silicates are the most abundant. The carbonaceous grains are assumed to be made up of graphite and amorphous carbon. SiC and MgS have not been observed directly in the interstellar medium, but their presence has been infered from observations of the mineral from red giant stellar outflows.

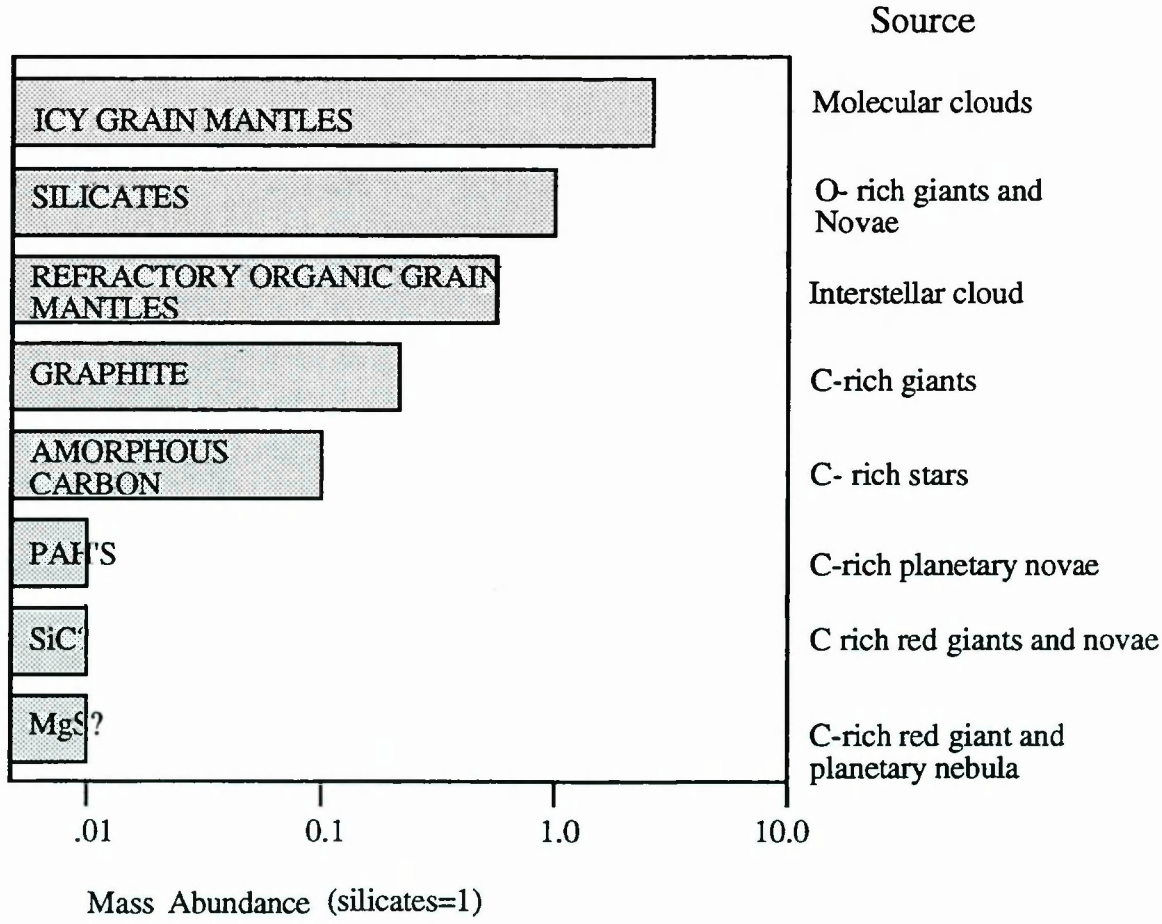

Figure 1.6. Grains in the interstellar medium (Data from Tielens, 1988).

Circumstellar grains undergo processing during their sojourn in the interstellar medium. In the dense dark clouds, material can condense into refractory grains and small grains can coagulate into larger ones (Seab, 1987). Polyaromatic hydrocarbons (PAHs) and ice accrete onto the grains to form a mantle (*e.g.* Tielens, 1988). Within the diffuse media ($n<20$ cm^{-3}) the predominant form of processing is destruction rather then accretion; shocks passing through the media can erode, vaporise and shatter grains (Seab, 1987; Tielens *et al.*, 1987).

Diamond in the interstellar medium can to some extent explain a strong extinction observed in the ultraviolet part of the interstellar spectrum (Saslaw and Gastad, 1969) although Wickramasinghe (1969) argued that no grain size of diamond would produce an extinction curve that is in agreement with the observed interstellar extinction curve. This point was refuted by Landau (1970) who maintained that the interstellar extinction could be explained by a diamond population with a grain size range of 0.001 to 10μm, although he pointed out that this did not represent proof that this mineral was present.

1.6 The early Solar nebula

The Solar system began about 10^{10} years after the formation of the galaxy (Reeves, 1978). The initial collapse of the protosolar nebula lasted for 10^5-10^6 years (Safronov, 1991); during this time the Sun formed and began to burn hydrogen. Gas falling into the nebula would have been decelerated and compressed as it encountered the shock front at the nebula boundary, which would have heated it up for a short period of time. The infalling grains would not be decelerated by the shock front but would slow down because of the drag from from surrounding gas; as a result the grains would become even hotter than the gas. A pressure and temperature gradient in the Solar nebula almost certainly existed, with convective motions away from the sun, although the exact figures on this gradient are still controversial (Moore, 1985). The amount of alteration and destruction of interstellar grains during the early stages of the Solar system is therefore unknown.

There is some debate about the exact conditions under which the planets formed from the Solar nebula. The angular momentum and turbulence of the Solar nebula are unknown and this means that a unique modelling of the condensation process is impossible. Many theories of the formation of the planetary bodies have been advocated, but the Kroto model is currently the most widely accepted. According to the Kroto school of thought, the infalling grains in the Solar nebula, under the

influence of Van der Waals forces, aggregated into clumps, of around 10μm across (but some of up to 10cm), within a few thousand years. After the Solar nebula had finished collapsing inwards, the turbulence in the nebula would have decreased to allow the aggregates to settle into a central rotating disc (Safronov, 1991; see figure 1.7). Gravitational instabilities in the disc then caused the collapse of these clumps into planetesimals, or protoplanets. The growth of the planetesimals into the planets could have then occured either by fast "runaway" growth of the larger bodies or by steady agglomeration (Wetherill, 1989). By analogy with observations of present day star forming regions, it is believed that after this stage the Sun, which would already have begun hydrogen burning, would have passed through a "T-Tauri" phase characterised by a variable stellar outflow that would blow off most residual dust and gas (Moore, 1985).

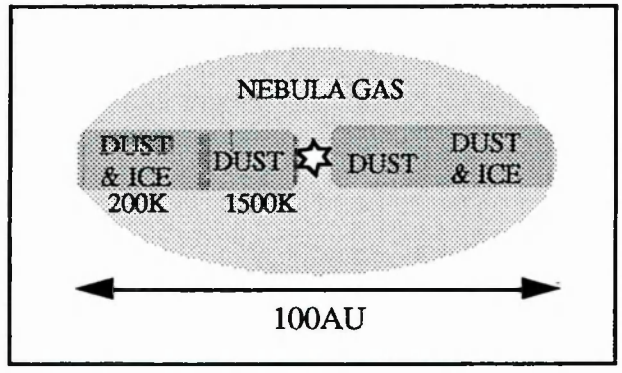

Figure 1.7. Structure of the early Solar system ("side view") after settling of dust towards the midplane. Diagram after Reeves, 1978.

1.7 Meteorites

A meteorite is a recovered fragment of an extraterrestrial object that has fallen onto the Earth. They are categorised as irons, stoney irons, and stones. Some stoney meteorites have suffered relatively little heating and so are the most likely host to any unaltered interstellar grains that would have survived processing in the meteorite parent body. Most meteorites are believed to have originated in the asteroid belt, between Mars and Jupiter, and have been chipped off these bodies by relatively recent collisions (*e.g.* Wetherill and Chapman, 1988). The formation of the planet Jupiter, which may have been completed just 10^6 years after the start of condensation in the Solar system, could have caused a gravitational perturbation that ensured the asteroids were prevented from accreting into a single planet (*e.g.* Wetherill and Stewart, 1987; Weidenschilling, 1988).

The stoney meteorites are further divided into chondrites, or meteorites with a sedimentary texture, which usually contain spheroidal silicate particles called chondrules, and achondrites, which have an igneous texture. This thesis is entirely concerned with the chondrites, as these are believed to have been relatively unchanged since their accretion. Chondrites have radiometric ages of around 4.55 billion years, probably similar to the condensation age of the whole Solar system (*e.g.* Tilton, 1988).

The chondrites are subclassified by their chemical and metamorphic characteristics. Chemically, the meteorites can be carbonaceous (volatile enriched), ordinary (depleted in volatiles and less oxidised than the carbonaceous chondrites) or enstatite (reduced mineralogy). Further classification of the carbonaceous class splits the meteorites into groups that contain similarities to a type specimen; for example "CV" meteorites are carbonaceous chondrites of the Vigarano type and "CM" meteorites are carbonaceous chondrites of the Murchison type. Ordinary chondrites are further categorised into H, L, and LL, representing decreasing amounts of total iron in the stone.

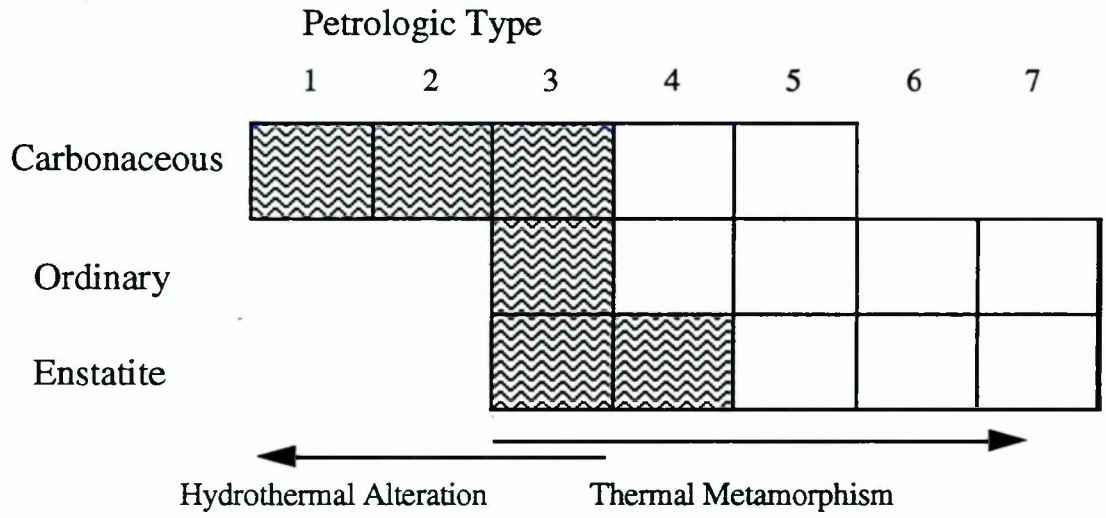

Figure 1.8. Meteorite types from which presolar grains have been reported (shaded regions indicate meteorites from which carbonaceous grains associated with isotope anomalies have been isolated).

The metamorphic classifications are denoted by number (Van Schmus and Wood, 1967): types 3-1 have suffered increasing amounts of hydrothermal alteration, and types 3-7 show increasing amounts of thermal metamorphism. Some chondrites also show signs of shock metamorphism from impacts in space. In the search for interstellar grains in meteorites, the least thermally altered chondrites have been prime

targets as an primitive material is more likely to have survived in these pristine samples. Interstellar grains, found in the meteorite classes shaded in figure 1.8, have not yet been isolated from meteorites of petrologic type 4 or above except in enstatite chondrites, which may provide a more stable environment for chemically reduced carbonaceous grains. Although the restriction of interstellar grains to primitive meteorites is most commonly attributed to grain destruction in the meteorite parent body in higher petrologic type meteorites, heterogeneous accretion in the Solar nebula may also play a role (*e.g.* Huss, 1990).

1.7.1. Oxygen isotopes: evidence for Solar system heterogeneity

It has been well established that the Solar system is largely isotopically homogeneous; the bulk isotopic compositions of meteoritic material is similar to that of terrestrial samples and any differences can usually be explained by fractionation or radioactive decay (Reynolds, 1967). Isotopic homogeneity supports the long held belief that the early Solar nebula was hot, vaporised and well mixed (*e.g.* Cameron, 1962). However, in the early seventies, evidence emerged that nebulae mixing was incomplete. During fractionation processes, the proportions of the three isotopes of oxygen - ^{16}O, ^{17}O, and ^{18}O should be related by $\delta^{17}O = 0.52\ \delta^{18}O$ (this is true only when $\delta^{x}O \sim 0$). Oxygen isotope data would therefore be expected to lie on a straight line that represents fractionation effects from an original source.

Clayton *et al.* (1973) found that calcium aluminium inclusions (CAIs) in carbonaceous chondrites fall on a slope of 0.94 (figure 1.9), which is interpreted as an input to these components from an ^{16}O rich source that was not fully mixed into the Solar system reservoir. A theory supported at that time, although not widely believed today, suggests that the additional ^{16}O may have come from a supernova, that injected fresh material into the early Solar nebula, inferred by the presence of ^{26}Mg from the extinct supernova-produced isotope ^{26}Al in the same inclusions (Cameron and Truran, 1977).

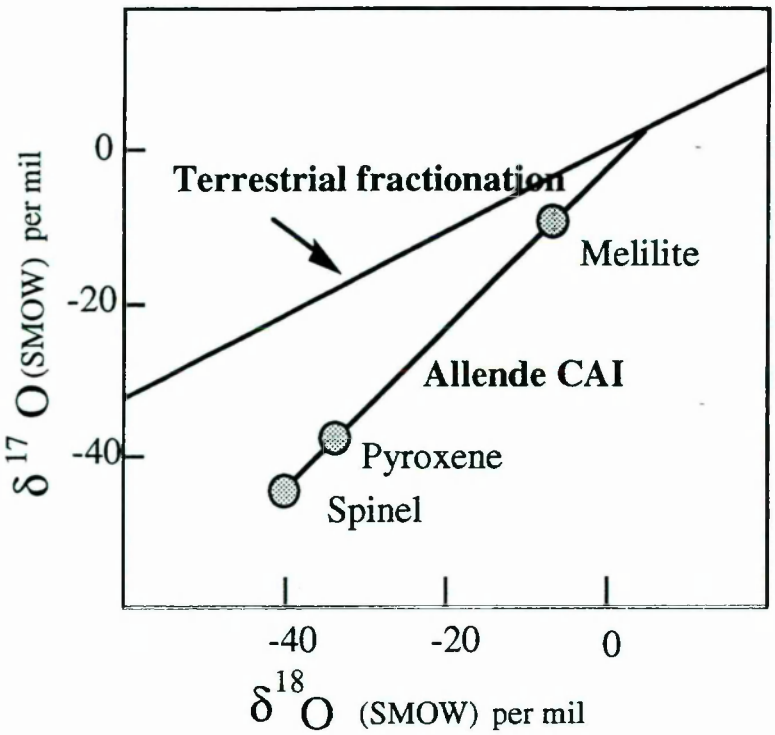

Figure 1.9. Oxygen isotopes from refractory inclusions in Allende (Data from Clayton *et al.*, 1973). The oxygen isotope compositions are plotted as $\delta^{17}O$ and $\delta^{18}O$, which are measures of the enrichments in these isotopes compared to a terrestrial standard (Standard Mean Ocean Water or SMOW); this notation is defined in Chapter 2.

Evidence for large scale isotopic heterogeneity in the Solar system is provided by whole rock oxygen isotope abundances of the different chemical types of chondrite, which do not fall on one line, indicating that they condensed in isotopically distinct regions (Clayton *et al.*, 1984). The isotopic composition of the various chondrite classes discussed in this thesis are represented diagrammatically in figure 1.10. However, many of the components in the meteorites, such as the anhydrous minerals, have similar oxygen isotopic compositions. The oxygen data thus demonstrate that the Solar system, although well mixed overall, was not completely isotopically homogenised before condensation.

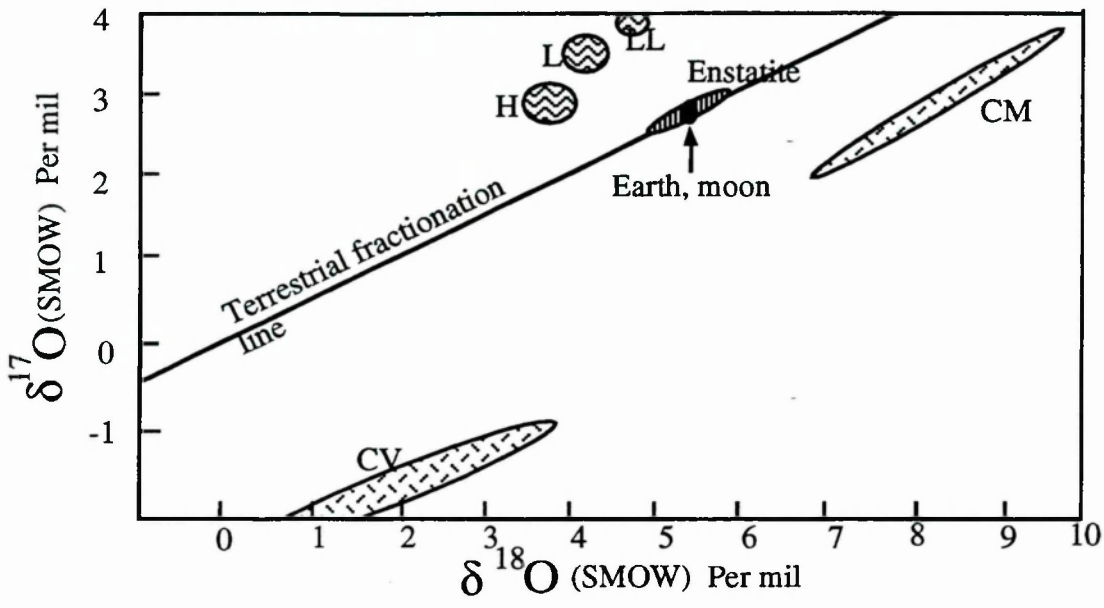

Figure 1.10. Whole rock oxygen isotopic compositions of chondritic classes of meteorite discussed in this thesis. Data from Clayton *et al.*, 1984.

1.7.2. Secondary processing in meteorite parent bodies

The study of alteration processes in meteorites is of great significance to the study of interstellar grains. Extensive alteration of the meteorite in its parent body may alter or destroy fragile grains and it can be seen that anomalous isotopic signatures are observed only in the the most primitive meteorites (*e.g.* Anders, 1987; Alexander *et al.*, 1990a; Huss, 1990) suggesting that the grains that once existed in the higher petrologic type meteorites were destroyed by either nebula or parent body processes. The most extensive form of post-accretion alteration was that caused by parent body heating, which caused recrystallisation and speeded up the homogenisation of elements and isotopes in the higher petrologic type meteorites. Several paleothermometers have been used in an attempt to constrain the temperature at which metamorphism took place. These include metal compositions, partitioning of the iron and magnesium in orthopyroxene and diopside and distribution of Ca in pyroxenes (Olsen and Bunch, 1984), phase transformations in feldspar which can be monitored by thermoluminescence (Guimon *et al.*,1985) and studies of $\delta^{18}O$ (Onuma *et al.*, 1972). The results point to an approximate maximum temperature of metamorphism of 400°C for type 3 ordinary chondrites, rising to 1000°C in type 7 chondrites. The heat source for the thermal metamorphism is likely to have been short lived radionuclides such as ^{26}Al (Lee *et al.*, 1976) but electromagnetic induction from the early Solar wind

(Sonnett *et al.*, 1970) and additional condensation of hotter particles (Larimer and Anders, 1967) have also been suggested.

Alteration by aqueous fluids appears to have been an important process in the more primitive chondrites, which has resulted in the crystallisation of secondary minerals (*e.g.* phyllosilicates and carbonates). Although the processes are most pervasive in the CM/CI meteorite groups, there is also some evidence for alteration of the CO and CV3 meteorites (Zolensky and Mc Sween, 1988) and the unequilibrated ordinary chondrites (*e.g.* Alexander *et al.*, 1986). Ice would have accreted onto the parent body, but must have then been heated to the liquid state to permeate the rock. The heat sources for this process may have been similar to those responsible for thermal metamorphism (DuFresne and Anders, 1962; Larimer and Anders, 1967; Sonnett, 1971); alternatively, impacts on the surface of the asteroid may have caused local heating that melted the ices. An oxygen isotope study of the CM chondrite Murchison (Clayton and Mayeda, 1984) indicate that its temperature was between less than 0°C and +20°C, with a water/rock ratio of *ca.* 1. Orgueil (CI1) appears to have experienced higher temperatures: ~140°C, and a water/rock ratio of >1.

Because of the comparatively small diameter of asteroids, pressures in meteorites appear to have been low except during shock events, which were caused by asteroidal collisions as well as terrestrial impacts. Shock metamorphism can be found in all the meteorite types, and shock features were once used as diagnostic tools in the earliest meteorite classification systems (*e.g.* Brezina, 1904), but are now considered to be unrelated to the meteorite origin. On collision, a high pressure shock front passes through the meteorite and heats it, causing recrystallisation or even melting, and this process may destroy any fragile interstellar grains. Hence highly shocked meteorites would not be the best candidates for hosting primitive grains.

1.7.3. Noble gases

The noble gases are extremely incompatible and so are present in meteorites and the Earth at only small fraction of their Solar abundance. They do however, provide a good marker for exotic meteoritic components as they are easy to study in small quantities, using static type mass spectrometers of the type pioneered by Reynolds (1956), and because the heavier noble gases have many isotopes, allowing distinct patterns to be characterised, and local isotopic compositions to be distinguished from

exotic ones. Two types of noble gases were believed to have be incorporated originally in meteorites: local, or "planetary" gases that have been affected only by fractionation processes, and "exotic" or presolar gases (*e.g.* Anders, 1988). Other noble gas components have since become part of the meteorite noble gas inventory: radiogenic (*e.g* ^{40}Ar, produced from ^{40}K), spallogenic (*e.g.* ^{21}Ne), and Solar (implanted Solar wind particles).

1.7.4. Carbonaceous grains

Only three types of circumstellar carbonaceous grains have been well characterised: diamond, silicon carbide and graphite; these are all grains that were first recognised as presolar by their anomalous noble gas signatures. Before the identification of the carbonaceous carrier phase, the presolar components were named C with a greek letter subscript: Cα, Cβ, *etc.* (see table 1.2); these nicknames have largely become redundant for the now identified components. Many other anomalous isotopic signatures have been observed, *eg.* light carbon ("Cλ") in Allende (Ash *et al.* 1989), heavy nitrogen in Bencubbin (Prombo and Clayton, 1985, Franchi *et al.* 1986); in polymict ureilites (Grady *et al.*, 1985); and in the unusual chondrite ALH 85085 (Grady and Pillinger, 1990), and a new xenon isotope pattern in Efremovka (Verchovsky *et al.* 1990) *etc.* None of these signatures have yet been positively related to a carrier phase, but it is apparent that circumstellar grains are abundant in primitive Solar system material.

Phase	Abundance in CM2's (ppm)	Associated noble gas anomalies	Associated C and N anomalies	Old name
Diamond	400	XeHL, Ne A-2	Light N	Cδ
Silicon Carbide	10	Xe-S, Ne E(H), Kr-S	Heavy C, light N	Cβ, Cε
Graphite	5	Ne E (L)	Some grains made of heavy C, some light C	Cα

Table 1.2 Carbonaceous grains and associated anomalies.

1.8 Carbon in the galaxy

Carbon ([He] $2s^2p^2$) has two stable isotopes: ^{12}C and ^{13}C, of which ^{12}C is the more abundant. In addition, the isotope ^{14}C is known in nature and has a half life of 5730 years. The bulk of the carbon in the galaxy is believed to have been produced by He burning reactions in red giants. ^{12}C is predominantly formed by $3\alpha \rightarrow {}^{12}C$ reactions and released into the interstellar environment by supernova explosions or in red giant winds/planetary nebulae. ^{13}C is a product of mature CNO cycling, and (p,γ) reactions in red giants. There is evidence that different stellar sources can produce carbon of very different isotopic compositions. The $^{12}C/^{13}C$ ratio of carbon rich red giants is very variable but the mean is around 30-50, (*e.g.* Knapp and Chang, 1985; Lambert *et al.*, 1986) although this figure may fall as low as 20 during dredge ups (Obaravic *et al.*. 1991), and is much lower (2-3) in a few anomalous stars called "J type" (Lambert *et al.*, 1986). The $^{12}C/^{13}C$ ratio of oxygen rich red giants is believed to be higher at around 89 (Tielens, 1988). Novae are a prolific source of ^{13}C enriched carbon ($^{12}C/^{13}C$ <1, Starrfield *et al.*, 1985), whereas supernovae produce carbon that is more ^{12}C rich. Surprisingly, the galaxy does not appear to have a significant $^{12}C/^{13}C$ gradient despite the heterogeneous distribution of these stellar sources throughout the galaxy (*e.g.* Tielens *et al.*, 1988); observations of interstellar dust in different directions indicates the mean value of the $^{12}C/^{13}C$ ratio of interstellar dust in the Milky Way to be 43±4 (Jura, 1988, see table1.3).

Direction	**$^{12}C/^{13}C$ ratio**
ζ Oph	43±6
ξ Per	46±11
P Cyg	44±11
20Tau	41±9
23Tau	41±8

Table 1.3. $^{12}C/^{13}C$ ratios observed in the Milky Way interstellar medium.
From Hawkins and Jura, 1987.

The bulk $^{12}C/^{13}C$ ratio of stoney meteorites is 90±4 (Pillinger, 1984); and of the Earth, 89 (*e.g.* Hoefs, 1987). A range of $^{12}C/^{13}C$ values have been recorded for the other planets, although because of experimental difficulties this measurement has proved hard to make accurately; the data falls within error of terrestrial values (*e.g.* Hoefs, 1987; Courtin *et al.*, 1983; Nier *et al.*, 1976; Epstein and Taylor, 1970). Comets, however, appear to be enriched in ^{13}C compared to the rest of the Solar system, with a

$^{12}C/^{13}C$ value of 65±9 recorded by Wyckoff *et al.* (1989). A $^{12}C/^{13}C$ ratio of ~90 for the Solar system as a whole is somewhat higher than the measurements of the rest of the galaxy, indicating that either the galactic evolution has increased its ^{13}C inventory, or else the Solar system condensed from a region of the galaxy that was of unusual carbon isotopic composition, possibly because it was dominated by a single stellar source material.

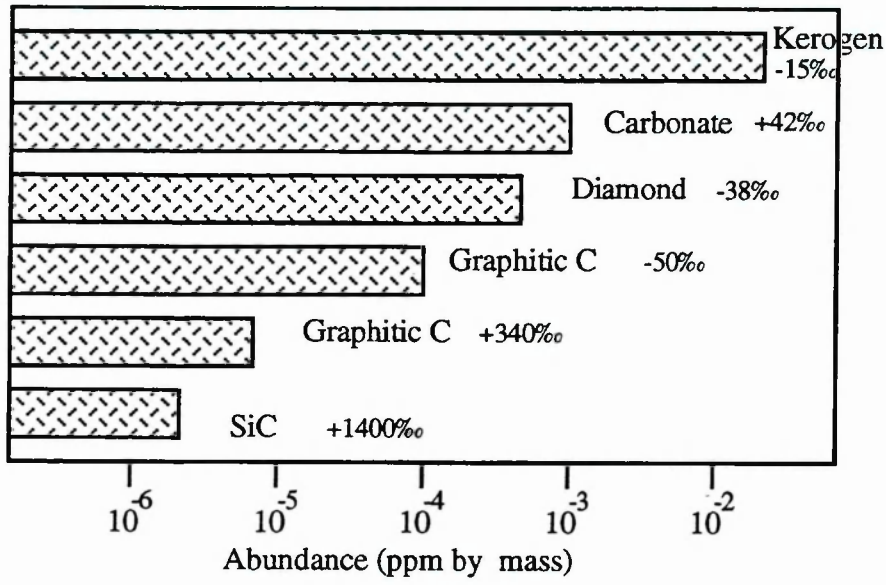

Figure 1.11. Relative abundance of carbonaceous components in Murray (adapted from Tang *et al.*, 1989). Carbon isotopic compositions are expressed as $\delta^{13}C$ values using the delta notation that is defined in Chapter 2.

An interesting insight into the carbon in the Solar nebula can be achieved by study of the carbonaceous components in primitive meteorites, which are believed to have been little changed since their accretion. The carbon inventory of Murray (CM2) is depicted in figure 1.11, along with the $\delta^{13}C$ values of the major components. The dominant species are organic materials that were formed either in the interstellar medium and/or in the early Solar nebula. Carbonates, the most abundant carbon bearing inorganic minerals, are probably secondary, formed by hydrous alteration processes in the parent body. Although their isotopic composition tends to be heavy, this is believed to be due to Fischer-Tropsch synthesis in the Solar nebula (Lancet and Anders, 1970). The putative interstellar grains, that have kept distinctive isotopic signatures from presolar circumstellar condensation, make up a surprisingly high proportion of the total carbon content. In contrast, the higher petrologic type meteorites have lost most of their carbon, probably through metamorphic processing (Grady, 1983). The ordinary and

enstatite chondrites contain carbon only in reduced forms: predominantly graphite, diamond, and SiC. Most of their carbon is made up of grains that have formed in the Solar system, indicated by their carbon isotopic composition.

1.9. Nitrogen in the galaxy

Nitrogen ([He] $2s^2\ 2p^3$) has two stable isotopes- ^{14}N and ^{15}N, of which ^{14}N is the more abundant. ^{14}N is produced mostly by equilibrium CNO cycling and released to the interstellar medium mostly by red giants and planetary nebulae. ^{15}N is produced by hot CNO cycling and is released into the interstellar medium when the cycling is interrupted, *e.g.* by a nova explosion.

The $^{14}N/^{15}N$ of the Earth's atmosphere is 272 and the value of the bulk Earth is probably close to this value. Indeed, N isotopic fractionation on the Earth gives isotopic variations that rarely exceed 20‰ (*e.g.* Javoy *et al.*, 1984; Boyd *et al.*,1988; Boyd, 1988). The $^{14}N/^{15}N$ value of the Sun, estimated by Geiss and Bochsler (1982), is thought to be around 250, similar to the value of the Earth. However, nitrogen studies of meteorites and other Solar system bodies have shown that much greater variations exist. Many of these heterogeneities can be explained by Solar system processes; for example, the martian atmosphere has $\delta^{15}N = +650‰$ (Nier *et al.*, 1976) which is thought to reflect escape of N from the planet's gravitational field to produce a large fractionation in the nitrogen residue. Spallation reactions (*e.g.* from ^{16}O to ^{15}N) act to decrease the $^{14}N/^{15}N$ ratio of some meteoritic and lunar minerals (usually those released at high temperatures during stepped heating). The isotopic composition of nitrogen in lunar samples has been the subject of some debate. The samples contain several N components, one of which, released at low temperatures during stepped heating, with a $\delta^{15}N$ of +125‰, appears to have been implanted by the present day Solar wind. At higher temperatures, a light component is released, which may be either ancient Solar wind (Kerridge 1980), a light planetary nitrogen component (Geiss and Bochsler, 1982) or input of isotopically anomalous grains from meteorites (Norris *et al.*, 1986). The carrier of the putative light planetary nitrogen component has not been isolated or identified, but a change in Solar $\delta^{15}N$ of 300‰ in the Sun is difficult to explain. It would have important implications for our understanding of nitrogen containing early Solar condensates.

It has been suggested (Geiss and Boschler, 1982) that the differences in nitrogen isotopic composition observed could reflect incomplete mixing of the Solar nebula. For example, Franchi (1988) identified four distinct nitrogen reservoirs in iron meteorites.

Some meteorites contain compounds that have extreme nitrogen isotopic values (*e.g.* Bencubbin:- Prombo and Clayton 1985; Franchi *et al.*,1986; Acapulco:- Stugeon and Marti, 1990; ALH 85085, Acfer 182:- Grady *et al.*, 1991). Despite the wide variations in $^{14}N/^{15}N$ produced by Solar system processes, there is evidence that some of the more extreme nitrogen isotopic values represent the survival of an exotic nucleosynthetic signature.

1.10 Aims of this thesis

Noble gas studies have indicated that interstellar grains in meteorites are concentrated in acid resistant fractions (Tang and Anders, 1988a). In particular, HCl/HF is often used to dissolve away silicates, to allow a more focused study of the remaining carbonaceous components; oxidising acids such as perchloric can then be used to remove the less resistant carbon phases such as organics. The acid residue left by this treatment is rich in isotopic anomalies that have been found to be associated with diamond (Lewis *et al.*, 1987), SiC (Tang and Anders, 1988b) and minor, unidentified phases (*e.g.* Ash *et al.*, 1989). The aim of this work was to further characterise the many perchloric resistant carbonaceous components in primitive meteorites. A suite of different meteorite types, all prepared in a similar way, were studied so that differences between meteorite types could be observed.

The work involved the setting up of a system of simultaneous nitrogen and carbon yield analysis, so that firstly, the relationship between carbonaceous minerals and nitrogen could be ascertained, and secondly, accurate C/N data could be collected from the components in an attempt to characterise the grains and detect any differences between similar minerals in different meteorites. It was therefore necessary to undertake an assessment of the reproducibility and accuracy of C/N measurements, using a variety of sample types and techniques, so that the errors involved in the measurements could be quantified.

The small size (~2nm) of diamond crystals associated with isotopic anomalies makes study of individual grains impossible and stepped combustion provides an accurate method for obtaining carbon and nitrogen isotopic and abundance information. Although values for the $\delta^{13}C$, $\delta^{15}N$, and rough estimates of nitrogen content in chondritic diamond have been acquired in the past (*e.g.* Alexander *et al.*, 1990; Arden *et al.*, 1989; Ash, 1990), there was a need for a systematic study of the stable isotopes of diamond rich separates from all the chondrite groups using samples that had been isolated in sufficient purity to ensure minimal contamination from other carbon and

nitrogen containing species. Careful, high resolution stepped combustion were performed on these samples to (i) attempt to constrain the number of sources of the diamond, (ii) investigate their distribution in the early Solar system and (ii) determine the extent to which parent body processes had altered the component.

The mechanism of the diamond formation is unknown. Samples of synthetic diamond produced both by high pressure mechanisms (shock) and low pressure mechanisms (chemical vapour deposition) were characterised in an attempt to compare these to meteoritic diamond and hence constrain their formation conditions.

The second part of the thesis was concerned with stepped combustion of silicon carbide, a mineral that is characterised by heavy carbon and light nitrogen, as well as "s process" isotopic signatures of heavy elements (*e.g.* Srinisavan and Anders, 1978; Ott *et al.*, 1985). These have a grain size range of up to 10μm, and so have been extensively studied in recent years by ion probes, which can analyse individual grains and have demonstrated that this mineral has multiple sources. However, this technique can only analyse the largest grains and so there is an intrinsic bias in the ion probe data. Mass spectrometry using stepped heating techniques, in which many thousands of grains area analysed at once, gives a more accurate picture of the mean data allowing meteorites of different classes and types to be compared. The development of a new accurate and sensitive mass spectrometer, "MS86" allowed high resolution stepped combustion experiments to be performed on the meteorite suite in an attempt to (i) recognise possible differences in the SiC inventories of different meteorite types, (ii) assess the extent to which they had been altered on the meteorite parent body and (iii) resolve possible less abundant interstellar components in these samples.

By stable isotope analysis of acid resistant residues it was thus hoped that a greater understanding of the origins and distribution of interstellar grains could be achieved, and also of the Solar system processes that altered and destroyed them.

CHAPTER 2 :
EXPERIMENTAL TECHNIQUES

The analysis of carbon and nitrogen isotopic compositions of acid resistant residues was performed by mass spectrometry. This technique separates isotopes of different masses by passing their ions through a magnetic field. The lighter isotopes are deflected by a greater angle than the heavier ones and so can be separated, then collected and counted. For the work described in this thesis two mass spectrometer types were used. For the precise measurement of microgram amounts of carbon a traditional dynamic mass spectrometer (SIRA 24) was used to analyse the CO_2 released from the combusted samples. For the nitrogen work and for smaller carbon samples this technique was not sensitive enough. Static mass spectrometry, in which an aliquot of gas is expanded into the source and measured, followed by the similar measurement of a reference aliquot, was more suitable. The nitrogen work was performed on a mass spectrometer described by Wright *et al.* (1988), using an extraction system modified from Boyd *et al.* (1988). The carbon analyses were conducted mostly on "MS86": a SIRA 24 analyser with a closed source, 80mm flight tube and 90° deflection described by Prosser *et al.* (1990), using techniques adapted from Carr *et al.* (1986), Ash *et al.*, (1989) and Yates *et al.*. (1992).

Most of the data are presented using the delta notation, where

$$\delta X(‰) = \frac{(R\ sample - R\ std)}{Rstd} \times 1000$$

where R = heavy isotope/light isotope (for carbon and nitrogen isotope measurements) and X is the isotope measured.
Laboratory reference materials are used for convenience during experiments, but all data quoted here have been adjusted to the international standards; for carbon, this is the carbonate from a belemnite of the Pee Dee formation of South Carolina (PDB), for nitrogen, air is employed.

Samples were typically analysed by a bulk carbon technique first, to obtain accurate yield and isotopic data. Separate aliquots were combusted by high resolution stepped

combustion to 550°C using dynamic carbon mass spectrometry or static nitrogen mass spectrometry. After removal of the more abundant lower temperature components, the residue was transfered for combustion to higher temperatures on a more sensitive mass spectrometer ("MS86"). A sample number of specimens were continued to high temperature for nitrogen isotopic measurements. In this chapter, the techniques used for the bulk measurements of carbon will be discussed, followed by a description of the standards and blanks used to test the static carbon instrument and techniques. It includes a description of a pilot study into a new system for measuring aliquots of standard gas (the capillary aliquotting system). In the second section of the chapter, C/N ratio measurements will be discussed. A system in which carbon yields of the samples could be measured simultaneously with the nitrogen measurements was an important development for the research effort to be undertaken. The conjoint nitrogen / carbon technique is described, and an analysis of its uses and limitations is made. Finally, the procedures used to isolate the acid resistant components in the meteorites will be described.

2.1 CARBON

2.1.1 Bulks

Whereas stepped combustion can separate the multiple components invariably found in meteorite residues, a useful check on the data can be provided by bulk analysis which gives an accurate value for overall isotopic composition and carbon content. The bulk analyses were performed in sealed tubes using an oxide as oxidising agent, with the samples (of around 100μg in mass) usually weighed into platinum buckets that had been baked out according to the protocol of Grady (1983). The samples were combusted at 1000°C for at least ten hours and then the tubes cracked under vacuum, measured by capacitance manometer and analysed by dynamic mass spectrometry.

Oxygen suppliers

Copper oxide (of Specpure, now called Puratronic grade, supplied by Johnston Mattey, Orchard Road, Royston, Hertfordshire, SG8 5HE) was used as the oxygen supply for most samples. CuO exists in equilibrium with oxygen, with the reaction $2CuO \leftrightharpoons 2Cu+O_2$ shifting towards the right at high temperatures. The brand of copper oxide used contains around 2ppm carbon, so that typically when a 100 fold excess of reagent is used in the experiment, a full procedural blank of 25ng carbon can be expected. The blank contribution to a 100μg sample is therefore less than 1% for samples containing 25%

carbon. The CuO dissociation is not 100% efficient and an experiment in which diamond chips were combusted using known amounts of CuO showed that at least 40x excess relative to the carbon content of the sample is needed to obtain a full carbon dioxide yield, compared to the stoichiometric amount of 13x as much CuO:

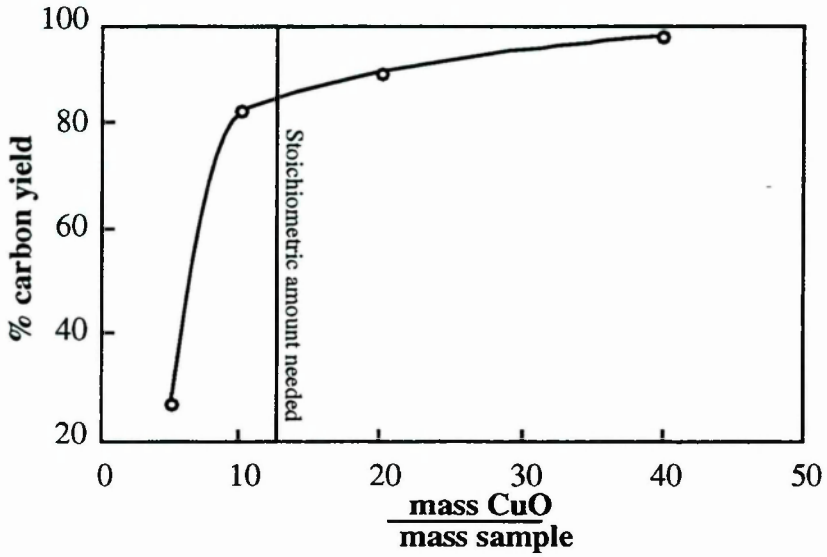

Figure 2.1. Combustion of diamond chips in different masses of CuO shows that CuO>40xC is needed to obtain a full combustion. This is three times more than the stoichiometric amount.

The use of silver oxide as an oxygen source was also investigated. Silver oxide decomposes above 100°C and so would be useful for preparative precombustion experiments (where the sample is combusted for a long time at low temperatures to slowly combust the less stable components while leaving the higher temperature ones intact - Ash, 1990). To investigate this oxygen source, samples of varying amounts of AgO were heated to 1000°C for ten hours and the carbon yield then measured. The results have been plotted in figure 2.2.

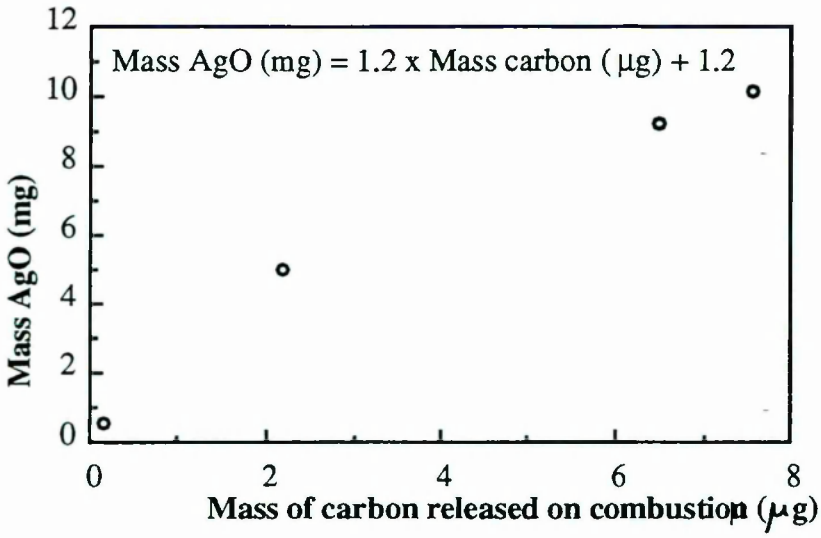

Figure 2.2: An analysis of the mass of carbon released during combustion (at 1000°C) of specpure AgO.

Unfortunately it was found that the silver oxide contained 815 ppm carbon making the blank prohibitively high for most isotopic work, although the relative uniformity of the carbon content suggests that blank corrections could be made on data using this technique.

More recent work by J. Gibson (*pers comm.*.) has shown $KMnO_4$ to be a suitable oxygen source associated with a low carbon blank that could be used for preparative precombustion. However, since this technique did not form an important part of this experimental work it has not yet been explored further.

2.1.2. Carbon Stepped combustion techniques

Stepped analysis of carbon

Stepped combustion is a technique whereby components of different thermal stability in oxygen can be separated, by increasing the temperature of the sample at well defined increments, and analysing the released gas at each step. Originally, this technique was designed to separate low temperature contaminants from material indigenous to the sample. In more recent times the technique has become more sophisticated, with high resolution experiments (*i.e.* raising the temperature in small increments) allowing the separation of many different components in each sample, and even allowing investigation into the mechanism of combustion of single components (see diamond work in chapter 3). For the data in this work, an extraction line similar to that described by Ash (1990)

was used. Diamond samples, in which the carbon was relatively abundant, were analysed by dynamic mass spectrometry and the scarcer silicon carbide analysed by static mass spectrometry using the system described by Yates *et al.* (1992).

Standards for static mass spectrometry

The newly developed static carbon mass spectrometer (MS86) can analyse picomole quantities of carbon to permil precision. This poses a problem for the preparation and transfer of standards; procedures must be capable of producing extremely pure gas even in small amounts. The standards were therefore prepared individually each time they needed replacing, rather than stored in glass bulbs. They were produced by combusting diamond chips, of 300-700μg in mass, which liberates very pure CO_2. An aliquot of the CO_2 produced was measured by dynamic mass spectrometry to 0.05‰ precision and the rest transfered to MS86 (~15μg to the fixed volume bulb and 100-150μg to the variable volume). Typically, a synthetic diamond ($\delta^{13}C$ =~-20‰) was used in one standard bulb and a natural diamond ($\delta^{13}C$=~-10‰) in the other for comparison.

The reference gases were checked independently by running standard samples. Three have been used for this purpose:

i) A $CaCO_3$ sample (PSU 2), whose $\delta^{13}C$ had been measured by phosphoric acid dissolution (Grady, 1983), was pyrolysed and the released CO_2 measured. This sample had the advantage of using up no oxygen in the low oxygen pressure system and so relatively large samples could be measured. The carbonate gave reproducible isotopic ratios for samples of ~60μg in mass (figure 2.3), but on 3 three occasions smaller sized samples (<10μg) were used. In all these experiments, the results obtained varied randomly by up to 5‰, or about 10σ, suggesting that the powder was not homogeneous on this scale.

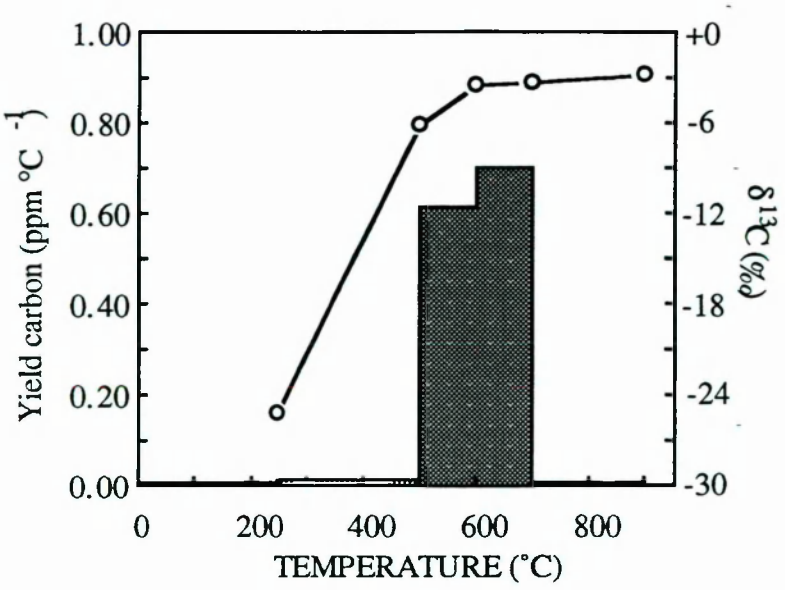

Figure 2.3 Stepped combustion of a $CaCO_3$ sample PSU 2. Bulk $\delta^{13}C$ = -3.6‰, *c.f.* bulk measured by Grady (1983) for the same sample: $\delta^{13}C$ = -3.5‰. The yield of this experiment was 13.3%C compared to the expected 12.0%.

ii) An industrial 5μm diamond powder, analysed several times by Boyd (1988) to give a mean $\delta^{13}C$ of -9.63 (σ= 0.06)‰ was also used as a standards check; for this technique it was important to use extremely small aliquots (~3μg) because of the low oxygen pressure of the extraction system. Thus yield data were subject to large errors using this system.

iii) Because of the difficulties in weighing small samples accurately, 50μm whole rock Allende was also analysed (Yates, 1992). By measurement on several mass spectrometers by half a dozen operators, it was found to be very homogeneous and have a low carbon content (0.25 wt %C), allowing larger aliquots to be used. In addition, this sample is free of organics and interfering species that make the measurement of some other meteoritic samples difficult. It therefore makes a suitable intralab standard.

Blanks

The stepped combustion experiments described in this thesis were usually performed at high resolution (25°C steps for the carbon work). Although a large number of blank stepped experiments have been performed by Yates (1992) these were only in 100-200°C temperature steps; in particular, the high temperature regime (600 - 1200°C) was usually covered in a single step. An investigation was therefore undertaken to find the dependence of the total blank on temperature step size, over the high temperature regime which was vital to the combustion of silicon carbide. Two experiments using baked out platinum buckets, identical to the containers used to contain samples, that had been

combusted at 500°C overnight to simulate the low temperature stage of the stepped combustion, were performed. The first experiment used temperature increments of 50°C and the second 25°C. It was found that the 25°experiment produced a lower yield per step than the 50° one, although the yield per °C was similar in the two experiments (figure 2.4). This may reflect the increased number of consecutive steps performed rather than a strict temperature related dependence. After 1000°C the blank appeared to marginally increase in both experiments, perhaps because because the bucket was baked out to only 1000°C, although the system contribution may also increase above this temperature (Yates, 1992). The source of the "blank" carbon is believed to be a mixture of CO_2 released from the extraction system and carbon associated with the platinum, as surficial dust and organic deposits and as carbon dissolved in the metal (*e.g.* Yates *et al.*, 1992). Blank corrected data in this thesis have been adjusted according to these data.

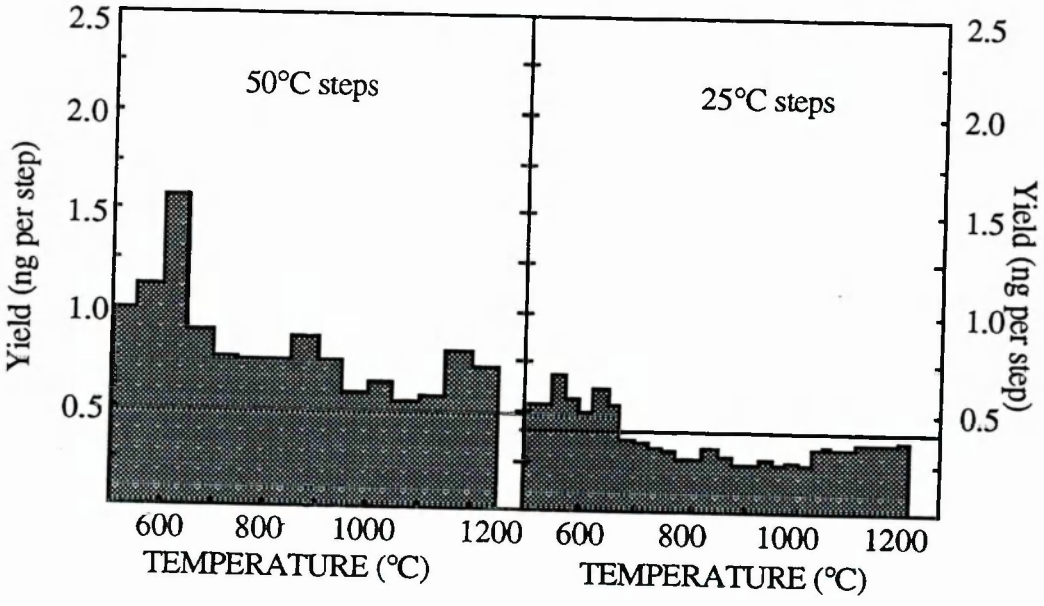

Figure 2.4 Blank stepped combustion experiments for the temperature regime 500-1200°C. The scales are such that the yield per step (rather than per °C) can be compared. The lines on the diagram indicate the beginning of day system blank (0.5ng for the 50°C step experiment and 0.4ng for the 25°C step experiment). Note that the carbon yield for the 25°C step experiment fell below that of the system blank, after several steps had been performed. Total carbon yields were 21.8ng for the 50°C step combustion and 29.1ng for the 25°C step combustion.

The Capillary aliquotting system

The system for aliquotting reference gas described by Carr *et al.*. (1986) uses a variable volume aliquotter to meter out an amount of reference gas that will give a major ion beam intensity in the mass spectrometer matched with that of the sample gas. Although this system has worked well for manually operated extraction lines, the automated equivalent is cumbersome, time consuming and expensive. A new system for aliquotting reference gas has therefore been developed.

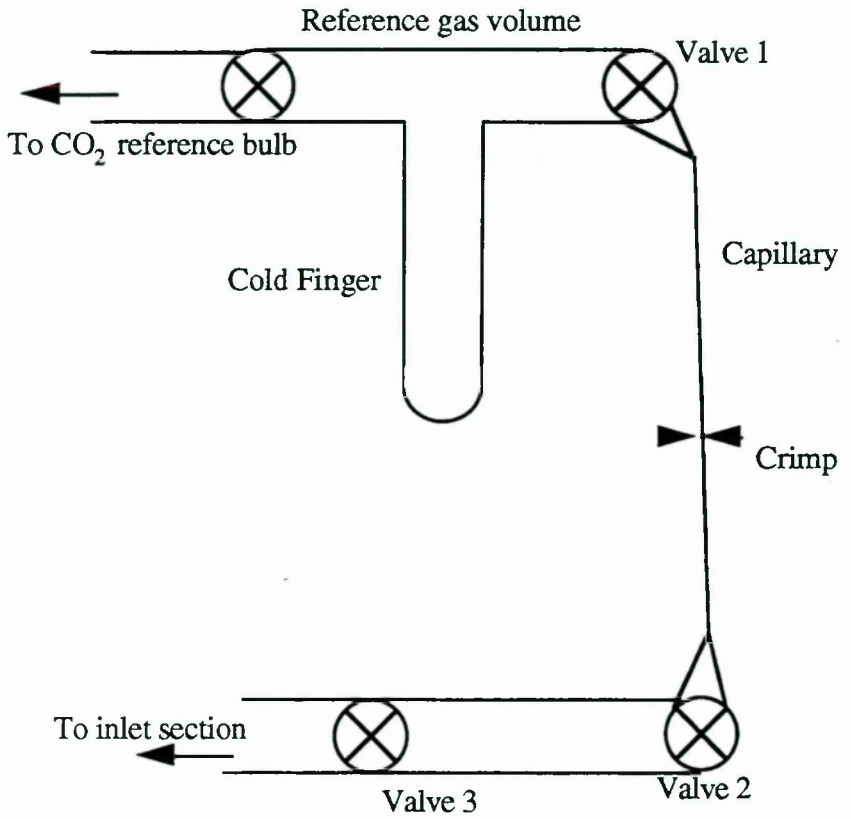

Figure 2.5. The capillary aliquotting system

This new system, shown schematically in figure 2.5, uses time, rather than aliqotter volume, as the variable factor. Reference gas at a high pressure (about 100 torr) is bled down a capillary tube of 60cm in length that has been crimped to restrict the flow to a measured rate of around 10 ng or less per minute. At this stage valves 1 and 2 are open and valve 3 is shut, to allow collection of the gas into the small reservoir volume. After a

calculated amount of time - proportional to the amount of gas needed - valve 2 is shut and valve 3 opened, to expose the gas to the inlet section to be fed to the mass spectrometer. An extremely simple prototype, using simple, cheap materials was tested on the static carbon mass spectrometer described by Carr *et al.* (1986). It was a system made of pyrex using Youngs valves (address) with a metal capillary tube that was bonded to the glass with Aqueson black wax.

The high pressure of reference gas ensures that there is no isotopic fractionation in the capillary bleeding process (Halsted and Nier, 1950) and that the gas flow rate does not significantly decay, over the time scale of a few days. Indeed, it can be calculated that for an original flow rate of 10ng per minute, the half life of the gas in the gas volume is around one and a half years. To demonstrate the constancy of the flow rate over the timescales of an average experiment, an experiment was performed in which gas was bled from the capillary for periods of up to 20 minutes and the total gas released was collected and measured in a capacitance manometer. The results, shown in figure 2.6, indicate a good correlation between the flow time and gas collected. The data were not collected cumulatively, but rather each point represents a separate bleed experiment. The bleeds were performed over several days and hence the linear relationship indicates that there was no noticeable depletion of the standard gas pressure over that time.

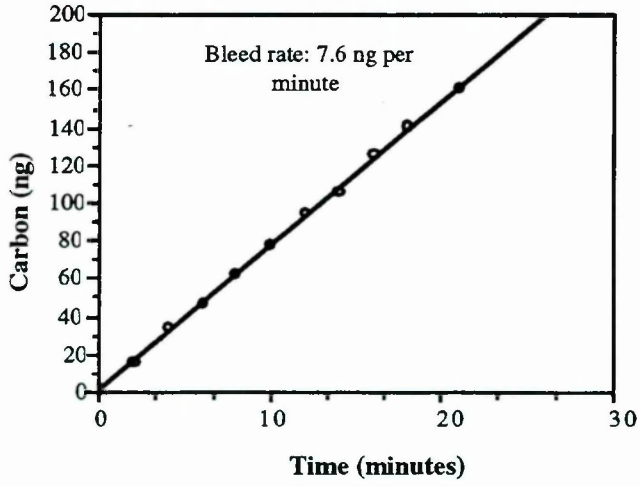

Figure 2.6. The relationship between bleed time and the yield of carbon dioxide collected.

The system was then tested by allowing the bled standard gas into the mass spectrometer, using bleeding times of 0 to 2 minutes which gave 0 to 10 ng of gas. A comparison of the

scatter in the major intercept from the variable volume and capillary methods was similar (micrometer method gave a correlation coefficient of 0.92 and the capillary method a correlation coefficient of 0.94; figure 2.7), and so the data scatter can be assumed to be due to machine imprecisions.

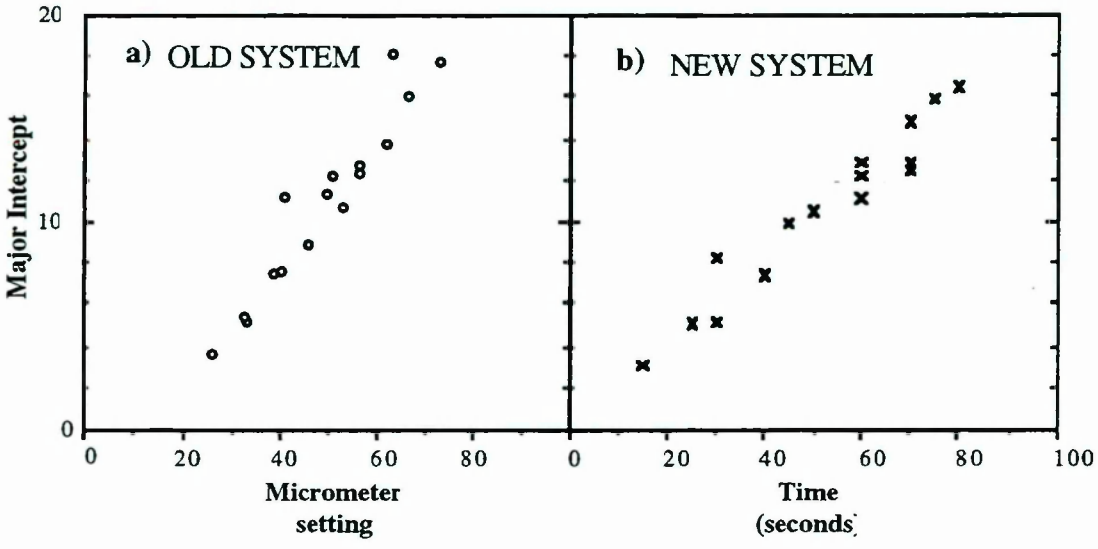

Figure 2.7. (a) The micrometer reading vs. major intercept (a measure of the ion beam current of the mass spectrometer) of the variable volume system and (b) capillary data of bleeding times from 0 to 100 seconds versus major intercept.

The isotopic fractionation involved in the capillary aliquotting was then investigated. An aliquot of standard gas was split, with a proportion frozen into the variable volume standard bulb and the rest into the capillary volume. Aliquots of the two reservoirs were then run against each other, and the difference in isotopic composition between the two gases was recorded. It was found that the mean of several isotopic deviation measurements was close to 0‰, indicating that there was little fractionation involved in the capillary procedure (Figure 2.8a). The mass spectrometer used in this test is however, rather more imprecise than the one for which this system was designed and so further tests will be necessary to investigate if a small fractionation effect is involved. Zero enrichment experiments (in which capillary aliquot was run against capillary aliquot) shows a similar data spread to variable volume zero enrichments. The mean deviation from zero was 1.8‰± 1.6 (n=19) for the micrometer technique and 2.1‰± 1.6 (n=22) for the capillary technique, demonstrating that the two systems are approximately equally reproducible (figure 2.8b). Again, the poor statistics affordable on this instrument demonstrate the need for this technique to be tested thoroughly on the more precise mass spectrometer for which it was designed.

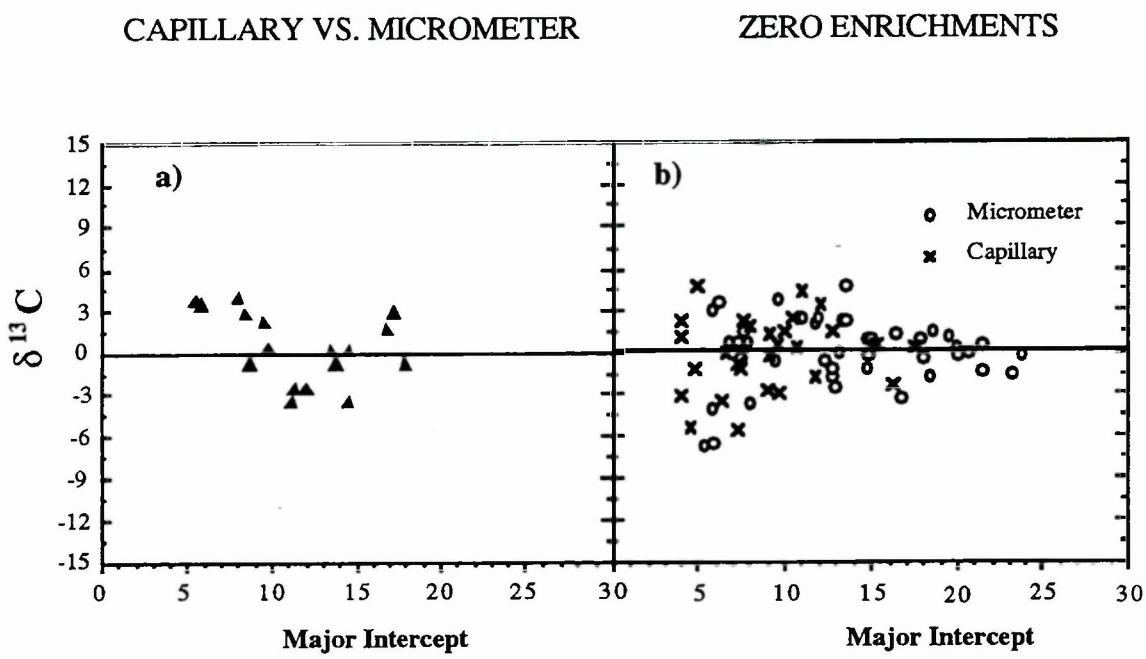

Figure 2.8: (a) Runs of capillary system aliquots against variable volume aliquots do not show any fractionation. (b) Zero enrichments of capillary gas against capillary gas give similar results to those of variable volume gas against variable volume gas. A major intercept of 30 corresponds a mass of approximately 15ng carbon.

An unexpected result was obtained when the errors for the zero enrichment experiments were compared. When fresh reference gas is used in both reference volumes the calculated errors on individual runs are consistently lower for the capillary method, at any major intercept value (*i.e.* the scatter of separate measurements during a single run is smaller); the mean error for the capillary technique was 1.2‰, over a spectrum of major intercept values, whereas the micrometer technique gave a mean error of 1.7‰ (figure 2.9). This could be because the gas pressure in the capillary reservoir is much higher than that behind the variable volume and so the effect of contamination is less noticeable. Also, the larger surface area of the old reference bulb may allow it to become contaminated more quickly.

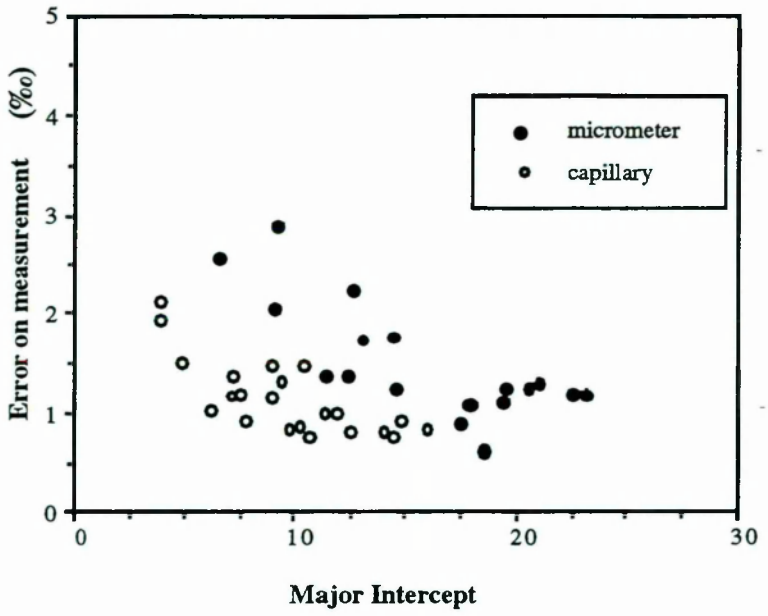

Figure 2.9. A comparison of the errors produced by the two aliquotting methods

The capillary system has been tested during sample runs. An artificial diamond formed by carbon vapour deposition (CVD residue 151) underwent two stepped combustions using first the variable volume then the variable time methods.The resulting bulk isotopic data obtained by the two experiments agreed to within 0.25 ‰; the experiment performed using the micrometer gave a bulk $\delta^{13}C$ = -60.5‰, and using the capillary, -60.7‰.

There are three main conclusions that have been drawn from this pilot study of the capillary aliquotting system:

1) The relationship between the amount of gas accumulated and allowed bleeding time is linear.

2) Bleeding the gas through the capillary appears to cause no isotopic fractionation.

3) The system is reasonably simple to use, and works well within the limits of this static mass spectrometer (the triple collector); although it must be remembered that the automatic machine this system was developed for is rather more precise. Before this technique replaces the variable volume system it is important that it is tested on a more accurate machine, to assess its reproducibility more thoroughly.

The capillary aliquotting method is likely to be preferable over the variable volume system

for automated machines where the timings can be controlled by computer. As a result of this pilot study, a fully automated system was built for a new nitrogen mass spectrometer (funded by the Paul Instrument Fund of the Royal Society). Unfortunately, the new instrument was not completed in time for it to be used for this work described in the thesis. Some preliminary data acquired by the new system however suggests that its performance is adequate for high sensitivity mass spectrometry (I.A. Franchi, *pers comm*).

2.2 NITROGEN AND C/N RATIOS

Introduction

A major thrust of the work in this thesis addresses the question of nitrogen abundance in meteoritic diamond (chapter 3). Very early in the study, it was deemed necessary to adapt the nitrogen extraction line to allow the measurement of carbon dioxide from diamonds simultaneously with the nitrogen released during the experiments. The system used for conjoint carbon and nitrogen measurement has been adapted from that of Boyd *et al.* (1988) that was designed for the analysis of nitrogen only; to measure the carbon yield of small samples, a capacitance manometer was incorporated. Measurement of C/N values simultaneously rather than on separate aliquots involving different instruments eliminates (i) inaccuracies due to weighing errors (ii) comparisons made on experiments performed using different step sizes and timings (iii) errors due to poor temperature control and (iv) differences in combustion rate due to variation in oxygen pressures.

The importance of this new procedure is observed in the discussion of nitrogen content in diamonds in Chapter 3, but the conjoint measurement also has uses in other applications, for example it allows: (i) the form of a nitrogen carrier to be constrained (carbonaceous or non-carbonaceous) (ii) characterisation of components to be more fully made and (iii) differences in C/N ratios between samples to be reliably measured.

2.2.1. Description of the extraction line

The extraction line used for the separation and purification of CO_2 and N_2 gas is shown schematically in figure 2.10. The samples were loaded into the combustion vessel where they could be heated by the furnace, either without oxygen, or, if the CuO finger was heated, in a pure oxygen atmosphere. They were then step or bulk combusted using the protocol of Boyd *et al.* (1988). After each step, the gases present in the combustion section were frozen to the molecular sieve in the clean-up section for two minutes, which was then isolated and heated to 180°C to release trapped N_2 and CO_2. The clean-up CuO was heated to 850°C for 5 minutes to ensure full oxidation of CO to CO_2, and then cooled to 650°C and 450°C for 5 minutes each to resorb all the excess oxygen in the section. Simultaneously, the hot Pt finger catalysed the breakdown of nitrogen oxides to their constituent elements, and the variable temperature cold finger (called a "cryotrap" herein) cooled to -175°C to freeze all the condensible gases (CO_2 and H_2O). After the clean up, the nitrogen was transferred to the mass spectrometer and the clean up section cryotrap warmed to -145°C to release any further condensed CO_2, which was also cryogenically transfered to the manometer. In this way, a simultaneous carbon yield measurement could

be made for each step in addition to obtaining nitrogen data. For some samples with high C/N ratios a cryotrap in the combustion section could be cooled to -173°C (after Boyd *et al.*, 1988) during the sample combustion stage to trap out some of the CO_2 produced. After transfer of products that remained uncondensible at -175°C at the end of each step, the combustion section cryotrap was heated to -145°C to release its CO_2, which could be frozen over to the manometer. The CO_2 from the clean up stage was then added to this gas to calculate the total CO_2 released. The use of the combustion section cryotrap was however found to be unsuitable for most samples - see section 2.2.4.

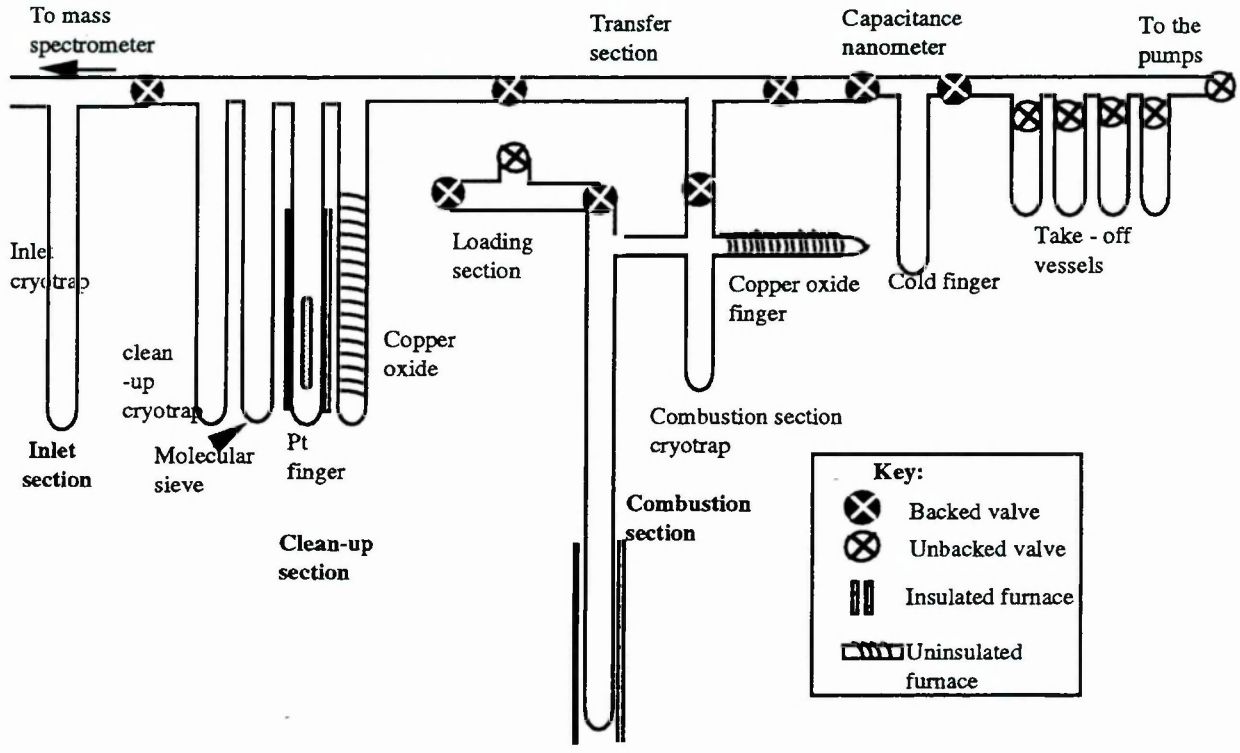

Figure 2.10: The nitrogen extraction line adapted for carbon measurement.

The individual measurements of carbon and nitrogen use slightly different preparative protocol. In particular, the CuO from the combustion section in the nitrogen extraction line is left at 450°C overnight (Franchi, 1988), with the combustion section open to the pumps, to ensure that the vacuum is as low as possible in this section. In contrast, the carbon isotope protocol involves the heating of the CuO to 850°C overnight, with the combustion section closed to the pumps. This ensures the combustion of carbon containing contaminants such as pump oil which could otherwise become absorbed onto the CuO. An experiment was therefore undertaken to determine which of these two

approaches would be the most suitable for conjoint nitrogen /carbon measurement. On consecutive days, the combustion section was left at 450°C overnight and then at 850°C overnight, and a stepped combustion with an empty combustion section performed during each day. The results (figure 2.11) were surprising: when the CuO was at 850°C overnight it gave lower carbon blanks (as expected) and also lower nitrogen blanks. This protocol is thus now used for all the conjoint C/N measurements.

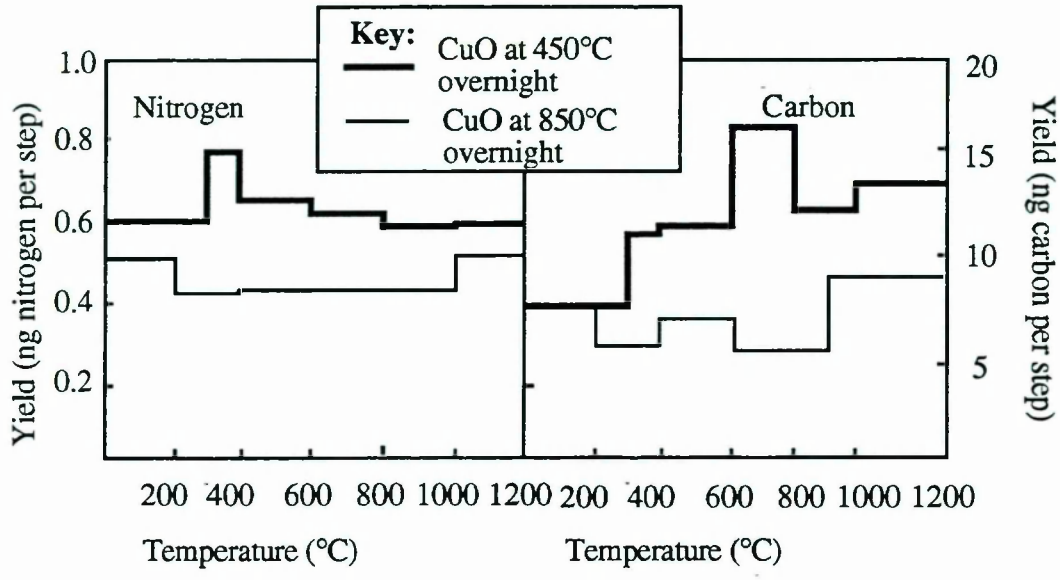

Figure 2.11: A comparison of carbon and nitrogen blanks with the CuO at 450° and 850°C overnight.

2.2.2. Platinum bucket preparation

Conjoint analysis of carbon and nitrogen poses a problem for the preparation of the platinum buckets used as sample containers. The procedures currently used for carbon and nitrogen individually are no longer applicable. Conjoint work typically involved combustion of each sample up to 550°C on the C/N system followed by transfer to a high sensitivity carbon machine for high temperature combustion to 1250°C. Thus, the buckets had to be cleaned sufficiently so that they released as little as possible of both carbon and nitrogen during the entire combustion experiment. The cleaning system described by Franchi (1988) for nitrogen is unsuitable for carbon because: i) the combustion time is too small (around half an hour) and ii) the method is time consuming, involving the use of ~14 hours of a pumping system, which makes it unfeasible to prepare the platinum buckets individually for each run. Instead they are made in bulk and then stored in clean room conditions. This greatly increases the risk of carbon contamination from organic

material and dust.

Similarly, buckets prepared specifically for carbon combustion experiments are unsuitable for nitrogen experiments. The cleaning protocol (Ash, 1990) involves the combustion of the buckets in sealed tubes at 1000°C for 10 hours followed by cooling to 600°C to resorb the oxygen onto the CuO; the tubes are cooled under vacuum. This procedure gave high nitrogen blanks (Franchi, 1988), possibly because vacant sites on the metal absorb nitrogen when the bucket was opened to the air. To adapt the Ash method for joint carbon and nitrogen use, after combusting at 1000°C overnight, the sealed tubes were quenched to room temperature so that oxygen resorption onto the copper oxide was prevented. The buckets were allowed to cool in an oxygen rich atmosphere so that oxygen filled the vacant sites on the platinum, thus preventing the nitrogen in air from sticking to its surface. This is a very simple technique which allows the buckets to be prepared individually for each run.

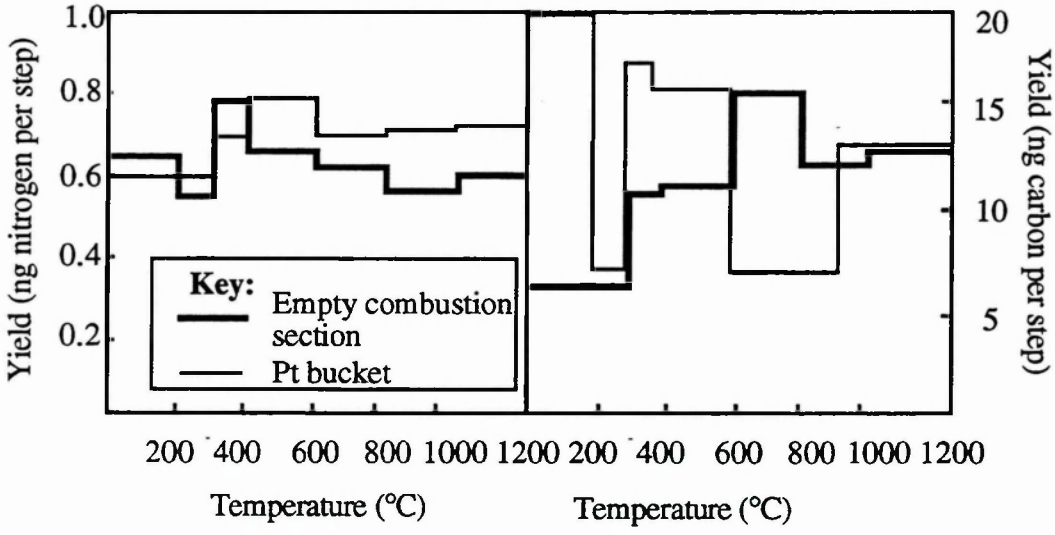

Figure 2.12: Nitrogen (left) and carbon (right) blank stepped experiments for Pt buckets baked out as above.

It can be seen from figure 2.12 that the nitrogen yields from platinum buckets baked out according to the new protocol are barely higher than for an empty combustion section (system blank). It is more difficult to assess the carbon blank using this technique as the system blank for carbon was rather high, but blank experiments using these buckets on a more sensitive carbon instrument have been described in section 2.12. The carbon blank of the nitrogen extraction line reduced gradually to around 2ng per step after several

weeks of the combustion section CuO being left at 850°C overnight.

2.2.3. Accuracy of C/N measurements

Carbon measurements. The carbon yield during sample combustion is measured by a capacitance manometer, which has been calibrated from two other similar instruments. Diamonds were weighed to ± 0.5 μg accuracy on a micro-balance, combusted completely using the bulk protocol of Grady (1983), measured on a manometer and a conversion factor calculated (figure 2.13). Aliquots of gas were then measured, transfered to the nitrogen extraction line and the manometer voltage recorded, to obtain a conversion factor for that instrument. As a calibration check, samples were then transfered to a third manometer which had been independently calibrated; the two conversion factors obtained this way were the same to three significant figures.

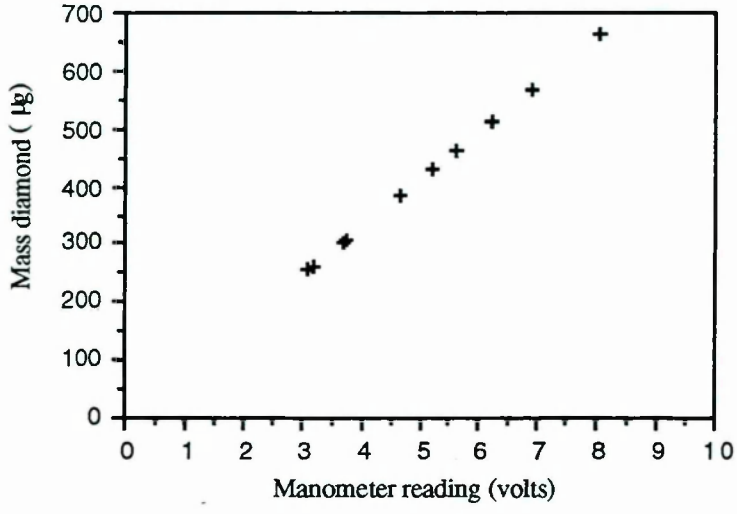

Figure 2.13 Calibration of the capacitance manometer. Diamond chips were weighed (mass indicated on the ordinance axis) and then combusted, and the evolved CO_2 frozen to the capacitance manometer and the pressure recorded.

Diamond rich residues were then oxidised using both the combustion section of the nitrogen extraction line, and the carbon extraction system of the dynamic carbon mass spectrometer, to allow a comparison of yields obtained by the two stepped combustion methods to be made. The carbon yield obtained using the nitrogen extraction line was found to be 91(±4)% of that from the carbon extraction system (figure 2.14). This result is in good agreement with results from R.D.Ash (*pers comm.*) who, using the conjoint C/N system, obtained carbon yields that were 91% of those obtained by static mass spectrometry. The low carbon yields indicate that a small loss of CO_2 may occur due to

gas retention in the molecular sieve.

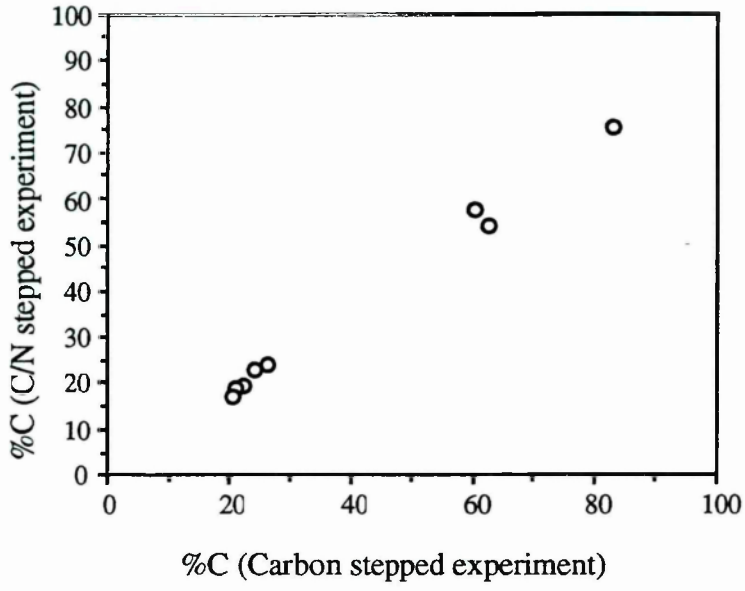

Figure 2.14. Comparison of yields obtained by carbon stepped combustion of diamond residues to the results from carbon and nitrogen conjoint analysis.

Nitrogen measurements. After cryogenic purification, nitrogen yields were measured by measuring the major intercept of the ^{14}N beam in the mass spectrometer. Calibration for this system was provided according to the protocol of Boyd and Pillinger (1991) using standard ammonium sulphate which has a nitrogen content of 21.2%. As this procedure evolves more nitrogen than can easily be handled, and is rather time consuming, in the future routine checks could be made using a new system which utilises a solid solution of ammonium sulphate in rubidium sulphate (Boyd and Pillinger, 1991).

2.2.4. Reproducibility of C/N measurements in natural terrestrial diamonds

a) Bulks

A homogeneous diamond powder (4-8 μm) was used to test the reproducibility of the system. Samples varying in mass from 7μg to 110μg were weighed out and combusted, first at 400°C for half an hour to remove organic contamination and then for one hour at 900°C to burn the diamond. For the last fifteen minutes of combustion, the combustion

section cryotrap was cooled to -173°C to trap out some of the CO_2.

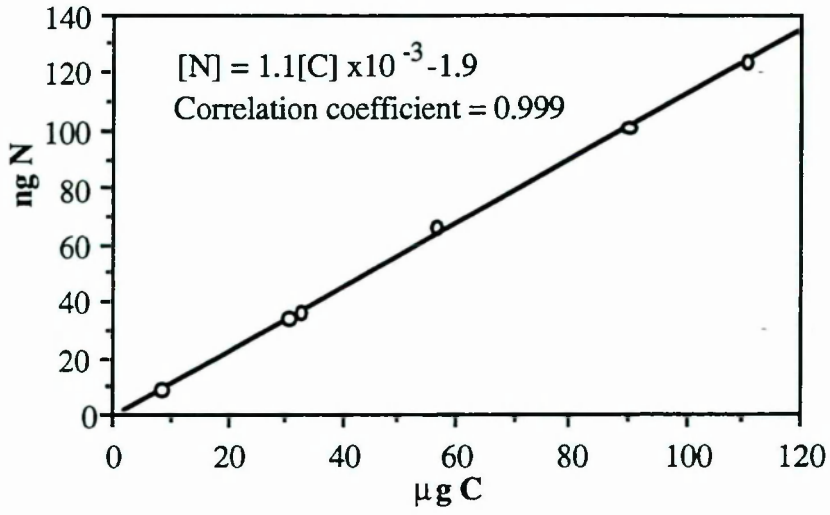

Figure 2.15: Yields of carbon and nitrogen measured for different sized aliquots of Ia diamond powder. The good correlation indicates the homogeneity of the powder and the reproducibility of C/N measurements.

The standard diamond C/N[1] ratio measurements (figure 2.15) had a mean value of 921 and a standard deviation of 32 (±3.5%), demonstrating that the C/N measurements are reproducible for a wide range of sample sizes. Interestingly, the line did not pass through the origin but intersected the abscissa at -1.9 ng nitrogen, suggesting that a finite amount of about 2 ng of nitrogen is frozen down with the carbon dioxide in the cryotrap. This would become important for very small samples and samples with a very high C/N ratio.

b) Stepped combustion

Because much of the work in this thesis involved high resolution stepped combustion, the terrestrial diamond powder was also analysed by stepped combustion. Firstly, the combustion was performed without using the combustion section cryotrap, so that all the carbon dioxide and nitrogen released were transfered to the clean-up section at the end of each step, where the CO_2 and N_2 were separated and quantified. The total carbon oxidised and total nitrogen released were summed and a value for the C/N ratio of the whole experiment calculated. The $\Sigma C/\Sigma N$ ratio lies very close to the values obtained by the bulk technique (see table 2.1 and figure 2.16). In a second experiment using identical step temperatures and a similar sample size, the combustion section cryotrap was kept cool throughout the experiment. During the combustion it was held at -170°C and then, at

[1]Herein, C/N ratio are recorded by mass rather than as atomic ratio values.

the end of each step,after the nitrogen had been transfered to the clean-up section, heated to -140°C to release the carbon dioxide. The cumulative yields of carbon and nitrogen were calculated by summing the yields from individual steps. The ΣC/ΣN ratio for the second experiment is higher than that obtained by the other techniques; in fact the nitrogen yield was only 80% of that released by the first stepped combustion technique. A possible explanation is that 2 ng nitrogen is frozen "in" the combustion section cryotrap and lost at each step; this would make a bigger difference for stepped combustion experiments than bulks for any one sample size.

Experiment	ng N	µg C	C/N
Bulk	97	88	913
Bulk	120	109	904
Bulk	30	28	935
Bulk	32	31	968
Bulk	62	55	885
Bulk	5.6	7.1	1271
Stepped (no cryotrap)	29	31	1116
Stepped (cryotrap)	27	38	1417

Table 2.1: Comparison of C/N ratios measured for the same terrestrial diamond sample by different techniques.

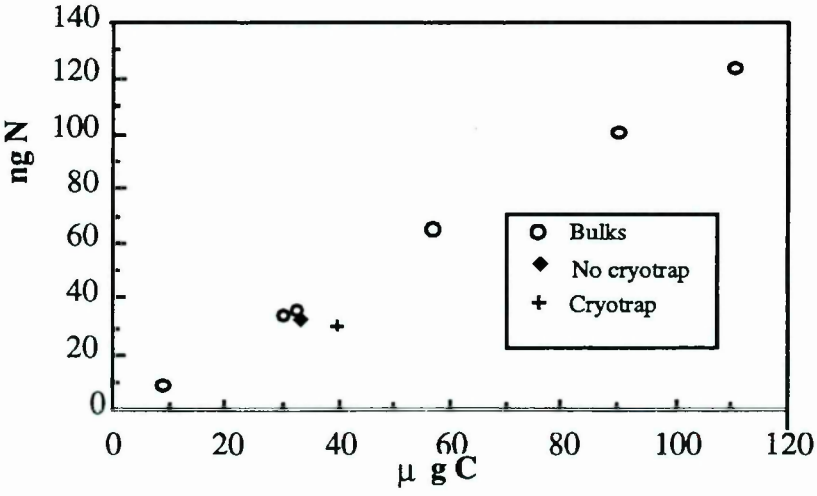

Figure 2.16: Stepped analysis of diamond powder compared to bulk values.

2.2.5 Analysis of other samples

The "combustion cryotrap problem"

The use of the combustion section cryotrap as described by Boyd *et al.* (1988) for the combustion of diamond powders appears to produce accurate C/N measurement for single step combustion. With large terrestrial samples, it is necessary to trap out some of the CO_2 before the clean-up stage, particularly if the C/N ratio is very high. The use of the combustion section cryotrap had therefore become an entrenched part of the nitrogen extraction procedure long before the experimental work on this thesis began. However, as has been shown in 2.2.4., the cryotrap causes problems for diamond during stepped combustion because of trapping of nitrogen in large quantities of CO_2. For types of diamond other than terrestrial Ia (in which the nitrogen atoms are present in pairs; Evans, 1976), the problem can be even more severe as nitrogen gas is not the only species evolved on combustion, but condensible nitrogen containing species are also produced.

This problem can be demonstrated by the experiment on diamond from the carbonaceous chondrite Allende shown in figure 2.17. The sample was combusted as in an ordinary stepped combustion, with the combustion section cryotrap kept at -173°C until 530°C, when most of the diamond had burned and the carbon yield was beginning to decrease. The sample was then torched off, *ie.* completely removed from the system, with the cryotrap remaining at -174°C, and the gas released during the glass blowing pumped away. The experiment was then continued, with the combustion section cryotrap still cool. There was no extra nitrogen gas released for three more steps. At 600°C, the temperature of the reaction vessel was kept constant whilst the temperature of the combustion section cryotrap was warmed to -140°C, which liberated all of the carbon dioxide released during the experiment, and some nitrogen gas. The combustion cryotrap was then further warmed to room temperature, which released no further carbon dioxide but a significant amount of nitrogen - approximately doubling the total nitrogen yield of the experiment. Note that this gas is released at temperatures higher than the CO_2 and so cannot be a CO_2 clathrate type condensate. The gas was similar in isotopic composition to the meteoritic diamond nitrogen demonstrating that it was not any form of contamination but undoubtedly originated in the meteoritic sample, and was released not as molecular nitrogen (boiling point -193°C) as it is condensible at -173°C. The nitrogen must therefore be present as another species - possibly an oxide which decomposes if given sufficient time in the presence of reagents in the clean-up section. The possibility of nitrogen condensing in the cryotrap could give rise to serious overestimates of C/N ratios in some specific samples.

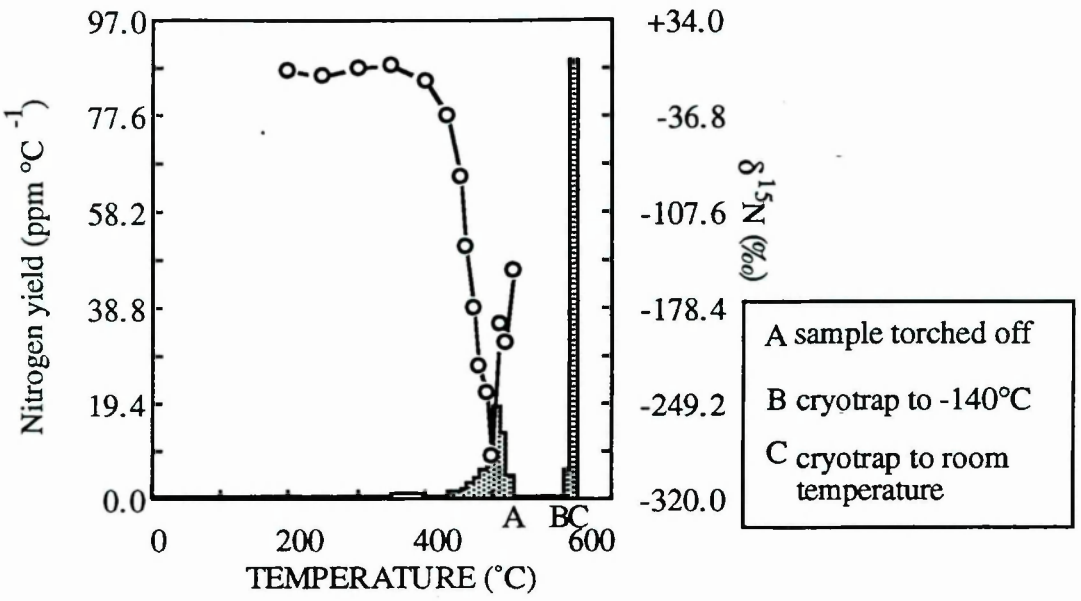

Figure 2.17: An experiment on the Allende meteorite to demonstrate the limitations of the combustion section cryotrap (see text)

Samples containing condensible nitrogen

To investigate if the production of "condensible nitrogen" is a feature unique to meteoritic diamond, other terrestrial diamond types were investigated. The samples (type Ib synthetic and C.V.D. diamond) were combusted at temperatures just high enough for complete combustion (this value depended on the diamond size and type). The combustion section cryotrap was held at -173°C during both experiments. During the analysis first non-condensible nitrogen gas was transfered to the clean up section and measured. Then the combustion section cryotrap was warmed to about +50°C to release completely the trapped carbon dioxide; nitrogen present in the cryotrap was cleaned and measured. The proportions of nitrogen that condensed into the combustion section cryotrap and remained uncondensed are shown in figure 2.18. The samples chosen for this study were a 4-8μm Ia diamond powder, the diamond from the Allende meteorite, Ib diamond chip and a diamond- like carbon sample that was produced by a CVD process.

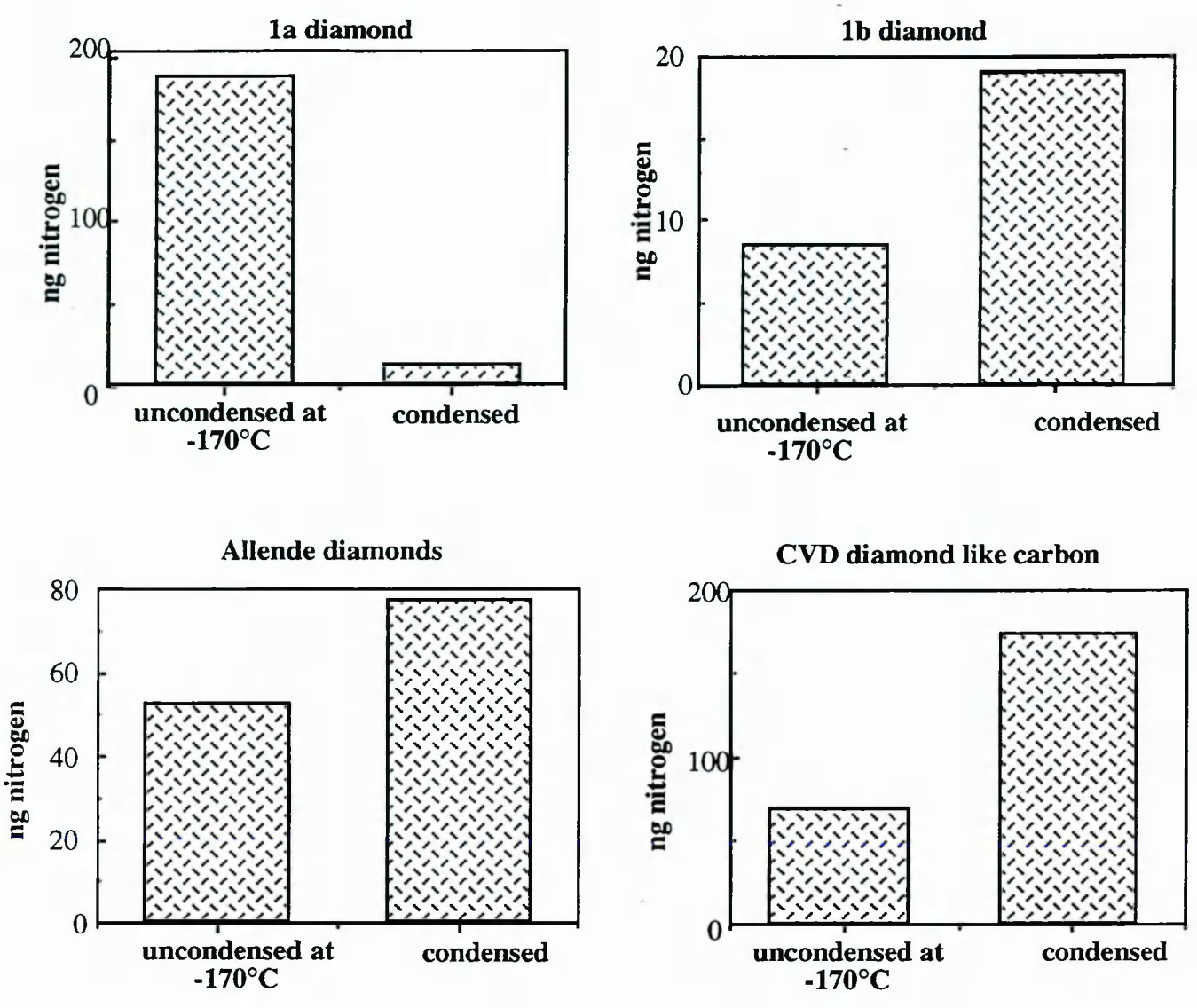

Figure 2.18: Comparison of the proportions of "condensible nitrogen" produced in various diamond types.

The proportion of nitrogen that remained uncondensed at -170°C was very high in the Ia diamond powder compared to the other samples. The Ib chip produced the most condensible nitrogen, with replicate experiments using different masses giving similar proportions of trapped and untrapped nitrogen. The CVD and Allende samples show greater similarity to the Ib diamond than to the Ia diamond, implying that the nitrogen is bound in a similar way to that in Ib diamond. The major difference between Ia and Ib diamond is the aggregation state of the nitrogen; Ia diamonds are believed to have matured at high temperatures allowing diffusion and subsequent aggregation of the nitrogen within the diamond lattice (Evans, 1976). Thus condensible nitrogen could be a result of single substitution that results in the formation of species other than N_2 on combustion.

It is likely that the CVD sample has not experienced high temperatures for a sufficiently long time for the nitrogen it contains to diffuse around the lattice and pair up with another nitrogen atom to form Ia diamond, but instead remained mostly as Ib (nitrogen unpaired) diamond. Similarly, it seems that the meteoritic diamond also contains nitrogen in an unaggregated state. Indeed, for the very small meteoritic diamonds, nitrogen degassing rather than pairing would probably be the preferential process during metamorphism (this will be dealt with more quantitatively in chapter 3). However, the possibility that the nitrogen in the meteoritic residue remains condensed because it reacts with other phases present (such as surficial hydrogen, Lewis *et al.*, 1989) cannot be ruled out.

Although the nitrogen release from the diamond is not well understood it seems clear that the proportion freezing down in the cryotrap is in some way dependant on the nitrogen substitution in the the sample. After more study, the combustion cryotrap could become a useful tool in identifying the bonding type of nitrogen in meteoritic samples; *e.g.* it is not yet known whether diamonds from different meteorites contain the same amount of trapped and untrapped nitrogen. This technique has already been used tentatively by Wright *et al.* (1992) to suggest that the fluorocarbon xylan contains at least two isotopically distinct nitrogen components, one that forms N_2 on combustion and one that forms condensible products.

Technique for the analysis of samples other than Ia diamond

Following the recognition of the cryotrap problem which must lead to inaccurate C/N ratios this facility was abandoned from the experimental procedure. The absence of the cryotrap, however, makes the experiment more tricky to perform. Problems encountered when the combustion cryotrap is not used include:

1. Complete separation of carbon dioxide from nitrogen is more difficult. Usually the clean up section cryotrap needs to be a few degrees cooler than usual to prevent carbon dioxide from reaching the mass spectrometer. The ideal temperature is dependent on the C/N ratio of the sample.

2. The potential for carbon loss exists from carbon dioxide sticking to the molecular sieve. To minimise the risk it is critical to ensure that the molecular sieve is heated to at least 180°C during the clean -up time.

3. The sample size must not be too large. The clean-up procedure is only effective if the sample contains less than 50μg of carbon (S.R. Boyd, *pers. comm.*). During stepped

combustion carbon abundance is not a critical problem because the CO_2 release is spread out over a range of temperatures, and so this proviso is usually met.

Even when these conditions are satisfied the reproducibility of Ia diamond powders cannot be obtained for samples that contain condensible nitrogen. However their C/N ratio can be estimated to within ~ 20% (see figure 2.19), an improvement on the separate system method of measuring C/N ratios which produce 42% to 25% 1σ reproducibility (see table 2.2) for meteoritic diamond samples.

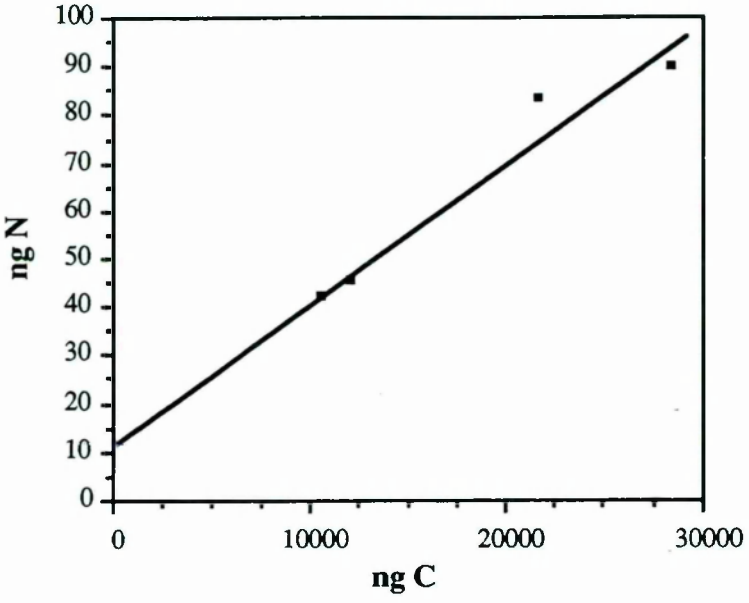

Figure 2.19. Reproducibility of C/N measurements of diamond from the Allende meteorite, without using the combustion cryotrap, using the procedures described above. The data give a mean C/N value of 272 ± 29.5. Also plotted is the best fit line.

Measurement	Separate aliquots method	Conjoint C/N method
1	2022	3752
2	1046	4613
3	2057	4289
4	4075	2281
5	2846	2729
Mean	2409 (σ=42%)	3533 (σ=25%)

Table 2.2: Comparison of the reproducibility of the C/N data of diamond from Allende obtained by the separate aliquots method (using separate carbon and nitrogen instruments to acquire data), and the conjoint method described here (Data from stepped experiments only is included for each experimental technique). Data from separate aliquots method from R.D. Ash, *pers. comm.*

Table 2.2 indicates that the separate aliquots method can give C/N data in serious error; these data includes yields that have been summed for each element over the diamond combustion range and so the additional (and more significant) error for the separate aliquots method of non-comparable temperature scales is excluded. The mean values are also different using the two techniques; this is probably because the separate aliquots method data were acquired using the combustion section cryotrap and so these data may have been subject to some nitrogen loss.

2.3 SAMPLE PREPARATION BY ACID DISSOLUTION

For this work, the resistant phases were separated from bulk samples by acid dissolution. To allow comparisons to be made between meteorite types, the same protocol was used for each meteorite. The samples were prepared by acid dissolution by J.W. Arden, of the University of Oxford. Typically, the meteorites were first etched in HF/HCl to remove surficial contamination, then crushed and dissolved in HCl/HF (to dissolve silicates), CS_2 (to dissolve sulphur) and $Cr_2O_7$2- and $HClO_4$ (to remove organics, amorphous carbon and graphite). A more detailed account of the procedures used can be found in Ash (1990) and the exact history of individual samples used in this work is listed in Appendix 1. All the samples discussed in this thesis have been treated in this way (except some specified donated residues), but in addition some extra treatments were occasionally found to be necessary:

i) Separation of diamond by ammonia or NaOH colloid.

The nanometric meteoritic diamond crystal apparently has acidic groups on its surface (Lewis *et al.*, 1989), and so forms a colloid in weak basic solutions. For experiments in which the purity of the diamond sample was important, the residue after $HClO_4$ treatment was treated with weak ammonia or sodium hydroxide solution (pH ~8+) to separate the diamond from the rest of the acid resistant material. Whereas ammonia was preferred by Tang and Anders (1988a), in this work sodium hydroxide was preferentially used because nitrogen containing components were considered a potential contamination source.

ii) Concentrated NaOH solution

Silicon carbide is known to dissolve in fused strong alkali solutions (Greenwood and Earnshaw, 1984). To investigate the nature of the high temperature components, residues after $HClO_4$ treatment were exposed to 25% NaOH at 150°C for 16.5 hours to dissolve SiC. This technique worked well with meteoritic SiC (high temperature carbon was removed by this reagent: see chapter 6), although the effect could not be reproduced on (more crystalline?) terrestrial SiC.

ii) Phosphoric acid

Phosphoric acid has been used by some authors (*e.g.* Tang *et al.*, 1988) to dissolve spinel. However, attempts to replicate this technique (by heating the sample at 150°C for

13 hours with H_3PO_4) appeared to affect the combustion temperature of SiC in the meteorite: see chapter 6.

Effect of Acid on Diamond

All the samples discussed in this thesis have been through acid treatments of HCl/HF and oxidising acids. It is important to consider whether the acid treatments in any way affect the diamond they isolate. HCl/HF is unlikely to damage diamond, but strong oxidants are often used as etchants in the diamond industry. The effects of $HClO_4$ and $Cr_2O_7^{2-}$ on terrestrial diamonds was therefore investigated as follows: fine diamond powders were photographed by electron microscopy and their isotopic composition measured. Weighed samples were placed through a similar acid dissolution treatments as the meteoritc samples and restudied. The acid treatment had no effect on either the isotopic composition, surface texture or mass, indicating that the diamond was left undamaged by the dissolution treatment.

CHAPTER 3

METEORITIC DIAMOND ASSOCIATED WITH ISOTOPE ANOMALIES

3.1 Diamonds

The word diamond comes from the greek "adamas" meaning invincible, reflecting the hardness and chemical resilience of the mineral. Today the term seems particularly appropriate to cosmochemists studying the enigmatic meteoritic diamonds, as they appear to be especially resilient to attempts to unravel their history and origins. Diamond is an allotrope of carbon, arranged so that each atom is covalently bonded to four other atoms in a tetrahedral structure, with the electrons hybridised to form sp^3 bonds, each with a length of 0.1545nm. Diamond is the high pressure polymorph of carbon (figure 3.1), although it is possible to form diamond metastably at low pressures, a process that may be of relevance to meteorites, which are generally unlikely to have experienced the high pressures necessary except during transient shock events (see chapter 5).

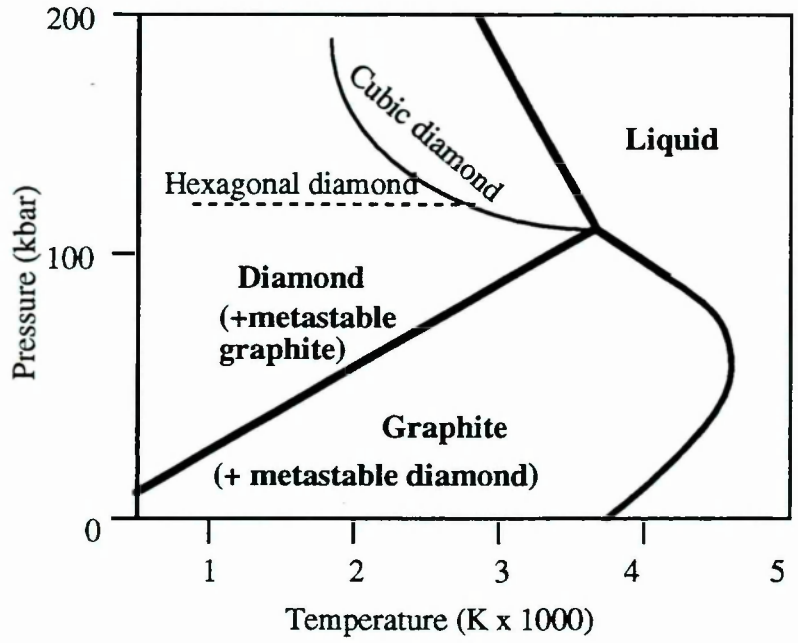

Figure 3.1. The stability field of carbon allotropes (from Hanneman *et al.*, 1967) showing the usual P,T formation regions of hexagonal and cubic diamond.

Cubic diamond is typically formed at high temperatures and pressures, whereas hexagonal diamond, usually associated with shock, is formed independently of temperature.

It has recently been suggested (Badziag *et al.*,1990), that for extremely small crystals (<3nm), diamond may actually be the most stable form of carbon at all pressures as surface tension factors come into effect. Nanometre diamond may therefore be an expected condensate in many environments where C > O.

The presence of diamond in acid resistant residues of extraterrestrial samples: ureilites (Ierofeiff and Latchinoff, 1888) and an iron meteorite (Weinshank, 1889), was first reported over a century ago. Meteorite parent bodies are thought to be no more than ~100km in diameter, and so would not produce high enough static pressures to form diamond in a way analogous to the formation of diamonds on the Earth. It now seems that a number of processes must have been involved in the formation of such meteoritic diamonds. In Canyon Diablo (Lipschutz and Anders, 1961), the iron meteorite from Meteor Crater, Arizona, diamond is associated with hexagonal lonsdaleite, which is usually associated with shock processing, and so it became widely accepted that in this case the diamonds were produced in the terrestrial impact event. Recognition of the diamond polymorphs in an unshocked Antarctic iron meteorite has, however, implied that at least some diamonds were produced by a mechanism other than impacts (Clarke, 1981). Most, but not all ureilites (for example ALHA 78019 is an exception: Berkley and Jones, 1982) contain up to 1 wt% diamond (Ierofeiff and Latchinoff, 1888) in matrix veins intergrown with graphite and lonsdaleite (Vdovykin, 1970). The favoured explanation for the origin of these diamonds is formation by shock during collisions 'in space' (Vdovykin, 1970; Lipschutz, 1964). An alternative mechanism, akin to chemical vapour deposition, has also been suggested (Fukunaga *et al.*, 1987).

Whatever the exact mechanism of formation of the ureilite and iron meteorite diamonds, their existence can almost certainly be explained by processes acting in the solar nebula/solar system at some time. The situation is clearly different for the diamond associated with isotopically light nitrogen (Lewis *et al.*,1983) and anomalous xenon (Reynolds and Turner, 1964; Manuel *et al.*, 1972). This diamond type is found only in the lowest petrologic grade chondrites and so cannot have formed by a shock mechanism involving the whole rock; it is believed to have been formed before the meteorite accretion in a presolar circumstellar shell. "Cδ" was the sobriquet given to the carrier of the anomalous xenon before diamond was found in residues enriched in Xe-HL, by Lewis *et al.*, in 1987. In this thesis, the term "Cδ" is generally avoided as the assumption that diamond is the carrier of the xenon is

only an inference, but it is used occasionally to differentiate between diamond associated with isotopic anomalies and the other chondritic diamond type.

3.2 The combustion of diamond

The analysis of diamond in this thesis was performed largely by combustion of the mineral, followed by measurement and isotopic analysis of the CO_2 and N_2 evolved. For this reason, it is important to try to reach some understanding of the mechanisms of diamond combustion. The combustion of diamond is apparently a simple first order reaction:-

$$C + O_2 \rightarrow CO_2$$

The oxidation is complicated by a thin graphitic layer that forms on the surface of the diamond during combustion at low oxygen pressures (Evans and Phaal, 1962). This causes the combustion rate of the diamond to fall, and the recorded activation energy to change from 230 kJ mol^{-1} (true value) to 139 kJ mol^{-1} (the apparent value for diamonds that form a graphite coat).

The combustion temperature of diamond is highly dependant on grain size (Ash *et al.*, 1987); nanometre diamonds typically combust at 500°C and diamond chips of ~1mm in diameter at around 800-850°C.

This reaction is highly exothermic with ΔH (diamond+O2 = CO2)= -395.8 kJ mol^{-1}, to produce more heat per unit mass than a coal fire (ΔH(graphite+O2 = CO2) =-393.3kJ mol^{-1}). Thus the combustion of the diamond may influence the combustion of other, slightly more thermally resistant components, and even diamonds of a coarser grain size, and this may be of importance during stepped combustion experiments. An investigation was therefore carried out in which diamonds of different sizes (and hence combustion temperatures) were mixed in approximately equal proportions and analysed by stepped combustion. The size fractions used were 0-2μm, 8-15 μm and 20-40μm. It was found that the profile produced from this experiment (figure 3.2) was slightly narrower than the profile produced by adding together data from 3 stepped combustion experiments of the grain size separates and that the diamond had almost completely burnt by 700°C, at which temperature the coarsest grain size was still combusting in the individual experiments. This effect (which may have been slightly enhanced by the difference in step sizes between the two experiments) shows that the reaction of diamond is exothermic enough to affect the combustion of components of slightly higher thermal stability but is not as pronounced as may be expected from theoretical

calculations; it is possible that the platinum bucket in which the samples are combusted acts as an efficient heat sink.

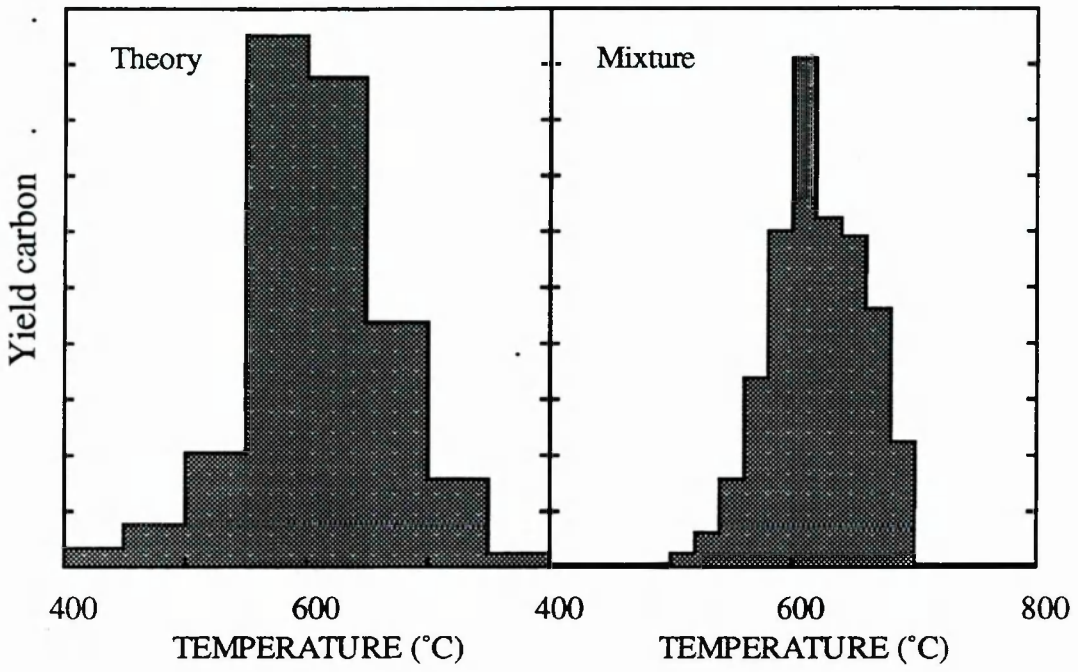

Figure 3.2. (a) "Theory": Stepped combustion profiles added together of three individual experiments of different grain sizes of diamond (data from Ash 1990). (b) "Mixture": Profile obtained from a single experiment in which the diamond fractions analysed for (a) were mixed in equal proportions and then step combusted.

3.3 The discovery of Xe-HL

In 1964, an isotopic anomaly in xenon (now called Xe-HL[2] as it consists of an enrichment in both Heavy and Light isotopes of xenon; figure 3.3) was noted by Reynolds and Turner during a stepped heating experiment on the CR meteorite Renazzo. The significance of this isotopic signature was not immediately understood; it was at first believed that this anomaly was produced from the fission of a heavy element such as ^{244}Pu (Reynolds and Turner, 1964) although it was also interpreted as the fission product of an extinct superheavy element (Anders and Heymann, 1969; Dakowshi,1969; Srivinsan *et al.*, 1969, 1977; Lewis *et al.*, 1975, 1977; Anders, 1981). This process would be expected to cause an enrichment in the heavy isotopes only, but Kuroda and Manuel (1972) explained the light enrichment as a fractionation signature imposed on the fission products. In 1972 Manuel *et al.* suggested that Xe-HL was a primitive nucleosynthetic product, produced during a supernova explosion, and it is this theory which is most widely

[2]The anomaly in xenon was at first named CCF Xe for Carbonaceous Chondrite Fisson Xenon because it was originally interpreted as a fission product.

accepted today. Clayton (1989) has shown that in a collapsing core of a type II supernova, which produces high energy neutrinos that can liberate neutrons, Xe approximating to Xe-H can be formed *via.* the r process in the He shell. The formation of Xe-L is not quite so easy to explain but the p process (proton capture) and photodisintegration that are believed to take place in the O shell of supernovae (Heymann and Dziczkaniec, 1979) may be important.

The modern mean values recorded for the isotopes of Xe-HL are $^{136}Xe/^{132}Xe$ = 64.2 and $^{124}Xe/^{132}Xe$ = 0.774 (Huss, 1990); or $\delta^{136}Xe$ = +1300‰, $\delta^{124}Xe$ = +700‰, relative to ^{132}Xe, using the standard BEOC - 12 (Nichols *et al.*, 1991, recorded for Tieschitz and Inman)

Samples which contain Xe-HL are also associated with other isotopically distinctive noble gas components in He, Ne (Ne-A2), Ar, and Kr (Kr-H) (Tang and Anders, 1988b), that are released at similar temperatures to the xenon during pyrolysis. In addition, low temperature argon, krypton and xenon are released that are "normal" (*i.e.* planetary) in isotopic composition.

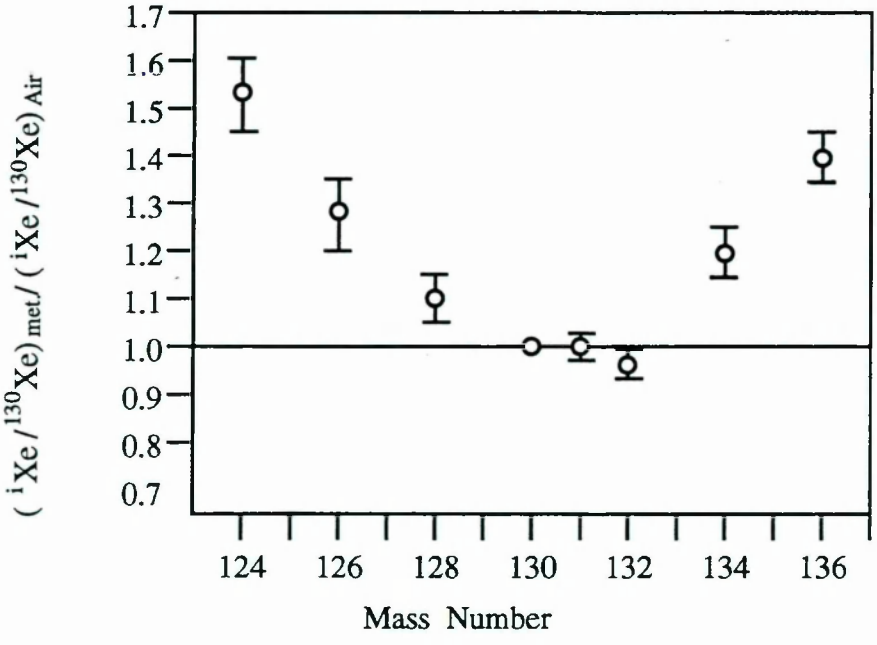

Figure 3.3 The abundance of isotopes in Xe-HL (from Manuel, 1972)

Although the Clayton theory requires that Xe H and Xe L were formed in separate parts of the stellar shell, it seems that they were at some stage extremely well (if not inseparably) mixed; the possibility of separating the isotopes has been discussed by, for example, Alaerts (1980) and Schelhaas *et al.*, (1990). A study by Huss (1990) of a wide range of samples was unable to distinguish Xe-L from Xe-H whereas more recent work by Nichols *et al.* (1991), using comparatively small

temperature step sizes, has tentatively suggested that the diamond in Tieschitz may have a Xe signature that is depleted in Xe-H compared with other meteorites. The carbon isotopic composition of the acid resistant residue was, surprisingly, found to fall in the Solar system range, with a $^{12}C/^{13}C$ ratio of around 93 (Swart *et al.*, 1983).

The carrier of Xe-HL remained unidentified for over 23 years after its discovery, although it had been ascertained that it was carbonaceous and and associated with an isotopically light nitrogen signature (Lewis *et al.* 1983). Finally, after misidentifications as chromite and carbynes (Lewis *et al.*, 1975; Alaerts *et al.*, 1980; Anders, 1981), the carrier was concentrated in sufficient purity by acid dissolution from Allende, Murray, Murchison and Indarch, to allow Lewis *et al.* (1987) to show, by electron diffraction in the transmisson electron microscope, presence of ~5nm diamond crystals. Later, the acid-resistant residues were found also to contain up to 50% diamond-like hydrocarbon associated with the diamond (Bernatowicz *et al.*, 1990, Huss 1990: oral presentation to the Royal Astronomical Society) as well as diamond *senso stricto*.

If Xe-HL is a primitive nucleosynthetic signature, then other elements would be expected to show a similar enrichment to xenon in "r" and "p" process elements (Clayton, 1981). Recent measurements of the barium and strontium associated with the diamond however, revealed these elements to be extremely underabundant in diamond and they did not show the expected isotope profile (Lewis *et al.*, 1991). Barium is slightly enriched in ^{137}Ba, the "r" process isotope, but strontium shows no significant overabundance of the heavy isotope ^{88}Sr. The Ba isotopic signature agrees in spirit, although not in magnitude, with models of a weak neutron burst in the helium shell of a supernova (Howard *et al.*, 1991).

3.4 A review of current theories about the origins of "Cδ" diamond

The grain size distribution of the diamond associated with Xe-HL was measured by TEM counting (Lewis *et al.*, 1989) and found to be log-normal. This suggests that the diamond was formed in a single event, by a growth mechanism rather than by the destruction of larger grains (Cartensen and Rodriguez-Hornedo, 1985), and implies the diamond population is very young, since the diamond has apparently been subjected to little damage after formation and before incorporation into the meteorite. The production of Xe-HL in a supernova environment has now gained widespread acceptance. One problem with this model, however, is that the stars massive enough to form supernovae are not thought to be carbon rich. If C<O, then carbon will condense as CO rather than as solid grains. The conclusion of Lewis *et al.* (1987) was therefore that the diamond was produced in a presupernova red giant

and then implanted with Xe during the explosion. Jorgensen (1988) pointed out a drawback of this theory is that carbon rich red giants ($M_o < M < 8M_o$) are not believed to be massive enough to undergo evolution to a Type II supernova event. Jorgensen therefore suggested two stars must be involved: that the diamond could have condensed in a carbon rich red giant star which lost some mass to a binary companion allowing the companion to reach its Chandrasekhar limit and explode as a supernova (a relatively common occurrence in astronomy). The grains that condensed around the red giant could then be implanted by xenon by the Type I supernova. In contrast, Clayton (1989) maintained that a single massive star would suffice as type II supernovae are sufficiently heterogeneous to contain carbon rich pockets in the He burning shell in which diamond may form. Carbon with a $^{12}C/^{13}C$ value of ~93 is not produced in any part of a supernova; the carbon that makes up the Solar system, which has a similar $^{12}C/^{13}C$ ratio, is thought to be a mixture of carbon from a variety of nucleosynthetic environments. According to the Clayton model, the primary carbon source for the diamond would be provided by $3\alpha \rightarrow C$ reactions in the convective part of the He burning shell in the pre-supernova star. This layer produces pure ^{12}C, so to reach a $^{12}C/^{13}C$ ratio of 93, mixing would have to take place with the radiative He burning layer just above it to give a $^{12}C/^{13}C$ ratio of 93. Although this upper layer has a $^{12}C/^{13}C$ ratio of ~0.2, (Clayton, 1989), it is extremely depleted in carbon content and so the mixing would have to be reasonably efficient to result in the observed carbon isotopic composition. The radiative layer would also be the source of ^{14}N to produce $^{14}N/^{15}N = 428$, corresponding to the measured value of the nitrogen in the diamond at ~ -340‰ (Lewis *et al.*,1983; see also section 3.8.1.). Unfortunately, it is not possible to produce both the correct carbon isotopic composition and nitrogen isotopic compositions if it is assumed that all C and N in diamond comes from a certain amount of mixing of these two layers.

None of the theories of diamond production can account for all the observations of and requirements for the diamond formation:

1) The normality of the carbon isotopic composition.

2) The need for the formation environment to be carbon rich compared to oxygen, a rare stellar condition that is more easily fulfilled in the lower mass stars that produce red giants than in supernovae.

3) The high abundance of diamond in meteorites. (The grains make up to 2% of all the carbonaceous material in the least altered CM2 meteorites, and are 100x more abundant than the other carbonaceous interstellar grains - see chapter 1).

4) The lack of a positive ^{129}Xe anomaly. This implies that the ^{129}I was not

preferentially incorporated into the crystal and points to either a non-selective (*ie.* ion implantation) mechanism for the Xe incorporation (Clayton,1989), or else diamonds must have formed a long time after the elements were produced (which seems unlikely since ^{129}I survived in many early Solar system condensates).

5) The high abundance of xenon in the diamond. Xe/C ratio=2.2×10^{-3} of solar, indicating an efficient trapping process (Clayton, 1989).

6) Xe-H and Xe-L cannot be formed in the same astrophysical environment and yet are apparently inseparably associated with each other (Clayton, 1989).

7) The high abundance of nitrogen associated with the diamond (see section 3.8).

8) The variations in nitrogen content between meteorite classes (see section 3.8).

9) The "log-normal" grain size distribution of the diamond is not to be expected for grains that have experienced a post supernova turbulent environment where grain-grain collisions would have been frequent.

10) The paucity of Ba and Sr compared to Kr and Xe, and lack of an anomalous isotopic signature in Sr, with only a weak "r" process signature in Ba, is difficult to explain. Precondensation of these lithophile elements before diamond formation and "contamination" with a Solar system Sr and Ba source may help to explain the results.

The formation mechanism of the diamond also needs to be considered. Two models have been proposed: formation of the diamond metastably at low pressure by a chemical vapour deposition (CVD) process (Lewis *et al.,* 1987), and a shock origin due to graphite grain collisions in a supernova shock wave (Tielens *et al.,* 1987; Blake *et al.,* 1988). The presence of diamond-like carbon associated with the diamond has been claimed as evidence for both mechanisms, whereas the log-normal grain size distribution is sited as evidence for the CVD (*ie.* growth) mechanism rather than a destructive mechanism like shock. Although the formation of nanometre diamonds by shock of other carbonaceous grains seems to be energetically feasible, the carbon isotopic composition of the diamond and their precursor grains would be expected to be similar, and their noble gas and nitrogen inventory may be expected to remain unchanged except for degassing processes. However, the diamond seems to be totally unrelated to other carbonaceous components in the meteorites. The tightly jointed aggregate texture of the diamonds is however is thought to be similar to that of shocked diamond, and thermoluminescence (TL) data indicates a similarity between Cδ and diamonds produced by an ultradispersion shock technique (Fishenko *et al.*, 1992). A

description of terrestrial diamonds made by CVD and shock processes, and a comparison with meteoritic diamond, will be made in chapter 5.

3.5 Diamond Abundance in the Primitive Chondrites

The abundance of the diamond was acquired by determining the carbon content of the perchloric resistant residues by the bulk carbon technique (chapter 2), and from this by calculating the amount of the carbon that can be attributed to diamond in the bulk meteorite (table 3.1). This assumes that none of the diamond-like material has been lost during the acid dissolution process. Huss (1990), however, has made measurements of Xe-HL and Ne content on the residues at an earlier stage of their acid processing, assuming that the diamond has a uniform Xe-HL quota, and the abundance data for diamond calculated from this process are uniformly higher than data acquired for the more processed samples. (The lone exception to this is Murchison, for which Huss reported a sample loss during processing). The most likely explanation for this is that there is some loss of diamond or diamond-like carbon containing Xe-HL. The same effect is found if the diamond content is calculated from the light nitrogen release in similarly prepared samples although this technique is somewhat unreliable because of the plethora of non-diamond, nitrogen containing components in these carbonaceous residues.

Meteorite	**Class**	**Abundance (ppm) (this thesis)**	**Abundance (ppm) (from Huss, 1990)**
Orgueil	CI1	424	941
Cold Bokkeveld	CM2	318	
ALH 83100	CM2	272	
Murchison	CM2	467	360
Allende	CV3	125	250
Efremovka	CV3	120	
Vigarano	CV3	37	497
Krymka	L3.0	136(?)	109
Adrar 003	L3.0/3.2?	74	
Inman	L3.4	8	20
Tieschitz	H3.6	8	36
Indarch	EH4	17	50

Table 3.1. Abundance of diamond in meteorites (not matrix normalised).

3.6 Morphology

The morphology of the diamond isolated using strong oxidants has been studied by several authors using transmisson electron microscopy (e.g. Lewis *et al.* 1987; Bernatowicz *et al.*,1989). These studies indicate that the diamonds are present as ~2nm grains in clusters of up to 100nm, and of a similar appearance in all meteorite types. The effect of the oxidising acids on the morphology of the grains has not however been very carefully considered. The residues before the perchloric acid treatment (from Allende, Cold Bokkeveld, Murchison and Adrar 003) were analysed using the TEM by K. Gilkes of the University of Cambridge. He found that the diamonds were actually >10nm in diameter in the residues treated only with HCl/HF, and had a pristine appearance (figure 3.4). Thus, it appears that the perchloric acid treatment either causes the diamond to disintegrate into smaller particles so the true size of the diamond in the meteorite is >10nm (*ie.* at least $1x10^5$ atoms of carbon), or else the 10nm diamond must be destroyed completely by the oxidative acid treatment, leaving only a population of more resilient small grains. The first option appears the least improbable, as no other perchloric acid soluble diamond has yet been reported.

The perchloric residues were also studied by TEM, and the major carbon bearing phase found to be diamond. However, in addition, K. Gilkes also identified a hexagonal allotrope of carbon "choaite" in the residues.

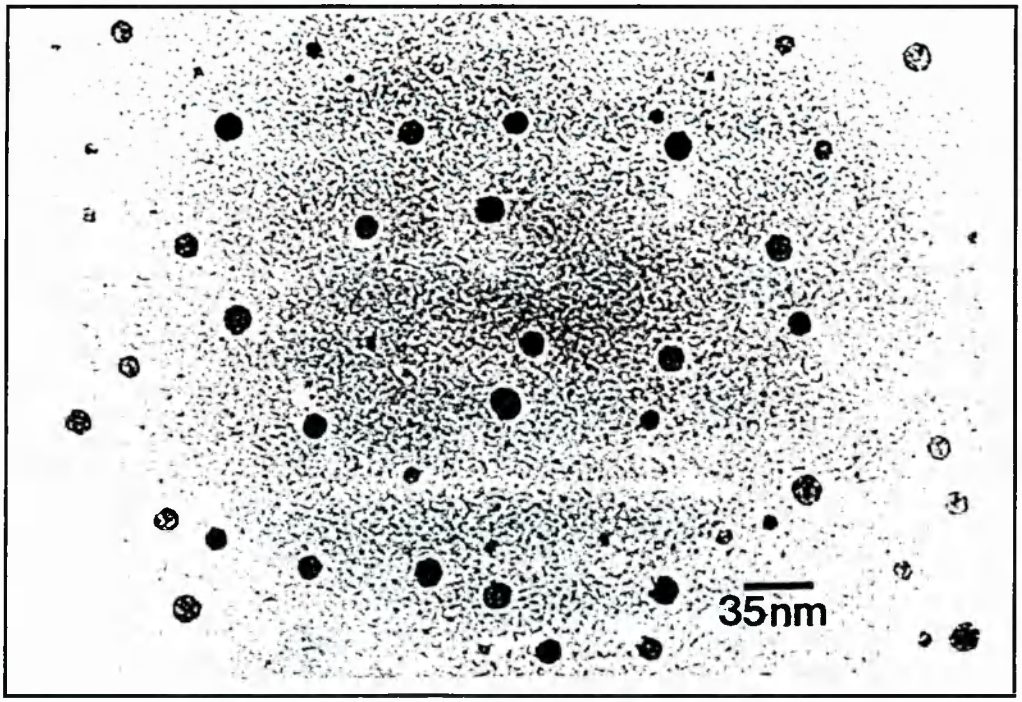

Figure 3.4 Morphology of the diamond crystallites before perchloric acid treatment.

3.7 Carbon isotope composition of the diamond

The isotopic composition of the carbon that makes up the diamond is poorly

characterised. Although it was believed that the diamond had a $\delta^{13}C$ of between -32‰ and -38‰ (Swart *et al.*, 1983; Ash, 1990) and a difference between meteorites was suspected, the absence of a systematic suite of experiments on similarly prepared residues using high precision mass spectrometry had ensured that the question of whether the carbon isotopic composition was constant, or varied between meteorite types, was open to some debate. A series of experiments was therefore performed, using dynamic mass spectrometry, on samples treated with HF/HCl, chromic acid and perchloric acid, from a range of carbonaceous, ordinary, and enstatite chondrites.

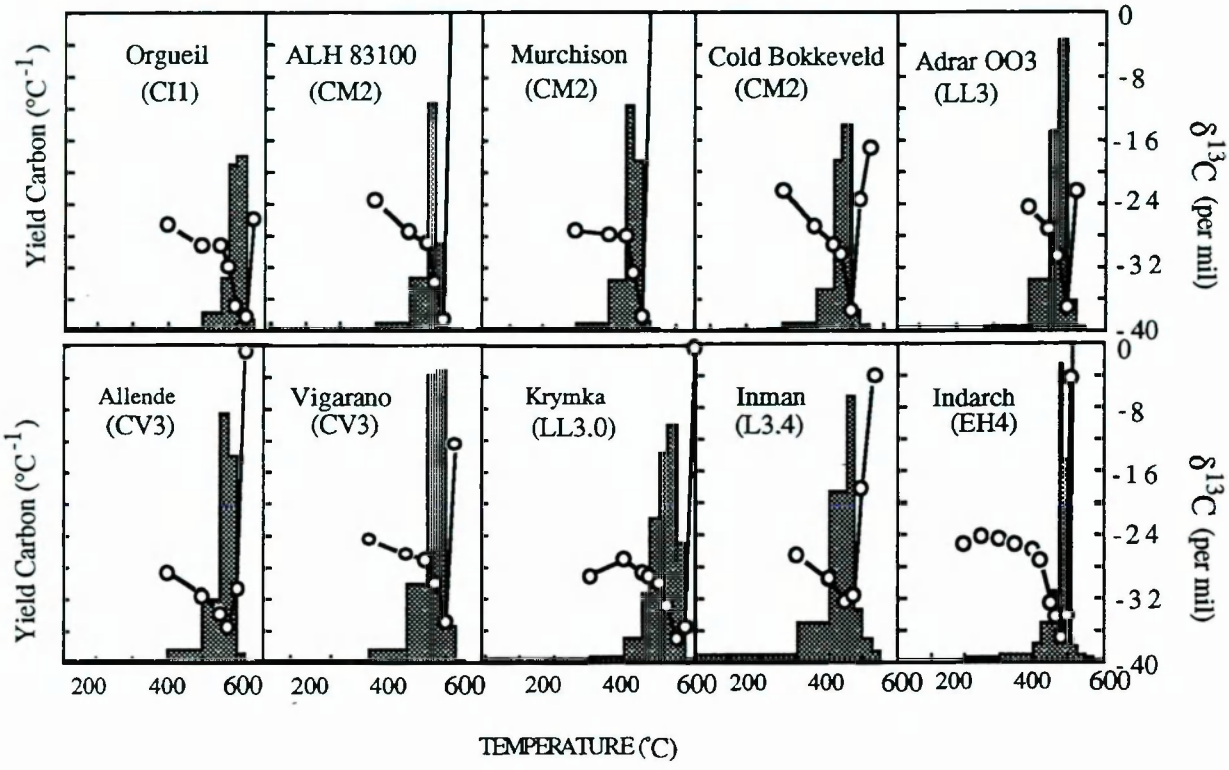

Figure 3.5 Examples of carbon stepped combustion plots for diamond from several meteorite types.

The stepped combustion of the diamond residues was performed using the same steps for all meteorites to facilitate comparisons, unless too little gas was released to analyse in which case the step size was increased. The steps used were 300°, 400°, 450°, 475°, 500°, 525°, and 550°. The exception to this procedure was Indarch which was analysed by static mass spectrometry because of the small amount of sample available, allowing smaller step sizes to be utilised. The peak attributable to diamond was typically extremely sharp (figure 3.5), as would be expected for the combustion of a single component, and the peak yield step usually 475 or 500°C. By 550°C, the component was completely combusted.

General differences between the isotopic data are more easily seen in the plots depicted in figure 3.6, which show $\delta^{13}C$ against the percent C released. This ensures that the differences between meteorites can be demonstrated more clearly and that differences in combustion temperature due to oxygen pressure, temperature monitoring *etc.* are eliminated.

It can be seen that diamond from different meteorite groups show differences in carbon isotopic composition during combustion. The CM2's are similar to each other, showing a decline in isotopic composition as the combustion progresses to a minimum of -38‰. The CI1 Orgueil reaches the same minimum value but becomes lighter than the CM2's at an earlier stage in the combustion. The CV3 Allende has a similar pattern of decline in $\delta^{13}C$ during the combustion as Orgueil but is around 3‰ heavier. Similarly, the ordinary chondrites Tieschitz and Inman are 3‰ heavier again than Allende, reaching a minimum of only -32‰. The most primitive ordinary chondrites, Krymka and Adrar 003, show greater similarities to the CM2 meteorites than to Tieschitz and Inman. The minimum values reached during stepped combustion over the diamond burning range are listed in table 3.2.

Meteorite	$\delta^{13}C$ **(minimum)‰**
Orgueil	-38.5
Cold Bokkeveld	-37.8
Murchison	-38.2
ALH 83100	-38.8
Allende	-35.5
Vigarano	-35.1
Adrar 003	-37.3
Krymka	-37.3
Inman	-32.5
Tieschitz	-33.9±1.4
Indarch	-37.0±0.4

Table 3.2. Minimum $\delta^{13}C$ values recorded during stepped combustion of perchloric residues over the diamond burning temperature range. The error on each isotope measurement is < 0.1‰ except where an error is indicated; the less precise runs were performed by static rather than dynamic mass spectrometry because of the small amount of sample available. The Tieschitz measurement was performed by C.M.O'D. Alexander.

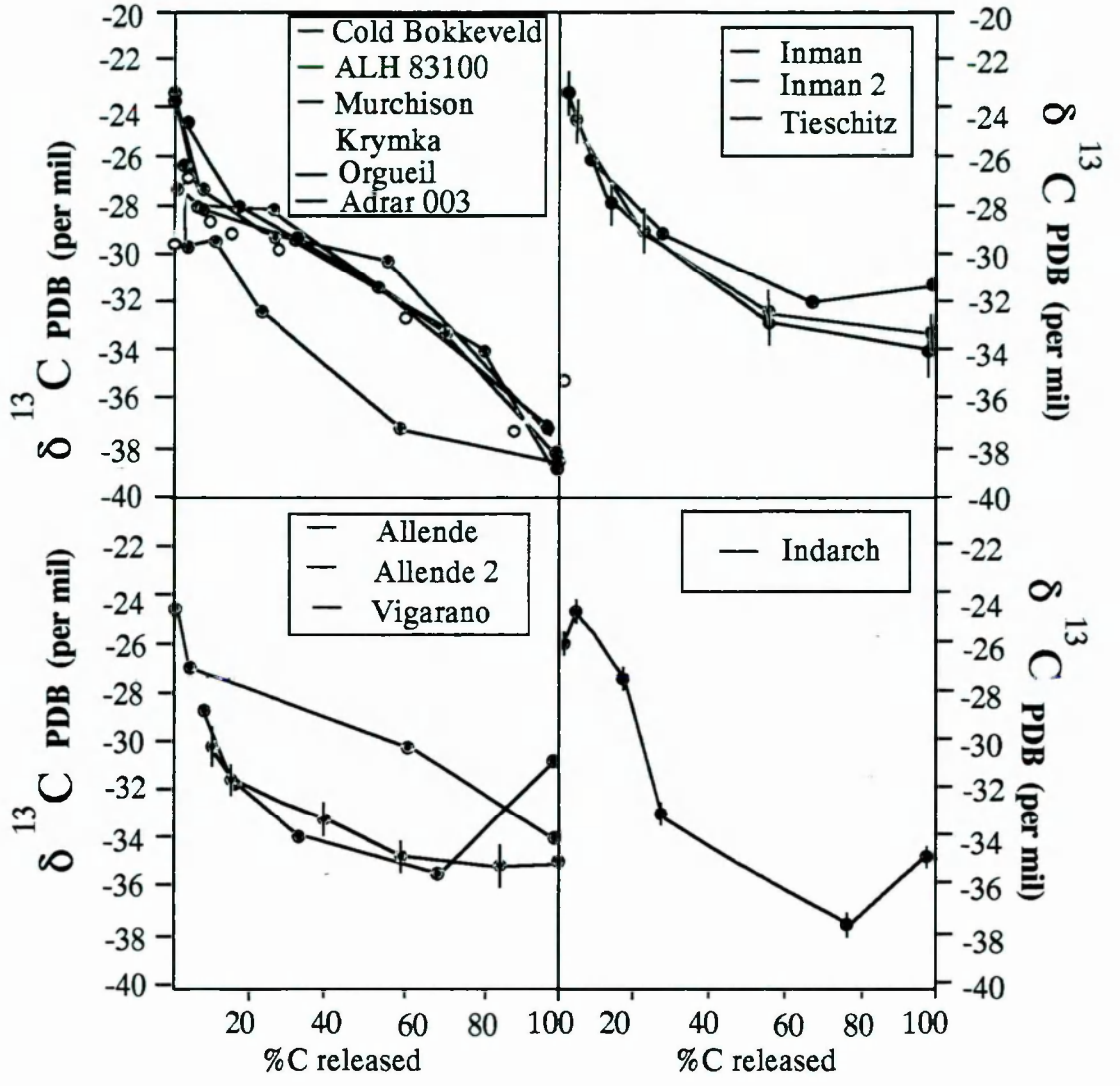

Figure 3.6. A comparison of the isotopic composition of diamond released from various meteorites. Most of the samples were measured by dynamic mass spectrometry and so have errors of <0.1 per mil, except for the following which were analysed by static mass spectrometry: (a) Indarch, (b) Allende 2 which was analysed by R. Ash and (c) Inman 2 and Tieschitz, analysed by C. Alexander.

It is possible, however, that the differences are the result of other components co-combusting with the diamond. Although Arrenhius plots (*e.g.* figure 3.7) indicate that any additional phases must be poorly abundant, an isotopically anomalous component need only be present in very small amounts to affect the isotopic ratio of the released CO_2. There is evidence that an isotopically heavier species combusts immediately after the diamond combustion in all the samples; however this component appears to be more abundant in the samples which have the lightest diamond related carbon (*e.g.* the CM2's) and so can not explain the differences in $\delta^{13}C$ seen during the diamond combusting peak. It is more probable that any interference involves a heavier component combusting before the main diamond peak.

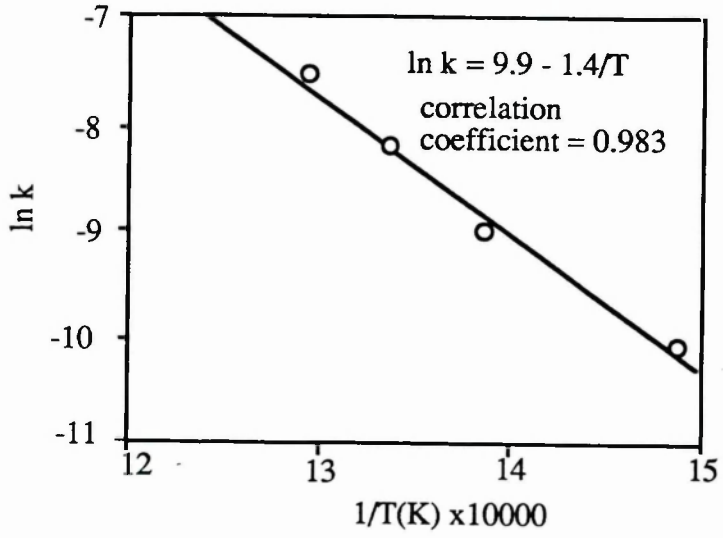

Figure 3.7. An arrhenius plot of the diamond combustion (this diagram plotted from the data for the Allende meteorite). The gradient indicated that the activation energy of the combustion was 112 $kJmol^{-1}$ compared with literature values of diamond of 139 $kJ\ mol^{-1}$ (Evans and Phaal, 1962).

One-step experiments (in which the perchloric acid resistant residues are combusted at 1000°C in sealed tubes for ten hours) are expected to release both the diamond component and the meteoritic SiC in the form of CO_2, which can then be analysed by mass spectrometry. The results of these experiments are shown in table 3.3. Since diamond and SiC are the most abundant carbonaceous phases in the residues, the isotopic composition of the CO_2 can be used to estimate the diamond/SiC ratio. If the isotopic composition of SiC is assumed to be +1400‰ (chapter 6), and that of diamond variable, given for each meteorite in table 3.2, then the ratios given in the third column of the table are obtained. It appears that this ratio is very variable

between meteorite types. The lowest ratio, indicated by the heaviest bulk carbon composition, is given by the enstatite chondrite Indarch at 25, and the highest ratio (*ie.* lowest SiC content meteorite) was the CV3 Allende. These data are likely to be accurate for the more SiC rich meteorites (see chapter 6 for SiC abundance information), but for meteorites such as Allende and Inman which are SiC poor, the data are likely to be less accurate because the abundance of other minor carbonaceous components becomes critical. This information suggests that SiC is more easily destroyed than diamond during metamorphism (as the diamond:SiC ratio rises with increasing petrologic type). This effect has also been noted by other authors (Huss, 1990; Alexander *et al.* 1990) and is somewhat curious since the SiC is more thermally resistant than diamond during stepped combustion experiments. The one exception to the general trend is the enstatite chondrite Indarch, which is extremely abundant in SiC despite being petrologic type 4. This may reflect the different conditions in the enstatite chondrite parent body (lower Po_2) or could be due to the presence of a different, additional SiC population in this chondrite (chapter 6). The diamond:silicon carbide ratios measured by high resolution stepped combustions will be presented and discussed further in chapter 7.

Meteorite	Type	$\delta^{13}C$ (bulk residue)	Diamond/ SiC (mass)
Orgueil	CI1	-15.1‰	62
Cold Bokkeveld	CM2	-25.5	114
Murchison	CM2	-24.0	102
ALH 83100	CM2	-21.1	76
Allende	CV3	-31.1*	371
Inman	L3.4	-28.4	307
Indarch	EH4	+19.0	25

Table 3.3. A comparison of the diamond/SiC ratio measured for several meteorites by bulk $\delta^{13}C$ measurement. * $\delta^{13}C$ for this meteorite may be less than the +1400‰ assumed: see chapter 6.

3.8. Nitrogen

Nitrogen is typically the major impurity in terrestrial diamonds and is present in quantities usually of up to 2500 ppm (although recent unpublished work by Mr L. Van Heerden, *pers. comm.* has extended the nitrogen content field to just above 4000 ppm in some Ellendale diamonds). The nitrogen isotopic composition of terrestrial diamond is typically within the range -10‰ to +10‰ (Javoy *et al.*, 1984;

Boyd, 1988) which is believed to be a similar value the mantle nitrogen from which it originates. As nitrogen has the electronic structure [He] $2s^2\ 2p^3$ a single nitrogen in the lattice leaves a single unpaired electron (*ie.* the crystal becomes paramagnetic which stretches the normal C-C bond length by 10% causing a distortion to the lattice). Although nitrogen is believed to be originally incorporated into diamond in this single state (called Ib), if diffusion is allowed to occur (*i.e.* the diamond is sufficiently heated) then the nitrogen will aggregate to form more stable structures such as nitrogen pairs (the Ia state) (Evans, 1976). This process, studied experimentally by Evans and Qi (1982), has shown that the time for nitrogen to aggregate completely from the Ib to the Ia state in diamond at 700°C is 1.5×10^{11} years, more than the age of the Solar system. Clearly this process would therefore not be of great importance to diamond metamorphism on meteorite parent bodies, which are not believed to have been exposed to very high temperatures. However, Collins (1978, 1980), increased the diffusion (and hence aggregation) rate by irradiating diamonds. This is believed to be because irradiation increases the vacancy concentration allowing nitrogen to diffuse more easily around the lattice. Meteoritic diamonds are likely to have been heavily irradiated throughout their lifetime, in their putative circumstellar formation environment, and also in the early solar nebula. Irradiation may in addition have the effect of destroying small grains.

Studies of nitrogen in terrestrial diamond have only been performed on diamonds which are large enough that it can be assumed that the crystal lattice is infinite, and only nitrogen movement within the crystal is considered. For the nanometre meteoritic diamond, in which around 50% of the atoms are surficial, and effectively all of the lattice is distorted by edge effects, such an assumption clearly cannot be made. It is likely that for nanometre diamonds, especially if they have a high concentration of lattice defects, nitrogen degassing rather than aggregation would be a more significant result of nitrogen diffusion and comparison to nitrogen in terrestrial diamond is of only limited use. In analogy to terrestrial diamond, the nitrogen does appear to diffuse around the crystal, as indicated by its peak release temperature during pyrolysis of 1000°C (see section 3.8.2), much lower than that for xenon. One explanation for this could be that whereas N can diffuse around the crystal lattice, Xe, like He (Luther *et al.*, 1964) may be completely immobile in the interstices of diamond crystals. So why is xenon released at all during stepped pyrolysis experiments? Stepped combustion after pyrolysis of the diamond to 1250°C indicates a carbon release temperature of 600-700°C, 100-200°C higher than that of unheated Cδ but similar to the expected temperature release of graphite (figure 3.8). This may indicate that the diamond has undergone recrystallisation to graphite when pyrolysed at 1250°C. This is somewhat lower than reported temperatures for diamond/graphite conversion (Davies and Evans, 1972), perhaps

reflecting the low crystallinity of the meteoritic diamond. The release of Xe, therefore, may occur only when the diamond structure itself is destroyed, and hence Xe may be much more resistant to low grade metamorphic degassing than nitrogen.

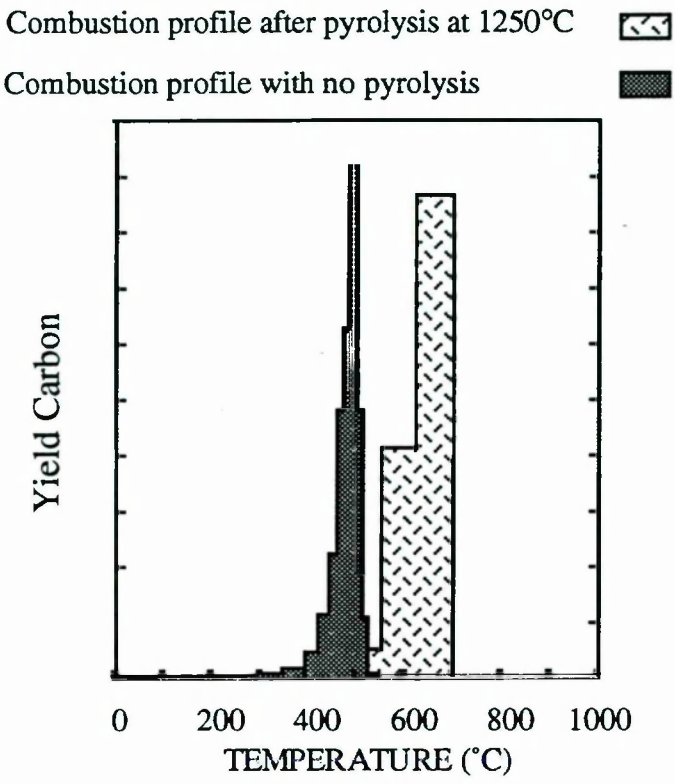

Figure 3.8 Comparison of carbon combustion profiles of diamond from Cold Bokkeveld after high temperature pyrolysis to a sample that had not been heated. Very little nitrogen was released during the combustion following pyrolysis.

In summary, the nitrogen in Cδ diamond cannot be treated in a completely analogous way to terrestrial diamond because (i) the crystals are too small (ii) the crystals have most likely been irradiated and (iii) their P,T, histories are so different; but it seems the overall behaviour of both nitrogen and xenon in the crystal lattice is similar to that in terrestrial diamond.

3.8.1 The siting of nitrogen in diamond

The diamond rich residues were studied by electron spin resonance (ESR) by Mark Newton and Andrew Cox of the Clarendon laboratory, Oxford to determine a) if nitrogen was a lattice element in diamond or merely an associated phase and b) how the nitrogen was bonded within the diamond. The spectra obtained indicated a

paramagnetic feature that could be due to a line defect in the lattice, typical of irradiated diamond, which may or may not contain nitrogen. The asymmetry of the peak obtained (figure 3.9) suggested that some unaggregated nitrogen may also be present, but the lattice was distorted by edge effects which made firm conclusions difficult. A second attempt to locate the nitrogen within the residues was made by K. Gilkes, using electron energy loss spectrometry (EELS). No evidence of the presence of nitrogen in any of several perchloric acid resistant residues could be obtained, suggesting that the nitrogen may be finely dispersed throughout the sample. From this it can be inferred that the nitrogen is more likely to be bound within the abundant diamond than within any minor phase, such as a nitride, although work is still in progress to identify nitrogen using this technique. The nitrogen is assumed to be located within the diamond, the most abundant carbonaceous phase in the perchloric resistant residues, but the possibility of a separate components hosting the light nitrogen is discussed further in section 3.9.

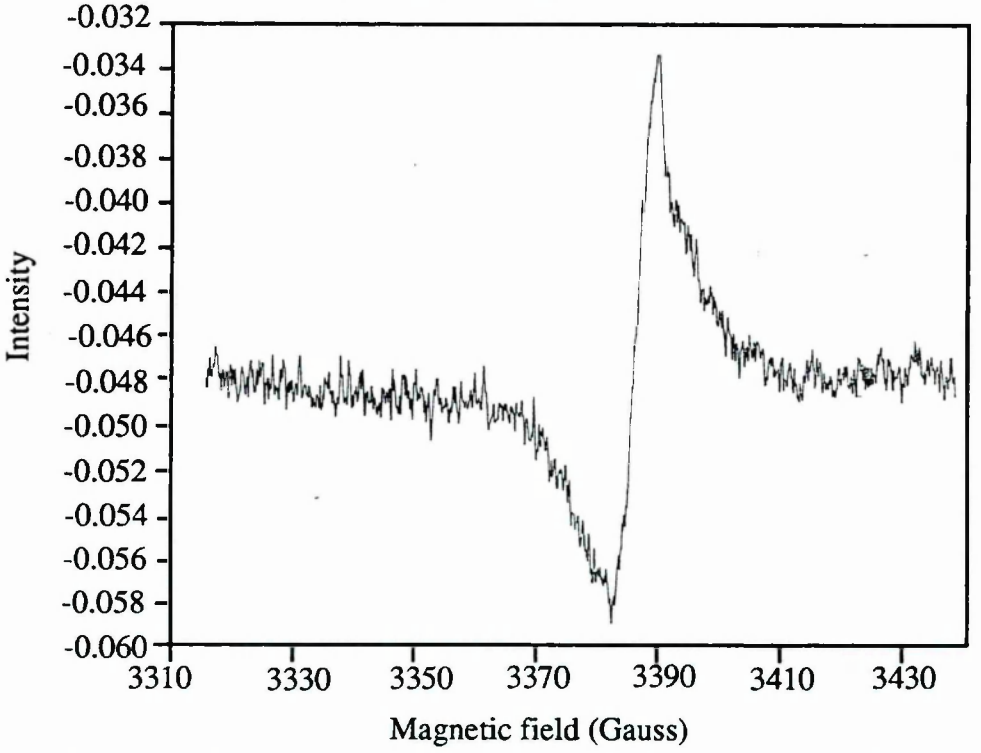

Figure 3.9. The ESR spectra of diamond from Murchison (acquired by M. Newton and A. Cox, University of Oxford).

3.8.2 Investigation of the diamond nitrogen by Mass Spectrometry

The nitrogen content of diamonds in different meteorites has been determined using two techniques: (i) a pseudo-bulk procedure involving combusting in two or three steps and (ii) multiple-step combustion of a single sample at very high resolution (10° steps) with quantification of both N_2 and CO_2 gas at each stage. The nitrogen isotopic composition was more accurately determined using the high resolution data as the atmospheric contamination and any minor phases present in these

experiments were better resolved from the diamond combustion. Using all the available data the nitrogen isotopic composition of the diamond from various meteoritic samples has been determined and is presented in table 3.4. It can be seen that for all the meteorites the nitrogen isotopic composition remains indistinguishable between meteorite types with a mean blank corrected value of -351.5‰ (σ = 7.9). Although there is a variation in individual measurements of ~20‰, the differences are not reproducible and so are designated instrumental errors. Stepped combustion experiments at 10°C intervals revealed that the carbon and nitrogen release occurs over a narrow temperature range of ~460°C to 520°C. The peak release temperature of C and N were typically within 10°C of each other, implying that the nitrogen is closely associated with the diamond, although the C/N ratio was not constant during the entire combustion. Two examples of the carbon and nitrogen release plots are shown in figure 3.10., and data for the other experiments has been listed in Appendix 2.

Meteorite	**Type**	**Number of measurements**	**$\delta^{15}N$ (‰)**	**$\delta^{15}N$ blank corrected**
Orgueil	CI1	1	-333	-337
C. Bokkeveld	CM2	2	-347	-351
Murchison	CM2	3	-341	-348
ALH 83100,78	CM2	2	-344	-346
Allende	CV3	4	-344	-360
Krymka	L3.0	1	-347	-349
Adrar 003	LL3.0, 3.2	1	-308	-311
Inman	L3.4	1	-325	-342
Tieschitz	H3.6	1	-192	-247
Indarch	EH4	2	-328	-358
Mean			**-338**	**-352**
Standard Deviation			**13.4**	**7.9**

Table 3.4. Isotopic compositions of chondritic diamond. C. Bokkeveld = Cold Bokkeveld. The mean $\delta^{15}N$ column shows the mean value of the lightest measurements recorded during stepped combustion over the diamond combusting interval; "$\delta^{15}N$ blank corrected" is the mean of the same measurements after undergoing a blank correction that assumed the system blank was 0‰ and remained unchanged during the experiment. The mean total value excludes the data from the apparently anomalous Adrar 003 and Tieschitz stepped combustion which was performed on an extremely small sample mass. Data from Alexander *et al.*, 1990, shows that the nitrogen in Tieschitz diamond is no heavier than that from the other meteorites.

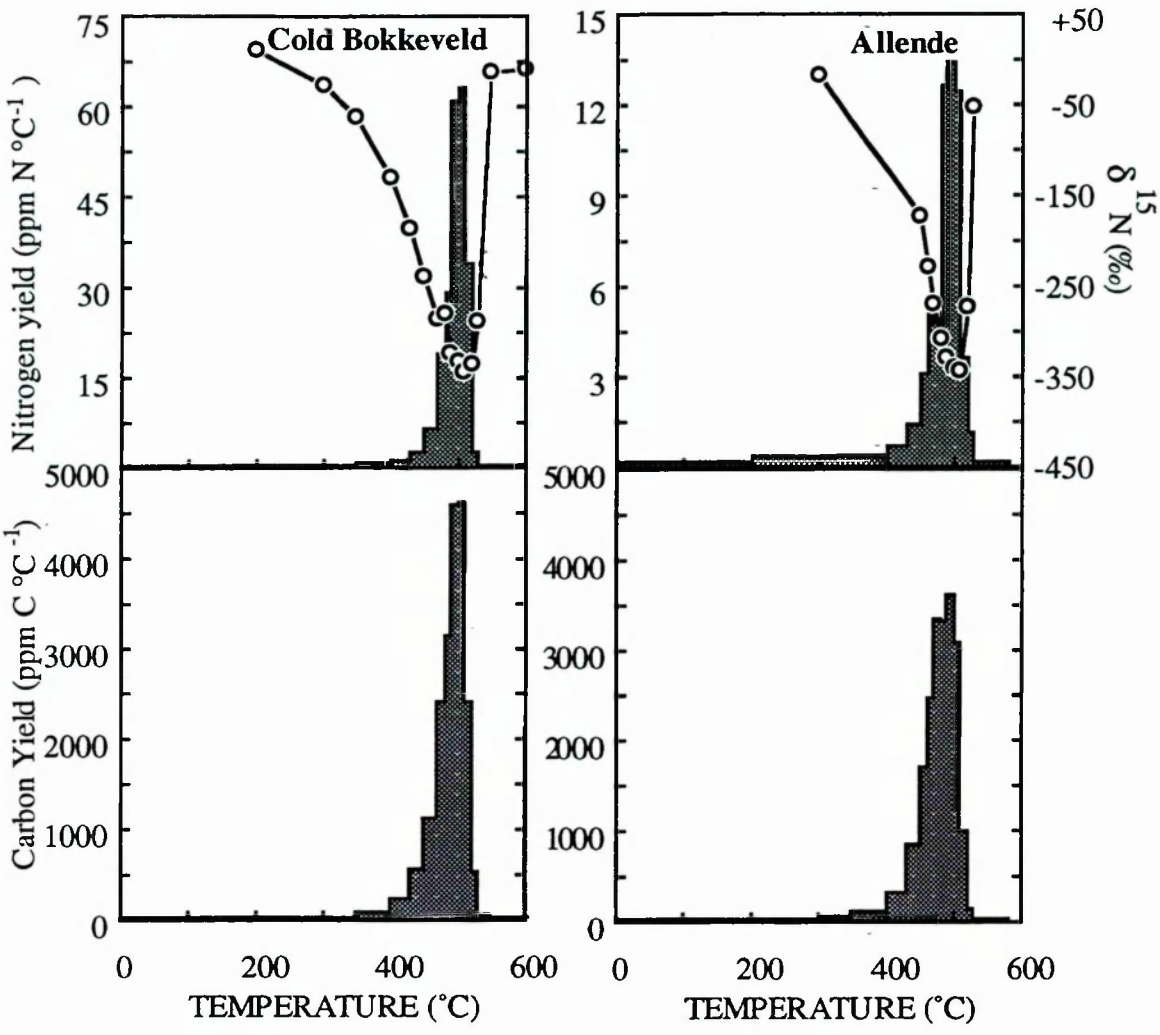

Figure 3.10. Examples of stepped combustion profiles of two diamond residues; note the different nitrogen yield scales. (Data from similar experiments on the other meteorites is in Appendix 2).

It can be seen from the stepped combustion plots (figure 3.10) that the nitrogen and carbon co-combust, at around 500°C, suggesting that they are closely related. The diamond combusts in a very narrow peak, as expected for a single component. The yield and isotope profiles for diamonds from different meteorite groups superficially appear very similar, but closer analysis of the data reveals that there are significant differences between meteorite groups.

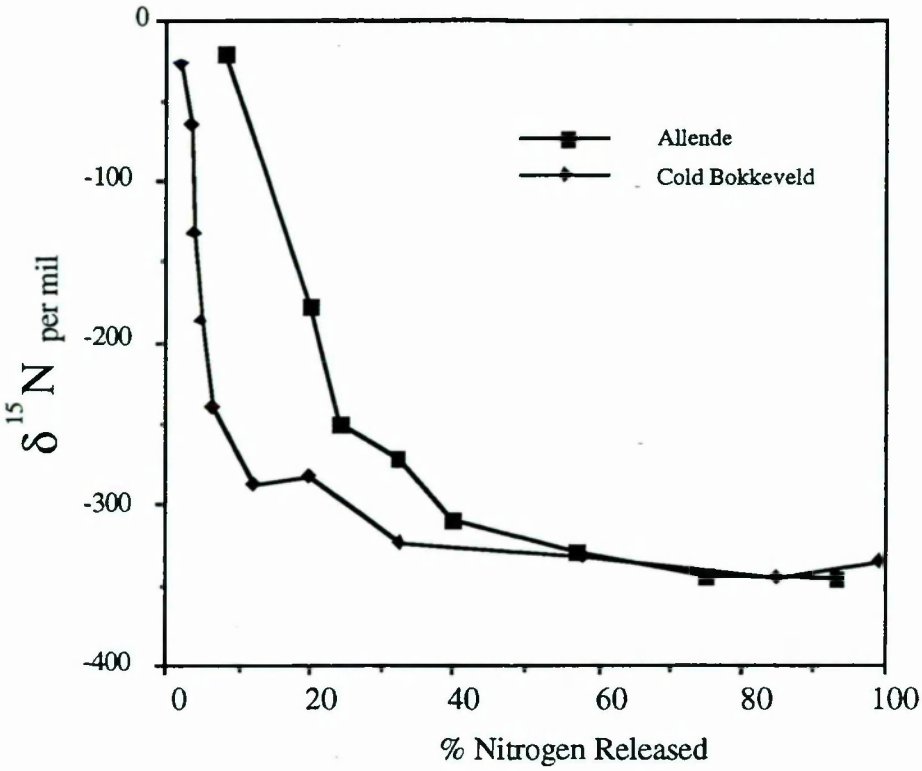

Figure 3.11. A comparison of the nitrogen isotope composition of the diamond from Allende and Cold Bokkeveld during combustion.

Although the lowest $\delta^{15}N$ value is constant, within the limits of the mass spectrometer used, if atmospheric contamination is considered to be the same for both meteorites, the isotopic composition of the nitrogen liberated by stepped combustion of the Allende residue (which is typical of the CV3s) is heavier than that released by diamonds from Cold Bokkeveld (typical of the CM2/CIs) at the same stage of the extraction (figure 3.11). The temperature intervals considered were the same for both meteorites. The higher $\delta^{15}N$ in the early stages of the combustion could be interpreted as isotopic fractionation and preferential loss, by degassing, of some of the ^{14}N-enriched nitrogen, possibly as a result of a metamorphic overprint (see section 3.9).

All the samples contained minor amounts of atmospheric contamination. The nitrogen abundance was calculated correcting for such a component using the assumption that mixing occurred between air at $\delta^{15}N = 0‰$ and indigenous nitrogen at an assumed value (-351‰). A compilation of all the data accumulated (table 3.5, and represented diagrammatically in figures 3.12 and 3.13) shows that the N concentration of diamond ranges from 1984 to 13369 ppm, and is systematically variable between meteorite types. The values for the lower petrologic type meteorites are very much higher than those typically associated with terrestrial diamonds (Figure 3.19).

Meteorite	Type	ppm N (bulk)	C/N (bulk)	(σ)	C/N (plateau)	(σ)
Orgueil	CI1	7735 (n=3)	130	(8)	141	(5)
ALH 83100	CM2	8994 (n=4)	112	(9)	91	(15)
Cold Bokk.	CM2	8926 (n=4)	110	(8)	81	(14)
Murchison	CM2	7864 (n=5)	135	(14)	89	(14)
Allende	CV3	3943 (n=11)	287	(90)	265	(11)
Efremovka	CV3	3185 (n=2)	342	(97)	213	(70)
Vigarano	CV3	3668 (n=3)	290	(78)	295	(17)
Krymka	LL3.0	9730 (n=1)	103		102	(11)
Adrar 003	L3.0?*	13369 (n=2)	75	(1)	71	(16)
Inman	L3.4	3098 (n=4)	342	(83)		
Tieschitz	H3.6	1984 (n=3)	555	(158)		
Indarch	EH4	4212 (n=3)	242	(32)		

Table 3.5. Nitrogen content associated with chondritic diamond. Cold Bokk = Cold Bokkeveld. "bulk"= values summed over the diamond combustion range. * grade estimate 3.2 from TL data (Sears, 1991); 3.0 from petrologic description (Hutchison, *pers. comm*). The "plateau value" is the average C/N value over the temperature regime in which the C/N is approximately constant (*ie.* this does not include the first few steps of the combustion).

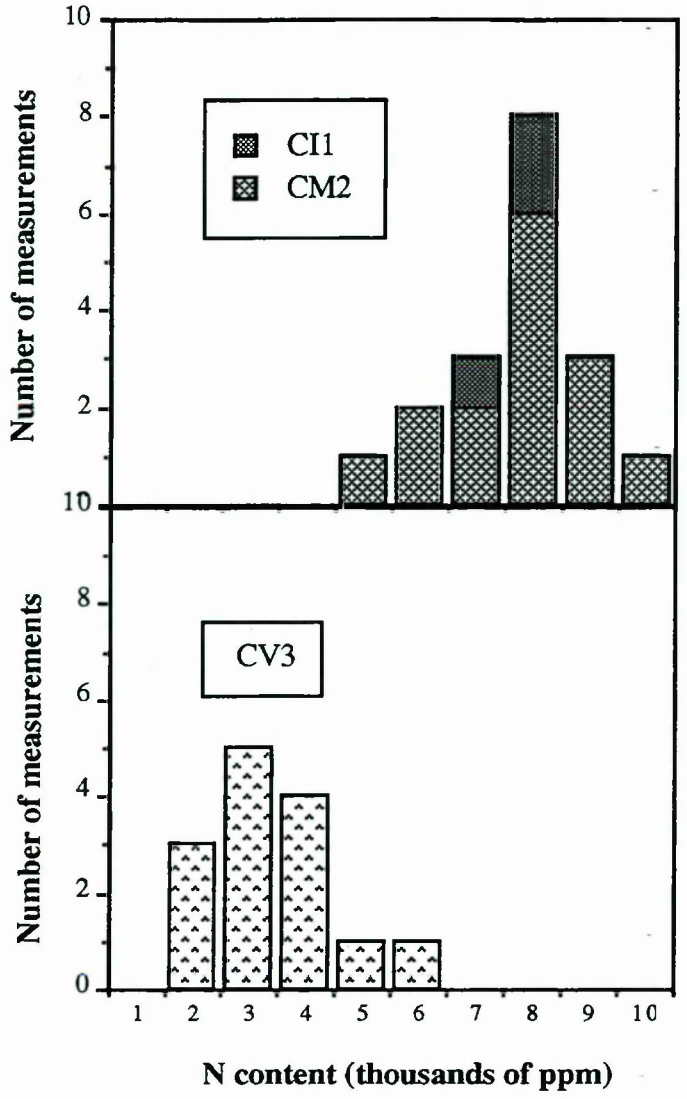

Figure 3.12. Nitrogen contents of diamond from the carbonaceous chondrites.

A comparison of nitrogen contents from the carbonaceous chondrites reveals two distinct groups (figure 3.12). The CI1 (Orgueil) and CM2s (ALH 83100, 78, Murchison and Cold Bokkeveld) have similar nitrogen contents of between 7500 and 9000 ppm (bulk value). The CV3s, however, (Allende, Efremovka, and Vigarano) contain only between 3000 and 4000 ppm. These differences cannot be explained by scatter of the data, but are statistically valid. The consistency of the nitrogen isotopic composition and shape of the yield profiles, which indicate the combustion of a single component, argues against the presence of contaminating components in quantities likely to significantly affect the nitrogen yield in some meteorites, giving an apparent difference in nitrogen content in the diamond.

The mean N content recorded for the CI/CM2 dataset is 8400 ppm N (σ = 1067), and for the CV3 dataset, 3800 (σ = 1313). The difference between the two

means is therefore 4600 with a variance of the difference equal to 418. This corresponds to a greater than 99.7% probability that the two datasets are truly different.

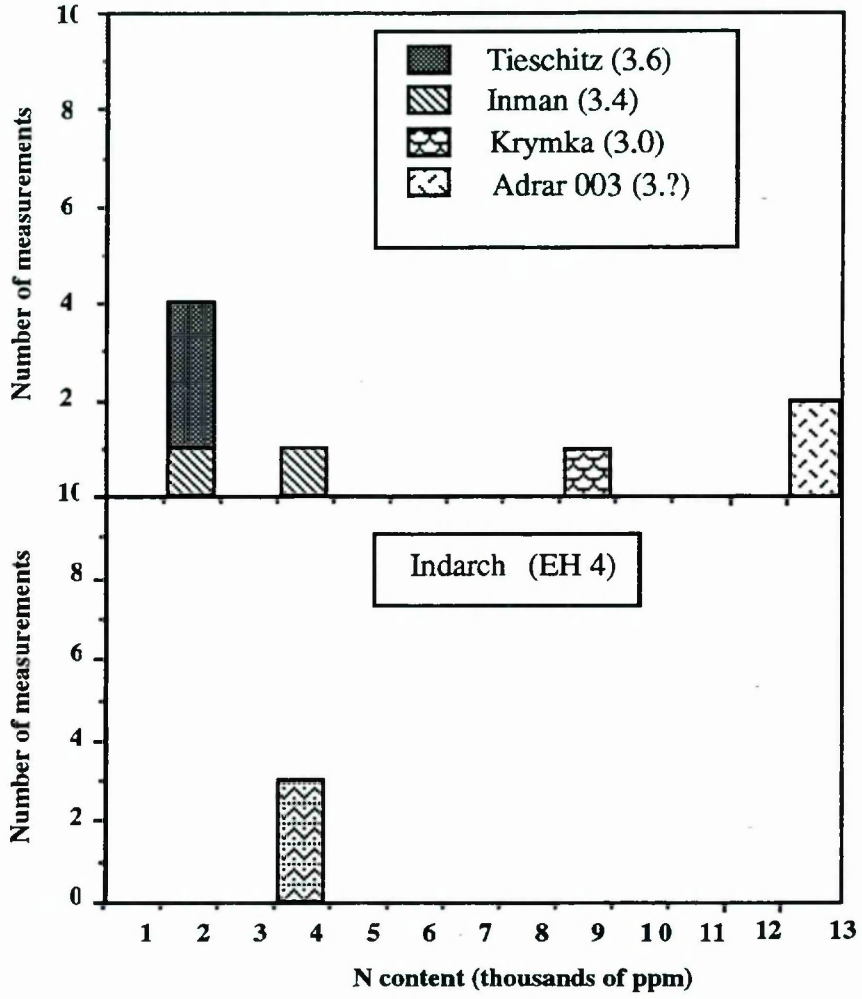

Figure 3.13. The nitrogen content of diamonds from ordinary and enstatite chondrites.

A larger range in nitrogen contents is observed in the ordinary and enstatite chondrites (figure 3.13). The lower petrologic type ordinary chondrites (Krymka and Adrar 003) have nitrogen contents as high as the CM2 and CI1 meteorites. In fact, Adrar 003 has a N content of over 13 000ppm after normalising the data, the highest value of any of the meteorites studied. The higher petrologic type ordinary chondrites, in contrast, have the lowest values recorded of all. Cδ diamond from just one enstatite chondrite (Indarch) has been studied; three measurements gave a mean of 4200ppm putting it in the middle of the nitrogen content range.

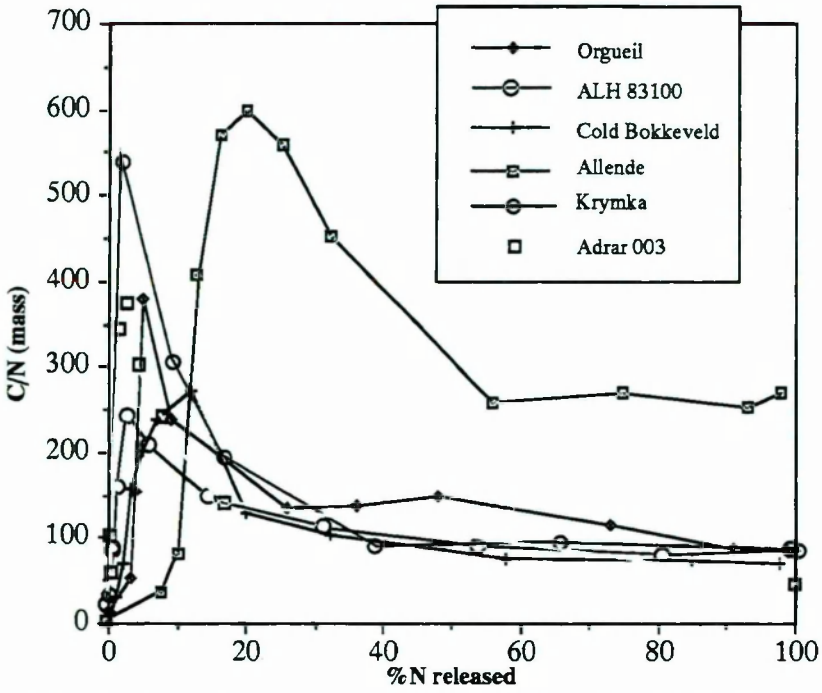

Figure 3.14. The variation of C/N during individual stepped combustion experiments

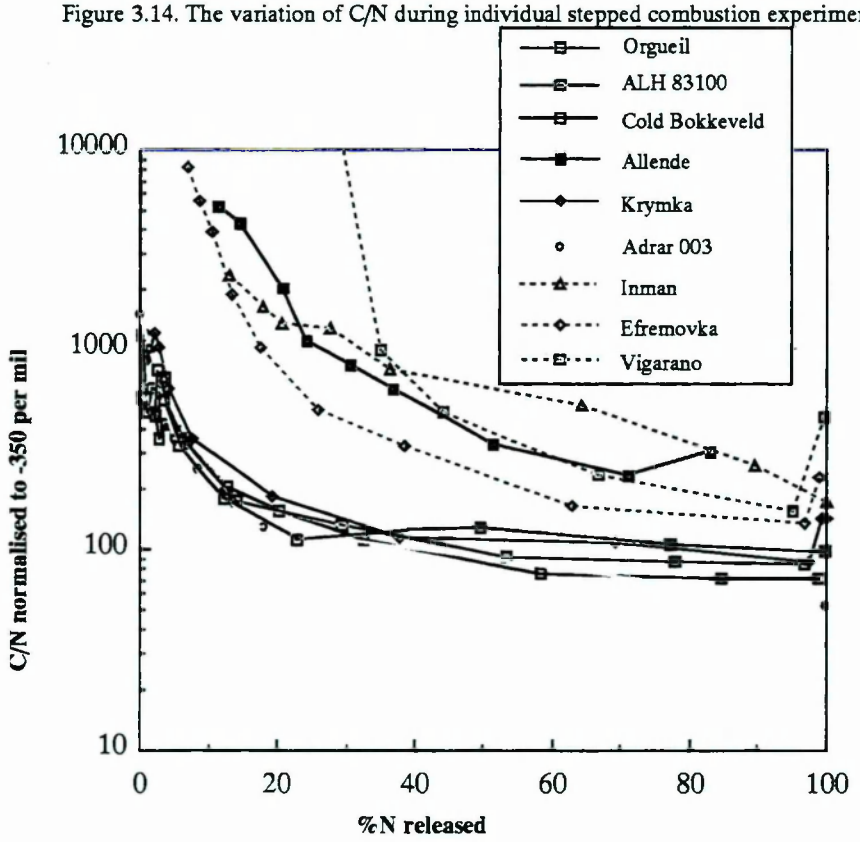

Figure 3.15. The variation of C/N during individual stepped combustion experiments, with nitrogen yields normalised to -350 per mil

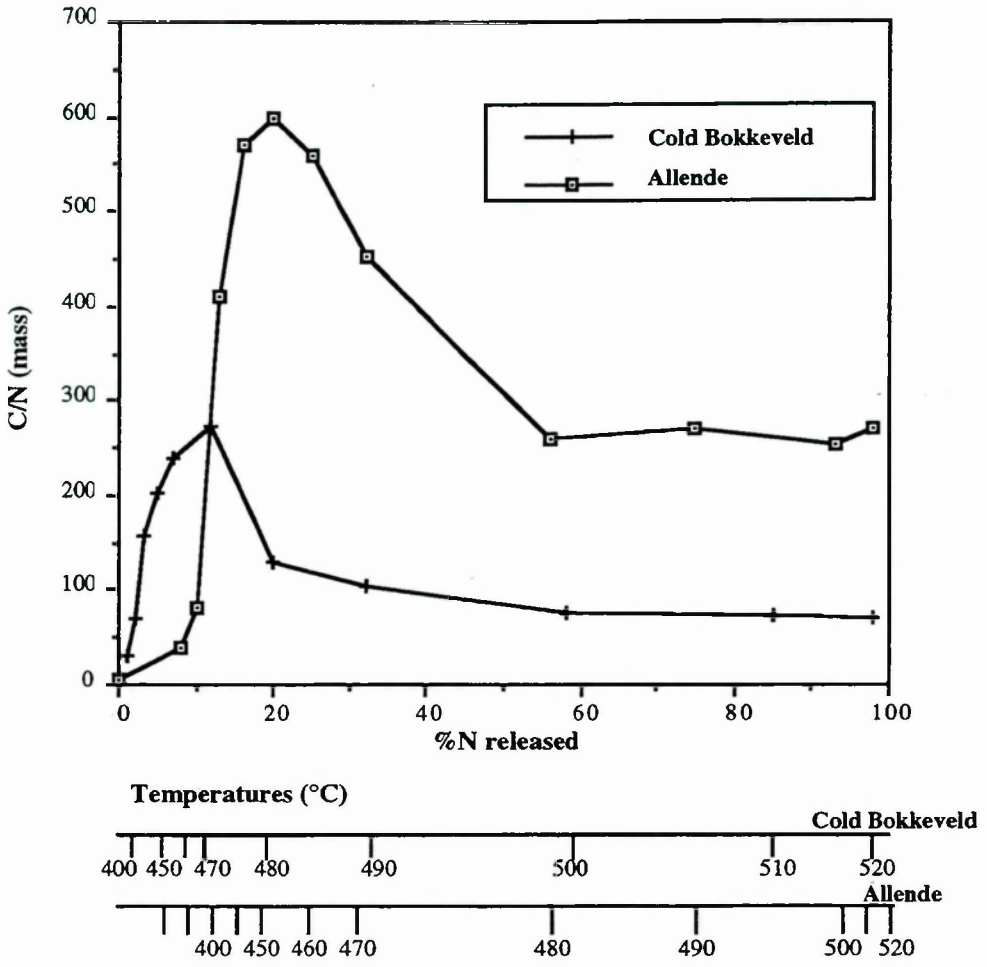

Figure 3.16. C/N ratio variations during the stepped combustion of diamond residues. Data from room temperature to the end of the diamond yield peak.

The relationship between the nitrogen and the diamond can also be studied by the careful measurement of C/N ratio variations as the experiment progresses. Figure 3.14 shows the results of all the experiments not unduly affected by blank/contamination nitrogen, plotted as the C/N variation against percent nitrogen released. The percent nitrogen released is used as an indicator of the progression of the combustion rather than temperature as this eliminates experimental artifacts due to differences in temperature, positioning of the thermocouple, oxygen pressure *etc.* Figure 3.16 shows, for clarity, only the Cold Bokkeveld and Allende experiments, which will be used as examples of a high nitrogen content and low nitrogen content diamond respectively. The Cold Bokkeveld experiment has been performed twice and the Allende experiment four times, giving reproducible results. All the samples considered show a consistent pattern with heating in that the C/N increases from low values (that is, a N-rich

component, $\delta^{15}N$ ~0‰ and $\delta^{13}C$ ~-25‰ from carbon isotope measurements, presumably terrestrial contamination) to a maximum then falls to an approximately level plateau. The low temperature component is rather more abundant than may be expected for typical laboratory contamination. It is possible that the diamond, on drying after the perchloric acid treatment becomes extremely susceptible to absorbing air/organic particles onto its activated surface. This process is analogous to the one suggested by Russell *et al.* (1990) to explain the unreplicable appearance of "recondite carbon" (Ash *et al.*, 1990) after precombustion of an Allende acid residue.

For diamonds from CI and CM2 chondrites the plateau is constant for 80% of the nitrogen released, whereas in diamond from Allende it is <70% because the peak in the C/N ratio is considerably broader. If the nitrogen in diamond concentration is calculated on the basis of the plateau C/N ratio then the abundances given in table 3.5 are obtained. These are generally higher (3185 to 13369 ppm) than abundances obtained by earlier methods which included the C/N ratio peak in the early stages of the combustion. The carbon rich combustion period followed by a plateau in the C/N ratio could be due to some parent body metamorphic degassing of the nitrogen in diamond leaving the diamond edges (which combust first) nitrogen depleted. The presence of atmospheric nitrogen can be compensated for by normalising all the data to -350‰ (figure 3.15). Although this treatment obviously ignores any real differences in $\delta^{15}N$ that may exist during combustion, it allows comparisons to be made between meteorites that have varying blank contributions (and so data from meteorites which contain diamond of very low nitrogen content have been added here). After normalising, the data shows a high C/N ratio at the beginning of the experiment, which then falls to a plateau value. The pattern is broadly similar for the CI1, CM2, and low grade ordinary chondrites, but the CV3 meteorites and Inman show extreme light nitrogen depletions. The high C/N ratio at the start of the experiment, even after normalisation, demonstrates that this C/N variation is a real effect and probably not a function of the diamond combustion mechanism.

The increased C/N ratio at the beginning of the combustion was investigated by performing a long precombustion experiment on diamond from the enstatite chondrite Indarch.

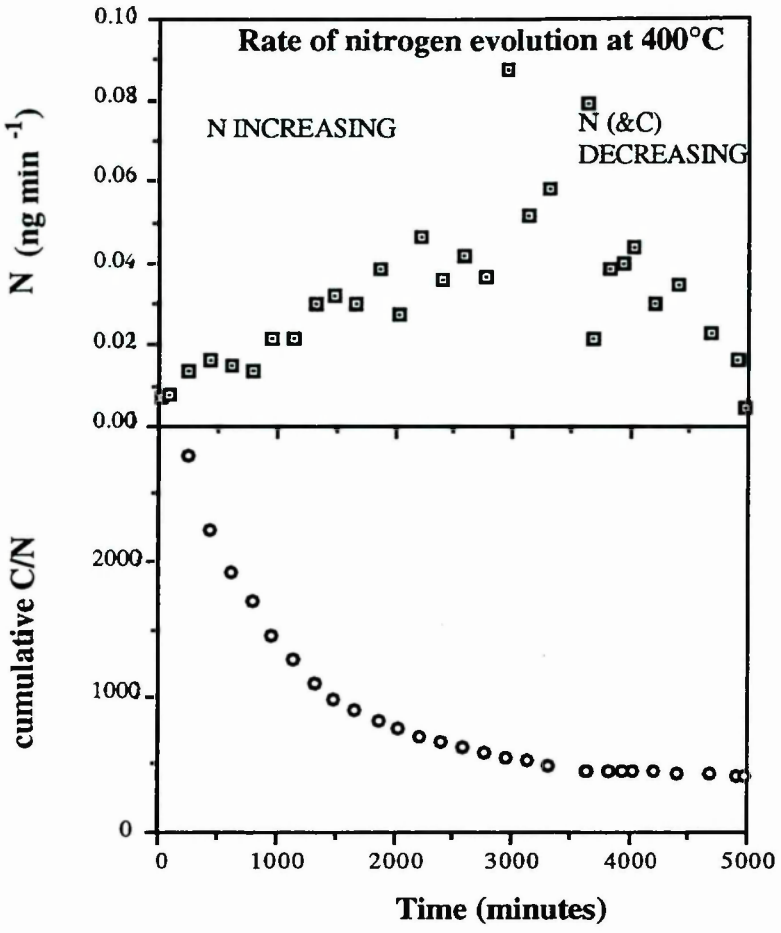

Figure 3.17. Nitrogen yield and C/N variations during a precombustion experiment on Indarch.

A residue from Indarch (~65% carbon) was combusted at 400°C for four days (figure 3.17), after several lower temperature steps had been performed to combust any organic contaminants (note these early steps have not been plotted on the figure). During this time all the carbon attributable to diamond was removed. The gas evolved was analysed approximately every 3 hours for the duration of the experiment. It would be expected that if the temperature remained constant, and the rate constant (k) remained constant, then the rate of any reaction would decrease with time as the reactants are consumed. For the first 3500 minutes (60% of the experiment) the absolute nitrogen yield (normalised to the known isotopic composition of the N in diamond: -350‰) was surprisingly found to *increase* in evolution rate as the experiment progressed despite the temperature remaining the same. After this stage the nitrogen evolution decreased with time as expected for a simple first order reaction. The situation can be seen more clearly when the nitrogen yields are normalised by plotting C/N ratio rather then nitrogen. This eliminates problems with temperature drifting etc. which would affect the reaction rate, and cancels out the effect of the N evolution decreasing because of the decrease in reactant concentration (as carbon would be

expected to decrease in supply at a similar rate). It can be seen that the C/N ratio is very high at first then declines to a constant value, as the nitrogen and carbon yield start to decrease at the same rate. This pattern mimics the effect seen during stepped combustion. There are two possible reasons for this C/N variation: either there is a less thermally resistant, carbonaceous, nitrogen poor component (another diamond type?) that combusts first, or the nitrogen evolution is blocked at the beginning of the experiment (presumably because the nitrogen is trapped in the centre of the diamond and so the surface has to be destroyed first before it can be released). Since the nitrogen yield in absolute terms increases with time, while the temperature is not increased, the second option is apparently correct, and it appears that the diamond surfaces are nitrogen depleted, possibly indicating the the diamond has been degassed to some extent.

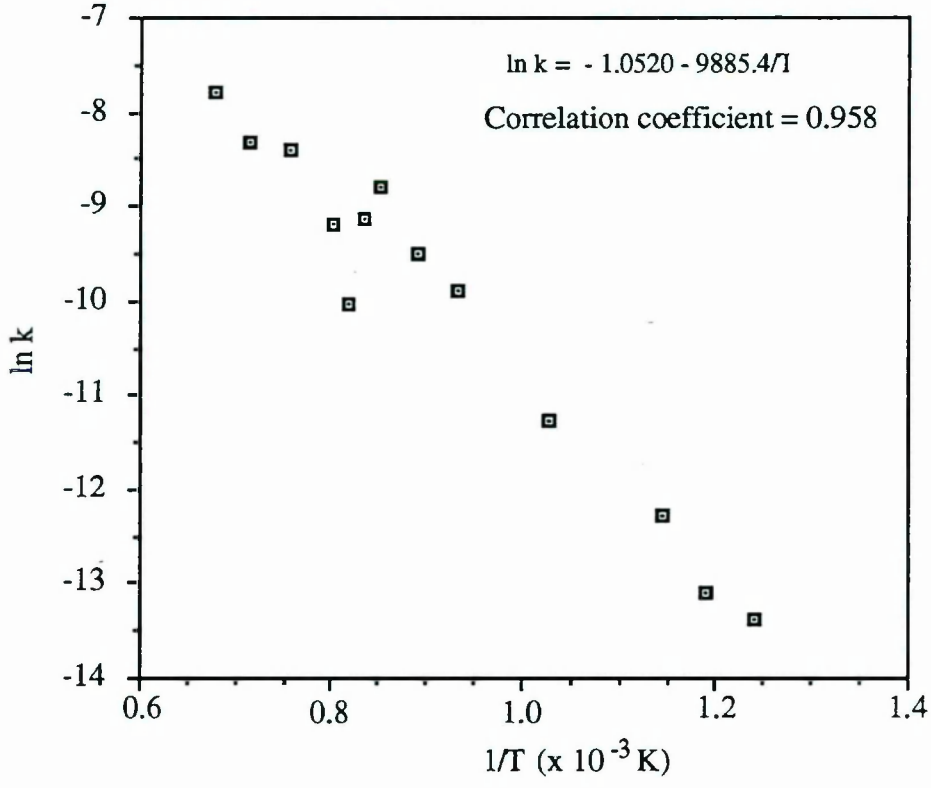

Figure 3.18. Arrhenius plot of a pyrolysis of Cold Bokkeveld diamond.

The degassing of nitrogen in the parent body has been mimicked by an experiment in which diamond from the CM2 meteorite Cold Bokkeveld was pyrolysed. Surprisingly, light nitrogen began to be released from the residue at ~300°C; the nitrogen containing grain seems improbably fragile for putative interstellar grains. An Arrhenius plot (figure 3.18) of the experiment gives a good straight line from which the constants of the reaction can be calculated (this was *not* plotted using normalised nitrogen yields). It is tempting to use these data to estimate the maximum possible temperature conditions on the parent body by extrapolating the best fit line; although an calculation of this type is bound to be oversimplistic, if it

is performed anyway as a purely academic exercise it can be estimated that the parent body must have been <-15°C for all Cδ containing meteorites if any light nitrogen was to have survived intact in the diamond. A temperature much higher than this attained for any length of time would cause the diamond to become completely degassed. This does not fit with estimated temperatures of parent bodies, especially for the more processed meteorites, which are believed to have experienced a heating event soon after accretion, and so it seems likely that the same rules did not apply during the sojourn of the diamond in the parent body. The pyrolysis data can be reconciled with the believed parameters of the parent bodies if the diamonds are assumed to have been larger when intact in the meteorite and so less prone to degassing. This conclusion could be understandable if the observations of K. Gilkes are recalled; the perchloric acid apparently reduces the grain size of the diamond from ~10nm to ~2nm. The grain size of the diamond is apparently >10nm in the less processed residues (after the chromic stage) and ~2nm in the perchloric resistant residues used in the experiment described here. Thus, it is likely that the diamonds were of the larger morphology, and so not as prone to degassing, when in their parent body.

3.9. Discussion

Isotopically anomalous meteoritic diamond has light nitrogen associated with it in very large amounts (up to >1%), making it the most abundant element after carbon that is within the lattice (Lewis *et al.*, 1991), and far more abundant in most meteorites than any natural terrestrial diamonds (figure 3.19). The high abundance of nitrogen in diamond, and the lack of positive evidence that the nitrogen is contained within the diamond lattice, has lead to the suspicion that the nitrogen is not in fact carried by the diamond at all but is in a closely associated phase. This phase would most likely be a nitride as the presence of other elements by various analytical efforts have all produced a null result. No associated phase has been observed by TEM or SEM and most known nitrides dissolve in HF or HCl so a nitride, if present , may be protected by the diamond (*i.e.* be surrounded by it), allowing it to survive, a difficult scenario to envisage considering the small grain size of the diamond in perchloric resistant residues. Furthermore, a second component has not yet been isolated from the diamond residues by either chemical or physical means. Stepped combustion of various candidate nitride materials (*e.g.* Si_3N_4, Si_2N_2O and CBN) with grain sizes of <1μm, indicate a combustion temperature of 1200° or above, much higher than that of the light nitrogen release. It is unlikely that the combustion of Si_3N_4 *etc.* could be promoted by ~700°C by exothermic burning of diamond, (see section 3.1), since SiC, a high temperature component within the residues, survives the diamond combustion. Although the

presence of a second nitrogen containing component has not been disproved, its existence seems improbable.

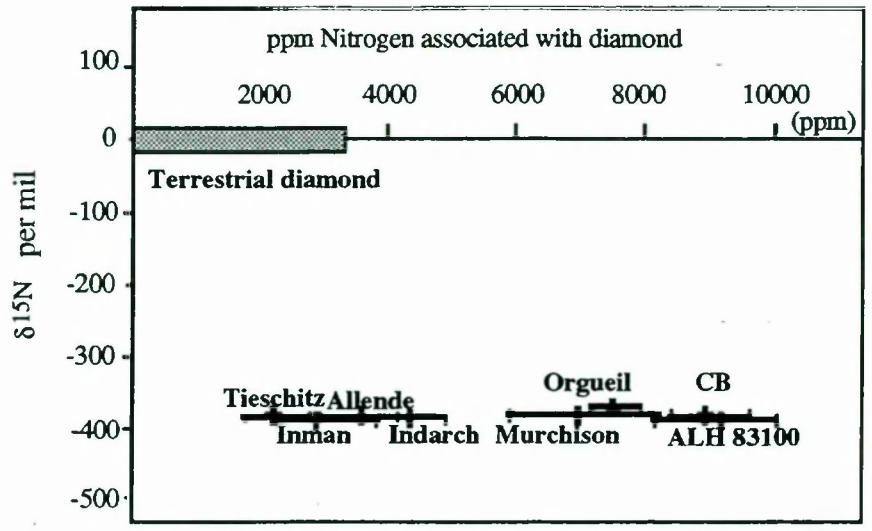

Figure 3.19. Nitrogen content and isotopic composition in terrestrial and meteoritic diamond.

The nitrogen abundance for diamond from different meteorites seems to be related to petrologic type; the higher grade meteorites have, in general, lower nitrogen contents (although there are exceptions to this rule, *e.g.* Indarch has a middle range nitrogen content despite being petrologic type 4). Below, the possibility that a petrologic relationship could be due to metamorphic degassing is discussed; alternative theories explaining the differences are then considered. The degassing of nitrogen in diamond due to metamorphism and its effect on these nitrogen content data has been investigated in the first instance by computer modelling of the nitrogen diffusion profiles; experimental heating of the diamond residues to simulate parent body metamorphism is also discussed.

3.9.1. Theoretical modelling

The computer program used for this work was written by R. Becker of the University of Minnesota and was kindly offered to the author to investigate the concept of nitrogen degassing in diamonds. It contains several assumptions: (i) that the diamonds are spherical, (ii) that the diamonds are similar in size (at 2nm in radius), (iii) that the nitrogen is originally distributed evenly throughout the crystals and (iv) that the diamonds combust in a simple way with the diamond pictured as being made up of a series of shells which are progressively destroyed as the

combustion progresses. Of course, these assumptions are somewhat idealistic, especially for chondrite diamonds that contain only a few thousand atoms, but it is assumed that if the diamond population as a whole is considered then the "average" crystal behaves in this way.

The equation describing the concentration profile for the reference species as a function of time is:

$$C(r,t) = \frac{-2C_0 a}{\pi r} \sum_{n=1}^{n=inf} \frac{-1^n}{n} e^{\left(-Dt\left(\frac{n\pi}{a}\right)^2\right)} \sin \frac{n\pi r}{a}$$

where C_0 is its initial (uniform) concentration, a is the radius of the sphere, r is the radial distance from the centre of the sphere, t is the time over which heating takes place, and D is the diffusion coefficient.

The total amount of the nitrogen remaining in the grain at time t is calculated by integrating this expression over the volume of the sphere which gives the expression:

$$M(t) = 8\, C_0 \frac{a^3}{\pi} \sum_{n=1}^{n=inf} \frac{1}{n^2} e^{-Dt\left(n\pi/a\right)^2}$$

where M is the amount of reference species.

The fraction of the original amount of nitrogen can then be calculated by dividing by the initial concentration.

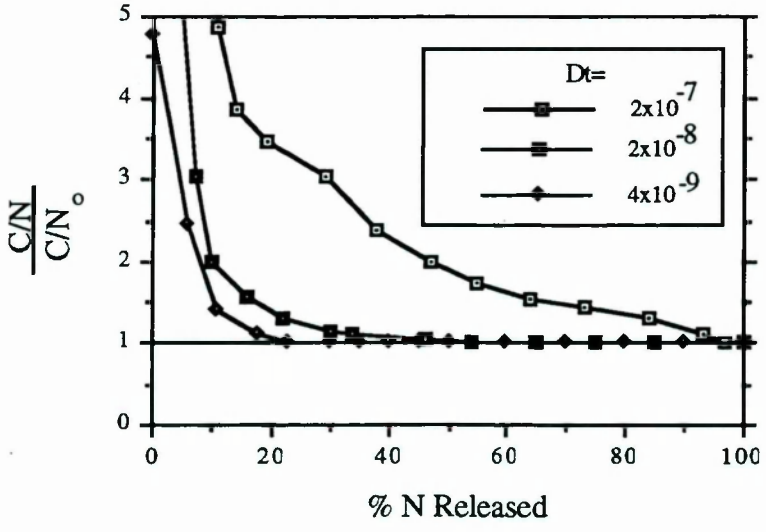

Figure 3.20. C/N variation during stepped combustion expected for diamond that has experienced increasing amounts of heating (represented by increasing Dt).

Using these equations, it can be seen that the C/N ratio of diamond would be expected to vary in a distinctive way during a stepped combustion experiment on a meteorite that had suffered thermal alteration. Figure 3.20 demonstrates the expected C/N profiles on stepped combustion for diamond that has experienced varying amounts of metamorphism. The outer layers of the diamond become nitrogen depleted on heating, and the depletion becomes more significant as the metamorphism increases (as the exact parameters of the metamorphic process are unknown, the degree of degassing is given here by Dt, where D is the diffusion coefficient and t is time). During a stepped combustion experiment the first steps of gas released -from the grain surfaces- would be N poor compared to the final steps which would release nitrogen from the centre of the diamond.

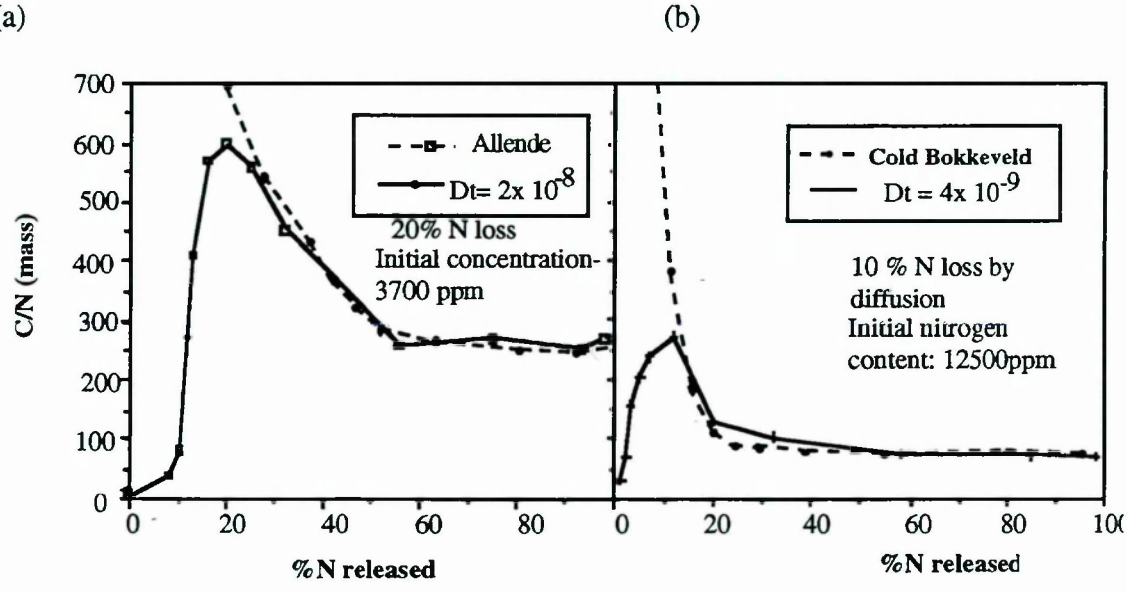

Figure 3.21. The C/N ratios of (a) Allende and (b) Cold Bokkeveld compared to the closest matching calculated diffusion profiles.

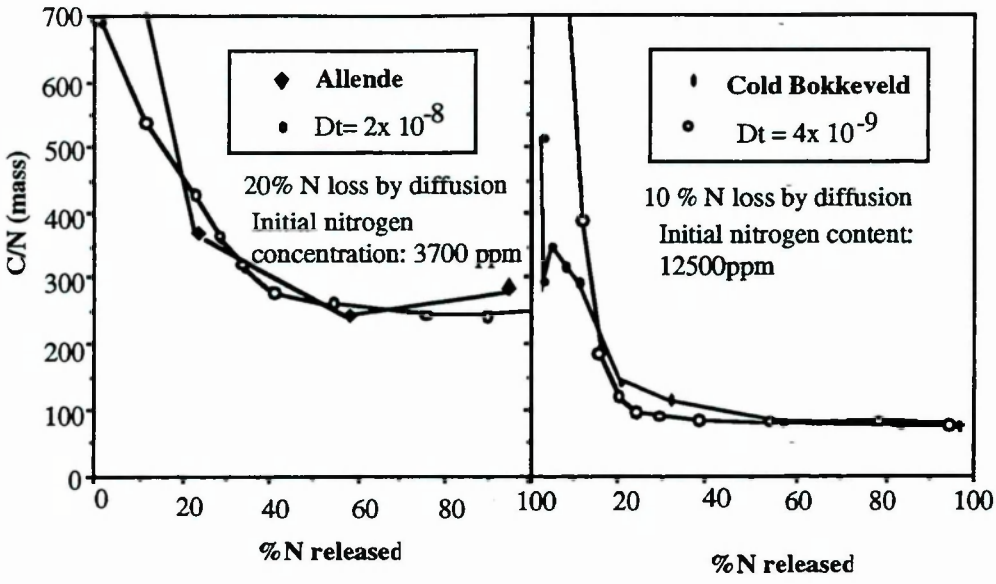

Figure 3.22. The C/N ratios of Cold Bokkeveld and Allende normalised to $\delta^{15}N$ = -350‰ compared to calculated profiles.

The profiles of nitrogen content after metamorphism bear some resemblance to those of the Cδ diamond (figures 3.21, 3.22), if the first nitrogen to be released is ignored (assuming it is atmospheric gas adsorbed onto the diamond surface). The parameters of the program can be adjusted to find the "best fit" situation. This is found to be Dt= 2 x 10^{-8} and an initial nitrogen content of 3700ppm for Allende and Dt = 4x10^{-9}, $[N]_{initial}$ = 12500ppm for Cold Bokkeveld. In order to obtain reasonable fits to the data it is therefore necessary to invoke different starting contents of nitrogen. The data can be interpreted as a loss, by metamorphic degassing, of some nitrogen, superimposed on an initial difference in nitrogen content. For Allende, this is around 20% of its original content and for Cold Bokkeveld, 10%. However, this amount is small compared to the observed inherent C/N differences of a factor of four.

3.9.2. Experimental modelling

The second way in which metamorphic effects were investigated was by degassing the diamond *in vacuo* to simulate metamorphism, followed by stepped combustion using the usual protocol. Although the laboratory conditions are clearly very different to those experienced by the diamond on the parent body, assuming a simple diffusion mechanism, the degassing of nitrogen is a function only of Dt, *i.e.* time and temperature, and is unaffected by pressure, oxygen fugacity *etc.* (although of course these will damage the diamond in other ways, probably

destroying them completely). Experimental pyrolysis at high temperatures (800-850°C) will therefore affect the nitrogen distribution in the same way as heating at lower temperatures for a longer time if the diamonds are in a similar form (ie. of the same size, shape and crystallinity) in the residues as they are in the parent body. A sample of the Cold Bokkeveld residue was therefore heated at 850°C until around 70% of the nitrogen had been released. The residue was then step combusted as usual. The step combustion yielded the most nitrogen during the 490°C step, a slightly lower temperature (10-20°C) to the unheated residues, and the isotopic minimum was just -315‰, 32‰ larger than the uncorrected mean value of Cold Bokkeveld diamond, and almost 2σ from the mean value of the dataset from all the meteorites (figure 3.23). This fractionation agrees well with that expected from theory. The difference in $\delta^{15}N$ between the degassing and pristine samples indicates that, as expected from the calculations discussed above, degassing of nitrogen causes an isotopic fractionation that is large enough to be detectable.

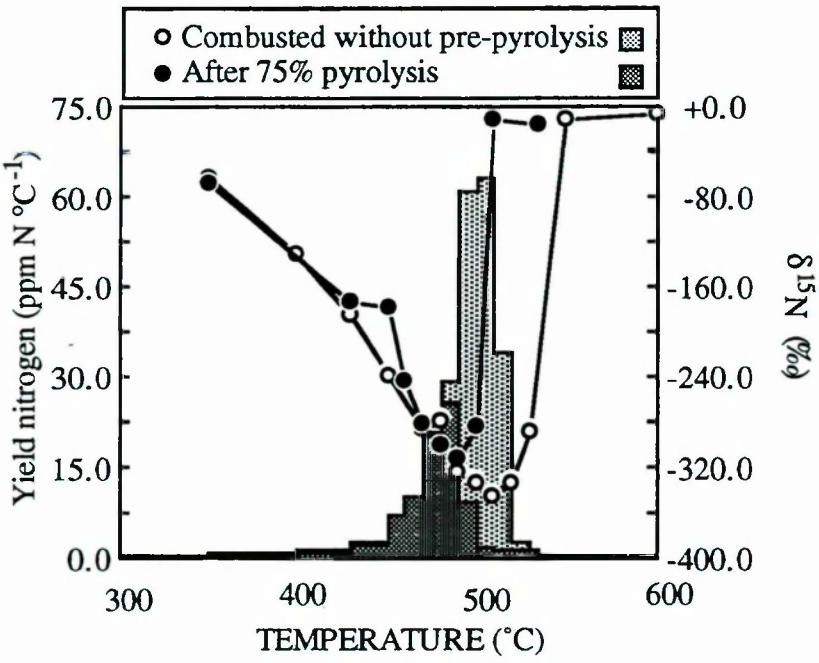

Figure 3.23. A comparison of the nitrogen release profile and nitrogen isotopes during stepped combustion of a diamond residue from Cold Bokkeveld that has been partially pyrolysed with an untreated sample.

The C/N *vs.* %N plot for this experiment (figure 3.24) demonstrates the higher C/N ratio overall of the sample after the nitrogen has been partially pyrolysed. In the first steps of the experiment, the pyrolysed sample mimicked the behaviour of the sample that had not been previously heated. In the later steps, the C/N ratio increased to 2-3

times the C/N value of the untreated residue, at the same stage of the combustion.

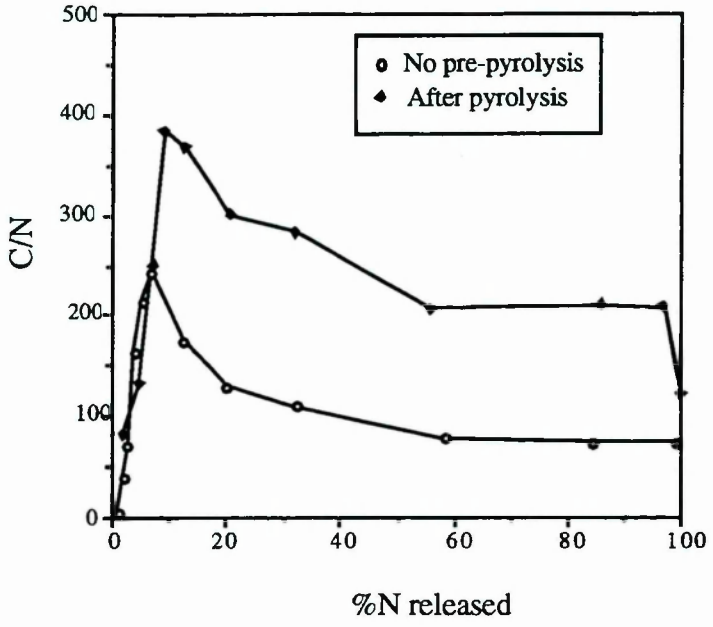

Figure 3.24. Comparison of the C/N ratio variations during combustion for pre-pyrolysed and untreated sample of diamond from Cold Bokkeveld.

3.9.3 Alternative explanations to degassing

There is evidence that diamond is only slightly degassed, and this cannot account for the observed differences in nitrogen content, that would require degassing of 80% of the nitrogen from the crystals. The lack of degassing is in some ways surprising as the diamond releases its nitrogen very easily during pyrolysis under laboratory conditions and this suggests that either the parent body was very cool or the diamond was in a more robust form (*e.g.* bigger) for most of its history. Since degassing provides a poor explanation for the observed differences, three alternative possibilities will be discussed.

(i) Heterogeneous distribution of diamond from different sources in the Solar nebula

Possibly the simplest explanation for the differences in nitrogen content is that the total population of diamonds in meteorites at the time of their accretion contained inputs from many different diamond sources, each having variable nitrogen contents. The different nitrogen contents seen in meteorites of different types would then suggest that they were originally distributed heterogeneously in the Solar nebula. Ion probe studies of SiC have shown that these interstellar grains may have come from a variety of stellar sources (*e.g.* Zinner *et al.*, 1989) indicated by the diversity of carbon and silicon isotopic compositions of separate

grains. It is thus quite possible that diamond also has a variety of sources. One would however expect some variation in nitrogen isotopic composition - and a greater spread in carbon isotopes- unless fortuitously the diamonds from different sources had similar isotopic characteristics. It is interesting to note that the mean carbon isotopic composition of SiC is constant between meteorite types (see chapter 6) indicating that the grains from separate sources were well mixed in the Solar nebula before its condensation. There is, however, strong evidence that the Solar nebula was *not* perfectly mixed before condensation. The oxygen isotopic compositions of meteorites from different groups show differences that cannot be due to fractionation (Clayton *et al.*,1976) and so reflect primitive Solar system heterogeneities. However, these differences are most pronounced between different chemical groups, which are believed to have been spatially separated in the early Solar system. The differences observed in nitrogen content in diamond are more difficult to explain in this way as the nitrogen contents appear to be related to petrologic rather than chemical type, with the least heated carbonaceous meteorites (the CM2s) having a similar nitrogen content to the least altered ordinary chondrites.

(ii) Single source of diamond with preferential destruction of the nitrogen rich crystals

The destruction of the diamond as a metamorphic process has been suggested (Huss, 1990) on the grounds that the diamond content of ordinary chondrites diminishes as a result of petrologic type. An extension of this theory is that some diamonds may be more resistant than others to metamorphism, and it seems likely that diamonds which are rich in nitrogen will be less resistant to destruction (Fishenko *et al.*, 1992). If it is assumed that the diamonds contain only ~2000 carbon atoms, then the average number of nitrogen atoms per crystal would be around 20, although clearly the crystals will show a range in the number of nitrogen atoms they contain. A property of the grains with a high nitrogen content will be that they will have many structural defects, making them structurally unstable, and so will be more vulnerable to metamorphic events during parent body processing. If the high N content diamond crystals are destroyed preferentially, then the overall nitrogen concentration of the diamonds from more metamorphosed chondrites would be lowered, without unduly affecting the nitrogen isotopic composition, provided the nitrogen isotopic composition is not dependant on nitrogen content. This theory elegantly explains the dependence of nitrogen content on petrologic type, which can be seen as a relationship between the nitrogen content of the diamond and its abundance normalised to matrix content (figure 3.25), and also the apparent consistency of the Xe content in diamond (Huss, 1990); although this correlation has still to be

fully established for meteorites from a variety of metamorphic grades. It could be argued that because the Xe probably exists as isolated atoms then the lattice deformities may be less for each Xe atom.
It is also worth considering that the parent body heating may actually anneal the more stable thus making them even more robust.

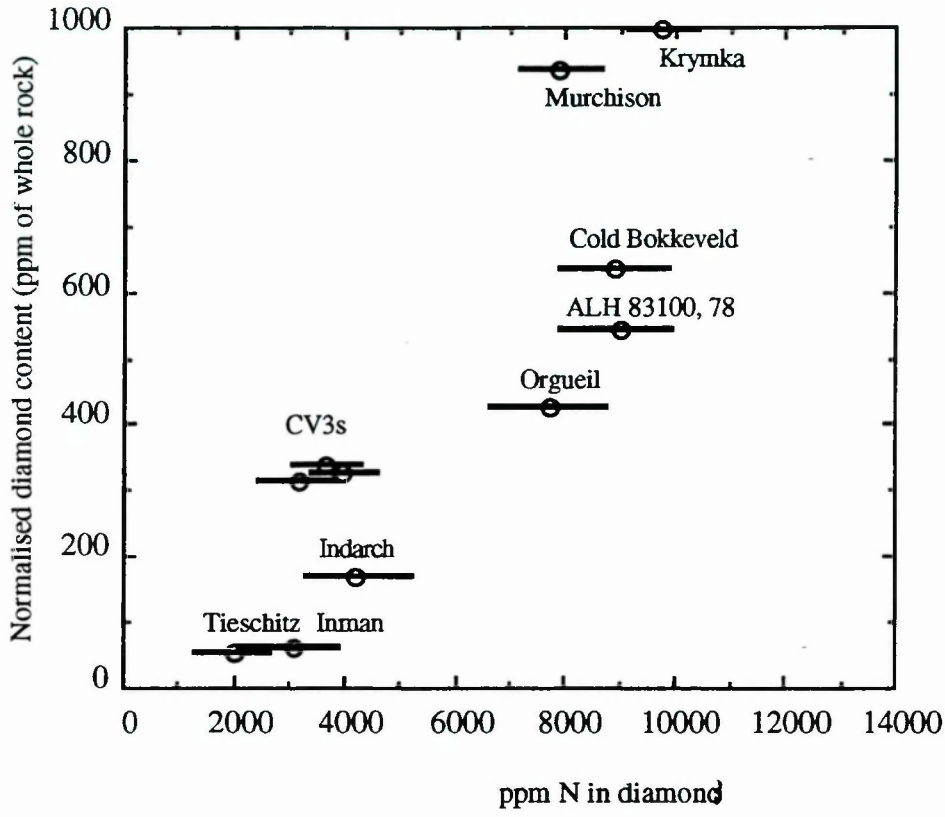

Figure 3.25. Correlation between nitrogen content of the diamond and their abundance in the whole rock meteorite normalised to matrix content. (Adrar 003, the meteorite with the highest ppm nitrogen in the diamond has been excluded as its matrix concentration is not known).

The nitrogen content is related to diamond abundance after subtracting the portion of the bulk that is made up of non- matrix (*i.e.* by matrix normalisation) using the very approximate equation:

nitrogen (ppm in diamond) = 14 x diamond abundance (ppm)

(iii) Multiple sources of diamond and preferential destruction of nitrogen-rich crystals

There are a few difficulties with the argument outlined above. Differences in nitrogen content of a factor of at least four between the most and least

metamorphosed meteorites cannot be achieved if a normal distribution of nitrogen contents is assumed (figure 3.26a), even if the metamorphic destruction is dependent only on the nitrogen content of the diamond, which is a very unlikely scenario in reality. The mean nitrogen content of the surviving diamond can be lowered by broadening out (*i.e.* increasing σ) of the distribution, but even if it is made completely flat (figure 3.26b), which in reality would be an impossible case, the mean nitrogen content of the grains is still just 25% of the original value. Further, it is not possible to determine a skewed or distorted distribution that could give the necessary depletion in nitrogen content. The easiest way to explain the relationship between diamond content and nitrogen concentration is to assume that more than one diamond population is involved, giving a bimodal (3.26c) or multimodal nitrogen content distribution.

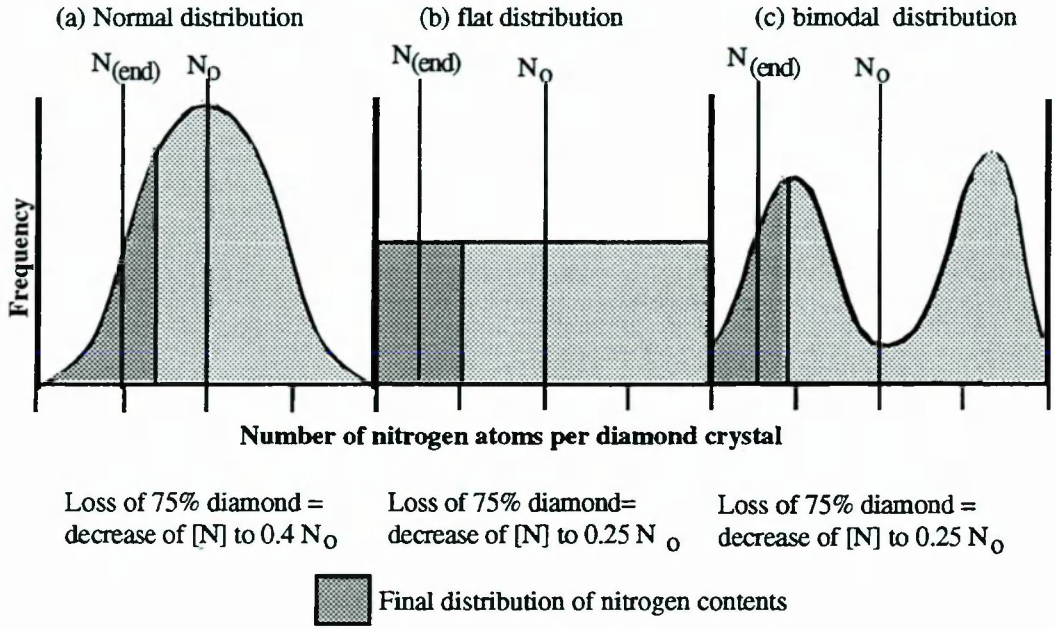

Figure 3.26. The effect of 75% metamorphic destruction of the most nitrogen rich grains on three original distributions of nitrogen concentration in the diamond crystals.

TEM evidence (figure 3.4) suggests that the diamond crystals may be much larger than previously suspected, and that the percentage differences in nitrogen content expected in individual crystal would be far less for diamond (such as those depicted in figure 3.4), that are ~10nm across, containing around 57000 carbon atoms and ~570 nitrogen atoms. If this many nitrogen atoms are involved then a broad normal distribution of nitrogen concentration such as that shown in figure 3.26a, with some grains containing twice the mean value, and some almost none, is far less likely. Furthermore, there is a correlation between the nitrogen content of the diamond and its $\delta^{13}C$ (figure 3.27). To explain this using the above theory, then the nitrogen poor diamond is isotopically heavier than diamond with

a high nitrogen content. It is difficult to see how this could be achieved in a single environment, unless this was highly stratified. Unfortunately, if the He burning layer in a supernova is the assumed source of the diamond, then it would be stratified in the opposite sense to help us here. The ^{12}C source (the convective shell) is directly below the nitrogen rich radiative layer, and this upper layer is the source of ^{13}C. So it would be expected that nitrogen rich diamonds would be associated with *heavier* carbon.

Therefore the data are most easily explained if it is assumed that the diamond is made up of two or more sources with variable nitrogen contents: figure 3.26c. This is most easily rationalised with the constant $\delta^{15}N$ value recorded for all the meteorites if one source is nitrogen rich and one nitrogen free.

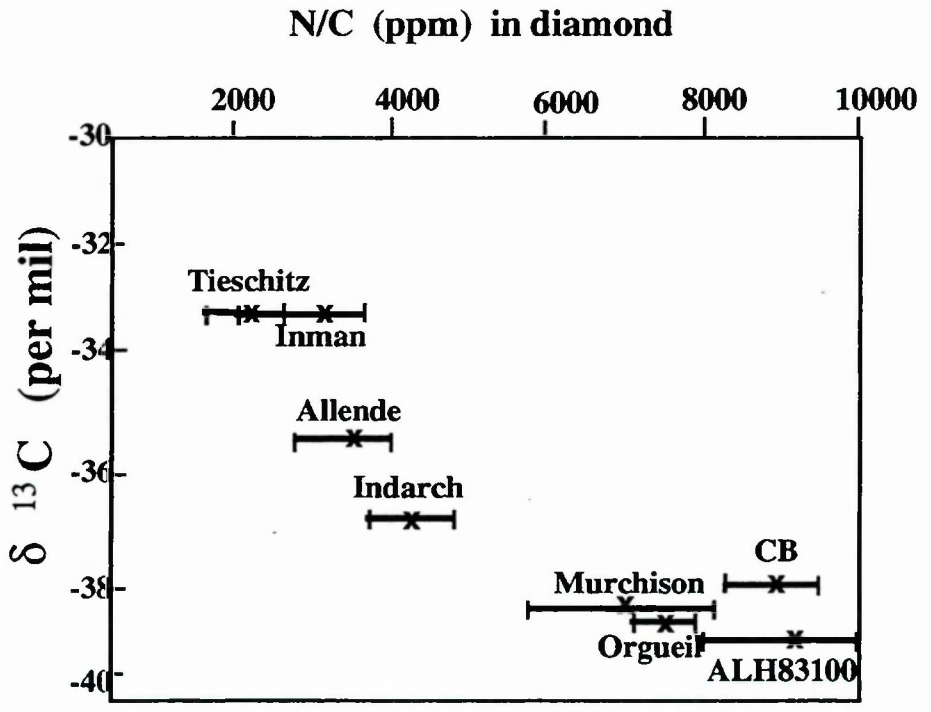

Figure 3.27. The relationship between carbon isotopic composition and nitrogen content of the diamond.

The multiple sources idea is explained diagrammatically in figure 3.28, using the simplification that only two populations are involved, although the model could be expanded to include several. One of these sources ("Population B") has to be a primitive interstellar grain, to account for the presence of Xe-HL. This diamond is isotopically light, and extremely nitrogen rich. In the early solar nebula, it was mixed with a second (or more) diamond type(s) ("Population A") that contains little nitrogen and has a carbon isotopic composition of around -25‰. Since it

contains no isotopically anomalous carbon or nitrogen, it may be a primitive solar system condensate rather than a circumstellar grain. The diamond populations would be well homogenised in the nebula (as the SiC grains apparently were) and a similar mixture incorporated into all the parent bodies, to account for the similarity between the most primitive ordinary and carbonaceous chondrites. During parent body metamorphism, the fragile, nitrogen rich population B grains are more easily destroyed and so the diamond characteristics as a whole moves towards the population A composition, becoming heavier in carbon isotopic composition and depleted in nitrogen. Because population A is nitrogen poor, this is achieved with little change in the nitrogen isotopic composition. Of course, the two or more populations do not need to be diamond; the choaite observed in the TEM (section 3.6) could, for example, form one of the populations of carbonaceous material.

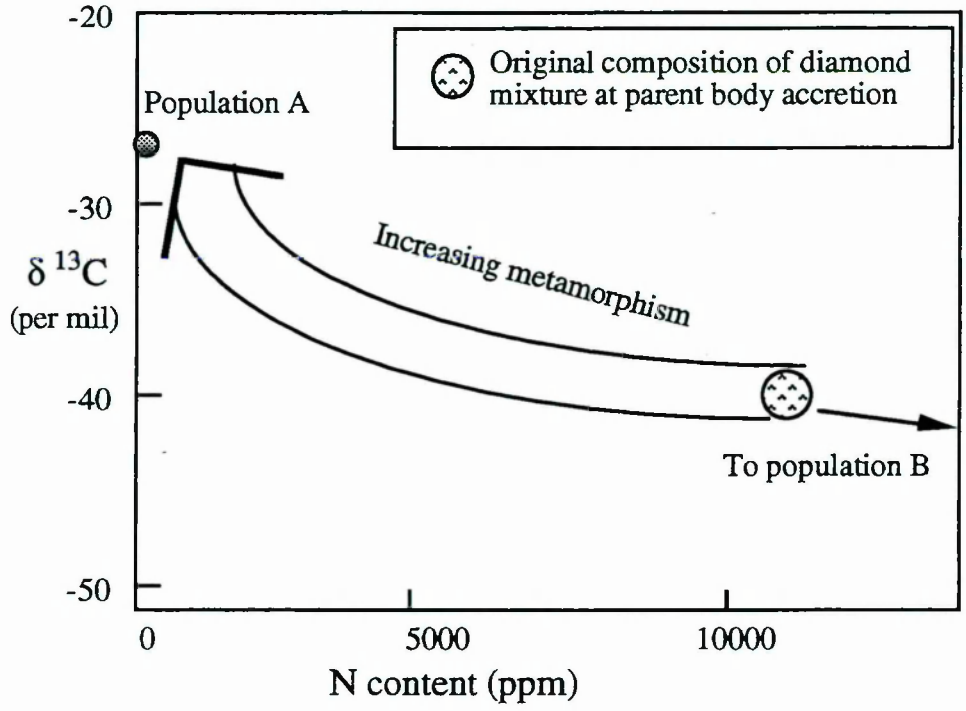

Figure 3.28. An explanation for the observed differences in carbon isotopic composition and nitrogen content in diamonds from primitive chondrites.

This theory can account for many of the diamond observations listed in section 3.4. It can also explain the differences in carbon isotopic composition and C/N ratios between meteorite groups that have experienced different amounts of thermal alteration. The high abundance of diamond in meteorites may reflect their dilution from a native source, which would also account for the normality of the carbon isotopes. The $\delta^{13}C$ of the true presolar component, population B, is in fact lighter. This is in the right sense to help Clayton (1989) to mass balance the mixing of the different supernova layers. The actual carbon isotopic composition of population

B is limited by the amount of nitrogen that can be held in the diamond structure; the more N that can be incorporated into the crystal, the further the line on figure 2.28 can be extrapolated to low $\delta^{13}C$ values. If the nitrogen is held as line defects (section 3.8.1), then this may allow large concentrations of nitrogen to be contained within the diamond with minimal lattice distortion. Kalish *et al.* (1991) have investigated the concentration of nitrogen that can be incorporated in to CVD diamond like films and induced a maximum of 10% nitrogen in the lattice. This would give a $\delta^{13}C$ of the presolar component of ~-175‰.

A Solar system component can also help to explain the presence of relatively "unanomalous" strontium and barium associated with the diamond, and could help explain the planetary noble gases although the difference in release temperature between the normal and exotic noble gas signatures would need to be rationalised.

Huss (1990) has suggested that the diamonds are destroyed during metamorphism and that this is reflected in the overall abundance of the diamonds in the parent meteorite. If the above theory is correct, then it may be expected that a relationship between the nitrogen content of diamond and their overall abundance in the meteorite exists, if it is assumed that the abundance of the diamonds was similar in all meteorites at the time of their accretion (Huss, 1990). It can be seen from figure 3.24 that this relationship does indeed broadly apply, although small variations in the trend could be from heterogeneous accretion of the diamond by the parent bodies.

3.9.4. Thoughts on the Origin of the Light Nitrogen

The most widely accepted theory for the production of light nitrogen is that it is a primitive nucleosynthetic product. ^{14}N is produced in many stellar environments, but not the ones in which either Xe-H or Xe-L are formed. In supernovae, the radiative He burning layer is believed to be especially important (Clayton, 1989) in producing nitrogen by CNO cycling. However, a study of the nitrogen in diamond would not be complete without a consideration of other possible sources.

The xenon associated with the diamond is widely believed to be presolar in origin; and by association the nitrogen is often thought to be a primitive nucleosynthetic signature. However, the possibility of a solar origin for the nitrogen must be investigated. The Solar wind nitrogen is believed by some authors to have become progressively heavy as the Solar system has aged with an original value of around -200‰ (Kerridge, 1975), and so diamonds formed early in the Solar system may be expected to be unusually isotopically light. Moreover Ash (1990) has shown

that diamonds formed by CVD can contain nitrogen that has been extremely fractionated (by up to 200‰); there is also other evidence that nitrogen fractionation in the Solar system can be extreme (*e.g.* Arrhenius *et al.*, 1978; Manuccia and Clark 1976). Is it conceivable, therefore, that the nitrogen is not presolar at all but the product of unusual solar processing?

^{14}C is an unstable nuclide that decays with a half life of 5760 years to ^{14}N. A possibility that needs to be addressed is whether the nitrogen in Cδ diamond is a decay product of this reaction:- this may make the extremely high concentration of nitrogen in the diamond easier to understand. However, close examination of the data makes this theory seem unlikely. An enrichment of ^{14}C (presumably formed in stellar environments which have a high neutron flux) would be expected to be accompanied by an enrichment also in ^{13}C, which is not seen. Also, combustion steps with a high C/N ratio would be expected to be the most enriched in ^{14}N, and it should in fact be possible to plot an isochron of the $^{14}N/^{15}N$ versus C/N. In reality, the reverse trend is seen, with the lightest combustion steps usually being comparatively nitrogen rich (an effect attributed to degassing in this thesis).

Since there is strong evidence that Xe-HL originated in a supernova, it can only be assumed that the nitrogen is also a primitive isotopic signature until any other evidence is revealed. However, if the diamond is found to be from a mixture of sources, then the presolar, supernova component is not necessarily the one that contains the light nitrogen signature.

3.10. Conclusions

This aim of this chapter was to provide a detailed characterisation of the carbon and nitrogen in isotopically anomalous diamond from chondritic meteorites. The carbon isotopic composition of the diamond was found to vary systematically between meteorites types by around 6‰, from -38 to -32‰, and although it is known that there are no other major carbonaceous phases in these diamond rich residues, the possibility that the differences are due to the presence of a small amount of isotopically anomalous carbon cannot be ruled out. The nitrogen isotopic composition in contrast is constant within the instrumental precision, (although a study on a more sensitive instrument may reveal small differences) whilst the nitrogen content varied between meteorite types by a factor of four. The size of the diamond has been shown by Gilkes *et al.*, (1992) to be much bigger than previous measurements which were based on the appearance of the diamond after they had been through harsh acids treatments.

Although it still has to be proved that the nitrogen is truly a trace element in the diamonds, ESR data suggest that this is the case, and TEM has yet to discover other more likely hosts. The high content of nitrogen can be explained adequately by the presence of nitrogen in line defects, which may imply that the diamond was formed in an environment with high levels of radiation. The origins of the nitrogen are not known. The extreme enrichment in ^{14}N may indicate a nucleosynthetic product ,*e.g.* from CNO cycling, but early Solar system processes cannot be ruled out as a source of light nitrogen. From this it follows that only the very rare xenon is almost certainly a circumstellar grain tracer.

There is evidence that some degassing of nitrogen from diamond has occured in all the meteorites (10 to 20%) but this effect is superimposed on a more substantial difference in nitrogen content. This can be explained in several ways: the most likely is that the difference is due to a mixing between diamond of two or more types, one extremely nitrogen rich and isotopically light, the other almost nitrogen free and with $\delta^{13}C$ close to -25‰, with the nitrogen rich source being less resistant to metamorphism. One explanation that is compatible with all the carbon and nitrogen data is that the diamond is made up of a supernova component and a solar-like component, (or more than two components), or the data has been influenced by an additional carbonaceous component (such as a carbyne). The supernova component (presumably containing all the Xe-HL) would be the site of all the light nitrogen and have a lighter isotopic composition than -38‰. This would be in the right sense to help Clayton (1989) (see section 3.4) mass balance the mixing of the $^{14}N + ^{13}C$ containing radiative He burning layer and the ^{12}C containing convective layer. The other "solar" diamond component would contain very little nitrogen and possibly no isotopic anomalies at all.

It is unsurprising that there is a possibility of diamond containing more than one component given that SiC, for which individual grains can be analysed, is believed to come from several sources. Indeed, given the high abundance of diamond in primitive chondrites, their Solar system like carbon isotopic composition and their apparently easy formation in many environments (e.g. Badziag *et al.* 1990; Jansen *et al.* 1990), it would seem unlikely that the diamonds originate in a single source. However, their "log-normal" size distribution (Lewis *et al.*,1989) has been used as evidence that only one formation environment was involved. If the presence of more than one source for the diamond is acknowledged then, since only one in two million diamonds contains a Xe atom, the xenon containing crystals may represent a small input from a very specific stellar source.

CHAPTER 4

DIAMOND AND OTHER ACID-RESISTANT COMPONENTS IN THE ABEE METEORITE

4.1. The Abee Meteorite

Abee is an EH4 enstatite chondrite, 47cm across, which fell in Alberta, Canada, on June 9th, 1952 producing a hole 2 metres deep and 1 metre in diameter in a wheat field belonging to a H. Buryn (Dawson *et al.*,1960). At 107kg (Millman, 1953), it is the largest enstatite chondrite that has yet been identified. Although strictly classified as an EH4, the presence of ortho- rather than clino- pyroxene is more reminiscent of a E5/E6. The stone consists of clasts (often metal rimmed), dark inclusions and matrix. The clasts and matrix have been thermally metamorphosed (at up to 900-1000°C) whereas the dark inclusions are less heated, implying that the main metamorphic event occurred before the breccia consolidated (Rubin and Keil, 1983). Carbon contents of enstatite chondrites are high, ranging from 0.15 to 0.70 wt%; Abee contains 0.42 wt% carbon, with a bulk $\delta^{13}C$ of -13.4‰ (Grady *et al.*,1985). Most of the carbon is in the form of graphite, which is particularly abundant in the silicate rich parts of the meteorite, as laths or lath clusters that are 1-3mm wide and 10-50 mm long (Rubin and Keil, 1983). In addition, organics and C dissolved in metal phases make significant contributions to the carbon inventory (Grady *et al.*, 1985).

A study was undertaken on the Abee meteorite to determine its interstellar grain inventory. As a more metamorphosed meteorite than the enstatite chondrite Indarch, it was not expected to contain diamond and silicon carbide in abundance. In particular, a previous study by Huss and Lewis (1990) had reported Abee to be free of Xe-HL, the Cδ noble gas tag, and so the presence of diamond in the meteorite was not expected. A sample was obtained that had been sawn as a slab from the interior of a larger fragment some time before 1960. Because the sample had been cut, probably by a diamond saw, a special effort was made to ensure that it was not contaminated by diamond from this operation. The surfaces of the Abee slab were etched for 5 minutes in 9M HF/1M HCl acid so that an initial mass of 86.8g was reduced by 1.4g. The residual block of meteorite was ultrasonicated in water, washed in acetone, dried, broken into chips, and processed according to the standard procedure for isolating

chondritic diamonds. After treatment with HF/HCl, CS_2, $Cr_2O_7^{2-}$, and $HClO_4$, a yield of 134.5 ppm of insoluble residue remained.

4.2. Diamonds in Abee

Four analyses showed that carbonaceous material made up an average of 78.3% by weight of the acid insoluble residue; the remainder was found, using TEM and X-ray diffraction, to be mainly oxide minerals. A scanning electron microscope investigation revealed crystals that were typically between 100 nm and 1 μm across, rather than of nanometre dimensions as for the "Cδ" diamond (chapter 3); the exact grain size distribution is discussed in more detail in section 4.3. Most crystals were clumped into rounded aggregates of 20 μm in diameter (figure 4.1). Electron diffraction data (table 4.1) demonstrated that these grains were diamond. Transmission electron microscopy showed that the diamonds have a face centred cubic structure, both platy and lath shaped crystals were evident (figure 4.2 a and b). Powder X-ray diffraction confirmed the electron diffraction results, giving a pattern consistent with well-crystalline cubic diamond (figure 4.3).

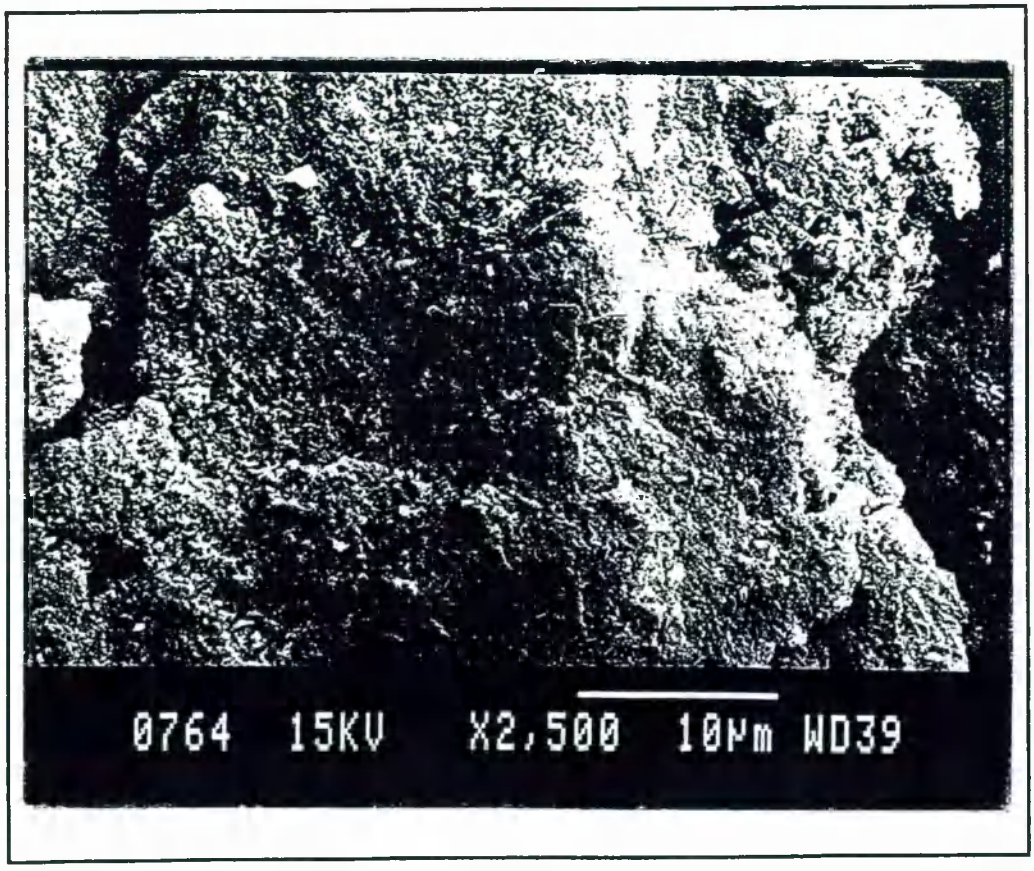

Figure 4.1 SEM photomicrograph of a cluster of diamond from Abee.

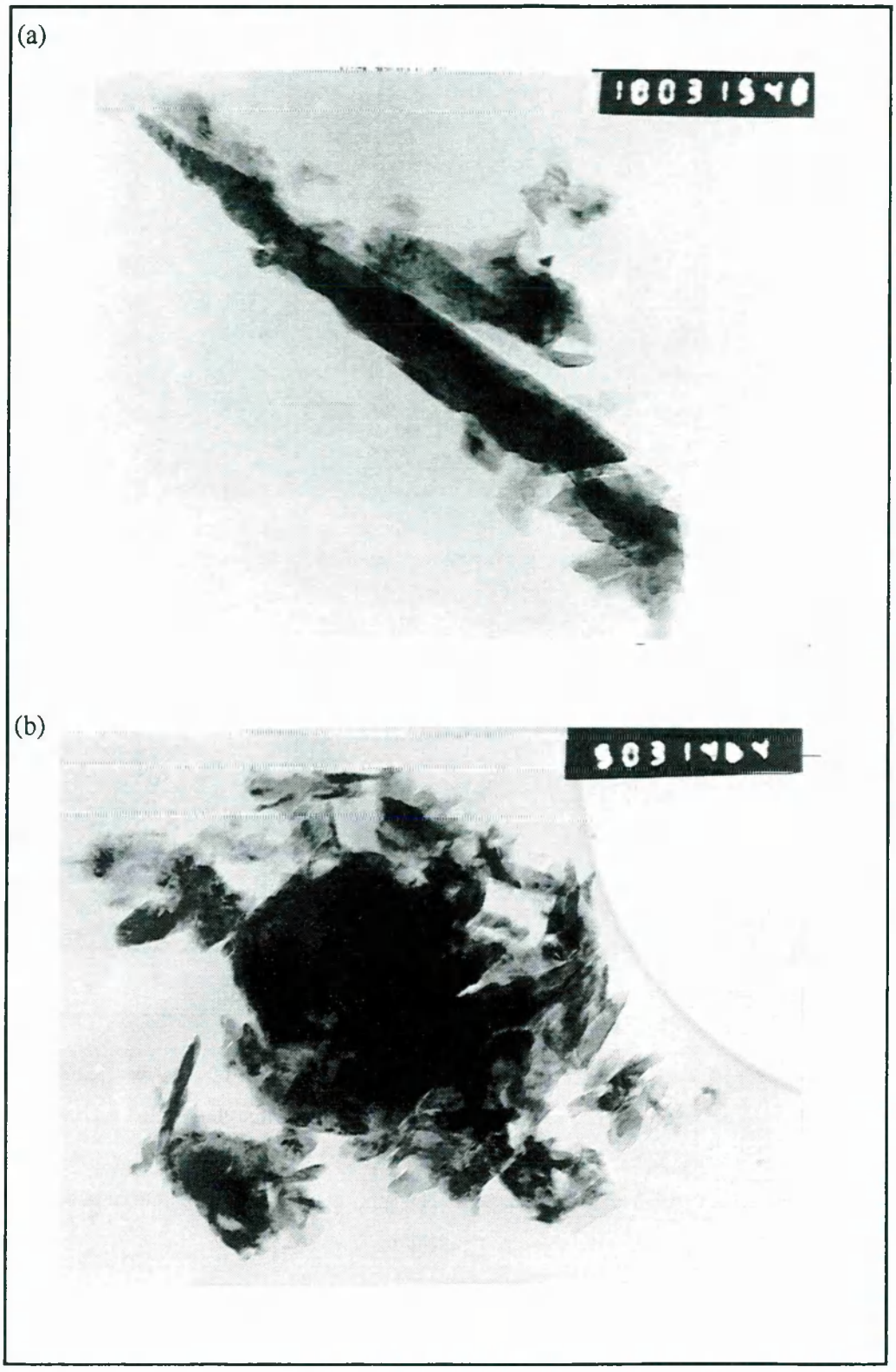

Figure 4.2 TEM photomicrographs of Abee diamond crystals: (a) a lath shaped crystal, scale 25mm = 167 nm, and (b) a platy crystal, scale 25mm = 320nm. These pictures were taken by M. Lee of the University of Essex.

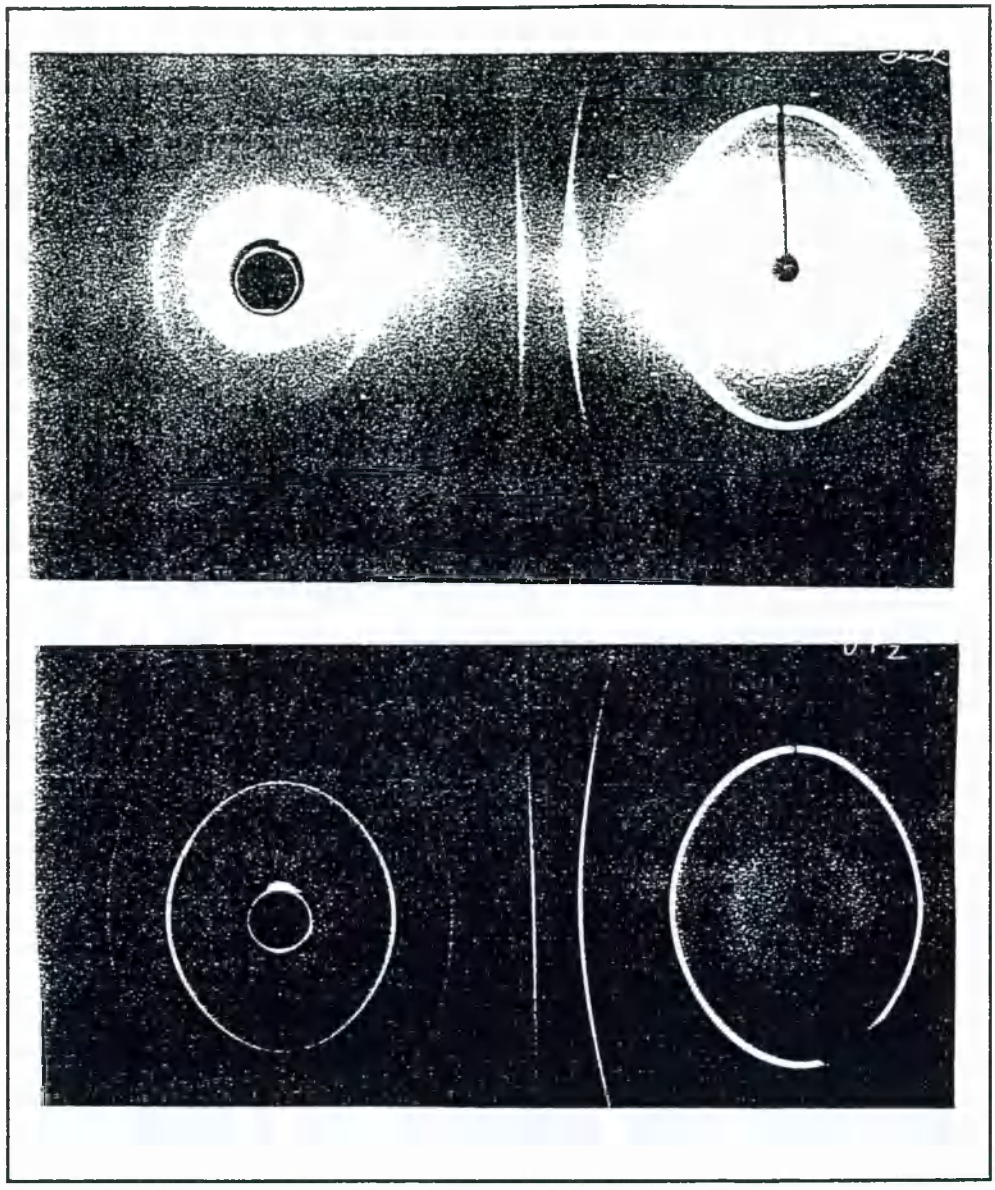

Figure 4.3. Comparison of the X-ray diffraction pattern of the Abee residue and a <1μm diamond standard. The patterns agree well, indicating that the residue is composed mainly of fine grained diamond, but the Abee sample gives a fuzzier diffraction pattern, suggesting that it is not as crystalline as the standard. The spots on the diffraction pattern indicate the presence of larger spinel grains. Patterns recorded by J. Milledge, UCL.

Line	Ring spacing (Å)	Cubic diamond (Å)
1	2.06	2.06
2	1.25	1.26
3	1.07	1.08
4	1.03	
5	0.88	0.89
6	0.81	0.80
7	0.72	0.73
8	0.68	0.69

Table 4.1. Diffraction spacings in the Abee meteorite compared to literature values for cubic diamond. Measurements were made by M.R. Lee of the University of Essex.

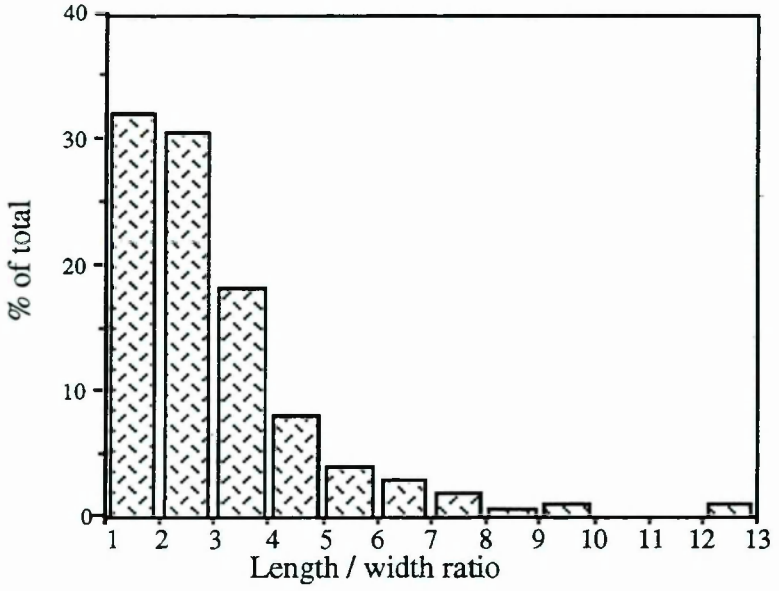

Figure 4.4. The length/width ratio of the diamonds from Abee: data from M.R. Lee of the University of Essex.

A study of the morphology of the diamonds was made; figure 4.4 indicates the length / width ratio (i.e. the deviation from roundness of the grains). It was found that 68% of the grains have a sufficiently elongated shape as to have a length / width ratio of >2.

During stepped combustion analysis of the Abee diamond, little carbon was combusted at temperatures below 400°C (figure 4.5); the peak yield of CO_2 occurred in the 550°

to 575°C steps [compared to 490° - 500°C for Cδ (chapter 3)]; some carbon was still being burned at temperatures as high as 800°C. The isotopic composition rose quickly on heating to a plateau of −1.86 ± 0.24 ‰ from a value below -20‰, which is probably indicative of terrestrial contamination. The overall bulk $\delta^{13}C$ measurement from repeat analyses was –2.2 to -2.5‰ (table 4.2).

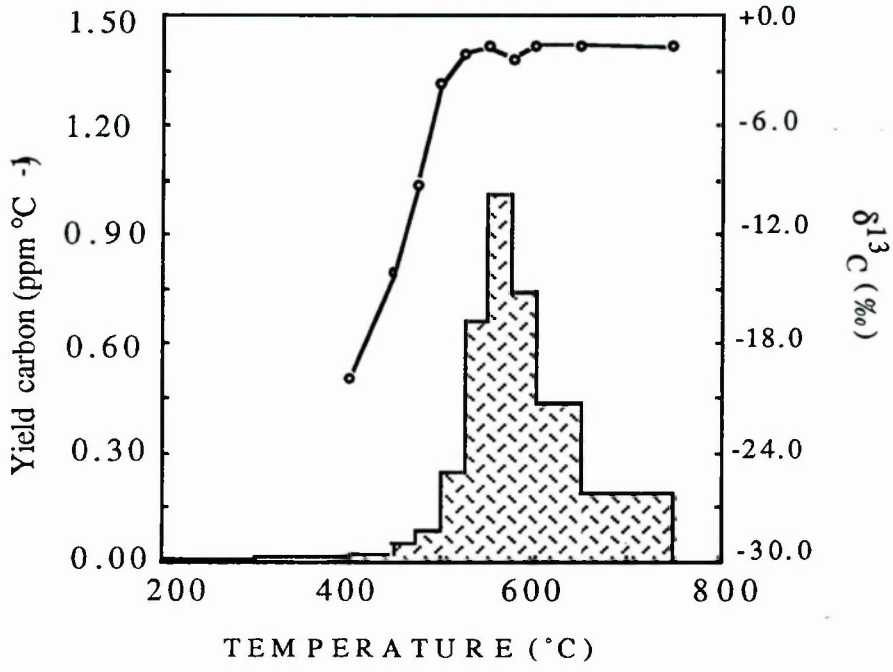

Figure 4.5. Carbon stepped combustion plot of diamond from Abee.

Measurement	bulk $\delta^{13}C$ (‰)	% Carbon	ppm of meteorite
C stepped combustion	-2.2	83	111
C stepped combustion (repeat)	-2.5	82	110
N stepped combustion		76	102
N stepped combustion (repeat)		72	97
Noble gas stepped combustion		66	89

Table 4.2. Carbon content and isotopic composition of the Abee perchloric residue.

A carbon isotopic composition of -1.86‰ is somewhat unusual for terrestrial diamonds; a recent review by Galimov (1991) of published data for over 2000 samples, indicated that most have a carbon isotopic composition of between -9 and -2‰,with a mode value of -4.6‰ (figure 4.6); only ~40 (2%) of the diamonds had a $\delta^{13}C$ as heavy as the Abee diamonds. These diamonds were from West and South

Australia, plus 5 from Siberia. The Galimov study indicated that $\delta^{13}C$ of terrestrial diamond is related to its geographic location and also to the rock type from which it originates, with ultrabasic rocks producing diamond with a higher $\delta^{13}C$.

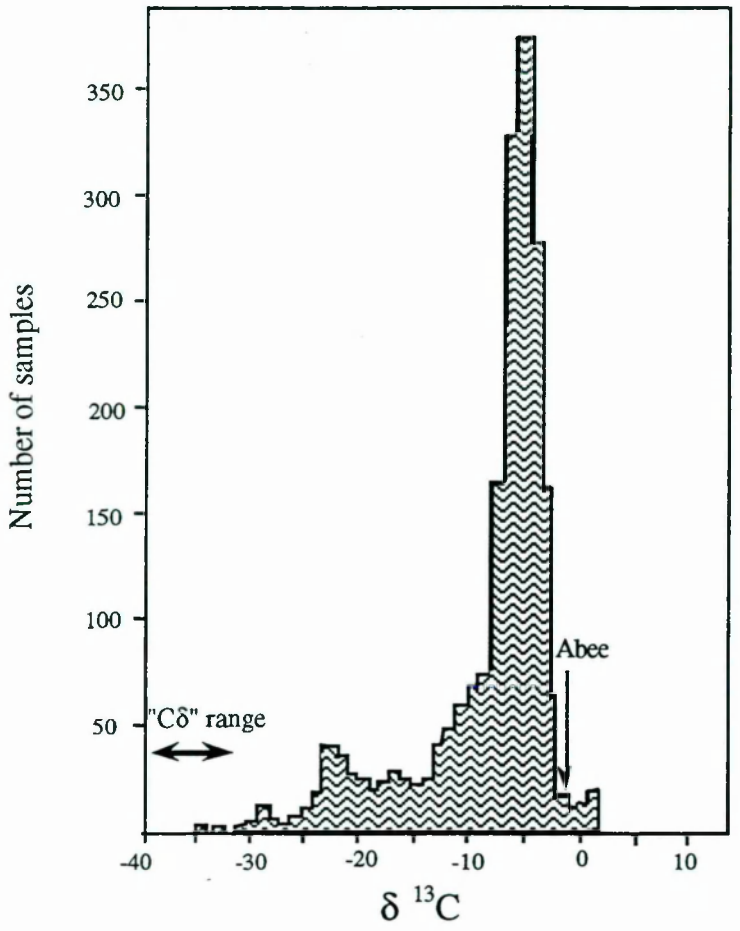

Figure 4.6. Carbon isotope data for terrestrial diamond, with Cδ and Abee diamond shown for comparison (Terrestrial data from Galimov, 1991).

The abundance of nitrogen released simultaneously as the diamond was combusted was low (figure 4.7), amounting to less than 50 ppm of the mineral. The C/N ratio was 2.0×10^4, much greater than the C/N ratio of Cδ of 80 to 270 (chapter 3). The exact nitrogen content of the diamond is difficult to determine as low resolution stepped combustion was necessary to produce adequate yields of nitrogen for measurement. Three times as much nitrogen as in the low temperature steps was liberated between 700° and 900°C, with a $\delta^{15}N = -22.7 \pm 1.0‰$. These data indicate the presence of a high temperature nitrogen component; the difference in combustion temperature to the diamond release suggests that it is not associated with the diamond. TEM analysis to date has not revealed the affinity of this nitrogen containing

component, which has a C/N ratio of ~50, if the tailing of the carbon peak is allowed for. A $\delta^{15}N$ value of -23‰ is rarely seen in terrestrial diamond samples: a study of the nitrogen isotopic composition of diamonds by Boyd (1988) reported no diamonds with a $\delta^{15}N$ less than -10‰; similarly, the lightest nitrogen from diamond recorded by Javoy (1984) had a $\delta^{15}N$ of -11‰. Out of over 300 diamonds analysed by L. Van Heerden (unpublished data) only four yielded $\delta^{15}N$ values lower than -20‰.

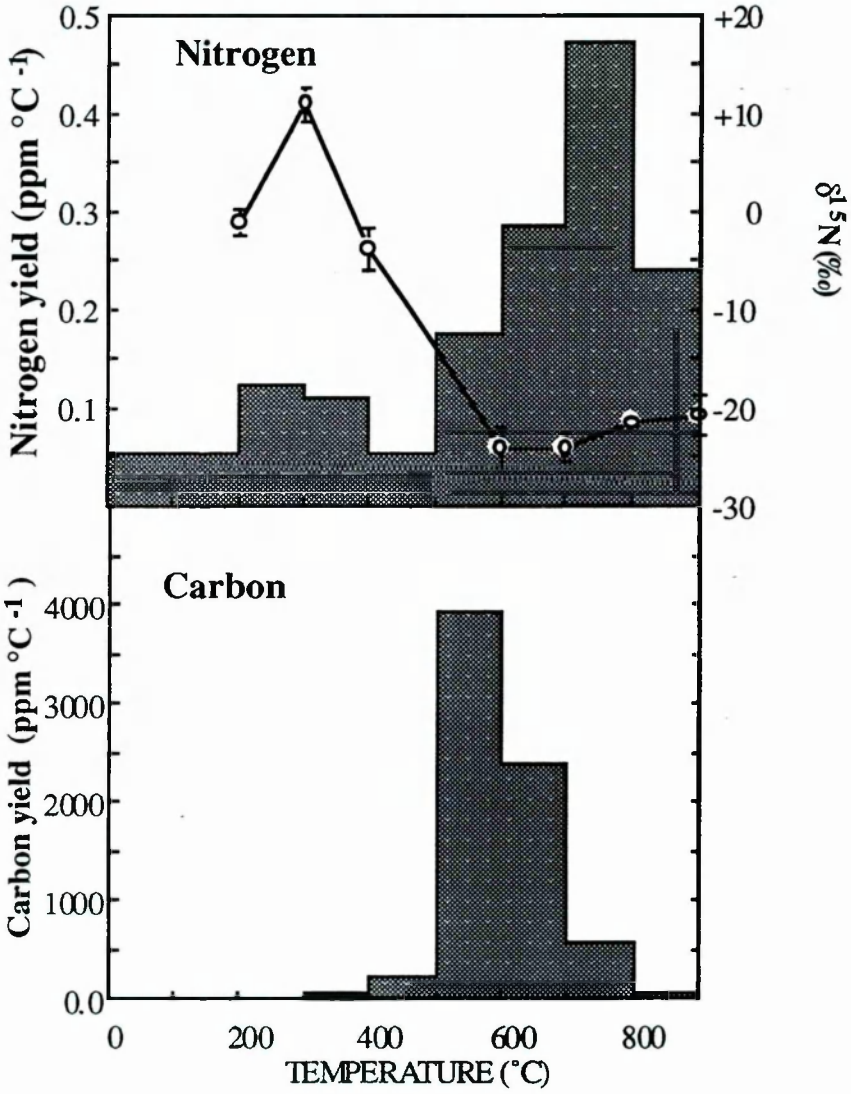

Figure 4.7 Nitrogen stepped combustion of diamond; the simultaneous carbon yield is also shown.

The noble gas contents and isotopic composition of the Abee diamonds were determined and interpreted by U. Ott of the Max Planck Institut für Chemie, Mainz, using a combination of pyrolysis and combustion steps (the data from his experiment are displayed in Appendix 3). The carbon abundance from combustion up to 600°C (*ca.* 64%) was in reasonable agreement with the carbon analysis. Major release of

noble gases occurred during combustion at 500°C and 600°C, whereas the preceding pyrolysis steps, although performed at higher temperatures liberated only minor amounts. The gases released included large amounts of cosmogenic ^{3}He and ^{21}Ne, in abundances similar to the concentrations measured for bulk Abee (Schultz and Kruse, 1989). These high abundances coupled with the release pattern, which closely follows that of C combustion (see appendix 2), demonstrates that these cosmogenic gases are contained in the carbon phase and thus the diamonds are indigenous. The presence of large amounts of cosmogenic Ne in diamond is somewhat surprising, because ^{21}Ne cannot be produced from carbon by spallation. The most likely explanation is that the Abee diamond is widely dispersed throughout the meteorite so that it acquired significant amounts of spallation Ne by recoil from the surrounding silicates. It follows that the aggregation of diamond into 20 μm clusters (figure 4.1) is an artefact of the isolation procedure. Trapped xenon and other gases were also released in the combustion steps. The $^{136}Xe/^{132}Xe$ ratio, at 0.325 for the main combustion step, is typical of planetary xenon and much lower than that of Xe-HL, and slightly higher than the value of ~0.318 established for Xe Q in carbonaceous chondrites (Wieler *et al.*, 1991), and Xe in ordinary chondrites (Schelhaas *et al.*, 1990) and ureilites (Göbel *et al.*, 1978). An upper limit for the abundance of Xe-HL in the Abee diamonds can be calculated from the $^{136}Xe/^{132}Xe$ ratio at $< 1 \times 10^{-9}$ cm ^{3} STP/g, less than 1/300 th of the concentration thought to be typical of Cδ diamonds (Huss 1990). Thus it is possible that Xe isotopes could reflect the presence of a small admixture (~0.1 %) of Cδ diamonds with diamonds containing planetary Xe. A proportion of Cδ this small would not be easily detectable by carbon or nitrogen isotope profiles. Alternatively, the Abee diamonds may not contain any Xe-HL, in which case the measured ratio could either be that of trapped Xe perhaps augmented by some ^{136}Xe from some other source such as fission. A third possibility is that some or all of the observed trapped gases could be carried by some other as yet unidentified carbonaceous phase. Unlike the cosmogenic gases, the trapped noble gases do not appear to be uniformly distributed in the carbonaceous material, because in the 500°C combustion step the ratio of trapped gas to C is significantly higher than in the 600°C step. Thus the trapped noble gases cannot be associated with the nitrogen containing component because whereas the noble gases are released at lower temperatures to the main diamond release, the nitrogen component is released at higher temperatures.

An unusual feature of chondritic (Cδ) diamonds is their ability to form a colloidal suspension in alkali. This property, thought to be due to carboxylic acid groups on the tiny diamond crystals (Lewis *et al.*, 1989), was accidentally brought to light for Cδ and became instrumental in identifying the nitrogen and noble gas carrier (Lewis *et al.*, 1987) as diamond. Abee diamonds treated with NH_3 (pH = 8) produced a milky

suspension, only a fraction of which could be concentrated in a centrifuge. On acidification the Abee diamonds reprecipitated and settled out as a grey deposit. To investigate the possibility that the acid moieties on diamonds were created by the harsh oxidizing treatments used in the isolation procedures a 0.25 to 1μm terrestrial diamond grinding powder was treated with $Cr_2O_7^{2-}$ and $HClO_4$. The properties of the Abee or Cδ samples could not be reproduced (although an anonymous reviewer to Russell *et al.* (1992) claimed to have done so). It appears that acidity is a characteristic of meteoritic diamonds and may be related to the way they are bound into the matrix or other carbonaceous phases. One possible explanation is that the diamond is bonded to a graphitic or organic kerogen-like material after incomplete diamond conversion by a shock or CVD process. The oxidising acid treatment would then cleave off the organic/ graphitic material leaving a COOH bond on the crystal surface.

The indigenous nature of Abee diamond is therefore indicated by (i) the carbon isotopic composition, which is unusual for terrestrial diamond, (ii) the presence of cosmogenic noble gases, (iii) the texture of the diamond crystals and (iv) their ability to form a colloidal suspension in ammonia. Furthermore, the combustion properties, N abundance, noble gas measurements, microscopy, and C and N isotope data confirm that the diamond in the residue isolated from Abee is not a variety of Cδ diamond (the differences are summarised in table 4.3), but is a new type of chondritic diamond. The higher temperature of combustion is in agreement with its observed size range.

Characteristic	**Abee diamond**	**Cδ**
Combustion temperature	550-575°C	500°C
$\delta^{13}C$	-1.8‰	–32 to –38‰
Xe-HL content	$< 10^{-9}cm^3STP/g$	$2 - 3 \times 10^{-7}cm^3STP/g$
^{20}Ne content	$<10^{-7}cm^3STP/g$	$1x10^{-4}\ cm^3STP/g$
N content	< 50 ppm	2000 to 10000 ppm
Colour	Grey	Brown
Reaction in NH_3	Milky solution	Brown solution
Grain size	<1μm	~2nm
Morphology	lath shaped	spheroidal

Table 4.3. A comparison of Abee diamond and "Cδ" diamond

4.3. Grain size of the Abee Diamonds

The grain size distribution of the diamonds from Abee has been investigated by TEM. This was a difficult undertaking because of the irregularities in shape of the diamond crystallites and so the area of the crystal was taken as a measure of the grain size; thus the equivalent diameter of the grain can be recorded as the square root of this value. A log plot of the size calculated in this way *vs.* the cumulative yield gives an approximately straight line (figure 4.8), although this was a simple pathfinder experiment and so the number of grains measured was comparatively small. The number of grains in the first size category, 0<area <0.1μm^2 was ~40% of the total, and so the finer size range is not well represented. These preliminary data are sufficient, however, to suggest that the grains size distribution could be log-normal, indicating that the distribution is governed by diamonds growth (*e.g.* Lewis *et al.*, 1989) rather than diamond destruction.

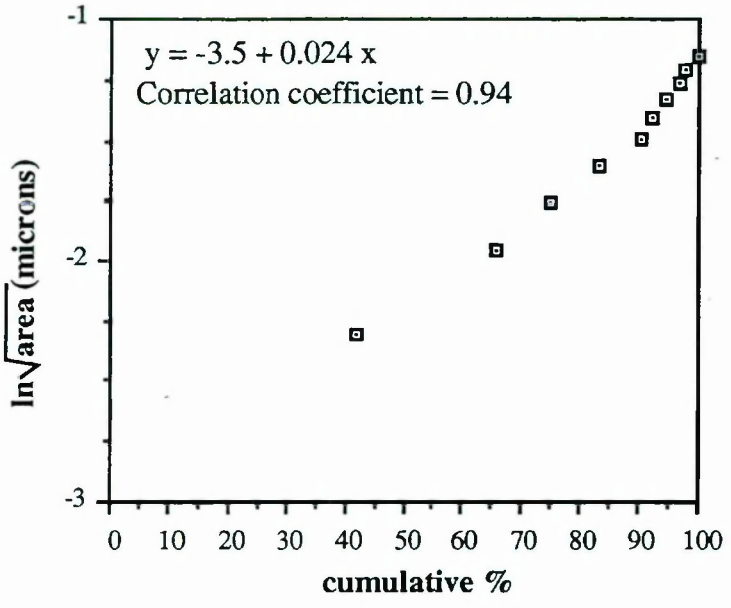

Figure 4.8. The size distribution of the Abee diamonds. Data from M. Lee of the University of Essex.

The Abee diamond clearly consists of a wide range of grain sizes that may not all be related. A study was attempted to separate out grain size fractions using their ability to partially form a colloidal suspension. The residue was split into four fractions in this way; F1 went into colloid most readily and F4 remained completely as sediment after centrifugation. The isotopic composition of F1 and F4 was found to be

indistinguishable (figure 4.9), both having a similar $\delta^{13}C$ to the bulk residue. Thus, it can be concluded that the diamonds, despite being diverse in size, are all of the same origin.

Interestingly, the fraction most susceptible to colloidal solution, F1, appeared to combust at a higher temperature than F4. Thus, F1 may in fact be made up of crystals with a coarser grains size than F4, an anti-intuitive result that should be confirmed by electron microscopy. This could be due to to clumping together of the smaller grains causing them to be less likely to form a colloid than larger, single grains.

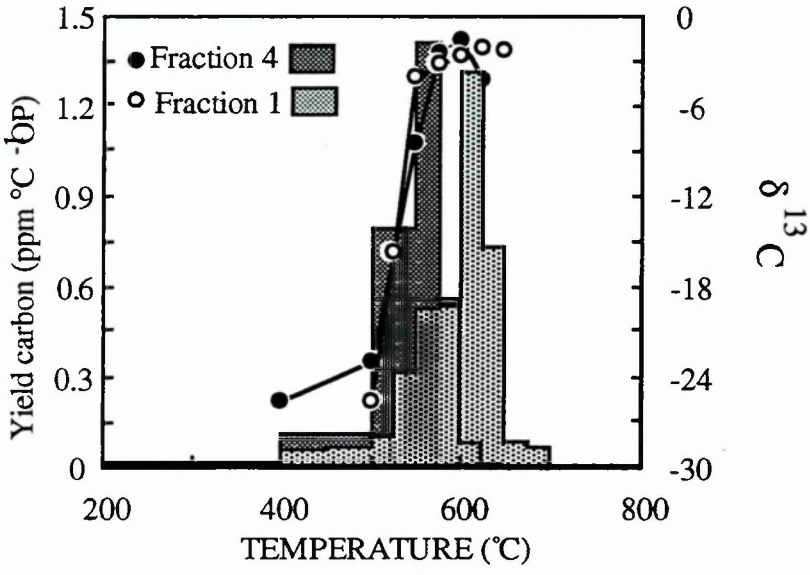

Figure 4.9. Comparison of the stepped combustion profile of grain size fractions from Abee

4.4 Formation of the Abee Diamond

The lack of associated isotopic anomalies in C, N or Xe in diamond from Abee argues against, but does not preclude, an interstellar source. Abee does contain free graphite (Rubin and Keil 1983), and therefore the possibility that the diamond formed by shock from graphitic material in the asteroid belt or on impact with the Earth must be considered. Minster *et al.* (1979) have suggested that Abee was situated close to the surface of its parent body and so was shocked by surface impacts during the early stages of Solar system history. However, the petrologic texture of Abee suggests that it has not been highly shocked; for example, it does not display any shocked veins, melt droplets, or eutectic sulphide/metallic intergrowths which are cited as evidence for shock in other chondrites. Thus, Sears *et al.* (1983) concluded that if the Abee meteorite suffered any shock (*e.g.* during the brecciation event) the petrologic evidence had become completely eradicated by thermal metamorphism. However, the retention

of clasts that have kept magnetic fields in random directions requires that the meteorite did not reach temperatures higher than 215°C after brecciation (Sugiura and Strangeway, 1983). Thermal equilibration would, therefore, have been unlikely to have occured. The mineralogical evidence is not suggestive of high pressure events: the only silica type observed in Abee is crystobalite (Rubin and Keil, 1983), a low density polymorph that is stable at low pressures (figure 4.10). Coesite, the polymorph stable at the same pressures in which diamond forms, is not present. It seems unlikely therefore that the mild shock experienced by Abee would have been extreme enough to have initiated the formation of diamond from graphite.

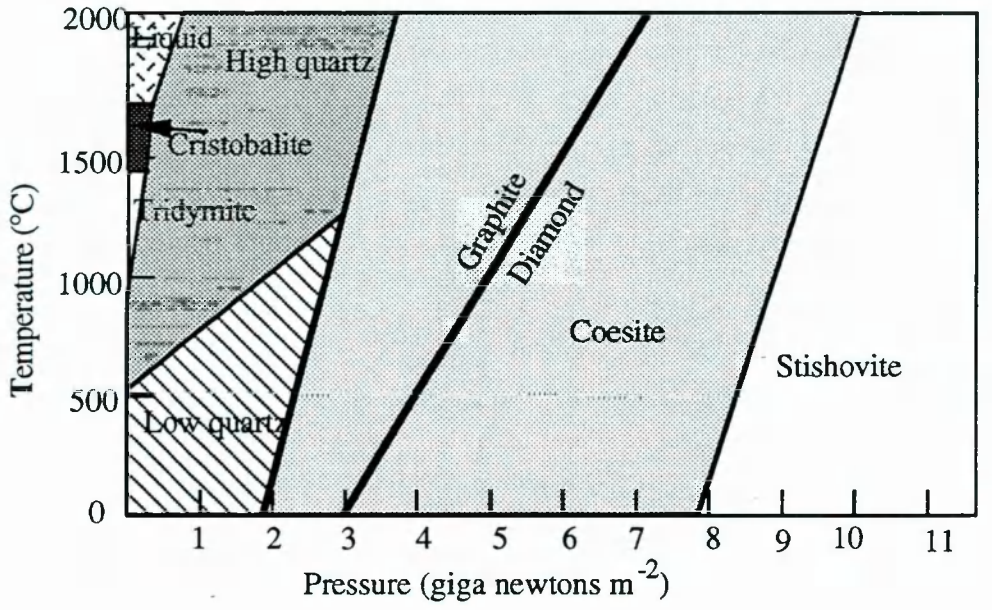

Figure 4.10 The stability field of silica polymorphs, on which the graphite diamond stability curve has been superimposed. (Data from Battey, 1982)

It is possible that the diamond could have formed before the parent body accreted by shock due to grain-grain collisions in the early Solar nebula. Experimental replication of this process causes large carbonaceous grains (0.1-1 μm) to disintegrate into tightly jointed poly-crystalline diamond aggregates of nanometre dimensions (Tielens, 1988), rather than the lath shaped, sub-micron grains observed in Abee.

Interstellar diamonds are believed to form in circumstellar environments by chemical vapour deposition (CVD) (Lewis *et al.*, 1987), and it has been suggested that this process could also occur in the early Solar system (Pillinger *et al.*, 1989). Abee diamonds could also have been produced by this mechanism in which case their coarse

grain size compared to Cδ could be a result of a difference in the formation environment (for example, Abee diamond could have been formed in a dust poor region where opportunities for nucleation were limited). A needle shaped morphology has been observed in CVD produced diamonds when the substrate is rich in iron (Angus and Gradner, 1969), and when diamonds are formed by the Vapour-Liquid-Solid technique (Deryaguin *et al.*,1968; see also chapter 5). For both of these mechanisms, the diamond growth is reported as being unusually fast, up to 250μm per hour.

An alternative possibility is that diamond formed as a result of substantial radiation by high energy particles, which are believed to produce carbonado diamond (Kaminskiy, 1987, Ozima *et al.*, 1991), from organic matter and coal. The enrichment of ^{136}Xe, which can be attributed to fission, adds weight to this argument. However, the presence of spallation neon suggests that Abee diamond was finely dispersed throughout the meteorite, whereas carbonado diamonds invariably occur as clusters. The stable isotope characteristics of these diamond types and their bearing on the origins of Abee diamonds, will be discussed further in Chapter 5.

4.5 Relationships to other meteoritic diamond

Abee diamond may confirm a link between enstatite chondrites and the other diamond bearing meteorites (the irons and ureilites) for which there is already some evidence. Ramdohr (1972) recognized obscure minerals common in enstatite meteorites, such as the sulphide niningerite, in the opaque part of the ureilite matrix. On the basis of trace element studies, Wasson *et al.* (1976) suggested that the graphite in enstatite chondrites may have come from the same source as the graphite in ureilite veins. Another possible link to other meteorite types is provided by the oxygen isotope data; these suggest that howardites, eucrites and IAB irons may lie on a fractionation line as shown in figure 4.11 (Clayton and Mayeda, 1988) and so could be related.

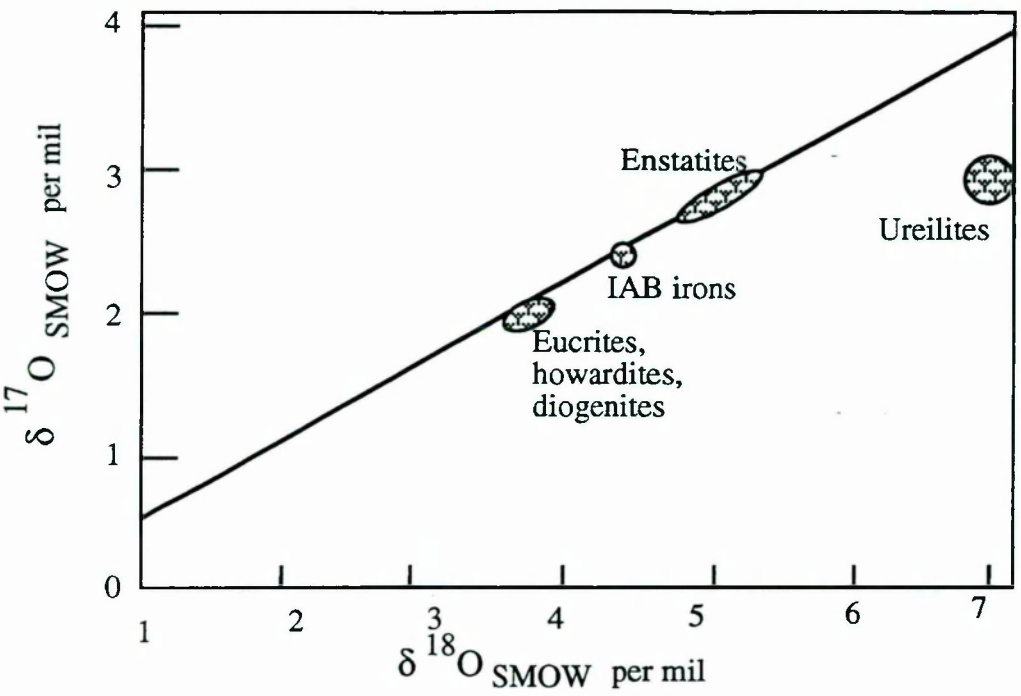

Figure 4.11. Oxygen isotope data for bulk meteorites. From Sears and Dodd, 1988.

Only a few isotopic data have been collected for diamonds from iron and ureilite meteorites, so their relation to Abee diamonds is uncertain. Vdovykin (1968) reported a $\delta^{13}C$ of –5.8‰ for a diamond from Canyon Diablo and a similar value (–5.7‰) for diamonds from the ureilite Novo Urei. A more recent study has shown that at least nine ureilites have a bulk carbon $\delta^{13}C$ of –2.2 ± 0.8‰ (Grady *et al.*, 1985) which may reflect the diamond composition because there is little evidence of fractionation between diamond and graphite (Vdovykin, 1968). The isotopic composition of carbon in silicate inclusions from type IAB iron meteorites, -3 to -4‰, is systematically 1 to 2‰ heavier than that of graphite nodules in the same samples (Deines and Wickman, 1975). The other enstatite chondrites might also contain Abee-type diamonds, although confirmation must await detailed analysis of acid-resistant residues. The carbon profile of the perchloric acid residue of Indarch, the only other enstatite chondrite that has been studied in this work, was dominated by Cδ and SiC and so the presence of a small amount of a different diamond type would not have been observed. Most of the carbon from relatively unprocessed carbonaceous residues of Qingzhen (EH3) and St. Saveur (EH5) (Grady *et al.*, 1985) burned from 500° to 700°C (slightly lower in the former than in the latter) and $\delta^{13}C$ values were between -4 and -6‰; Daniel's Kuil, an EL6, liberated carbon with a $\delta^{13}C$ of + 5 to + 7‰ at much higher temperatures (650° to 1000°C): the presence of diamond would not be detectable using these residues which are dominated by the presence of graphite. The graphite in Abee

was studied by measuring the $\delta^{13}C$ of the HCl/HF residue in two ways. The first experiment on this residue was a 50°C step size stepped combustion that gave a peak $\delta^{13}C$ of -1.40.03‰ at 700°C (figure 4.12); in the second experiment the residue was precombusted at 400°C for one hour to remove any organic/low temperature components and then combusted in a sealed tube bulk experiment. The bulked system yielded a $\delta^{13}C$ value of -3.4±0.03‰. The isotopic composition of the graphite is thus similar to that of the diamond, suggesting that there is a possible link between the two.

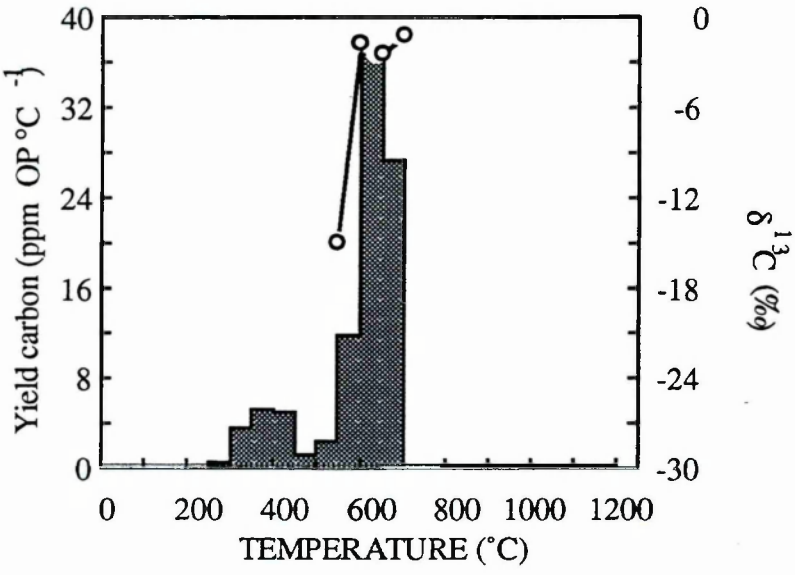

Figure 4.12 The carbon release profile of the HF/HCl carbonaceous residue from Abee. Below 550°C the CO_2 released was highly contaminated with SO_2, and so the $\delta^{13}C$ values obtained for this temperature regime were not reliable.

4.6. The Mysterite Connection

Ganapathy and Larimer (1980), during a study of unusual minerals in the enstatite chondrites, reported the presence of an unidentified volatile rich carbonaceous component in Abee, that occurs as "thin, delicate strands with a yellow tint". As this phase is ~90% carbon it would seem likely to be graphite, but Rubin and Keil (1983) pointed out that graphite is invariably black in colour. The discovery of diamond laths in Abee now provides a more probable suspect for the identity of this phase. The component identified by Ganapathy and Larimer was enriched in volatile elements (*e.g.* antimony, silver, zinc and mercury) compared to C1 chondrites that linked it to

"mysterite" seen in the Supuhee and other meteorites. Laul *et al.* (1969) suggested that mysterite may represent dust that formed at a very late stage in the Solar nebula, and hence became enriched in incompatible elements. A study of the concentration of these elements in Abee diamond, perhaps by ion probe, could thus be very informative; antimony has been detected by EDX analysis of residues of other meteorites, such as Murchison, that have been prepared using the same acid treatments (K. Gilkes, *pers. comm.*).

4.6. High temperature components in Abee

After investigating the $\delta^{13}C$ in the diamond by stepped combustion using dynamic mass spectrometry to 750°C, the sample was transferred to a static carbon system to investigate the higher temperature carbon components. The first gas to be released (figure 4.14) had a $\delta^{13}C$ = ~-1.9‰ and was presumably a residue of the coarsest diamond size. After 850°C very little carbon was released, and while the yields at this stage were >10ng per step, clearly higher than the blank value (0.6 ng per step), no clear peaks in the release pattern could be detected. The isotopic composition over this higher temperature range was -23.8±1.1‰. These values are distinct from the high temperature regime of the more primitive meteorites, which yield heavy CO_2 from the release of circumstellar SiC (Chapter 5). TEM analysis of the Abee sample revealed that it too contains SiC. The SiC grains are typically ~0.5 μm across and have an angular "chipped" morphology (figure 4.13). One highly distinctive lath shaped grain contained many stacking faults, (figure 4.15) and the electron diffraction data suggest that this crystal is a hexagonal polymorph of SiC (α-moissanite). In contrast, most SiC grains in other chondrites have a cubic structure (Bernatowicz *et al.*, 1987).

The stepped combustion data suggests that the SiC has a $\delta^{13}C$ that is within normal Solar values and so it may be a Solar system condensate rather than a presolar component, although the possibility that the SiC grains of this unusual polytype did not combust before 1200°C, and so the $\delta^{13}C$ of the SiC was not measured, cannot be ruled out. Unfortunately, the technique used for stepped heated prohibits the continuation of the experiment far beyond 1200°C.

The maximum abundance of the SiC can be estimated from the amount of carbon released at high temperatures in the residue; a value of 0.18 ppm of the whole rock is obtained if all the carbon released between 1000° and 1200°C is from SiC. This is a rough estimate as it assumes that there is no other contributions from other carbonaceous phases over this temperature range, and that all the SiC is measured.

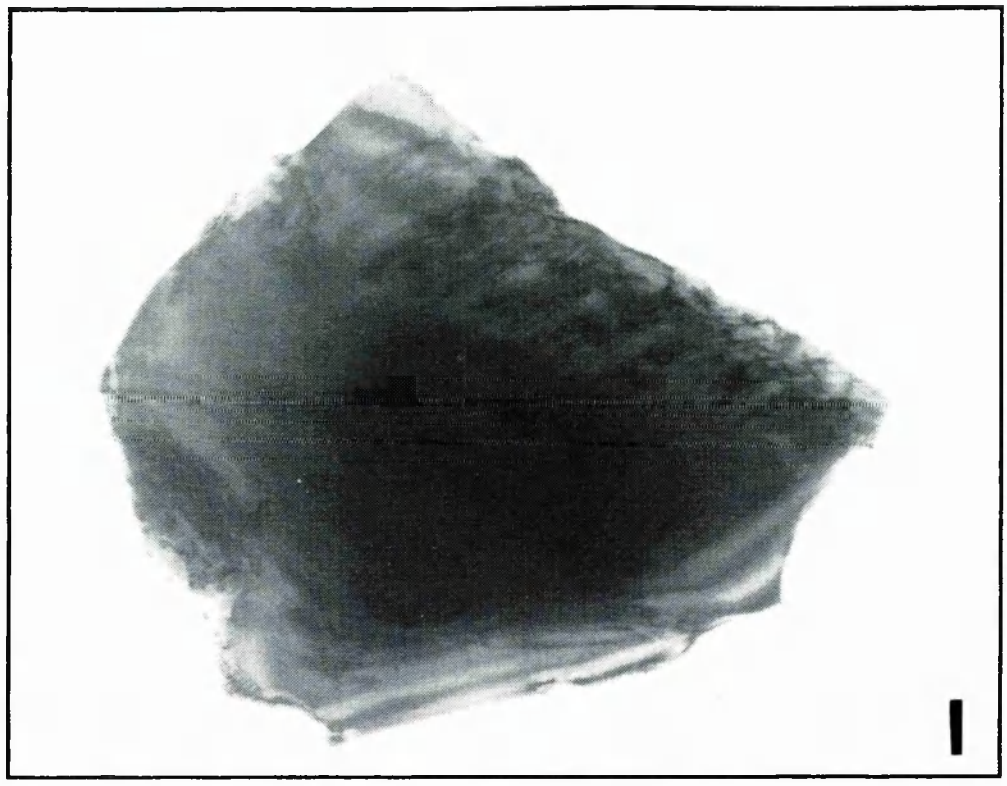

Figure 4.13. TEM photomicrograph of a typical SiC grain, taken by M. Lee. The scale is 25mm = 750nm.

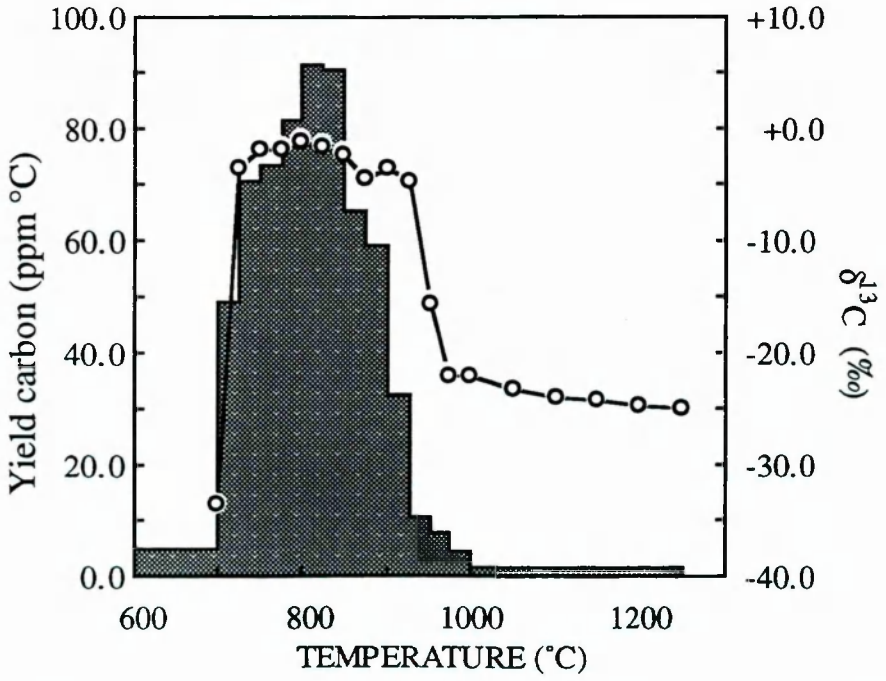

Figure 4.14. High temperature carbon stepped combustion of the Abee perchloric resistant residue.

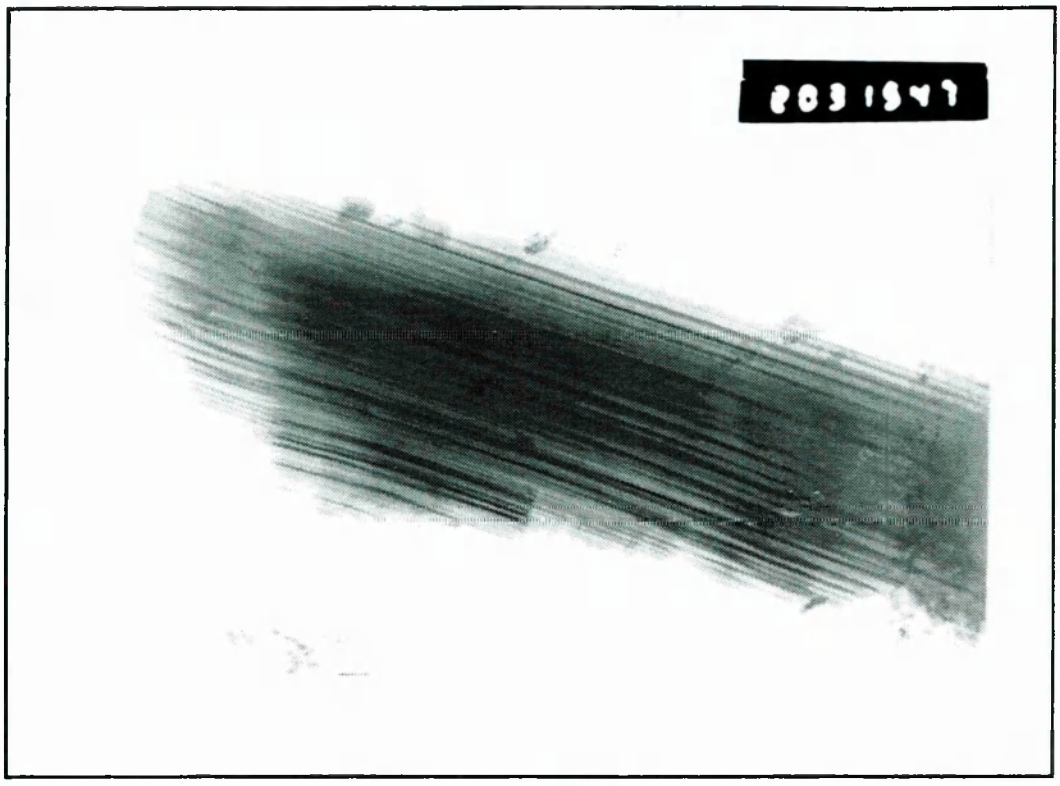

Figure 4.15. TEM photomicrograph of a SiC grain from the Abee meteorite, scale 25mm = 1.154 μm (taken by M. Lee of the University of Essex).

The presence of SiC of apparently normal carbon isotopic composition is as mysterious as the presence of diamond. Silicon carbide is only rarely produced naturally on the Earth but is formed industrially at high pressures and temperatures, although the mineral can also be made easily at low pressures by a chemical vapour deposition process. In fact, it is a common by-product of the diamond CVD manufacture. SiC has not been studied as thoroughly as diamond and so any interpretation of its formation environment would be even more tentative. It is possibly fair to assume that the diamond and SiC were formed by a similar process, since these unusual morphologies of both are found in the same meteorite, and so the presence of SiC adds weight to the theory of manufacture by a CVD mechanism.

4.8. Location of the diamond and SiC grains within the Abee meteorite

As Abee is a breccia, it is possible that the diamond and SiC grains are held within a clast that is extremely unusual or unique. The meteorite is made up of extremely diverse clasts; other chondrite breccias, such as the blackened ordinary chondrites, do

not display the same degree of heterogeneity (Rubin and Keil, 1983). The clasts have have been well equilibrated by thermal metamorphism; it is possible that the metamorphic temperature reached 950- 1000°C (Rubin and Keil, 1983): under which conditions the diamond would probably be destroyed. The exception to this general rule are the dark inclusions, which are mm to cm sized matrix inclusions that appear to be relatively unheated primitive condensates. Sears *et al.* (1983) found that the chemical composition of the dark inclusions is very different to that of the rest of the meteorite and, indeed, of any other meteorite class, or interpolations between classes. The "mysterite" reported by Ganapathy and Larimer (1980) was located in these primitive inclusions. The inclusions are characterised by a rare earth element enrichment of 4x the mean value for EH chondrites and an enrichment in sulphur. These primitive inclusions are thus the most likely suspects as hosts for primitive material.

The composition of the dark inclusions can in part be explained by condensation from a nebula gas which had a high pS/pO_2 ratio (Rubin, 1984), although a complex multi-stage process is believed to be necessary to explain the mineralogy exactly (Sears *et al.*, 1983). The condensation sequence for minerals from a gas of Solar nebula composition to explain the mineralogy of the carbonaceous chondrites has been well established (*e.g.* Larimer, 1967; Anders, 1987; Larimer, 1988) but the enstatite parent body forming region requires somewhat different starting conditions. If the C/O ratio is assumed to be ~1, rather than the value of 0.6 taken for the carbonaceous chondrites, then the appearance of silicates and oxides is depressed by 400K and new minerals are found to condense. The thermodynamics of this process has been modelled in some detail by Larimer and Bartholomay (1979) over the pressure range 10^{-6} to 1 atm and the temperature range 2500 to 300K. They predicted the synthesis of AlN, Fe_3C, MgS, SiC, TiN, graphite, and Si_2N_2O from a gas that deviated from Solar composition only in its C/O ratio. The modelling has been justified by the presence of all these minerals except SiC and AlN in the enstatite chondrites. Less optimistic workers may have found the absence of SiC somewhat problematical, but Larimer and Bartholomay declared "given the recent history of refractory compounds being predicted and subsequently discovered, this is better viewed as a challenge than as an embarrassment". The observation of SiC in Abee discussed here could thus justify their confidence. In addition, SiC grains of "normal " isotopic composition have subsequently been discovered in Indarch, although their relationship to presolar SiC is obscure. The Larimer and Bartholomay modelling used only the ten most abundant elements, but in addition, Sears *et al.* (1983) suggested that the condensation sequence of the more obscure elements could result in the formation of SiC within a reducing gas:

$$Ca + SiS + C \rightarrow CaS + SiC$$

and:

$$LaO + SiS + 2C \rightarrow LaS + SiC + CO$$

Although graphite is reported as a stable condensate in all modelling exercises, the possibility of diamond formation has not been discussed, probably because until recently, the formation of diamond from the vapour phase had not been a well known phenomenon.

In summary, if the diamond and SiC are primitive condensates then their most probable locality is in the relatively unprocessed dark inclusions. Thermodynamic modelling of the condensation sequence of these inclusions predicted the presence of SiC that has now been found.

Alexander *et al.* (1991) observed that the enstatite chondrite Qingzhen (EH3) contains Si_3N_4 as inclusions within metals and phosphides and suggested that these grains formed by exsolution from the metal phase, either during the original cooling of the grains or during subsequent metamorphism. An alternative mechanism to primary condensation for the production of isotopically "normal" SiC in Abee could be exsolution of carbide by an analogous mechanism. *In situ* studies of Abee to determine the locality of the SiC grains could resolve the primary/secondary debate.

4.9. Conclusions

The perchloric acid-resistant carbonaceous components in Abee are predominantly diamond and SiC, in line with the other chondritic meteorites used in this study. The isotopic composition, morphology and noble gas content of these phases are, however, clearly distinct from those in other chondrites and the carbon, nitrogen and noble gas isotopic composition of the residue suggests that the minerals could have been formed in a Solar, rather than presolar environment. Abee is perhaps the most heated chondrite for which a highly processed acid resistant residue has been prepared and studied, and presumably almost all the isotopically anomalous diamond and SiC has been destroyed by metamorphism (Huss, 1990; Huss and Lewis, 1990). Thus it is possible that the phases found in Abee could also exist in the more primitive meteorites but their signature is masked by the presence of the isotopically anomalous diamond and SiC. Alternatively, the grains may be unique to enstatite chondrites, or may also exist in ureilite meteorites that are known to contain diamond, which has not yet been closely studied. As Abee is a breccia, it may have contained a clast of a

highly unusual stone that may be unique, so a future study should examine separate clasts from Abee and the other enstatite chondrites. The formation mechanism of the diamond and SiC production is not yet known, although a low pressure system seems likely as the meteorite does not show any evidence of having experienced high pressures. There is little evidence that the diamond and SiC were formed post-accretion and so it is possible they may be primitive Solar system condensates that could potentially provide more information about the conditions within the part of the the Solar nebula in which the Abee parent body accreted, and about the associations between enstatite chondrites and other meteorite types.

CHAPTER 5

SYNTHETIC AND NATURAL TERRESTRIAL DIAMONDS: THE SEARCH FOR METEORITIC DIAMOND ANALOGUES

Diamond can grow under many diverse sets of conditions: although diamond is thermodynamically stable only at high pressures, it is also possible to produce diamond metastably at low pressure. This chapter discusses some preliminary work comparing nitrogen and carbon isotopes of meteoritic diamond to various synthetic and terrestrial diamonds of known origins, in an attempt to reach an understanding of the meteoritic, nebula, and circumstellar processes that may have been involved in their formation. Although this study concentrates on the formation of chondritic diamonds, diamond from ureilites and iron meteorites are also mentioned because of the possibility that they formed by a similar mechanism to diamond from Abee.

Firstly, the theory that meteoritic diamond could have been formed in an analogous way to terrestrial diamonds, at high static pressures over prolonged periods of time, is discussed. Since this is shown to be unlikely, alternative mechanisms for diamond production are then investigated. One of the most widely accepted possibilities for the production of some populations of meteoritic diamond is shock, by grain- grain collisions either of circumstellar grains in a supernova shock wave (Tielens *et al.*, 1988), or of presolar and nebula condensates in the early Solar system (Vdovykin, 1960) or by the impact of the meteorite with the Earth (Lipschutz and Anders, 1961). This latter scenario, although applicable for some iron meteorites, can be excluded for diamond from stony meteorites, and especially the lower petrologic type chondrites which tend to be too small to impact the Earth at great speeds and do not appear to be strongly shocked during terrestrial impact (Lipschutz, 1964) and do not show any evidence for pre-entry shock. Diamond can also form at low pressures by deposition from the vapour phase in a plasma (*e.g.* Deryaguin and Spitzyn, 1956), a process that clearly may have implications for the formation of diamonds before parent body accretion (Lewis *et al.*, 1987; Pillinger *et al.*, 1989; Fukunaga *et al.*, 1987). Finally, carbonado diamonds are described as a possible analogue to meteoritic diamond. These naturally formed diamonds from the Earth's crust are not associated with high pressure facies. Although their exact formation mechanism is still a cause of controversy, they

are always found in areas of high radiation and this may cause the conversion of carbonaceous material to diamond (Kaminskiy, 1987).

5.1 Formation of diamonds by hydrostatic pressure

The most common mechanism responsible for producing natural terrestrial diamonds is thought to be prolonged pressure due to deep burial. Terrestrial diamonds are believed to have formed in the mantle or deep crustal regions and uplifted to the surface by kimberlite intrusions. This process requires burial to depths of around ~100km, depending on the density of the overlying rock, to reach pressures sufficient that the diamond stability field is reached (40-60kbar: Berman and Simon, 1955). Although early comments on the formation of ureilite diamonds (Ringwood, 1960) suggested that these meteoritic diamonds could have formed in the same way, this is not an option for "Cδ" diamond because their anomalous noble gases restricts its formation to a pre-accretionary process. However, observations of present day asteroids indicates that bodies large enough to allow the formation of diamond are non-existent. Most asteroids are smaller than 100 km across: the largest, Ceres, is 385 km in radius. The central pressure would be only ~6 kbar in this asteroid (Dodd, 1981), less than the pressure at a similar depth in the Earth because of the lower gravitational force, and insufficient by a factor of ten for graphite-diamond conversion. In the early Solar system, the average size of the protoasteroids is believed to have been around 630km (Hayashi *et al.,* 1985); again too small for diamond formation.

Less circumstantially, there is petrologic evidence that the pressures experienced by unshocked meteorites were not extreme enough to initiate the formation of diamond growth. The presence of Widmanstätten structures (exsolution features of nickel and iron alloys) in iron meteorites suggests cooling rates of the meteorite parent bodies and thus puts a limit on the depth at which they cooled; Widmanstätten patterns are not produced where the pressure of the parent body was more than 12kbars (Dodd, 1981). The petrology of meteorites also suggests that they have not experienced long term high pressures; for example, ringwoodite, a high pressure equivalent of olivine, is absent from unshocked meteorites (*e.g.* Dodd, 1986), including all the chondrites in which diamonds have been isolated. Similarly, the high pressure polymorphs of silica, coesite and stishovite, that are stable at the same pressures as diamond, are absent. The most common silica polymorphs in chondrites are crystobalite and tridymite which are stable at pressures of less than 5 kbars. There is evidence that the ordinary and enstatite chondrites were thermally metamorphosed only when the parent body first accreted (McSween, 1986) suggesting that they were quickly cooled and hence not buried

deeply. Thus, the possibility that the chondritic diamond could have formed in an analogous way to terrestrial diamond, at high static pressures within their parent body, seems unlikely. Similarly, ureilite and iron meteorite diamonds are believed to have formed by alternative mechanisms (Lipschutz, 1964; Lipschutz and Anders, 1961; Clarke e*t al.*, 1981) which are discussed below.

5.2 Shocked diamonds

Whereas formation of diamond due to prolonged pressure from burial seems unlikely, formation of diamond by high pressure during impacts may be an important meteoritic process. These impacts may be from grain-grain collisions before the meteorite parent body accreted, impacts between parent bodies, or the impact with Earth. Of these, the latter two options are likely to have also affected the other minerals in the meteorite, and so should be relatively easy to identify. All of the meteorites discussed in this thesis are free of highly shocked features and so these processes can be excluded as candidates for the formation of diamonds in these chondrites. However, the possibility that pre-accretionary grain-grain collisions were an important diamond forming mechanism in presolar grains (Tielens, 1988), and in the Solar system (Vdovykin, 1968), will now be considered.

Supernova shock waves are believed to be the dominant destruction mechanism for interstellar grains (Draine and Salpeter, 1979). High velocity (~100kms^{-1}) gas from supernovae explosions has a higher elemental abundance for the grain forming elements than the interstellar medium in general (Cowie, 1978), implying that many dust grains are vaporised to gas in these regions. Tielens (1988) has suggested that under these conditions poly-crystalline diamond aggregates may form through graphite grain-grain collisions. He calculates that the expected fraction of elemental carbon transformed to small grains of diamond by a shock front would be ~5%, a figure which is surprisingly insensitive to the initial conditions, and which is similar to the proportion of carbonaceous material in the form of diamond in the carbonaceous chondrites.

Diamonds synthesized on Earth by shock processes that may be analogous to the meteoritic diamond formation, have been obtained for characterisation. Four specimens were donated for a stable isotope study by A.B. Fisenko and L. Semjenova of the Vernadsky Institute, Moscow in an attempt to demonstrate similarities or differences between meteoritic diamond and diamond of known shocked origin. The samples include: (i) diamond powder isolated from a Russian meteorite crater, (ii) diamonds

formed from graphite and soot by a detonation method and (iii) diamond from a TNT (trinitrotoluene) type material formed by an ultradispersion technique. The crater diamond may be comparable to diamond formed by asteroidal collisions, that would be expected to form other high temperature minerals in addition to diamond. The other techniques involve collisions of small particles and thus are to some extent comparable to grain-grain collisions "in space". The results of the carbon and nitrogen measurements of these diamonds is shown in Table 5.1.

Sample	$\delta^{13}C$ (σ)	$\delta^{15}N$ (σ)	C/N	ppm N
Crater	-10.44 (0.06)	+12.2 (1.4)	2520	397
from soot	-31.36 (0.07)	-2.2 (1.4)	1371	730
from graphite	-30.26 (0.06)	+7.2 (1.7)	150	6670
from TNT	-29.68 (0.04)	nm	58	17300

Table 5.1 Results of carbon and nitrogen analysis of shock produced diamonds.

The crater diamond was also analysed by x-ray diffraction and the binocular microscope and found to be in the form of cubic euhedral crystals, about 1μm in diameter, very similar in morphology to terrestrial microdiamonds. This sample was pale yellow in colour, suggesting that the nitrogen within the grains was in the singly substituted (Ib) state. This would be in keeping with their assumed shock origin, as it implies they have not been heated for any geologically significant length of time. The $\delta^{13}C$ of the crater diamonds, at -10‰, (table 5.1) is in the usual microdiamond range (Mr. L. van Heerden, unpublished data), presumably coincidental as the $\delta^{13}C$ reflects the initial starting composition of the carbonaceous material. However, their cubic morphology is somewhat surprising; diamonds isolated from the Barringer Crater, U.S.A. are intergrowths of cubic and hexagonal crystal structures. Similarly, the TNT sample was studied by T.E.M. analysis and found to consist of ~10nm grains that were also cubic in morphology. As the starting materials of the diamonds from TNT, soot, and graphite were unavailable, it was not possible to determine if the diamond formation process caused any isotopic fractionation: values of ~-30‰ are within the typical range in carbon isotopic composition for graphite and soot.

The nitrogen content of the shocked produced diamond suite ranged from 397ppm (crater diamond) to 1.7 wt% (TNT produced diamond). Evidently shock transformation processes allows the uptake or retention of a high concentration of nitrogen atoms, if nitrogen is present in a suitable form in the precursor material.

5.3 Chemical Vapour Deposition: formation of diamond from the vapour phase

Although diamond is perceived as a high pressure mineral, it is surprisingly easy to form nanometre sized crystallites metastably at low (< ~0.5 x atmospheric pressure), because of a small free energy difference between graphite and diamond (2.4 kJ mol^{-1}). The first reported attempt at diamond growth from the vapour phase (von Bolton, 1911) claimed to have grown diamond from diamond seeds using illuminating gas (C_2H_2) in the presence of mercury vapour. Attempts at reproducing this result with similar experiments were unsuccessful and low pressure diamond synthesis was not further pursued until the 1950's, when W.G. Eversole of the Union Carbide Corporation (Eversole, 1958;1959) and Derjaguin and co-workers of the Academy of Sciences, Moscow (Deryaguin and Spitsyn, 1956) achieved successful growth of diamond from CBr_4 and CCl_4.

There are three main processes used today to manufacture diamond by the chemical vapour deposition (CVD) method industrially: (i) hot filament chemical vapour deposition, (ii) high frequency plasma assisted CVD and (iii) DC plasma discharge. These varied approaches have several features in common: (i) hydrogen is always present, which saturates the carbon, encouraging the formation of sp^3 rather than sp^2 bonds (ii) the carbon source is always an organic compound (*e.g.* CH_4, CH_3OH, C_2H_6); (iii) a solid substrate on which diamonds can nucleate is usually necessary; many materials have been used to provide a nucleation site, including silicon, silicates and metals. However, some recent studies report the successful growth of diamond by homogeneous nucleation, in which no substrate was required (Frenklach *et al.*, 1989; Howard *et al.*, 1990). Less controlled conditions have also resulted in the production of metastable nanometric diamond; for example, small diamonds have been found as a deposit within internal combustion engines (DeVries, 1987) and have been detected as a precipitate from an oxygen acetylene flame (Janssen *et al.*, 1990). In addition, "hard carbons" have long been produced by the pyrolysis of hydrocarbon material (*e.g.* Ubbelhode and Lewis, 1960). Thus, the production of nanometre sized diamonds at low pressures may be an extremely common occurrence in nature, although this has only recently been appreciated because the observation of crystallites of this size requires sophisticated isolation and detection techniques.

Samples produced by chemical vapour deposition onto silicate substrates by Plessey, Towcester, U.K. were donated for carbon isotopic analysis to allow a comparative study to be made between meteoritic diamond and CVD diamond. The samples included (i) a diamond-like hydrocarbon, (ii) a diamond-like carbon, and (iii) three

senso stricto diamond samples, CVD 110, CVD 125, and CVD 151 from three different starting materials (see table 5.2, which is at the end of this section).

5.3.1. Effect of perchloric acid

One of samples donated by Plessey was a mixture of diamond-like carbon and diamond. As the meteoritic component "Cδ" is also believed to be a mixture of these two phases (*e.g.* Blake *et al.*, 1988), the samples represented an opportunity to observe the effect of acid treatments on this type of sample. The perchloric acid stage was of particular interest because this strong oxidant destroys most carbonaceous material.

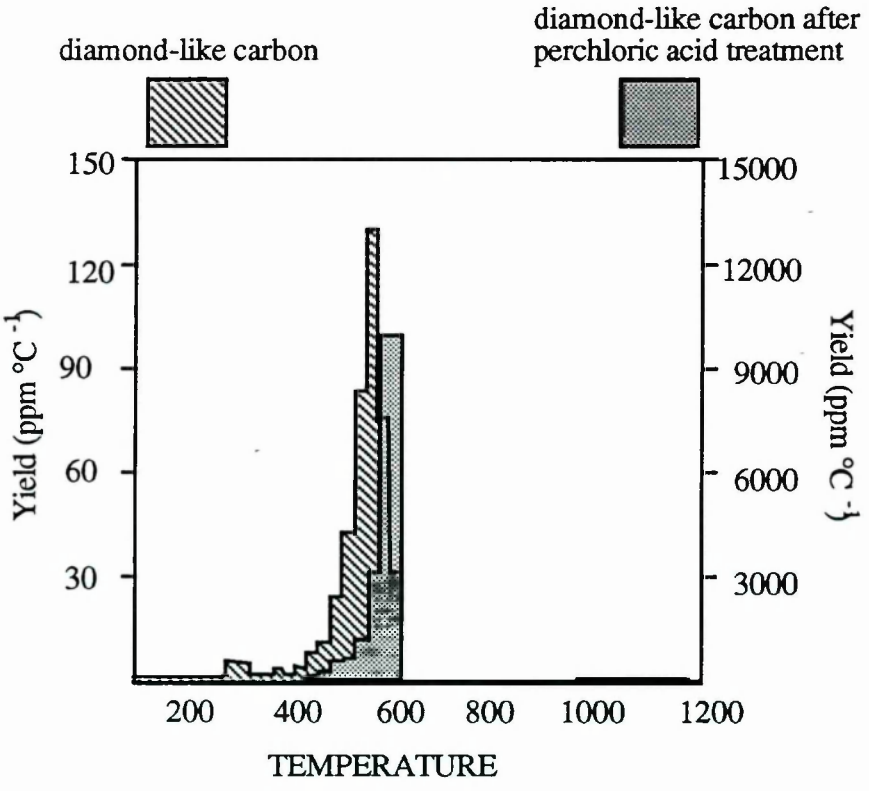

Figure 5.1. Comparison of combustion profile of a CVD diamond-like sample before and after perchloric acid treatment, demonstrating the difference in combustion temperature the treatment causes.

A before-and-after comparison was made of the stepped combustion profile of the perchloric treated diamond like carbon sample (figure 5.1). Before treatment the peak combustion temperature was 500°C; after the treatment the peak temperature had risen

to 600°C with less carbon burning at very low temperatures. The data indicate that the perchloric treatment dissolved most of the carbon in the sample but left a thermally resistant (true diamond?) residue. Unfortunately the weight loss of carbonaceous material is impossible to quantify as the acid treatment also destroyed the silicon substrate material, and thus the mass loss included both silicon and carbon in unknown proportions.

5.3.2. Stepped combustion of CVD diamond

The burning of CVD diamond during stepped combustion occurs over a very narrow temperature range, indicating that the only low temperature carbonaceous component in the samples was diamond, of approximately uniform grain size. The carbon was released at 500-600°C, around 50° higher than the usual release temperature of Cδ diamond (figure 5.2), suggesting a grain size of ~1μm, which is in keeping with electron microscopy observations of similarly produced CVD diamond (*e.g.* De Vries, 1987). The sharp combustion profiles indicate the CVD samples are well sorted grains of pure diamond.

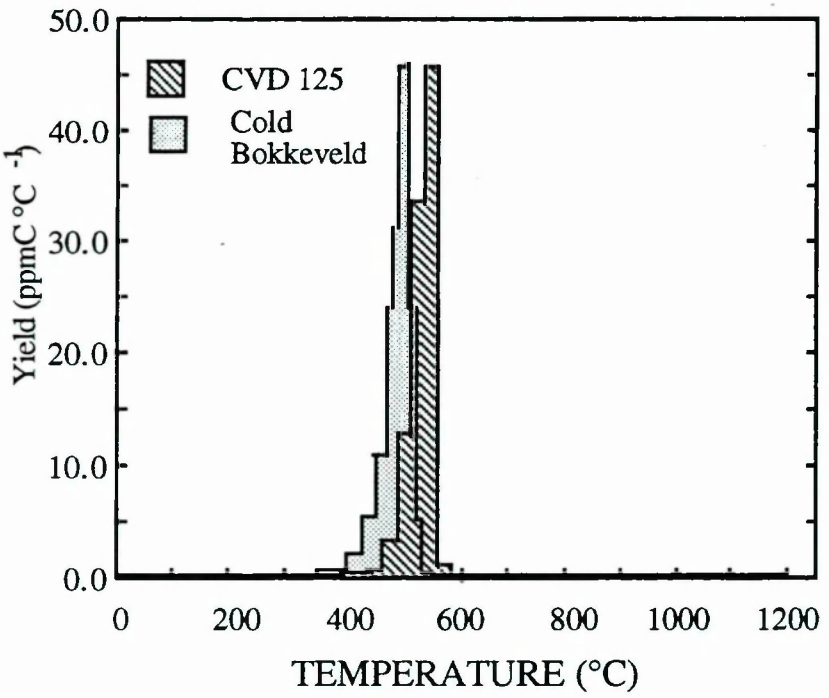

Figure 5.2. A comparison of carbon release profiles of diamond from a CVD sample and diamond from the CM2 carbonaceous chondrite Cold Bokkeveld.

In addition, some carbon combusted at high temperatures; probably SiC from the diamond/substrate interface. The diamond to (putative) SiC ratio varied from 26

(diamond like carbon) to over 700 (CVD 151) and there was a difference in $\delta^{13}C$ between the SiC and diamond; the high temperature release in the diamond like carbon sample for example was 9‰ lighter than the diamond release.

5.3.3 Carbon isotopic composition of CVD diamond

The isotopic fractionation of carbon involved in the reaction may provide clues to the diamond forming mechanism that would allow a more efficient production system to be designed. Surprisingly, few publications discuss the isotopic composition of diamond produced by CVD processes, though this may in part represent the publication-shy nature of CVD research.

The $\delta^{13}C$ of all the diamond samples *senso stricto* investigated was low, with values of -60 to -70‰ typical (table 5.2). Only one example of a starting material -the methanol used to prepare CVD 125- could be obtained. The $\delta^{13}C$ of the methanol was measured, although this experiment was somewhat difficult to perform as it was necessary to freeze the methanol using liquid nitrogen in a quartz finger with CuO powder, to allow the evacuation of the system without sample loss, before sealing the quartz and combusting the sample. However, the experiment was performed twice and gave a reproducible result. The methanol had a carbon isotopic composition of -47.6 ‰ (σ= 0.05), and the diamond produced from this had $\delta^{13}C$ = -59.9‰ (peak value), -58.3‰ (bulk [summed] value). This corresponds to a fractionation between starting material and product of ~12‰; the solid diamond formed was *lighter* in isotopic composition than its precursor. More work is clearly needed in this area in which the $\delta^{13}C$ of the starting materials are known and the experimental conditions more closely controlled so that the relevance of this behaviour to the diamond forming mechanism can be understood. The carbon isotopic composition of the diamond-like sample was also measured both before and after perchloric acid treatment; its peak isotopic composition remained unchanged at -2.6‰ (σ=1.54) before acid dissolution and -3.2‰ (σ=0.89) after the treatment, indicating that the diamond-like carbon and diamond have similar $\delta^{13}C$ values.

5.3.4. Nitrogen in CVD diamond samples

The diamonds produced by CVD are difficult to distinguish from natural diamonds, but one important difference is that they are believed to contain more lattice defects that are of a different type to high pressure diamonds which causes them to have a

broadened 1332 cm^{-1} Raman peak (*e.g.* Kalish, 1990). The increased number of defects in the CVD diamond lattice may allow them to hold more nitrogen (Kalish, 1990, Ash ,1990) than natural terrestrial diamond. Measurements of the CVD diamond suite indicated that the diamond can indeed contain large amounts of nitrogen compared to terrestrial diamond (in which values of <1000ppm are the norm); in this sense they are more reminiscent of the meteoritic diamond Cδ.

Sample	$\delta^{13}C$ (σ) peak	$\delta^{15}N$ (σ) mean	C/N	ppm N
CVD 110	-71.8 (2.55)			
CVD 125	-59.9 (1.29)			
CVD 151	-65.6 (1.09)	+2.9	485	2061
CVD dia like	-3.2 (0.89)	-7.7 (0.4)	1122	891
CVD dia like HC	-44.8 (1.0)	-4.3	600	1665

Table 5.2 C.V.D diamond data CVD dia like = diamond-like sample after perchloric treatment. CVD dia like HC = diamond-like hydrocarbon, data from this sample are from Ash (1990). Nitrogen data for CVD 151 are from R. Ash (*pers comm*, 1991). Starting materials: CVD 110 was produced from methane; CVD 151 from methanol, and CVD 125 from ethene.

5.4 Carbonados

Carbonados are natural aggregates of diamond or diamond-like crystals held together with sintered diamond (Orlov, 1977) with a characteristic porous texture. They are associated with crustal minerals and typically contain low pressure inclusions; hence a shallow origin for the diamond has been suggested (Kaminskiy, 1987). Possible origins of carbonado diamond include the subduction of carbonaceous sediment and impact metamorphism of organic crustal carbon but the absence of other high pressure facies argues against these theories. The first report of this diamond type was by Breger (1964), in uranium bearing Mesozoic and Cenozoic rocks of the Colorado Plateau. He linked the presence of diamond to the effect of radioactive emissions. It was later shown experimentally (Ergun *et al.*, 1974) that α particles from uranium causes dehydrogenation and crosslinking of the graphitic layers in carbonaceous materials, a process that may eventually allow the formation of diamond and diamond-like clusters. In nature, the initial carbonaceous material was possibly organic matter such as kerogen, coal, kerite *etc.* If the α particle has an energy of >~10eV, then during irradiation a localised region of 100 atoms can be heated to 4000K, sufficient

for the generation of diamond like film (Ergun *et al.*, 1974). Submicron clusters would form in this way which could then aggregate into larger crystals over time. This process would not be expected to cause any isotopic fractionation (Kaminskiy, 1987) and so the $\delta^{13}C$ of the resulting cluster will be the same as the isotopic composition of the starting material. Recent noble gas data (Ozima *et al.*, 1991) indicates the presence of fission products in the diamond and so provides further evidence for the irradiation formation theory.

Ozima and Zashu (1991) have suggested that this process may be important in meteorites. The presence of carbonaceous material in meteorites is well established and high radiation fluxes are a feature of the interstellar medium, so it is conceivable that diamonds may form in such an environment by the carbonado mechanism. A suite of carbonado diamonds were used in a preliminary study to determine if there is any similarity between carbonados and meteoritic diamond.

Sample	$\delta^{13}C$ (σ)	$\delta^{15}N$ (σ)	C/N	ppm N
JWF 1	-19.84 (0.05)	+4.7 (0.91)	4000	247
JWF 4	-2.89 (0.10)	nm	1.2×10^6	0.8
JWF 5	-2.42 (0.03)	nm	18000	55
JWF 11	-19.25 (.08)	+8.7(2.1)	13000	76

Table 5.3 Carbon and nitrogen in four Brazilian carbonado diamond samples

The samples investigated were from the JWF suite which originate in a locality in Brazil, donated by H.J. Milledge of University College, London. Carbonado diamonds are notoriously diverse in character but these particular specimens were chosen because they bear a resemblance in colour (grey) and macroscopic morphology to the diamond residue isolated from the Abee meteorite (chapter 4). The four samples had a very similar agglomerate texture to each other and the binocular microscope revealed them to be made of ~mm sized crystals, an observation confirmed by their combustion temperature of ~750°C. A study of the carbon and nitrogen isotopic composition of the diamonds demonstrated that these four samples consist of two distinct groups. One group (JWF 1 and JWF 11) was characterised by a $\delta^{13}C$ of -19‰, which lies just outside the range from a wide variety of localities in values reported by other investigators which lie between -20 and -30‰ (*e.g.* Ozima *et al.*, 1990; Orlov, 1977; Galimov, 1985; L. van Heerden, unpublished data), believed to be in keeping with an organic origin for the carbon. JWF 4 and JWF 5 have an even heavier carbon isotopic composition, at ~-2‰, a value not previously encountered for carbonado diamonds. This is well outside the range reported in other carbon isotopic

studies of carbonado diamonds indicating their precursor may have been a non-organic material. The carbon isotopic composition is more reminiscent of a carbonate origin, although it seems unlikely that such a well oxidised source could produce diamond. Thus, this small database is clearly atypical of the carbonado population as a whole.

The nitrogen content of all four of the samples is extremely low, especially for the JWF 4 and JWF 5 samples. Again, this is surprising if their putative source is biologically produced organic material, which is generally contains 5 to 10% nitrogen. It is possible that the mechanism by which these diamonds were formed is one which produces effectively defect-free diamond and so it would be difficult for nitrogen to become incorporated into the crystal lattice. Unfortunately there is an absence of reports of nitrogen contents in carbonados in the literature, and so it is possible that these samples are atypical of the carbonado population as a whole.

Interestingly, the JWF5 sample is similar in nitrogen content to diamond from Abee,but a wider suite of samples must be studied to determine if this feature is diagnostic of this diamond type. The similarity of $\delta^{13}C$ between JWF 4 and JWF 5 and Abee diamond is also striking but as this is believed to represent the starting material this must be purely coincidental.

5.5 Conclusions

A series of diamonds of diverse origins have been considered as analogues for meteoritic diamond formation. Of these, only one, diamond formed by prolonged static pressure, discussed first, is universally believed to be not relevant to meteoritics. Samples of diamonds from other sources (shock, CVD and carbonado) have been studied in an attempt to observe similarities between these diamonds and those found in meteorites. As "Cδ" diamond is found only in the least heated meteorites, it is believed to have been formed "in space" before the accretion of the meteorite parent body (*e.g.* Lewis *et al.*, 1987; Huss, 1990, Anders, 1988). Carbonado formation takes place terrestrially only in consolidated rocks and it is thus difficult to make an analogy between this process and the formation of diamond in a plasma or high vacuum, although it is possible that this *in situ* process may be important in the formation of diamond from the enstatite chondrite Abee (see chapter 4). Although there is some evidence for fission products in Abee (Wacker and Marti, 1983) these are not in greater abundance than the fission products in other meteorites.

Since their identification in 1987 by Lewis *et al.*, the formation mechanism of nanometric diamonds have caused some discussion. Lewis *et al.* favoured a CVD type formation whereas others, such as Tielens (1988) argue that they could have been formed from graphite in a supernova shock. Both mechanisms are feasible both in a circumstellar environment and in the early Solar nebula. From the limited and preliminary study made here of diamonds produced by both methods it is difficult to pass judgement on this debate. Diamond produced by different techniques cannot be distinguished by their stepped combustion release profiles or combustion temperatures, which depend strongly on diamond size, rather than other features. Similarly, the T.E.M. study indicated that the morphology of the diamonds produced by shock and by CVD were similar; both were cubic in structure. Although the shocked diamond was of nanometre dimensions whereas the CVD was made up of submicron grains, other CVD samples have a size range very similar to that of meteoritic diamond (*e.g.* Janssen *et al.*, 1990; DeVries, 1987). The nitrogen contents of diamonds produced by both techniques can be high, fulfilling that criterion necessary for an analogy to Cδ diamond, although only the diamond produced by explosive processes from a nitrogen rich source had a nitrogen content as extreme as that seen in Cδ diamond. Further study should include an investigation into the nitrogen content of CVD diamonds produced from similar nitrogen containing progenitors. The shock technique is not believed to cause any isotopic fractionation; although vapour deposition is not an equilibrium process and does fractionate the diamond formed, this has not yet been carefully studied and is probably very dependant on the exact starting conditions.

The argument of Tielens (1988) that carbonaceous material in meteorites comes from a common reservoir, of which 5% converted to diamond under the influence of a shock front, is difficult to justify as there is a large discrepancy in $\delta^{13}C$ between the diamond and other carbonaceous material in the meteorite, particularly the graphite which he considered the diamond precursor. In addition, the noble gas and nitrogen complement of the graphite and diamond are not the same, implying they have had diverse histories. The carbon isotopic composition and nitrogen and noble gas content and isotopic composition of the diamond imply it had a separate source from the other carbonaceous components in the meteorites. Hence, since a solid diamond precursor cannot be found in meteorites, with a $\delta^{13}C$ of -32 to -38‰, a vapour deposition mechanism of diamond production seems more likely.

CHAPTER 6

SILICON CARBIDE AND HIGH TEMPERATURE COMPONENTS

Silicon carbide was first made and identified by E. G. Acheson in 1891. Recognising its hardness and extreme thermal and chemical resilience, he founded the successful Carborundum Company that supplied an industrial demand for the new material. Silicon carbide (SiC) exists in over 170 crystalline modifications, based on the carbon atoms in a face-centred cubic (diamond type, "β–SiC") or polymorphs of the face centred hexagonal (wurtzite type, "α–SiC") arrangement, tetrahedrally bound to silicon atoms that lie at the half points in the structure. Pure samples of SiC are yellow or white, but small amounts of impurities such as iron and aluminium can change the colour to black, green, or purple.

SiC is produced industrially by the Acheson process in which high grade sand is mixed with coke or anthracite in a furnace at 2000-2500°C:

$$SiO_2 + 2C \rightarrow SiC + 2CO$$

The growth of SiC by CVD is also a well established process (*e.g.* Nishino *et al.*, 1983; Matsumami *et al.*, 1989; Glasgow,1989). Typically, the SiC is grown from a SiH_4-C_3H_8-H_2 mixture at ~1 atm pressure and at 1350-1500°C onto a Si or SiC substrate. Trace elements can be introduced to the crystal lattice *via.* the reaction gas (Kim and Davies, 1986) or by ion implantation after crystal growth (*e.g.* Edmond *et al.*, 1987). The diffusion coefficient of trace elements in SiC is negligible below 1800°C and so loss of these components due to degassing is unlikely at low temperatures (Kirchstein, 1984). The crystal size produced by both processes can be up to several millimetres across.

6.1 Combustion of silicon carbide

The thermodynamic properties of SiC are complex due to a thin layer of SiO_2 that forms on the surface of the crystal on contact with air:

$$2SiC + 3O_2 \rightarrow 2SiO_2 + 2CO$$

Because of the complicated combustion mechanism, fine grained SiC powders can be

more stable in oxygen than macroscopic crystals (Kirchstein, 1984). The oxidation of SiC occurs at the SiC-SiO_2 interface and the combustion follows a parabolic law, suggesting that the rate determining step is diffusion controlled, from the movement of oxygen through the silica layer. After several hours at ~1000°C the combustion rate increases, possibly because the SiO_2 layer crystallises and thus increases in porosity (Jorgensen *et al.*, 1959). Similarly, although the combustion rate is dominated by oxygen diffusion below 1200°C, above 1200°C crystobalite crystallisation is the rate determining step. The colour and polytype of SiC) is thought by some authors to have little effect on the combustion properties of SiC (Kirchstein, 1984) but some authors (Greenwood and Earnshaw, 1984) suggest that the β form is less stable to combustion than the α forms. Doping the crystal with Al affects the combustion rate (*e.g.* Kato *et al.*, 1963) but the exact relationship is obscure: the rate of oxidation can be either increased or decreased depending on the temperature and Al concentration.

6.2 Silicon carbide in meteorites

Although the first report of meteoritic SiC, from Canyon Diablo (Moissan, 1904), was made at the turn of the century, this observation was widely considered to be ascribable to terrestrial contamination. SiC of a clearly indigenous nature was not shown to be present in meteorites until a series of experiments were performed on primitive chondrites nearly seventy years later.

Chondritic SiC was identified and isolated because of its anomlaous isotopic signature. During a stepped heating experiment on the CM2 meteorite Murray (Srinivasan and Anders, 1978), xenon with an isotopically anomalous signature was evolved, that matched almost exactly that of calculations of s-process nucleosynthesis, in which a low flux neutron bombardment produces high atomic mass elements (consequently the Xe signature became known as Xe-S: figure 1.1). The experiment provided the first hint that, as predicted by Clayton and Ward (1978), interstellar grains were present in the carbonaceous chondrites that have an "s" process signature and hence were formed in a circumstellar environment around an evolved star. The discovery of Xe-S was quickly followed by the detection of an anomaly in neon isotopic composition (Eberhardt *et al.*, 1979, Lewis *et al.*, 1979), typified by an enrichment in ^{22}Ne and called Ne-E. Acid resistant residues, highly enriched in both these noble gas components, were found to be made up mostly of SiC (Tang *et al.*, 1988). The presence of this mineral in meteoritic residues had been suggested by silicon detection in an analytical SEM system (Tang *et al.*, 1987), and by TEM, ion probe and Raman spectroscopy (Bernatowicz *et al.*, 1987,

Zinner *et al.*, 1987). Many other anomalous isotopic compositions have since been associated with SiC, including the major elements, silicon and carbon (see Table 4.1), indicating that the grains are almost certainly presolar in origin. There was early evidence that silicon carbide was heterogeneous; before its characterisation two components, called Cβ and Cε, were postulated, where Cβ was the Xe-S carrier that had a grain size of 0.03 to 0.2μm and Cε was the carrier of Ne-E (now called Ne-E(H)) that was thought to be coarser grained (0.1 to 2 μm crystals). Silicon carbide has been isolated by acid dissolution from samples of all chondritic classes (*e.g.* Alexander *et al.*, 1990; Ash, 1990; Huss, 1990; Stone *et al.*, 1991) in amounts of up to ~10 ppm of the whole rock.

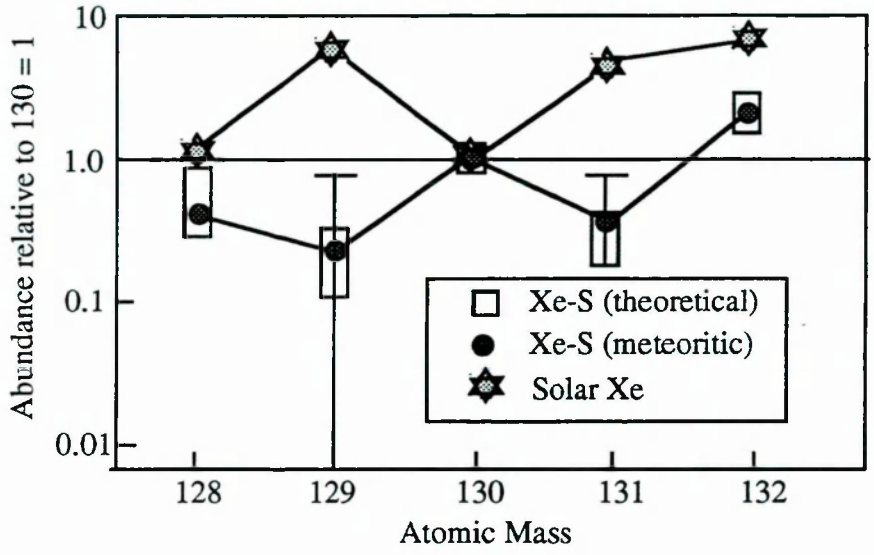

Figure 6.1. Theoretical Xe-S compared to Xe in meteoritic SiC and Solar values, normalised to $^{130}Xe = 1$. Figure after Anders, 1988.

Studies of silicon carbide using the ion probe technique have allowed considerable progress to be made in the understanding of SiC on a grain by grain scale. The ion probe technique allows the isotopic analysis of small (5μm) areas of sample using ion bombardment and subsequent high resolution mass spectrometry. In this way, individual grains above a minimum size can be analysed; this technique has demonstrated that the silicon carbide grains are isotopically diverse (Zinner *et al.*, 1989). In particular, the diversity of silicon isotopes has given support to the theory that the silicon carbide grains came from several different stellar sources, unless the stellar source was large enough to synthesize fresh ^{29}Si and ^{30}Si during the AGB stage (Clayton *et al.*, 1992). The carbon isotope composition of individual grains show extreme isotopic diversity (figure 6.2), but these data cannot be used as evidence for diverse sources as it would be possible to have extreme C isotope variations in a single red giant if dredge ups were frequent (Zinner *et*

al.,1989). The nitrogen isotope composition could also be affected by the same process. The mean $\delta^{13}C$ of SiC from ion probe measurements is heavy, at ~+1000‰,and nitrogen light, with $\delta^{15}N$~-400‰ (Zinner *et al.*, 1989; see figure 6.2).

Element	Anomaly	References
Helium	^{4}He enriched	Nichols *et al.*,1991
Carbon	^{13}C enriched	Swart *et al.*, 1983 Ash, 1990; Alexander *et al.*, 1990, Zinner *et al.*, 1989.
Nitrogen	^{14}N enriched	Zinner *et al.*, 1989; Ash 1990
Silicon	^{28}Si depleted	Zinner *et al.*, 1987, Stone *et al.*,1990
Neon	^{22}Ne enriched	Lewis *et al.*,1979; Eberhardt *et al.*,1979
Magnesium	^{26}Mg enriched	Zinner *et al.*, 1991
Calcium	s-process signature	Amari *et al.*, 1991
Titanium	s-process signature	Ireland *et al.*, 1991
Krypton	s-process signature	Ott *et al.*, 1988
Strontium	s-process signature	Ott and Begemann, 1990; Richter *et al.*, 1992. Prombo *et al..*, 1992
Xenon	s-process signature	Srinivasan and Anders, 1978
Barium	s-process signature	Ott and Begemann, 1990 Zinner *et al.*, 1990; Prombo, 1991.
Neodynium	possible s-process signature	Zinner *et al.*,1990; Richter *et al.*, 1992
Samarium	s-process signature	Richter *et al.*, 1992
The anomalous "X" grains		
Carbon	^{12}C enriched	Zinner *et al.*, 1991
Nitrogen	^{15}N enriched	Zinner *et al.*, 1991
Silicon	^{28}Si enriched	Zinner *et al.*, 1991
Calcium	^{44}Ca enriched	Amari *et al.*, 1992
Titanium	^{49}Ti excess	Amari *et al.*, 1992

Table 6.1 Elements for which isotopic anomalies have been reported in SiC.

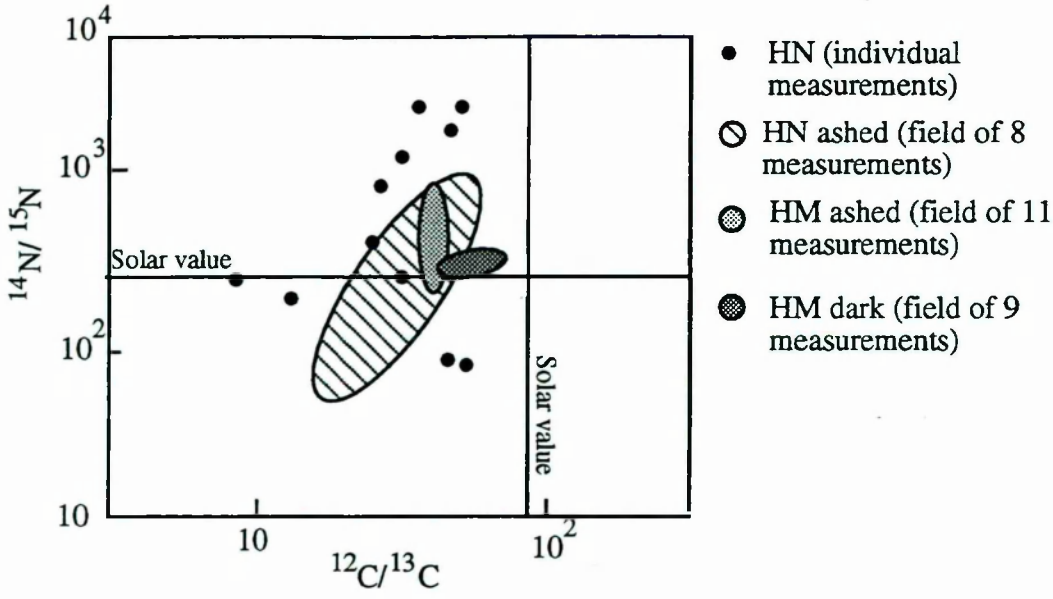

Figure 6.2. Variations in $^{12}C/^{13}C$ and $^{14}N/^{15}N$ observed in individual SiC crystals from four Murchison residues using the ion probe (from Zinner *et al.*, 1989)

The study of individual grains by ion probe is limited to the larger crystals, giving a biased dataset. The data have therefore been complimented by ion probe studies on groups of small grains. Such investigations ought to provide a greater insight into the SiC population as a whole (*e.g.* Amari *et al.*, 1990; Zinner *et al.*, 1990). The analysis of many thousands of grains in a single stepped combustion experiment is more useful in this regard, as it allows mean data to be accurately measured. A strength of stepped combustion is that, unlike the ion probe, it can potentially differentiate between SiC and minor components which must be investigated.

Assuming the s-process isotopic signatures are indicative of events occuring in a red giant carbon star, it is likely that the noble gases were implanted from the associated stellar wind after the grains had solidified. The Ne-E (H) was at first believed to come from a separate source (a nova component from the decay of ^{22}Na) but Lewis *et al.* (1990) suggested that a more likely source is "parentless" ^{22}Ne produced in the He shell of a red giant, an idea that has been supported by noble gas studies of individual grains using laser gas analysis (Nichols *et al.*, 1992). Thus, the carrier of Ne-E (H) and Xe-S (Cβ and Cε) could be indistinguishable, although the Ne-E (H)/ Xe-S ratio is slightly higher in the larger grains (Amari *et al.*, 1989). Some ion probe analyses indicate that a small proportion of the silicon carbide ("X" grains) have very different isotopic characteristics and maybe from a supernova environment (Zinner *et al.*, 1991); see table 6.1. Similarly,

anomalous "Y" grains are distinguishable from the main bulk of grains by a higher $^{30}Si/^{29}Si$ ratio (Amari *et al.*, 1992).

The isotopic compositions of the carbon, nitrogen, and silicon in SiC have allowed Gallino *et al.* (1990) to model the nucleosynthetic processes under which they formed. They concluded that the isotopic characteristics of SiC agree well with the expected evolution of a low mass ($M_o<M<3M_o$) star in its thermally pulsing AGB phase of giant evolution. Stars of this type dredge up "s process" elements (see section 1.3 for a summary of red giant evolution).

6.2.1. Silicon isotopic composition of meteoritic SiC

The apparently all-encompassing interpretation of Gallino and colleagues has been questioned by Obradovic *et al.* (1991), whose models of AGB star evolution predict higher $^{30}Si/^{29}Si$ ratios than those observed in SiC grains. The isotopic composition of the silicon most of the SiC grains (figure 6.3) falls on an array which has a $\delta^{29}Si/\delta^{30}Si$ of ~1.4 (Stone *et al.*, 1991). This array cannot be explained by fractionation of material of a Solar source, which would fall on a line with a gentler gradient on a 3 isotope Si plot. For similar reasons, the variation in Si isotopes cannot be explained by calculated abundances of Si formed by (n,α) and (n,γ) reactions in a neutron rich environment which would produce silicon with $\delta^{29}Si/\delta^{30}Si = 0.5$ (*e.g.* Gallino *et al.*, 1990). Although previous studies have attributed the silicon array to several stellar sources of SiC each with a different progenitor Si isotope composition (*e.g.* Zinner *et al.*, 1989), recent calculations by Clayton and Brown, (1992), and Brown and Clayton, (1992), have shown that the correlation can be explained if the AGB star is sufficiently massive to undergo magnesium burning. Then, shell flashes reach a higher temperature than predicted in previous models, allowing the conversion of ^{22}Ne to magnesium, and then the reactions $^{25}Mg(\alpha,n)\ ^{28}Si$ and $^{26}Mg(\alpha,n)^{29}Si$ to take place which would form extra ^{28}Si and ^{29}Si. This process would occur only in high mass AGB stars rather than the more common low mass ones. It is possible that only these larger stars are rich enough in silicon to produce SiC rather than graphite. Magnesium burning would allow the silicon isotopic composition to change during stellar evolution and mixing can then explain the position of most of the individual grains thus far analysed (except for the X and Y grains). Thus, it is possible that a single source could produce most of the meteoritic SiC showing the silicon isotopic diversity observed.

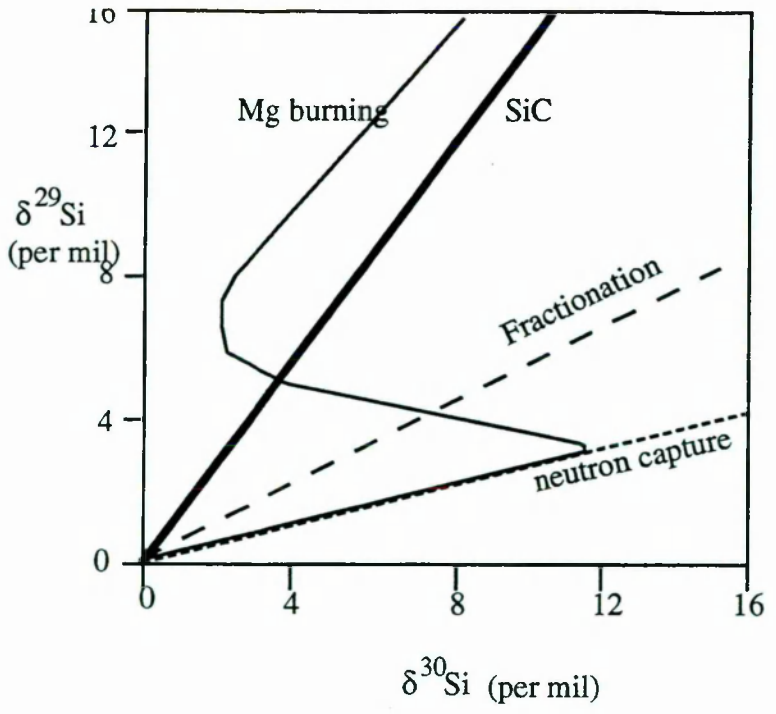

Figure 6.3. The array of Si isotopic compositions of most meteoritic SiC grains, compared with the line of expected values if the variations were caused by mass dependant fractionation and line of expected values if the variations were caused by neutron capture reactions in the red giant. Also shown is the evolution of Si isotopes during Mg burning. If Mg burning occured in an AGB star then the input of fresh ^{28}Si would shift the overall isotopic composition of Si towards more ^{28}Si rich values. Diagram after Clayton and Brown, 1992. SiC array and fractionation lines from Stone *et al.*, 1991, and neutron capture line from Gallino *et al.*, 1991.

6.3. Previous stepped combustion results and aims of the chapter

High-temperature isotopically heavy carbon was observed in bulk meteorite samples and simple acid resistant residues were first reported by Swart *et al.*, (1983) and the improvement in our understanding of acid dissolution and stepped combustion procedures have allowed increasingly sophisticated measurements to be made (*e.g.* Wright *et al.*, 1988; Ash, 1990). Previous carbon and nitrogen stepped combustion studies have demonstrated that meteoritic SiC is characterised by an enrichment in ^{13}C, with typical $\delta^{13}C$ values of between +1000‰ and +1400‰ reported (*e.g.* Wright *et al.*, 1988a; Ash, 1990; Alexander *et al.*, 1990). Nitrogen is extremely enriched in ^{14}N in Cold Bokkeveld (CM2) with a $\delta^{15}N$ value of -618‰ recorded by Ash *et al.* (1989b), the lightest N released during any stepped combustion experiment. In contrast, the acid-resistant residues of the ordinary chondrites Inman and Tieschitz released isotopically heavy nitrogen with $\delta^{15}N$ = +1607‰ for Tieschitz (Alexander *et al.*, 1990). None of the samples studied showed a sharp single peak or a distinct $\delta^{13}C$ plateau during stepped combustion, thus the residues must also contain several other high temperature acid-resistant components (*e.g.* McGarvie *et al.*, 1987; Tang *et al.*, 1988; Ash *et al.*, 1990). Confirmation of these components was often difficult because of restricted sample

availability, the necessity of large step sizes over the high temperature regime, and the absence of a systematic production technique for the residues involved. The development of a new higher sensitivity mass spectrometer (Prosser *et al.*, 1990; Yates *et al.*, 1992) provided an opportunity to study in more detail carbon in residues believed to contain SiC. Decreasing the size of the temperature increments from typically 50-100° steps over the high temperature regime to 25°C, would allow a more detailed appraisal of the structure in the step combustion pattern, and hence give a more favourable opportunity to characterise the minor components. Samples of the residues before and after stepped combustion were studied collaboratively with electron microscopists in the hope that minor components released during stepped combustion could be correlated with the mineral assemblage. The suite of similarly prepared residues from several meteorite classes allowed a systematic study to be made of SiC so that comparisons could be made between meteorites.

The objectives of this chapter can be summarised as: (i) to measure the abundance and mean isotopic composition of SiC within a suite of meteorite classes (carbonaceous, ordinary and enstatite) and (ii) to verify the existence of other minor carbon components so that in future these might be the subject of separate studies in their own right, as many of these components are probably also interstellar grains that could provide further information about the material that made up the Solar system.

Samples, of carbonaceous, ordinary, and enstatite chondrites were treated with HF/HCl and oxidising acids as described in section 2.3; further treatments with NaOH and H_3PO_4 were performed on some Murchison residues. The acid-resistant residues were then combusted incrementally to 550°C in order to remove the diamond component (data from this part of the experiment have been discussed in chapter 3), which constitutes around 99% of the carbon in these samples. The remainder, still in its platinum bucket, was then transfered to the high resolution static mass spectrometer extraction system (see section 2.1 for a discussion of the blank contributed by this process). The residues were studied both before and after stepped combustion experiments by X-ray diffraction analysis, SEM and TEM, by G. Cressey and R. Greenwood (British Museum) and M. Lee (University of Essex).

6.4. SEM and X-ray diffraction analyses.

The acid-resistant residues were studied by SEM and X ray diffraction to verify that the expected components of the samples - for example, spinel, SiC, chromite, and hibonite - were present and that no major contaminating components could be detected (table 6.2). Some samples were studied after the removal of diamond by stepped combustion, and after the combustion to 1200°C. The SEM evidence appeared to confirm that no

contaminants were present in the residues except possibly barytes and rutile, *e.g.* in CB2C (figure 6.4). The SEM analyses cannot be truly quantitive for minor components such as SiC, as observation of rare minerals often depends on seeing a single grain or not. If a grain is not observed this does not represent proof of its absence.

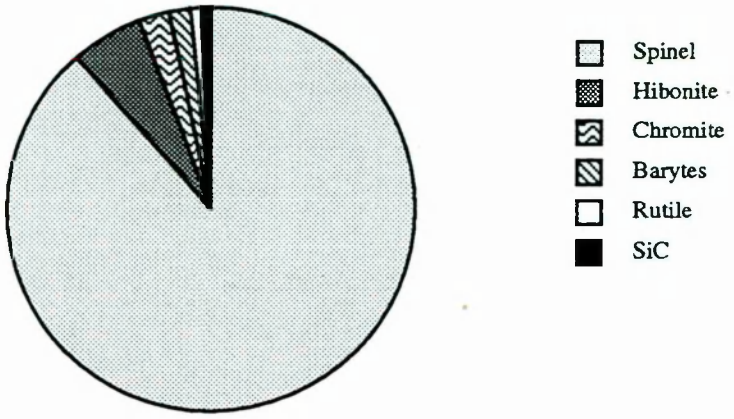

Figure 6.4. Composition of the perchloric acid-resistant residue of Cold Bokkeveld (CB2C). These are quantative results but only compounds which contain at least one element with z >10 are measurable; *i.e.* diamond and graphite are not included. Data from R. Greenwood (British Museum).

An important result from the SEM analyses was the observation that spinel recrystallises over the temperature range of the stepped combustion; residues heated to 800°C had partially recrystallised but this process was complete in residues heated to 1250°C; the crystals loose their stoichiometry and become more enriched in iron. The source of this iron is unknown although work is in progress to understand this phenomenon more fully. The recrystallisation process would be expected to cause the release of any carbon dissolved within the crystals at this temperature. The decrease in stoichiometry observed in some spinel samples (*e.g.* in CB3B) results from the presence of SiO_2 in the crystal lattice. The most likely source of the silicon is SiC. These preliminary results indicate the need for microscope characterisation of all the meteorite residues both before combustion and analyses at stages during the stepped extraction, to allow the monitoring of the components destroyed or recrystallised at each stage of the stepped combustion process.

Meteorite	Residue	Treatments	Composition	
C.Bokkeveld	CB2C		Spinel	88.8%
			Hibonite	5.7%
			Chromite	2.4%
			Barytes	1.6%
			Rutile	0.8%
			Silicon carbide	0.8%
Murchison	M2A	H_3PO_4	Carbon (diamond?)	
			Hibonite	
			Silicon carbide	
	M2B	NaOH	Spinel	95.4%
			Hibonite	3.4%
			Chromite	1.1%
ALH 83100	ALH 3		Carbon (diamond?)	
			Silicon carbide	
			No spinel	

Table 6.2 Minerals identified by X-ray diffraction and SEM analysis. All samples have been treated with HF/HCl, $H_2Cr_2O_7^{2-}$, and $HClO_4$; any additional treatments are listed above.

6.5 TEM analysis

Representative samples of the meteorite residues were prepared for TEM analysis at the Open University and then sent to M. Lee, at the University of Essex, for characterisation by transmission electron microscopy. The samples were prepared by ultra-sonicating in isopropanol to which a drop of ammonia had been added (after Bernatowicz *et al.*, 1990). Around 1ml of the solution was then pipetted onto a holey carbon grid and evaporated at 150°C for half an hour. A conclusion of the TEM study was that diamond is a major constituent of the samples in addition to the minerals seen using SEM. SiC and rutile were also observed. In addition, Si_3N_4 was detected in the Indarch residue, a mineral that had previously been observed in the enstatite chondrites Indarch (Stone *et al.*, 1991), and Qingzhen (Alexander *et al.*, 1990), and Si_3N_4 and ureyite (kosmochlor: $NaCrSi_2O_6$) were found in Tieschitz.

6.6 Combustion of meteoritic residues believed to contain silicon carbide

The combustion experiments were performed by static mass spectrometry using 25°C steps (unless larger steps were necessary because of low carbon yield). The temperature range of the experiments was 550-1300°C, using samples already precombusted in separate experiments to 550°C to analyse and remove the diamond (data from this part of the experiment has been discussed in chapter 3). Before the 550°C step, a step at 500°C was performed to combust any contaminant accrued from the sample transfer. The low temperature step released typically up to 20 ng of carbon, and the blank experiments suggested that almost all the contaminating carbon was released in this step. In this chapter "high-temperature components" refers to all the components that combust in the 550-1300°C regime, *i.e.* SiC and any other carbonaceous grains that are unstable to combustion below 1300°C. The stepped combustion results from the residues representing the entire suite of meteorites are shown in figure 6.5. The combustion plots indicate that more than one carbon containing mineral was released for each of the samples but they all release isotopically heavy carbon, attributable to SiC, at high temperatures. The isotopically heavy carbon is usually associated with a yield increase that presumably represents the breakdown of the silicon carbide.

For comparison to the meteoritic residues, a terrestrial SiC sample (0-2μm grain size) was mechanically mixed with ground Burma spinel (in the proportions 1:50) to form a "synthetic residue" and step combusted. To simulate the diamond combustion stage the sample was heated in air at 500°C overnight before the experiment was performed. The main carbon release (figure 6.6a) did not occur until > 1000°C, and the isotopic composition was constant over the carbon release peak, at $\delta^{13}C$~-31‰. The temperature of the main carbon release is very similar to the peak high-temperature yield of the residue of the enstatite chondrite Indarch (figure 6.6b) although in addition Indarch contained a low temperature carbon component released at 600-800°C. This lower temperature carbon component was not associated with a plateau in $\delta^{13}C$ and thus may represent a mixture of components. It is possible that the combustion of this heavy carbon carrier was affected by a "tail" from the diamond combustion in addition to some SiC that combusts at low temperatures: the other components and minimum combustion temperature of SiC are discussed in section 6.10.

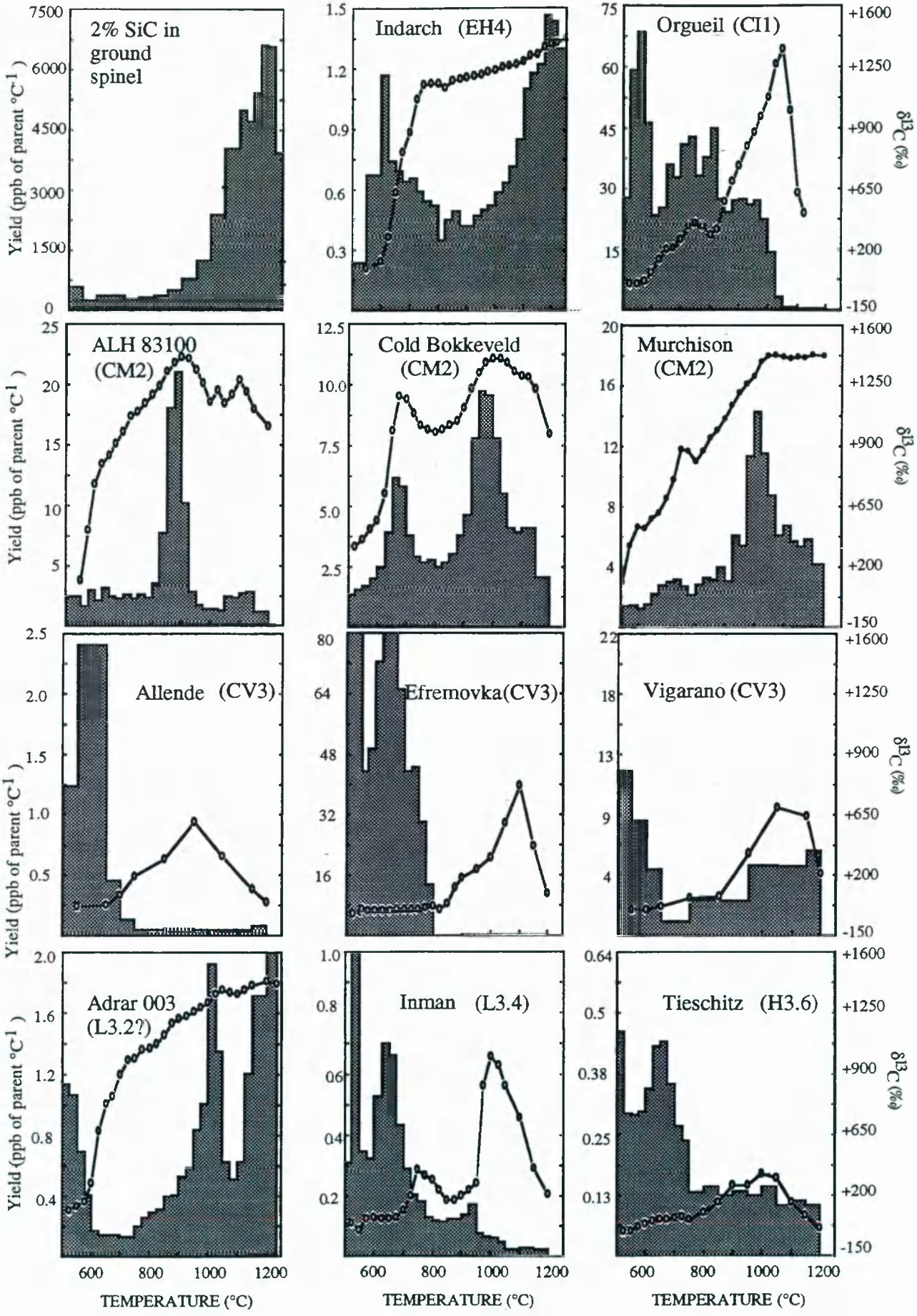

Figure 6.5. Stepped combustion analyses of perchloric resistant residues over the high temperature regime. Note that the temperature and isotope scales are comparable, but the yield scales vary from diagram to diagram because of the extremely wide range of SiC abundances.

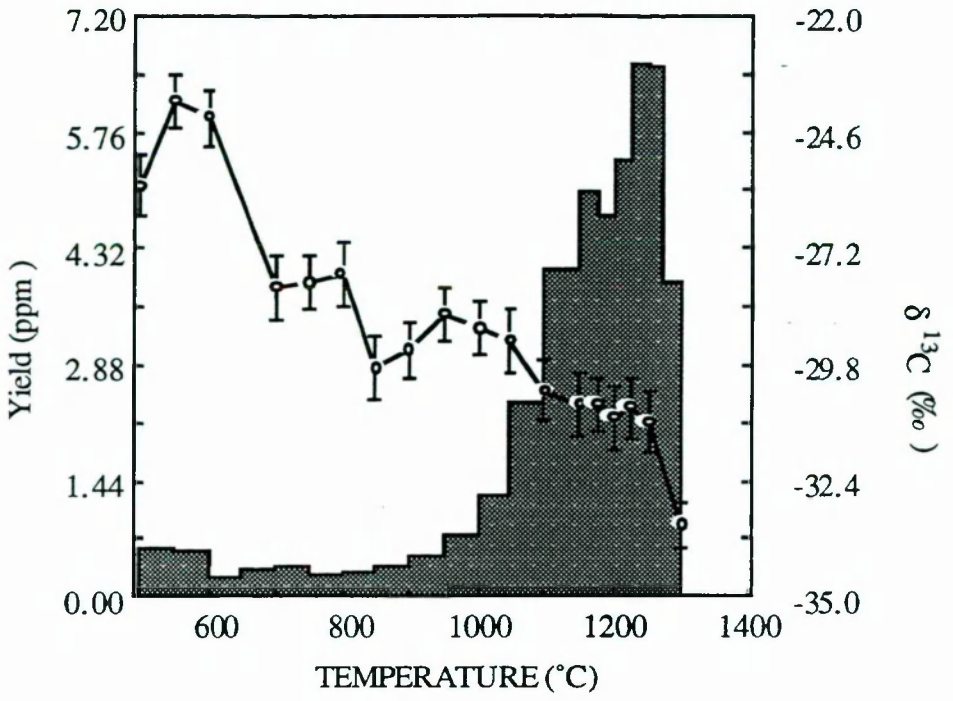

Figure 6.6a. Step combustion plot for a "synthetic residue" of SiC and spinel precombusted to 500°C overnight. (Yield profile is also shown in figure 6.5).

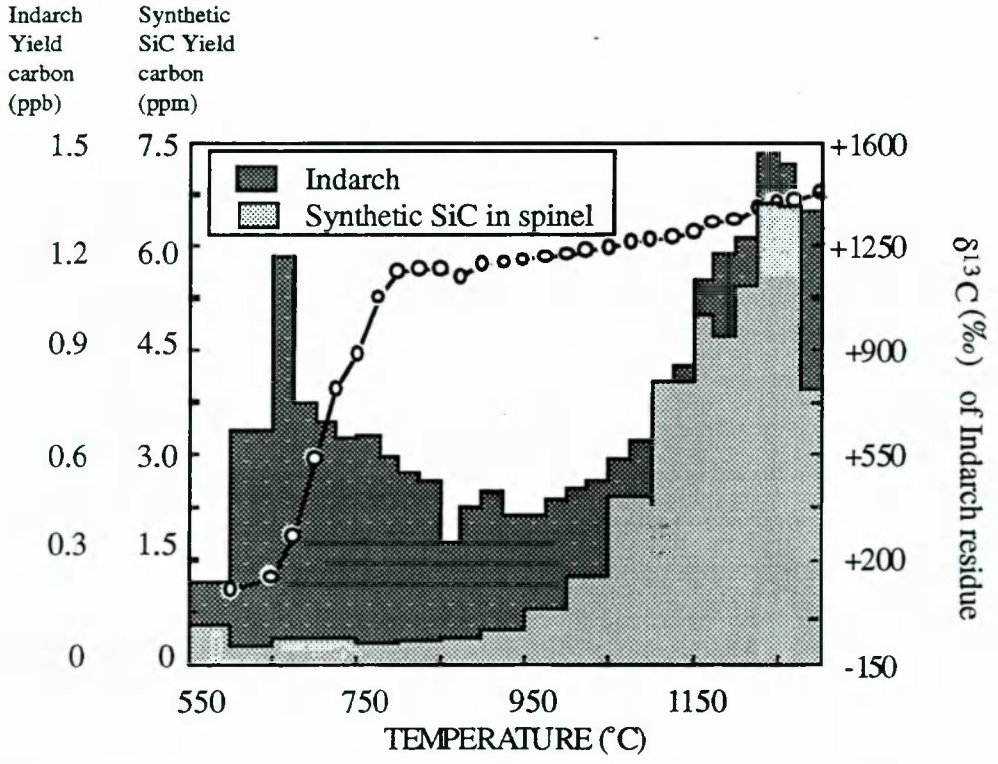

Figure 6.6. A comparison of the Indarch high temperature regime and the "synthetic residue"; data also shown in figure 6.5.

To establish the reproducibility of the experimental method, two aliquots of an acid resistant residue from Cold Bokkeveld were analysed (figure 6.7). One of the experiments (run 2) released substantial amounts of carbon at low temperatures (<700°C) suggesting it was contaminated by incompletely combusted diamond ($\delta^{13}C$ = -38‰). The presence of this component could have had the effect of lowering the $\delta^{13}C$ for the steps <700°C. Apart from this explainable discrepancy, a very good match between run 1 and run 2 in yield and isotope profiles above 800°C was demonstrated, indicating that any comparison between residues made during the study reflect differences in the make up of the residues rather than experimental artefacts.

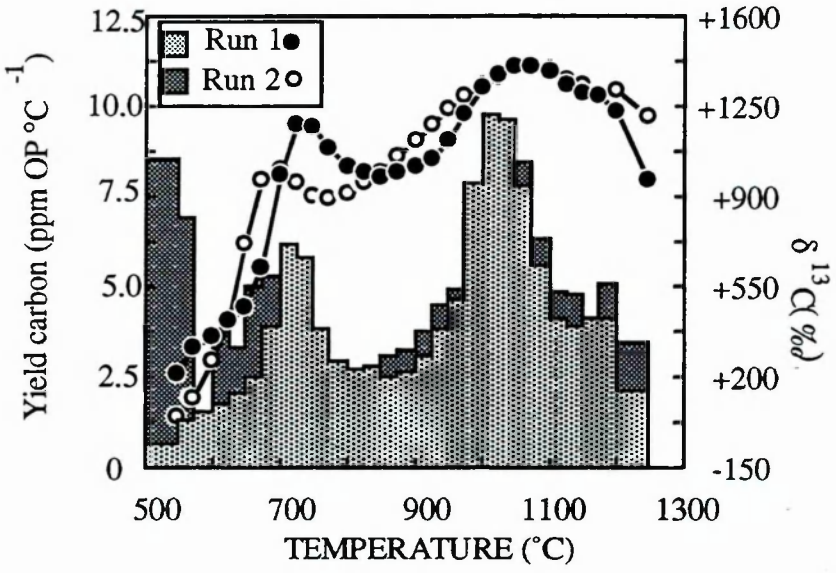

Figure 6.7. A comparison of two runs performed on a Cold Bokkeveld perchloric resistant residue to test the reproducibility of the stepped combustion experiment.

The CI1 Orgueil (figure 6.5) contains an abundant carbonaceous component that makes up 9 ppm of the whole rock with a $\delta^{13}C$ of ~+350‰ that combusts in the range 600-800°C. In addition, there is some evidence of some very heavy carbon ($\delta^{13}C$=+1370‰) that combusts at high temperatures and is more likely to be attributable to SiC. At lower temperatures this is hidden by the more abundant component but above 1000°C it makes up a greater proportion of the total carbon released. This higher temperature component is more likely to be the SiC, that may be masked at lower temperatures by the combustion of the component containing isotopically lighter carbon.

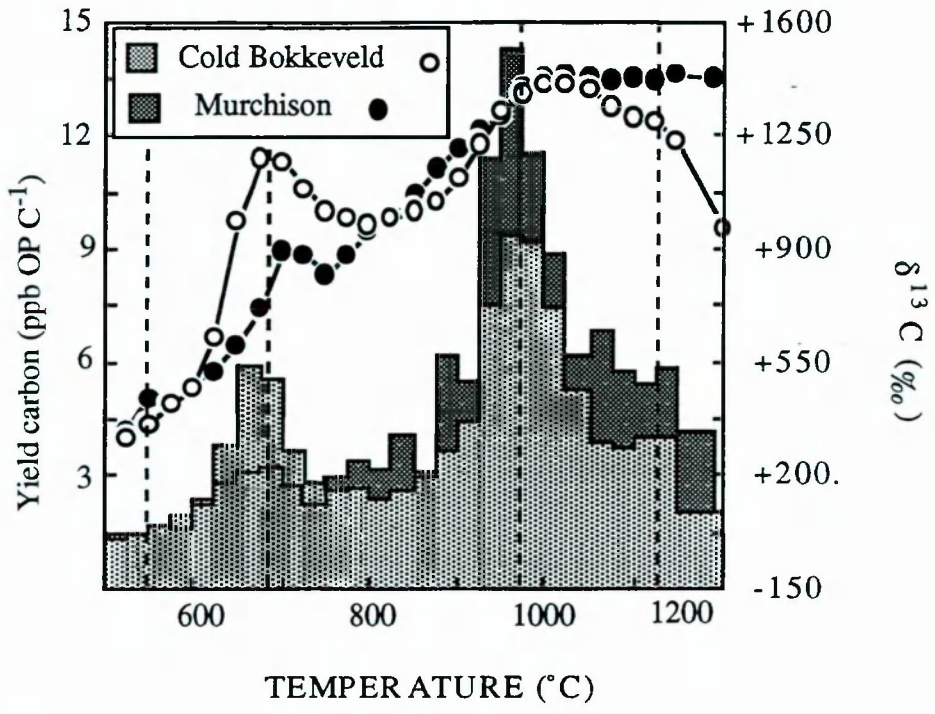

Figure 6.8. Comparison of Cold Bokkeveld (run 1) and Murchison meteorites. Data also shown in figure 6.5.

Most of the SiC from the CM2 carbonaceous chondrites combusts between 9000 and 1200°C with the major yield peak at 1000°C; in addition, Cold Bokkeveld and Murchison contain a hint of a second heavy peak close to 1200°C, a similar temperature to the main release of heavy carbon from the Indarch residue. The profiles from the CM2s Cold Bokkeveld and Murchison are similar (figure 6.8 and 6.5); both suggest the presence of constituents other than the main SiC component that combusts at around 900-1100°C; one that combusts at ~650°C, one *ca.* 800°C and one at higher temperatures than the main peak. The stepped combustion experiments do show some differences between the CM2s; ALH 83100 has a much sharper peak than the other two meteorites, and the heavy carbon is released at a temperature that is 50°C lower than the the major carbon release from Murchison and Cold Bokkeveld, making it clearly anomalous.

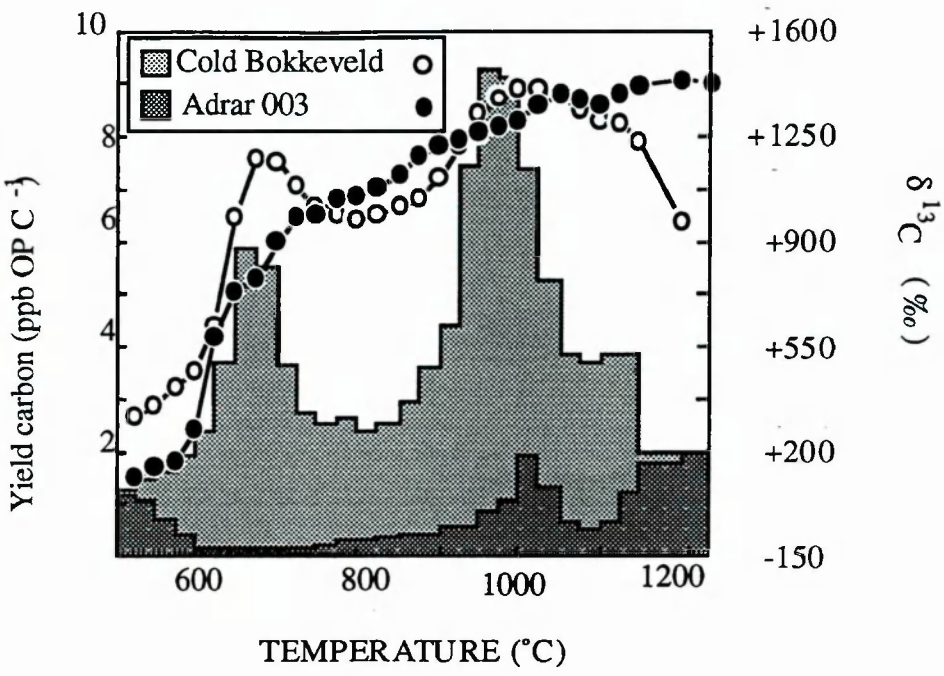

6.9. Comparison of Adrar 003 and Cold Bokkeveld; data also shown in figure 6.5.

The ordinary chondrites also contain heavy carbon that combusts between 900°C and 1100°C but the amount and maximum $\delta^{13}C$ are apparently related to petrologic type, with the least altered meteorite, Adrar 003, containing the most SiC. The profile obtained from Adrar 003 (figure 6.9 and 6.5) has two carbon release peaks. One component is similar in release profile and maximum yield temperature to the CM2 heavy carbon and the other is released at higher temperatures, similar to the Indarch release, at >1200°C. Figure 6.10 compares the L3.4 Inman to Cold Bokkeveld; the two runs indicate the meteorites contain similar components but that these are much less abundant in Inman; the low temperature heavy carbon peak may be affected by combustion of a component with $\delta^{13}C$ = +60‰ between 600 and 700°C.

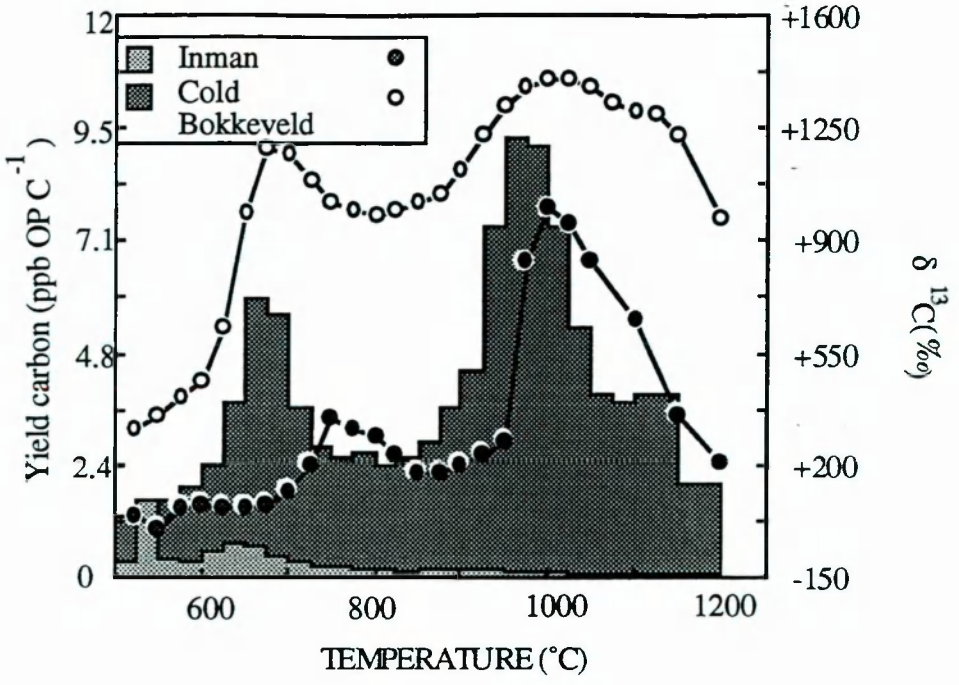

Figure 6.10. Comparison of Inman and Cold Bokkeveld meteorites; data also shown in figure 6.5.

The combustion results of all the meteorites suggest that two types of SiC may be present in these residues, if it is assumed that material burning below 800°C is not SiC (an assumption that will be further discussed in later sections): the Murchison and Cold Bokkeveld CM2 chondrites contain SiC that burns with the maximum yield between 900°C and 975°C but contain a minor additional component which produces a second yield peak at ~1200°C; the enstatite chondrite Indarch contains SiC that combusts between 800 and 1300°C but with the major peak at 1200°C. The ordinary chondrites contain the lower temperature component and in addition, Adrar 003 produces a second yield peak at 1200°C, a similar temperature to the main carbon release of Indarch.

6.7. Carbon isotopic composition of silicon carbide

The isotopic composition of the carbon released from all the meteoritic residues is heavy. Table 6.4. lists the heaviest carbon isotopic composition recorded from all the meteorite types and includes both raw data and blank corrected data. The blank corrections were calculated using typical full procedural blank stepped combustions that have been presented in section 2.1. The data are listed both using the delta system and as $^{12}C/^{13}C$ ratios.

Meteorite	$\delta^{13}C$ ‰(max)	$\delta^{13}C$ (‰) blank corr.[3]	min	max	$^{12}C/^{13}C$
Orgueil	**+1334.8**	**+1370.4**	**+1367**	**+1388**	**37.6**
ALH 83100	**+1402.9**	**+1413.4**	**+1408**	**+1418**	**36.8**
C.Bokkeveld	**+1398.6**	**+1450.4**	**+1426**	**+1466**	**36.3**
	+1405.6	**+1457.3**	**+1448**	**+1470**	**36.2**
Murchison	**+1429.4**	**+1479.0**	**+1461**	**+1506**	**36.2**
Allende	+503.6	+986.5	+797	+1441	44.8
Vigarano	+590.5	+758.7	+678	+891	50.6
Efremovka	+710.7	+833.1	+801	+941	48.6
Adrar 003	**+1431**	**+1444.7**	**+1442**	**+1448**	**36.4**
Inman	+993.7	+1133.9	+1097	+1254	41.7
Tieschitz	+319.7	+592.5	+453	+896	55.9
Indarch	**+1432.8**	**+1448.0**	**+1444**	**+1464**	**36.4**
Mean (n=6)		**+1437±32**			**36.6±0.5**
Mean (n=11)		+1166±317			41.5±6.6

Table 6.4. Most ^{13}C enriched steps of of SiC rich residues. Values in bold type are the least heated meteorites that are the most SiC rich (>1000 ppb SiC) and so are less likely to be affected by minor indigenous contaminating components.

The SiC rich meteorites (the CI1, CM2s, EH4 and Adrar 003) have a $^{12}C/^{13}C$ ratio of 36.6±0.5, with no discernible differences between meteorite classes. However, the picture is somewhat more difficult to see with the CV3 and higher petrologic type ordinary chondrites. The isotopic composition of the carbon associated with SiC is lighter in these samples, even after blank corrections have been applied. This could either be because the Solar nebula has sampled separate populations of the isotopically different grains, or the heavy carbon release in the meteorites that contain SiC in lower abundance has been diluted with carbon released from the spinel. Although the CV3 meteorite Allende is known to contain isotopically light carbon components ("Cλ": Ash *et al.*, 1988), the comparatively low $\delta^{13}C$ at 1000°C has been confirmed by preparative

[3] Blank corrections were determined using a program written by P. Yates. The range in parentheses indicates minimum and maximum reasonable values allowing for the error in the isotope measurements, fluctuations in the system blank during the run and errors in CO_2 yield measurement.

be due to the small sample size available for the Inman. A similar argument could be applied to the experiment performed on Tieschitz, which also utilised a small mass of sample. The CV3 experiments, in contrast, used much larger sample sizes. Another CV3, Leoville, in an *in situ* ion probe study appeared to contain a higher proportion of isotopically light ($\delta^{13}C$ ~0‰) SiC grains than CM2 meteorites (Alexander *et al.*, 1990b; Alexander *et al.*, 1992), and so a likely explanation is that the CV3 meteorites contain an mixture of SiC grains with a different mean isotopic value to the other carbonaceous chondrites.

If only the most primitive petrologic types, (shown in bold type in table 6.4), are considered then the carbon isotopic composition shows no systematic variation between meteorites at $\delta^{13}C = +1437\pm32$‰ ($1\sigma$, n =6) which corresponds to a $^{12}C/^{13}C$ ratio of 36.6±0.5.The similarity between SiC rich meteorites in all the chemical groups: carbonaceous (CM2 and CI) ordinary (Adrar 003) and enstatite (Indarch) chondrites suggests that a mixture of SiC grains, known to be of very different isotopic compositions from ion probe studies, were well mixed in the different parent body forming regions of the Solar nebula. The possible reasons for the apparent difference in $\delta^{13}C$ of SiC from the CV3s will be discussed later.

A question that can now be addressed is whether the $^{12}C/^{13}C$ value of 36.6±0.5 can be reconciled to an origin for silicon carbide within an AGB star. Measurements of $^{12}C/^{13}C$ of present day carbon stars in the red giant stage of evolution are summarised and compared below.

Mean $^{12}C/^{13}C$	No. stars	Technique	Reference
36.6± 0.5 (n=6 meteorites)		Stepped combustion	This study
56		Ion probe	Alexander, *pers. comm.*
5	18	Band line intensities	Climenhaga *et al.*, 1982
49	30	Infra red spectra	Lambert *et al.*, 1986
20	4		Dominy *et al.*, 1986
34.5	7	Fourier transform spectrometer	Dominy and Wallerstein, 1987

Table 6.5. Mean $^{12}C/^{13}C$ ratios reported in the literature for carbon stars compared to meteorite values.

The measurement of $^{12}C/^{13}C$ in carbon stars is a difficult one and in addition to the agreement amongst most authors that there is a wide variation among individual stars, the

mean values published are very diverse. The most extensive study, by Lambert *et al.* (1986), gives a mean $^{12}C/^{13}C$ of 49, with most stars falling into the 30-70 range. A small proportion were extremely enriched in ^{13}C, with $^{12}C/^{13}C$ ratios as low as 3 reported. Theoretical calculations by Obarvaric *et al.* (1991) predict that the $^{12}C/^{13}C$ ratio at the surface of the star at the beginning of the AGB phase is ~20, and then increases as the helium burning produces ^{12}C that can be dredged to the surface. Later in the star's evolution the $^{12}C/^{13}C$ decreases again as ^{12}C (p, γ)^{13}C reactions take place. Small stars should not become more ^{13}C rich than their original value by this process, however. Observations and theory thus do not contradict the idea that grains with a mean $^{12}C/^{13}C$ of ~37 can be formed in a carbon star environment, although the expected $^{12}C/^{13}C$ ratio in this case is not well constrained. Of course, the SiC found in meteorites is thought to be at least 4.55 x10^9 years old and so its $^{12}C/^{13}C$ will reflect a historic value of ancient stars. The galactic $^{12}C/^{13}C$ ratio is believed to have evolved since then to more ^{13}C enriched values. Thus, the somewhat lower $^{12}C/^{13}C$ ratio of meteoritic SiC than observed present day carbon stars is potentially problematical, perhaps implying that either SiC condenses only from a certain type of AGB star that tends to lower $^{12}C/^{13}C$ ratios than the population as a whole, or the material from which the Solar system condensed was affected by a single AGB source that was more ^{13}C enriched than the average AGB stars.

6.8. Minor components in perchloric acid-resistant residues

Although SiC is the major carbonaceous component left after the oxidising acid treatments and combustion to 550°C, a number of minor components are seen to combust in the 550-900°C temperature range. Clearly, the identity of these components is important; are they (i) a separate population of SiC (*e.g.* crystals with a very fine grain size), (ii) another carbon bearing, highly resistant, mineral or (iii) a less thermally stable carbonaceous phase that is protected by an acid-resistant mineral? To shed some light on this question, a perchloric acid-resistant residue of Murchison, called M2, was treated with some additional reagents in an attempt to constrain the origin of the carbon release: - (i) NaOH, to dissolve the SiC, (ii) H_3PO_4 to dissolve the spinel and (iii) a solution of NH_3 to give a separate of fine grained particles, and the resulting samples analysed by stepped combustion.

6.8.1. Treatment with NaOH

Fused sodium hydroxide is known to destroy SiC by attacking the protective silica

coating on the crystals, leaving it vulnerable to attack from the alkali and oxygen in air (Greenwood and Earnshaw, 1984):

$$SiC + 2NaOH + 2O_2 \rightarrow Na_2SiO_3 + H_2O + CO_2$$

This treatment was applied to the Murchison perchloric acid residue and the resulting sample (M2B) analysed by stepped combustion, which revealed that some of the <800°C temperature carbon components survived the treatment: a heavy component combusting at ~600°C and another at ~800°C, that have almost identical $\delta^{13}C$ values to the components combusting at similar temperatures in the untreated sample (figure 6.12). SEM and TEM analysis of the sample did not show any unambiguous evidence that SiC was present but a few unidentified Si-rich grains of nanometre dimensions were detectable. This component may have been SiC, although intuitively it seems unlikely that the alkali treatment would dissolve the larger (~μm sized) grains and leave the smaller (nm sized) ones intact. Thus, it cannot be ruled out that the heavy carbon release at 500 - 800°C is due to the combustion of nanometre SiC crystals, although it seems unlikely that they are present in this residue.

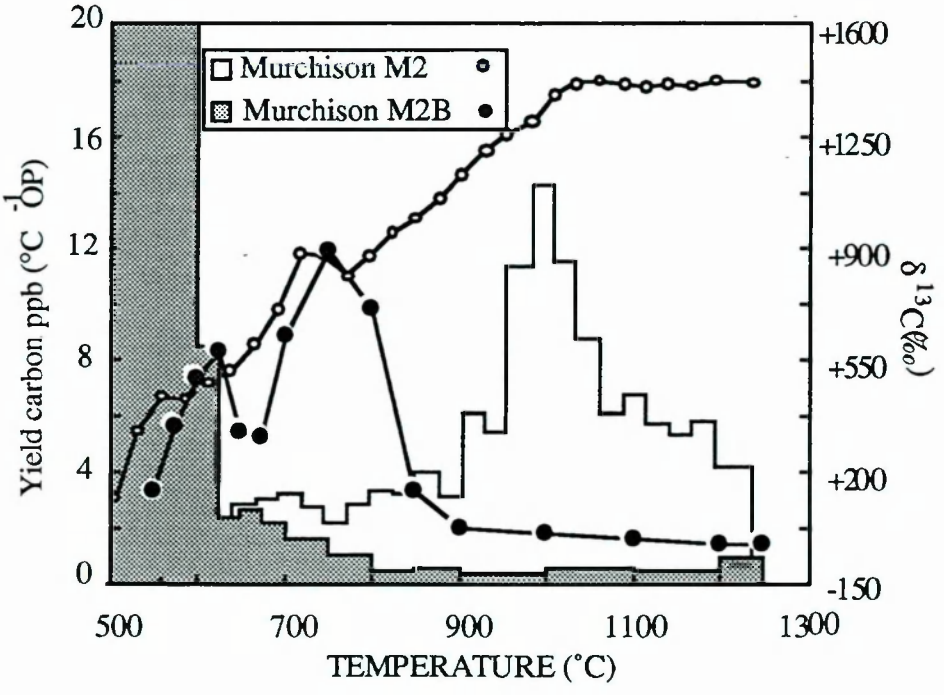

Figure 6.12. Stepped combustion profile of M2B (M2 perchloric acid-resistant residue after NaOH treatment), compared to the parent residue.

The NaOH treatment thus appeared to have been successful in dissolving the SiC grains. Subtracting the carbon stepped combustion plot after NaOH treatment from the parent residue allows the contribution to the stepped combustion profile of the

dissolved material to be calculated. The dissolved fraction is shown in figure 6.13. This plot should be viewed with a certain amount of caution; weighing errors, different blank contributions and non- comparable temperature scales all make the plot at best an estimate of the dissolved material. However, the smooth yield variations and isotope changes from step to step suggest that the plot is along the right lines. This could thus be the profile of pure meteoritic (NaOH-soluble) silicon carbide. Carbon is released at temperatures >700°C until the experiment was stopped at 1250°C. The bulk $\delta^{13}C$ is +1375‰ ($^{12}C/^{13}C$ = 37.8), with the peak yield step at $\delta^{13}C$ = + 1517‰ (higher than the maximum $\delta^{13}C$ of the M2 sample because M2B contained an isotopically normal component at high temperatures:- carbon from the spinel?) and the bulk yield was 2365 ppb C of the whole rock which is the equivalent of 7883 ppb SiC. Interestingly, the $\delta^{13}C$ increases steadily with temperature, suggesting a relationship between stability to combustion and grain type. This could imply that the smaller grains are less ^{13}C enriched although Amari *et al.* (1989) in an ion probe study of SiC grain size separates reported no relationship between SiC size and $\delta^{13}C$.

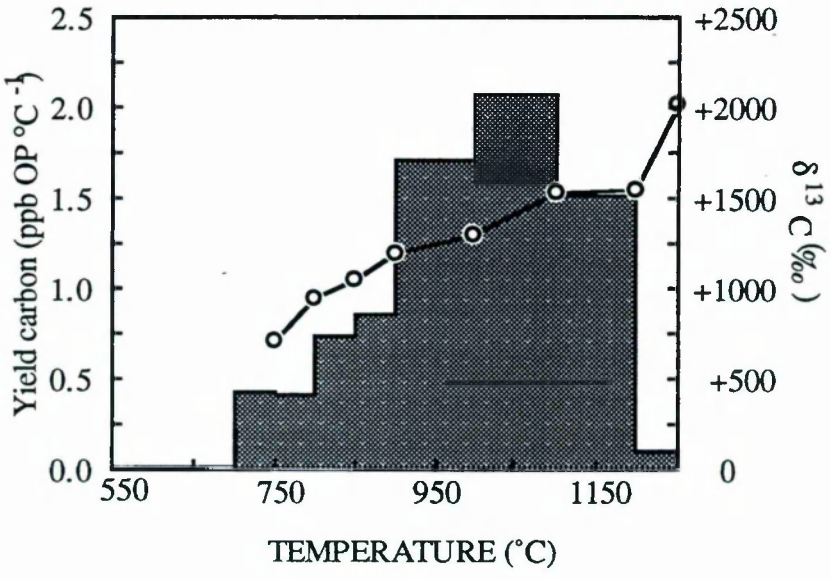

Figure 6.13. The NaOH - soluble component in the perchloric resistant Murchison residue M2, calculated using the blank correction program written by P. Yates.

6.8.2. Treatment with H_3PO_4

Phosphoric acid treatment has been used by the Chicago group (*e.g.* Tang and Anders, 1988a) to destroy spinel in meteorite residues while leaving the SiC intact for isotopic

study. This processing step was introduced because it was believed that some SiC was intimately associated with the spinel (Zinner and Epstein, 1987) and that the spinel removal would thus facilitate its characterisation. The acid has a potential use, therefore, for elucidating the nature of carbon contained within spinel grains from the samples (see also section 6.10.2 for a discussion of Cθ). However, some authors contend that SiC is soluble in H_3PO_4 (Greenwood and Earnshaw, 1984). The Murchison sample M2 was treated with H_3PO_4 for 16 hours at 150°C and the residue (M2A) then analysed by SEM. It was found to be spinel free, but still contained hibonite, and some ~1μm grains of SiC. When this residue was analysed by stepped combustion, the major high temperature carbon release occured between 700° and 850°C, nearly 200°C below the carbon release of the sample before treatment (figure 6.14) It is almost certain that this heavy peak represents the combustion of SiC as its abundance and isotopic composition is the same as in the untreated sample; the heavy carbon could account for 8330 ppb SiC in M2A compared to 8760 ppb for the parent sample, suggesting that the SiC has not been destroyed but simply altered. The low combustion temperature of the main heavy carbon component ensured it was not possible to observe if the lower temperature components were still present. The lowering of the combustion temperature of the SiC could be because the acid had attacked the protective SiO_2 coating of the SiC leaving it more vulnerable to combustion:

$$4H_3PO_4 + 3SiO_2 \rightarrow Si_3(PO_4)_4 + 6H_2O$$

The TEM evidence that SiC is still present in this residue supports this supposition. In addition, the SiC could have been partly destroyed and the carbon released altered to another phase:

$$6SiC + 8\ H_3PO_4 \rightarrow 2Si_3(PO_4)_4 + 6C + 12H_2$$

If this is the case, then the peak at 800°C is from the combustion of elemental carbon that originates from SiC (elemental carbon can have a combustion temperature in this range if it is very crystalline or coarse grained). The 800°C peak in earlier experiments has obvious parallels to the component observed in M2A. Thus, this lower temperature component could be from SiC that has been partially altered or destroyed, in the ways described above, in the residue processing.

An alternative explanation could be that 800°C is the "natural" combustion temperature of the SiC, but if spinel is present then the combustion is repressed until higher temperatures, perhaps because most of the SiC is in the form of inclusions within the spinel. Given that a combustion temperature of 1000°C for the meteoritic SiC is already lower than that of analogous synthetic samples, this explanation seems unlikely.

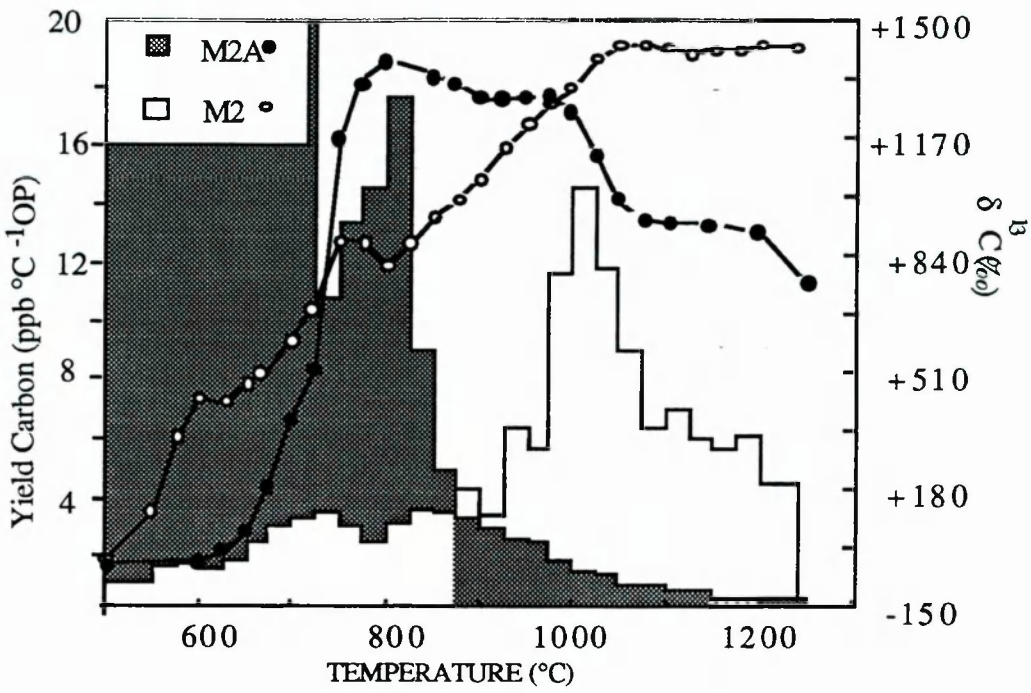

Figure 6.14 Stepped combustion profile of M2A (M2 perchloric acid-resistant residue after treatment with phosphoric acid), compared to the parent residue.

6.8.3. Treatment with NH_3 solution

Ammonia solution has been used to obtain samples of almost pure meteoritic diamond from perchloric acid-residues (*e.g.* Lewis *et al.*, 1987). The diamonds have acidic bonds on their surface (Lewis *et al.*, 1989) that allow the crystals to form a colloidal solution in ammonia, thus after decantation and reprecipitation with acid, the colloidal fraction provides a residue in which diamond is concentrated. However, it has been noted that the resulting meteorite fractions also always contain Xe-S (Huss, oral presentation at Lunar and Planetary Science Conference, 1991), implying that some SiC enters into the colloid. It is possible that the SiC which forms a colloid in NH_3 represents a different population from the SiC as a whole. In order to investigate this theory, a colloidal separate (M IL) from a Murchison residue that had been prepared using an identical protocol to M2, was step combusted. The stepped combustion profile of the colloid was very different to that of the meteorite at the perchloric acid treatment stage (figure 6.15). The carbon combusting at >1000°C in M2 had clearly been separated into the non-colloidal fraction. As a result, two components burning at temperatures higher than the diamond, could be resolved. Some heavy carbon with a $\delta^{13}C$ maximum at ~650°C and a $\delta^{13}C$ of at least

+660‰ was released, but the isotope peak did not correspond to the maximum yield that occured at a temperature of 700-800°C with an isotopic composition close to zero.

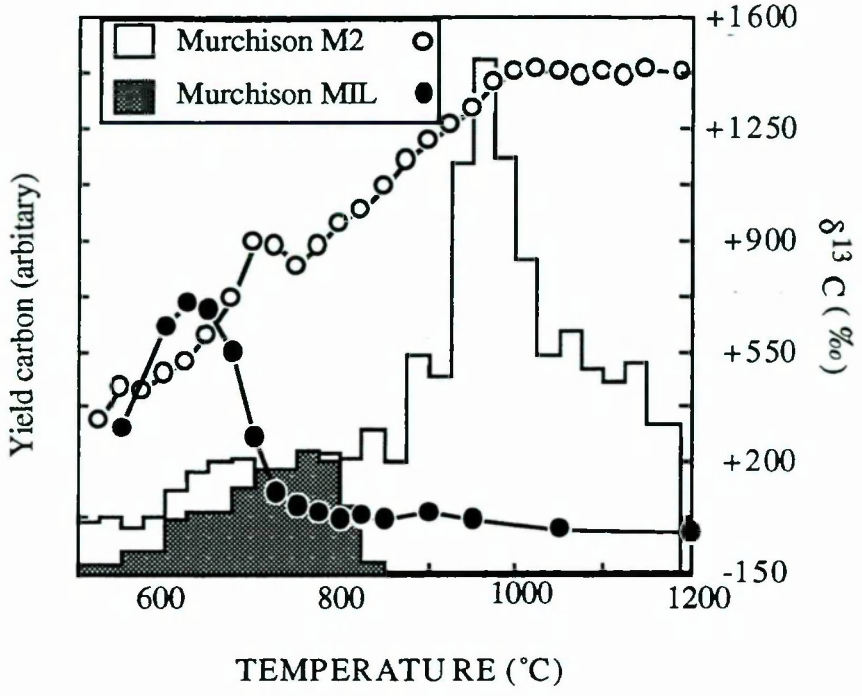

Figure 6.15. The Murchison MIL NH_3 colloidal fraction; the yield aXe-S are not comparable as this was a separation rather than a destructive treatment.

Because MIL was believed to represent an almost "pure" diamond separate, it was chosen for a trial experiment aimed at obtaining the diamond size distribution by a laser scattering technique. The experiment was performed by E. Pelan (Unilever plc) and employs a technique which measures the grain size of particles suspended into a liquid by measuring the extent to which they deflect a laser beam, which is related to their speed of Brownian type movement in the colloid, and hence size (Stock and Ray, 1985). Not surprisingly, the MIL sample in NH_3 colloid was dominated by 2nm particles (of diamond), but populations of larger grain size could also be discerned, one at ~18nm and others at 91 and 168nm (figure 6.16); the size distribution is not entirely accurate because the number of components appeared to be very large. These grains could be clusters of diamond or small SiC particles, which exist apparently in discrete grain size populations. Although diamond clusters are observed in TEM studies of diamond-rich residues (*e.g.* Blake *et al.*, 1989), it is not known if they retain this grouping when in colloidal solution. A few larger grains (>1μm), attributable to spinel or hibonite, were also noted (giving a peak at 1232nm) but their paucity made statistical measurement of their abundance impossible.

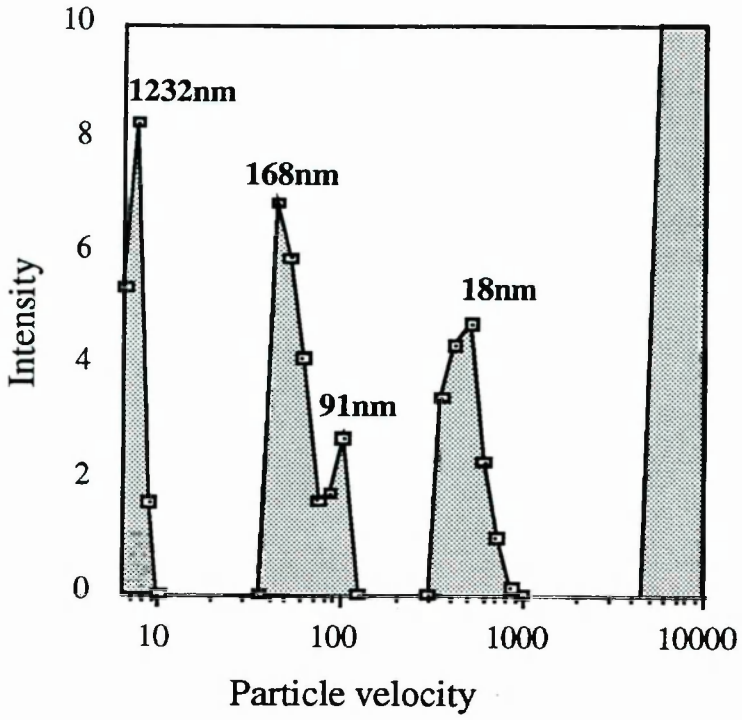

Figure 6.16. Results of the laser scattering experiment on MIL.

MIL was also studied by K.Gilkes (University of Cambridge) using scanning transmission electron microscopy (STEM). This showed that although the carbon in the residue was dominated by diamond, small (tens of nanometre) grains were also present that could be attributable to SiC, along with some hundreds of nanometre-sized sheets of well crystallised graphite. Thus, the main carbon release, with $\delta^{13}C \sim 0$, and the isotopically heavy carbon released in the high temperature regime of the stepped combustion could be graphite and SiC respectively, and are discussed further in the summary section.

6.9. SiC abundance in meteorites

The SiC abundance of bulk meteorites has been calculated in two ways: firstly, it can be assumed that all carbon combusting above a certain temperature (850°C) is due to the combustion of SiC (column 1 in table 6.6). Alternatively, it can be assumed that SiC in all the meteorites has a mean $\delta^{13}C$ of +1400‰ (possibly not true for some: see section 6.6) and the high temperature carbon assumed to be a mixture of SiC and other components with a lower $\delta^{13}C$ (arbitrarily assigned to 0‰, column 2). These two approaches give similar results for the meteorites that release a large amount of carbon at high temperatures, with obviously slightly lower yield using the second method. However, the two figures for the type 3 chondrites differed by over a factor of 3. Both techniques contain assumptions that may not be valid; from the results obtained it seems

that minor components other than SiC are present and these must interfere with the abundance measurement, particularly as their carbon isotopic composition is not well defined. Another method of determining SiC abundances (Huss, 1990) also has its limitations. This system calculates SiC abundances from Ne-E(H) concentrations of relatively unprocessed residues, assuming that the Ne-E (H) content of SiC is constant for all meteorites. However, the Ne-E (H) concentration of SiC has been found to vary both with grain size (Amari *et al.*, 1989) and between meteorites (Ott *et al.*, 1991).

The Huss method uses less samples at a less processed stage of acid dissolution, as the oxidative acid treatments may partially destroy the components to be measured. Although the C and N data indicate that this may be true for the diamond component (see chapter 3), the SiC is apparently not affected by the oxidative treatments. Comparisons of quantities of heavy carbon in residues processed to different extents indicate that no SiC is destroyed by oxidative acid treatments (R.D. Ash, 1992, *pers. comm*).

Given that both the method of calculating SiC abundances in this thesis and the Huss method are, at best, estimates, they agree remarkably well for some meteorites, such as Orgueil (16600 and 9700 *vs.* 14100), Murchison (9300 and 8800 *vs.* 9000) and Indarch (1500 and 1400 *vs.* 1300). There are significant differences between the two results for the CV3s, which are apparently richer in heavy carbon than their Ne-E (H) content predicts, and the ordinary chondrite Inman, which seems poorer in SiC than Huss estimates. Neither Xe-S nor Ne-E(H) have been detected in the CV3 Allende (Huss, 1990) although SiC has been observed by TEM in an Allende residue (Gilkes, *pers. comm.*). Possibly, this meteorite contains SiC that is made from a different source, as has been suggested for the CV3 Leoville (Alexander *et al.*, 1990; Walker *et al.*, 1992) which would cause the Huss technique to underestimate the abundance of SiC. In this case, the first abundance measurement of SiC in table 6.6 would be the more accurate because this measures all the carbon released over the SiC combustion range regardless of its isotopic composition. However the CV3 perchloric resistant residues are known to contain small amounts of thermally resistant carbonaceous components other than SiC (Ash *et al.*, 1989) that would cause the SiC abundance to be overestimated.

Meteorite	Type	ppb SiC (1) (σ[4])	ppb SiC (2)	ppb SiC (Huss, 1990)
Orgueil	CI1	16600 (17)	9600	14100
Cold Bokkeveld	CM2	6400 (57)	5700	
Murchison	CM2	9300 (93)	8800	9000
ALH 83100	CM2	7600 (43)	7100	
Allende	CV3	60 (3)	10	0
Efremovka	CV3	83 (4)	23	
Vigarano	CV3	520 (17)	170	70
Adrar 003	L3.0?	1400 (7)	1400	
	Low T peak	700 (7)	700	
	High T peak	700 (<1)	700	
Inman	L3.4	67 (<1)	23	330
Tieschitz	H3.6	170 (10)	23	63
Indarch	EH4	1500 (2)	1400	1300

Table 6.6. SiC abundances in meteorites. Data from (1) assumes that all the carbon combusting over the 800° to 1250°C temperature range is from SiC. Data from (2) assumes that all SiC has a $\delta^{13}C$ of +1400‰ and this is mixed with isotopically "normal " carbon over the high temperature regime. The data for Indarch and Adrar 003 must be underestimates as carbon was still being released when the experiment was terminated at >1300°C.

The abundance of silicon carbide in the most primitive meteorites (CI, CM2s, Adrar 003) agree within an order of magnitude, especially when matrix normalised (data after normalisation will be presented and discussed in chapter 7), suggesting that the meteorite parent bodies originally contained similar quantities of SiC. The paucity of SiC in the more metamorphosed meteorites (*e.g.* Tieschitz and Inman) suggests that the grains have been partially destroyed by metamorphic reactions in these samples.

6.10. Nitrogen in SiC

Nitrogen doped synthetic SiC has received some attention recently as a potential high temperature semiconductor (*e.g.* Powell and Matus, 1988). The presence of nitrogen can

[4]The errors in parthenses correspond to cumulative errors involved in measuring yields over a stepped combustion experiment: from a computer program written by J. Higgins and P. Yates

be detected by EPR spectra (Woodbury and Ludwig, 1961) although the effect of nitrogen on sample paramagnetism is not well understood. Nitrogen is believed to singly replace carbon in the cubic SiC lattice, and also co-exist with another trace element, aluminium, in Al-N donor pairs. In addition, it may exist in more complex structures associated with other defects (Bishop *et al.*, 1989). Nitrogen rich SiC can be produced by a CVD technique by introducing N_2 gas into the system (*e.g.* Okumara 1989); the nitrogen concentration of the resulting SiC is approximately proportional to the square root of the nitrogen partial pressure. There is a relationship between the polytype of SiC and nitrogen solubility; the solubility is highest for β-SiC and decreases with increasing degree of hexagonality of the polytypes (Gugel *et al.*, 1969). Nitrogen solubility in SiC has been studied by ion implantation of N^+ ions into the lattice, followed by annealling that allows the interstitial nitrogen to substitute into the lattice (Addamiano *et al.*,1972). This technique produces a maximum substitutional concentration of N in SiC of 1×10^{21} atoms cm^{-1} (Campbell *et al.*, 1975) which corresponds to a C/N ratio of ~48.

The "synthetic residue" discussed in section 6.4. was analysed for nitrogen. It was found that little nitrogen attributable to SiC was released during the stepped combustion experiment: the total C/N ratio was 920.

Nitrogen in meteoritic silicon carbide has been studied using stepped combustion techniques (*e.g.* Ash, 1990; Ash *et al.*, 1991) and by ion probe (*e.g.* Zinner *et al.*, 1989). Zinner *et al.* (1990) observed a correlation between nitrogen and aluminium which was interpreted as an indication of the presence of AlN associated with SiC, and a more recent study by Bernatowicz *et al.* (1992) concluded that the aluminium was evenly dispersed throughout the SiC grains and so was present as Al-N pairs within the crystal lattice rather than in discrete grains.

6.10.1. High temperature nitrogen in the Cold Bokkeveld perchloric acid resistant residue

Silicon carbide is present as a very minor component in even the most primitive meteorites. This makes the analysis of carbon in SiC by stepped combustion an onerous task, and the study of nitrogen, a trace element within the SiC, is even more difficult. The first part of this discussion concerns the nitrogen released at high temperatures from the CM2 meteorite Cold Bokkeveld, which is known to be ^{14}N enriched, with a minimum $\delta^{15}N$ value recorded of -618‰ (Ash, 1990). In particular, data from a conjoint C/N experiment performed on the Cold Bokkeveld meteorite residue CB3B/2 will be presented. This experiment used ~1mg of residue, nearly ten times the usual sample size, in an attempt to discriminate between blank contributions and the low level of indigenous

the CM2 meteorite Cold Bokkeveld, which is known to be ^{14}N enriched, with a minimum $\delta^{15}N$ value recorded of -618‰ (Ash, 1990). In particular, data from a conjoint C/N experiment performed on the Cold Bokkeveld meteorite residue CB3B/2 will be presented. This experiment used ~1mg of residue, nearly ten times the usual sample size, in an attempt to discriminate between blank contributions and the low level of indigenous nitrogen released after the diamond had been combusted. The diamond was step combusted using 10°C increments the day before before the SiC analysis was performed.

The experiment indicated that there were at least two isotopically light nitrogen components released at high temperatures. The first reached a minimum $\delta^{15}N$ value, at 800°C, of -437‰, or blank corrected -562±60‰ [5]. The second component reached a minimum $\delta^{15}N$ value, at 1050°C, of -626‰: blank corrected: -652±5‰*. These two light nitrogen components correspond well to the heavy carbon peaks found in Cold Bokkeveld.

A plot of C/N ratio against temperature (figure 6.17) indicates the presence of several components in this perchloric resistant residue. The carbon and nitrogen yield data have been blank corrected. The first half of the experiment produced a predictable C/N pattern due to the combustion of diamond and discussed in Chapter 3. After the diamond combustion was complete, the C/N ratio rose to a maximum value of 600, representing the combustion of a nitrogen poor carbonaceous component. This component accounts for only 0.5% of the carbon in the residue and is associated with heavier nitrogen (even after blank corrections) than that associated with diamond combustion, although the exact $\delta^{15}N$ is difficult to predict because of the tailing effect of the diamond combustion. A candidate for this component is crystalline graphite, known to exist in sheets of ~100nm across in perchloric resistant residues (K. Gilkes, *pers. comm*).

Above about 800°C, the C/N ratio appears more constant. However, if the C/N ratio is re-plotted for the high temperature regime (figure 6.18), with error bars on the measurements of 20% (see Chapter 2) there is tentative evidence that the C/N ratio of the light nitrogen isotope peak at ~800°C (60-70) is different to that of the 1050°C peak (25-30). Above 1050°C the C/N ratio is very constant, indicating the combustion of a single

[5] Blank corrections were calculated using a computer program written by P. Yates. The errors shown indicate maximum and minimum reasonable values allowing for errors in isotope measurements, fluctuations of the system blank during the day and variability (assumed to be 5%) in M/Z = 28 beam intensity giving errors in yield determination.

gives C/N of 32, and $\delta^{15}N$ of SiC as -652‰ (blank corrected). These values are in broad agreement with experiments on the other carbonaceous chondrites (table 6.7), although stepped combustions have not been performed using such large samples on any other meteorite. The value of 32 is rather lower than minimum recorded values for synthetic SiC (Kirchstein, 1984) and needs to be rationalised. It is possible that the meteoritic SiC crystals are highly defective and so can dissolve more N than terrestrial samples, or very Al-rich and so can contain the nitrogen as pair bonds. Alternatively, some of the nitrogen may be interstitial rather than substitutional, and thus more can be held. It is probable, however, that substitional nitrogen may have degassed from the mineral at some point during its long history. A third possibility is that another nitrogen containing component is co- combusting with the SiC. Although the constant C/N ratio at high temperatures argues against this theory, confirmation may not be achieved until higher resolution stepped combustions are possible. The measured C/N ratio of ~32 is lower than synthetically produced samples, but compatible with a CVD origin (nitrogen can be incorporated into SiC produced by CVD processes but is not renowned for substituting into SiC produced by the Acheson process).

The higher C/N ratio below 1050°C can be explained in two ways. Either no SiC is combusting over the lower temperature regime (*i.e.* it is a separate and as yet unidentified component), or, if SiC also combusts at lower temperatures, then the difference in C/N ratios must be rationalised by assuming that in addition, another component or components of a higher C/N ratios are co-combusting. For example, a "tail" from the combustion of graphite would raise the C/N ratio over the 800-900°C temperature range. The graphite has a higher $\delta^{15}N$ than the SiC and so the co-combustion would raise the $\delta^{15}N$ value from -652‰ the combustion of "pure" SiC- to -562‰.

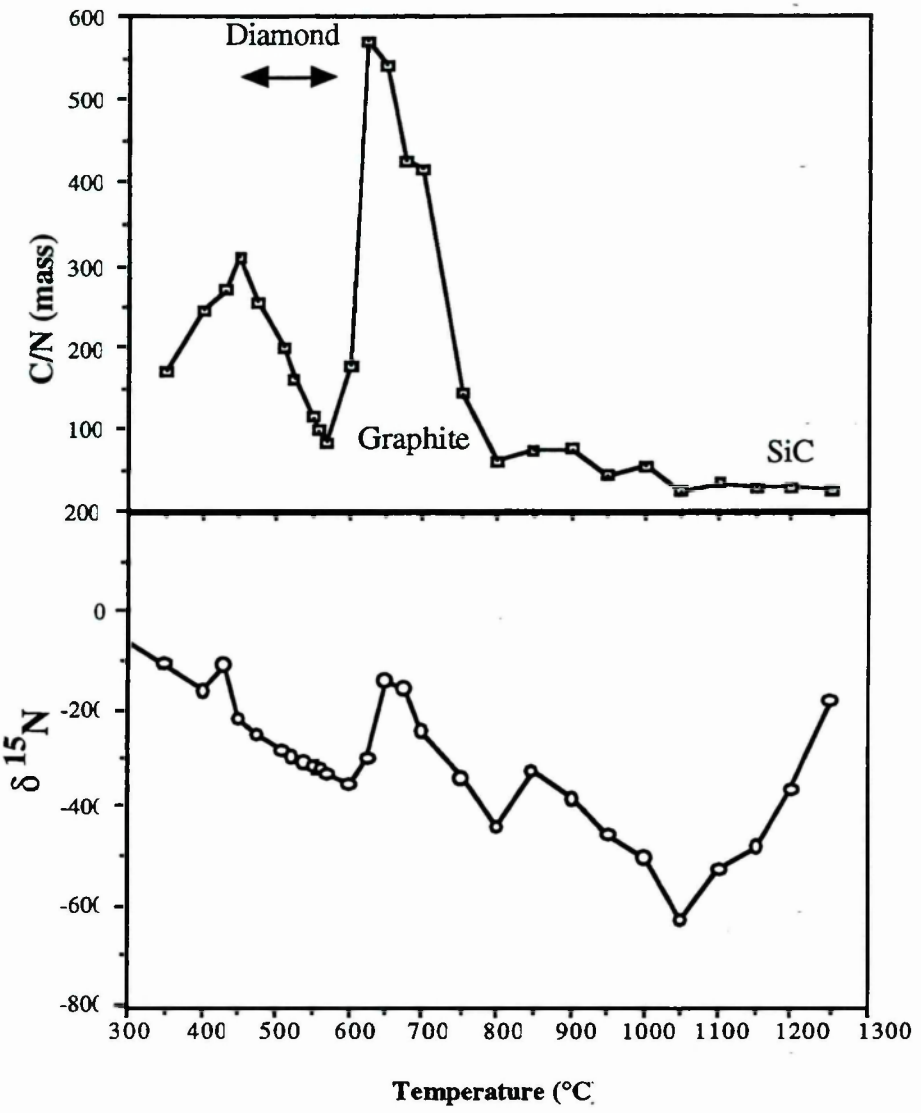

Figure 6.17. The C/N profile of Cold Bokkeveld residue over the temperature range 300 to 1200°C, also showing the $\delta^{15}N$ values. Peak carbon yields occured at 800° and 1000°C.

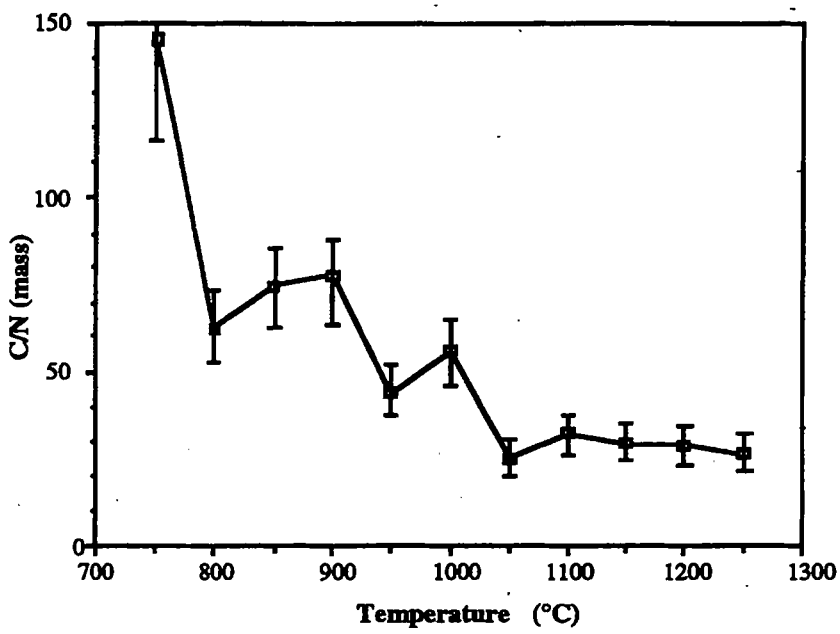

Figure 6.18. The C/N profile of the combustion of Cold Bokkeveld from 800° to 1200°C. Error bars represent 1σ reproducibility on C/N measurements; see chapter 2.

6.10.2. Ordinary and enstatite chondrites

Nitrogen stepped combustion release experiments on the ordinary and enstatite chondrites yield very different results to the carbonaceous chondrites (figure 6.19). Tieschitz and Inman both contain an isotopically heavy nitrogen component at high temperatures that was also noted by Alexander *et al.* (1990). The C/N ratio of this component reaches as low as 4 (for Inman), much lower than the solubility limit of nitrogen in SiC given by Kirchstein, 1984. Since it is known that SiC is present in the ordinary chondrites (Huss and Lewis, 1990; Nichols *et al.*, 1991) some nitrogen could be contained in the SiC as a trace element, with the rest located in a separate component, possibly attributable to Si_3N_4 which is observed by TEM. High-resolution stepped combustion analysis of SiC residues using more sensitive equipment, or chemical destruction of SiC in these meteorites is necessary to ascertain the exact relationship between the two components. The data for Adrar 003 can easily be rationalised if it contains more of the SiC component. The nitrogen released from the residue of Adrar 003 is ^{14}N enriched compared to air, but the minimum $\delta^{15}N$, at -122‰, was lower than the comparable step of the carbonaceous chondrite residues, and has a C/N of 12, intermediate between the 4 and 5 recorded for Inman and Tieschitz, and the value of ~32 obtained for the carbonaceous chondrites. An explanation for these results is that two nitrogen containing components are present in the ordinary chondrites, one that is similar to that seen in carbonaceous chondrites, that is associated with the SiC, and a second, isotopically heavy component (this can be seen

more easily in figure 6.20). It is possible to estimate the $\delta^{15}N$ of the second component if it is assumed that (i) the N in SiC is similar in concentration and isotopic composition to that in carbonaceous chondrites, and (ii) that the second component contains no carbon. Using these assumptions the isotopic composition of the second component appears heavy ($\delta^{15}N = +357‰$), suggesting affinities to the nitrogen components in Inman and Tieschitz. If the same SiC stripping exercise is applied to all three ordinary chondrites then the nitrogen isotope values obtained for the nitride component appear to be in reasonable agreement at $\delta^{15}N = 338\pm13‰$ (see table 6.9).

Similarly, the enstatite chondrite Indarch releases such an abundant amount of nitrogen compared to carbon at high temperatures (table 6.7) that it is difficult to see how it could be associated with the SiC. The Indarch residue has been studied by TEM analysis by M. Lee (University of Essex), and found to contain Si_3N_4, a probable candidate for high temperature release; a stepped combustion experiment on a synthetic Si_3N_4 sample indicated that the combustion temperature of this component is >1200°C. If the same assumptions as above are made then the calculations indicate the nitride has $\delta^{15}N$ of 12‰, making it clearly different to the component seen in ordinary chondrites, and more probably a Solar system condensate than a presolar grain.

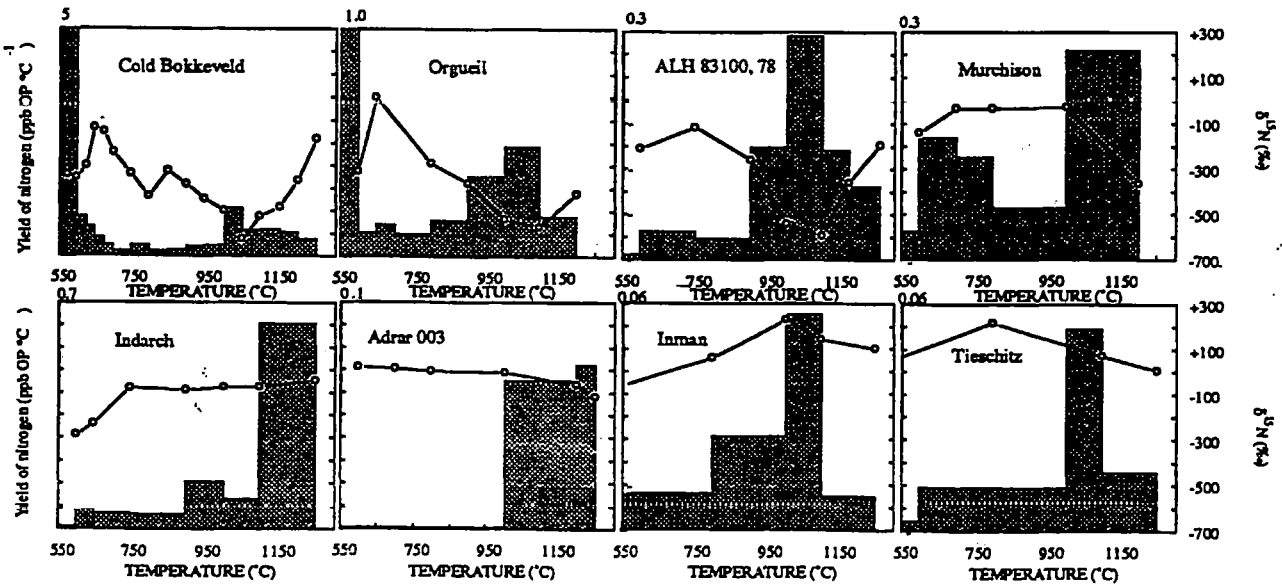

Figure 6.19. Nitrogen stepped combustion experiments over the high temperature regime for a series of perchloric acid-resistant residues (ppbOP= parts per billion of the whole rock).

Meteorite	$\delta^{15}N$‰ (1σ)	$\delta^{15}N$‰ blank corr.	C/N
Orgueil	-576.5 (3.0)	-625 (-605 to -655)	36
ALH 83100	-594.6 (2.7)	-630 (616 to 653)	37
C.Bokkeveld	-626.4 (6.0)	-652 (-650 to -659)	30
Murchison	-365.7 (2.1)	-515 (-453 to -653)	18
Allende	-24.1 (4.3)	-74 (-37 to -311)	27
Efremovka	-304.4 (4.0)	-369 (-330 to -384)	184*
Adrar 003	-122.1 (2.6)	-126 (-122 to -131)	12
Inman	+204.5 (1.2)	+235 (+223 to +256)	4
Tieschitz	+405.8 (1.2)	+839 (+473 to +1289)	5
Indarch	-51.7 (.38)	-51.9 (-51.5 to -52.4)	3

Table 6.7. "$\delta^{15}N$" represents the most extreme isotopic value recorded in the high temperature regime; the C/N given is the ratio recorded for that step. * The Efremovka component recorded here burns between 600° to 800°C (see the next section) and is not attributed to SiC: the heavy carbon peak, which is very minor in abundance compared to this phase, occurs at higher temperatures and contains no measurable nitrogen.

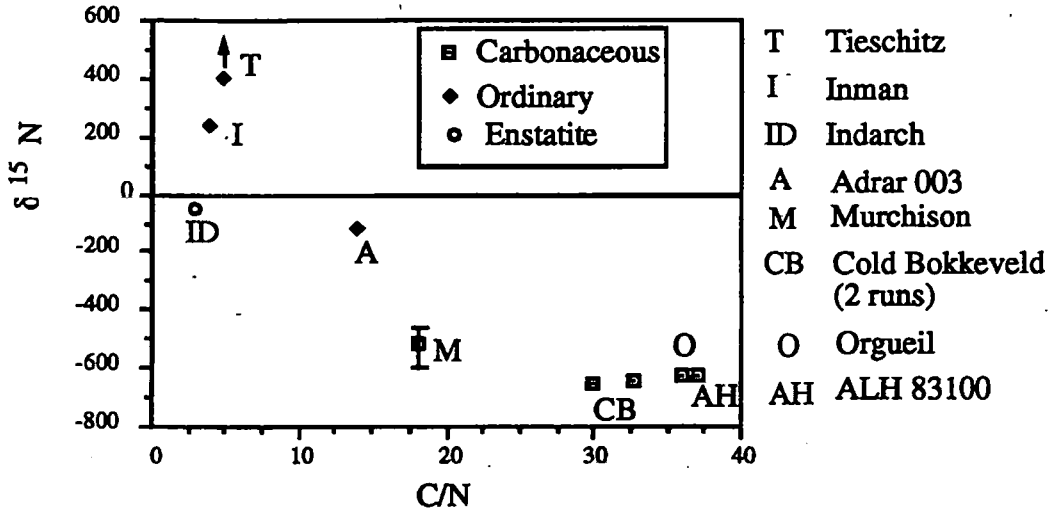

Figure 6.20. C/N ratios and $\delta^{15}N$ for the high temperature regime of the SiC rich residues, including two analyses for Cold Bokkeveld. The experiment performed on the Murchison residue may have been contaminated with some air. Data are all blank corrected, except for Tieschitz, because the errors involved in this correction were very large.

6.11. The high temperature component in Efremovka

Following the discovery of a new anomalous xenon isotopic signature in the CV3 Efremovka (Verchovsky *et al.*, 1991), a series of residues from this meteorite were donated for carbon and nitrogen study by A.B. Verchovsky, L. Semjenova and A.V. Fisenko (Academy of Sciences, Vernadsky Institute, Moscow). The residues (DE2 and

DE5) were found to contain stacks of carbon that is released at 600-800°C (the results from a C and N conjoint experiment on DE5 are shown in figure 6.21.). The carbon release is similar in temperature and isotopic composition to ones seen in Tieschitz and Inman, but it is a factor of 100x more abundant in Efremovka. The carbon made up 14 ppm of the whole rock meteorite and had an isotopic composition of ~-10‰; a component of comparable abundance and $\delta^{13}C$ is not observed in any of the other carbonaceous chondrites but this may reflect in part the difference in preparation technique between the Russian and British residues. The temperature range of the carbon release was in broad agreement with that of the isotopically anomalous Xe release but its $\delta^{13}C$ is within the normal Solar system range. A nitrogen extraction of the residue DE2 after diamond precombustion (figure 6.22) revealed the presence of a light nitrogen component, $\delta^{15}N$ = -304‰, or -369‰ (blank corrected); C/N = 186. The extreme ^{14}N enrichment of this component suggests that it may represent a presolar signature associated with the presolar Xe containing component; the high C/N ratio and combustion temperature is reminiscent of graphite, although it is possible that the presolar noble gas carrier may not be very abundant, and could be swamped by a more abundant "normal" carbon component that is not the host phase to the isotopic anomalies. The presence of at least two components (one of Solar system origin and one presolar) is also inferred by the C/N ratio, which is not constant but decreases towards the end of the experiment (figure 6.21). This suggests that the nitrogen rich component has a slightly higher combustion temperature to the most abundant carbonaceous component.

Carbon stepped combustion of the Efremovka residue at higher temperatures demonstrated that the residue also contained isotopically heavy carbon attributable to SiC; this could be easily resolved from the 600-950°C components.

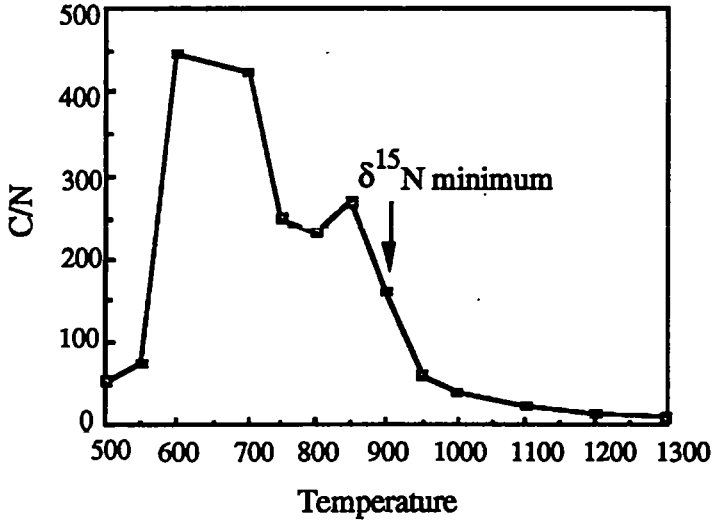

Figure 6.21. Variation in C/N over the main carbon and nitrogen burning regime in the Efremovka residue, after the combustion of the diamond component.

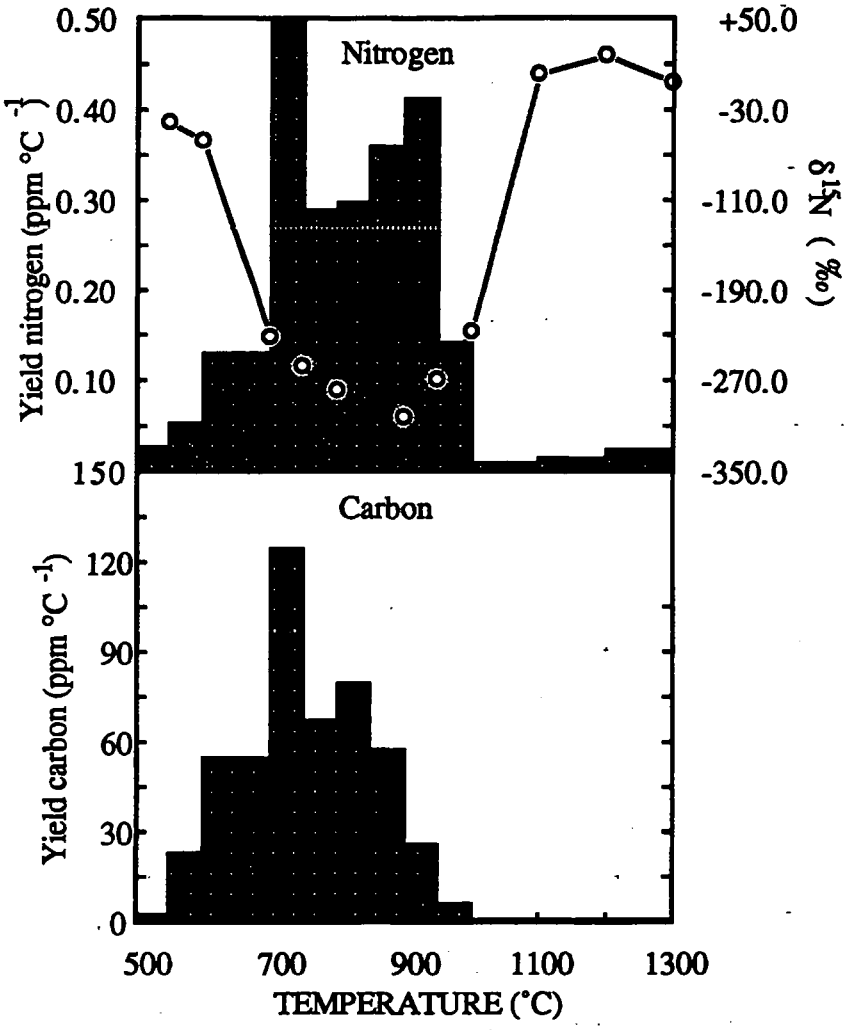

Figure 6.22. A nitrogen stepped combustion of the Efremovka high temperature regime.

6.12. Summary and Discussion

This section will attempt to address the two main questions raised by the experimental data: (i) are the observable differences in SiC combustion temperature between meteorites from different classes due to sampling of different sources, or parent body processing and (ii) what carbon and nitrogen components are present in addition to SiC in these residues?

6.12.1. Sources of silicon carbide

Despite the wide range of minor components combusting in the interval 500 to 950°C, above this temperature the combustion profiles for the lower petrologic type meteorites appear to be dominated by a material that has a consistent mean $\delta^{13}C$ value of

+1437±32‰ that can be attributed to SiC. The CV3 group apparently contains SiC with a lower $\delta^{13}C$ and the reasons for this are discussed at the end of this section. Similar $\delta^{13}C$ values to +1437‰ have been recorded by other authors (*e.g.* Murray, +1384‰ - Ash ,1990; Colony, +1350‰ -Newton *pers. comm.* 1992; Inman, 1375‰ - Alexander *et al.*, 1990). This study indicates that the SiC mixture has a similar mean carbon isotopic composition in all chondrites of low petrologic type but differs in combustion dynamics between meteorite groups. This apparent discrepancy can be explained in several possible ways:

(i) The SiC could be identical in all meteorites, and the combustion temperature differences an artefact of the acid dissolution prior to stepped combustion. Since, for example, the phosphoric acid treatment clearly changes the combustion temperature of heavy carbon by some mechanism, the other acid treatments may have similar effects. However, since all the meteorites were dissolved using as nearly as possible identical protocol, it would be hoped that the samples are still internally comparable. All the carbonaceous chondrites gave a peak carbon yield between 900° and 1000°C, agreeing with values of SiC from carbonaceous chondrites studied by other workers (Ash, 1990; Newton *et al.*, 1992). Not enough sample was available to replicate the Indarch result of silicon carbide combusting at a temperature ~200° higher than the carbonaceous chondrites, but the conjoint carbon data acquired during nitrogen analysis gave a similarly shaped profile to that of the carbon isotopic analysis. Similarly, the heavy carbon release of Adrar 003 was replicable during conjoint C/N analysis. Thus it is assumed that the observed differences are real, and that there is a variation in the SiC type -demonstrated by a difference in combustion temperature- with class of meteorites.

(ii) Meteorites may have sampled different mixtures of SiC sources that coincidentally have the same mean carbon isotopic composition. Recent work by Ott *et al.* (1991) has pointed to differences in Ne-E(H) and Xe-S content between SiC in Indarch and other meteorite groups and this may indicate that the enstatite chondrites are enriched in silicon carbide from a separate source to the main contributors to the carbonaceous chondrites. Stone *et al.* (1991) have observed that the majority of SiC grains in Indarch have a different morphology to those of the carbonaceous chondrites; the grains in Indarch are of a rounded, fractured morphology whereas those in the CM2s are mostly platey in appearance, although a few Indarch-like grains are also present in the carbonaceous chondrites. These differences may represent sampling from a alternative provenance. Thus, samples of SiC with distinguishable morphologies may have differing combustion characteristics, or else samples from separate sources may have differing aluminium contents that would affect combustion temperature (There is a correlation between morphology of SiC and Al content, described by Virag *et al.*, 1992). However, observations of present day red giant stars suggests that they have very diverse $^{12}C/^{13}C$

ratios. For example, the study by Lambert *et al.* (1986) of 30 cool carbon stars found a variation in $^{12}C/^{13}C$ ratio of between 2 and 70. Given the wide range of potential $^{12}C/^{13}C$ for SiC from carbon rich stars, it would be extremely unlikely that two separate mixtures of grains would fortuitously have the same $\delta^{13}C$.

(iii) The SiC mixture was originally the same in all meteorites but parent body processing has caused the SiC to be of variable stability to combustion. For example, the SiC from the carbonaceous chondrites may have been weakened by partial oxidation, whereas the reducing conditions in the enstatite parent body may have preserved the grains in a more pristine state. An explanation for the difference in combustion temperatures could thus be that the SiC of platey morphology combusts at 1000°C and anhedral grains at 1200°C. In this case, the morphology differences reported by Stone *et al.*, (1991) would have to reflect the extent of weathering in the parent body, which seems rather unlikely. A prediction could then be made that Adrar 003 residue, which has not yet been studied by SEM, contains grains of both types in approximately equal proportions. The most convincing evidence that the silicon carbide represents the same original mixture is the similarity in $\delta^{13}C$ between low petrologic types of the carbonaceous, ordinary and enstatite chondrites.

The $\delta^{13}C$ of the SiC in CV3s is apparently lower than for the other meteorites ($^{12}C/^{13}C$ for CV3= ~52; $^{12}C/^{13}C$ for CM2/EH4/Adrar 003 = 36.6), and this component appears to be underabundant in this meteorite group compared to the lower petrologic type meteorites. A possible explanation for the lower $\delta^{13}C$ is that the CV3s are relatively enriched in Solar system SiC. All the meteorites are known to contain a proportion of SiC with isotopically "normal" carbon, and it could be the case that on accretion all the chondrites contained the same proportions of Solar and presolar SiC. If the presolar component is more unstable than the Solar one (Solar SiC appears to survive in the Abee meteorite where all the presolar would have been destroyed), then as metamorphism progressed, the overall abundance of SiC would decrease and the $\delta^{13}C$ of the residual silicon carbide would decrease. This process would be expected to be mirrored in the other chondrites that have experienced a small degree of thermal metamorphism (e.g. the H3.6 Tieschitz) but the $\delta^{13}C$ values of SiC in these components are difficult to measure because the the overall abundance of SiC in these meteorites is so low that combustion is affected by co-release of the relatively more important blank contribution and carbon associated with indigenous minerals.

6.12.2. Other potential carbonaceous components in the high temperature regime

Carbon from spinel

Spinel is the major constituent of the residues after the perchloric acid treatment and diamond precombustion (see section 6.4) and so it is possible that carbon, contained as a trace element in the spinel structure or as inclusions within the grains contributed to the carbon release profile. The presence of carbonaceous inclusions within the spinel was discussed by Tang *et al.* (1988), who found that residues rich in spinel appeared to contain an isotopically light carbonaceous component in addition to the heavy SiC. A spinel-rich separate was prepared by Tang *et al.*, using the heavy liquid bromoform ($CHBr_3$), and the sample was then treated with H_3PO_4 to dissolve away the spinel. The resulting sample (Murchison GS) contained mostly carbon with a bulk $\delta^{13}C$ of -45.7‰. This was interpreted by Tang *et al.* as a pure separate of the carbonaceous phase contained within spinel that was dubbed "Cθ" and made up an estimated 14% of the spinel by mass. With hindsight, this remarkable finding appears somewhat unlikely. Ash (1990) has pointed out that the existence of a phase that oxidises at *ca.* 400°C within a spinel grain that condensed at 1240°C (Grossman, 1972) is chemically improbable, as carbon is oxidised to CO under the O-rich conditions under which spinel forms. In addition, the presence of carbon in abundance in meteoritic spinel has not been reported by other workers. This study found no major carbonaceous phase with a $\delta^{13}C$ =~-45‰ in samples that had been treated with H_3PO_4. SEM and X ray diffraction studies of heated residues after the perchloric acid stage indicates that the spinel recrystallises at ~800°C, and so it is at this temperature that any carbon components would be released, but a major carbon yield is not obtained during stepped combustion. Is it feasible that the carbon within the Murchison GS sample could simply be a terrestrial contaminant? A probable contamination source is the bromoform. Unfortunately the isotopic composition of the bromoform used was not measured and in any case the actual contaminant may have been a minor residue within this reagent. Although the exact chemical used can no longer be obtained for isotopic analysis, a similarly treated terrestrial sample could provide a clue to the identity of "Cθ". A clinopyroxene, isolated from its rock using a similar heavy liquid preparation technique, was analysed by carbon stepped combustion by S. R. Boyd, now of the University of Paris VII. The stepped combustion profile obtained from the clinopyroxene bears a striking resemblance to that of the Murchison GS sample made of the "Cθ" component plotted as a function of carbon released (figure 6.23). For the pyroxene sample, the existence of an indigenous carbonaceous phase, with a combustion temperature of 500-600°C and with a carbon isotopic composition of ~-45‰, is highly improbable. The sample must have become contaminated by the separation procedure; by analogy, the Murchison sample could have become

contaminated in a similar way.

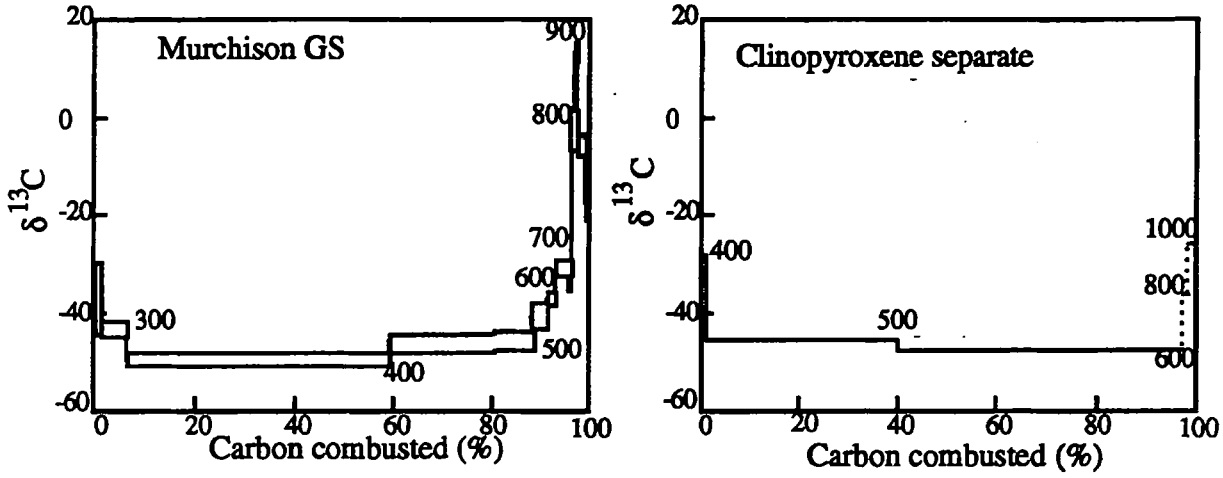

Figure 6.23. A comparison of the "Cθ" component in Murchison GS (figure plotted as a function of %C, from Tang *et al.*, 1988) to a clinopyroxene separate (Data from S. Boyd).

Thus, the evidence that the perchloric acid-resistant residues contain 14 wt % carbon in spinel (corresponding to ~12wt % of the residues) is poor. However, by Wexler's Law (there is at least one part per 10^8 of everything in everything) the spinel could contain trace amounts of carbon dissolved within the crystal lattice in measurable quantities that may be released during stepped combustion. The SEM work indicated the recrystallisation temperature of spinel was ~>800°C so it is above this temperature that the carbon would be released. The isotopic composition of the carbon within spinel is not known. Zinner and Epstein (1987) found carbon attached to spinel grains that was isotopically heavy (up to +7000‰) but concluded that this was probably entirely attributable to SiC. Stepped combustion evidence (McGarvie *et al.*, 1987) suggests that spinel may contain carbon with a $\delta^{13}C$ of close to 0‰. This study found a small amount of NaOH-resistant carbon released at high temperatures with $\delta^{13}C$ ~-25‰ that could thus be attributed to spinel.

Graphite

Graphite is a ubiquitous component of the meteorites used for this study, but the perchloric acid treatment used in the preparation of the residues was designed to destroy the graphitic material which would otherwise dominate many of the combustion profiles. TEM observations of the residues by M. Lee and K. Gilkes has however shown that while perchloric acid dissolves the "wispy" graphite, well crystallised graphitic sheets, that are typically ~100nm across, survive the treatment. Thus, the carbon from graphite must be released at some stage during the stepped combustion. The graphite standard NBS 21 combusts in the 700-800°C temperature regime (Grady, 1983) but it is probable

that grains of hundreds of nanometre dimensions, by analogy to diamond, combust at lower temperatures, and so it is perhaps the ~600 to 800°C part of the stepped combustion that should be considered. The nitrogen analysis of the Cold Bokkeveld residue may provide some more specific clues. After the main diamond combustion release, the C/N ratio of the residue rose to a maximum of 600 at around 600-650°C before dropping to >60. The C/N ratio remained at low values for the remainder of the experiment. It is extremely unlikely that well crystalline graphitic material could have a C/N ratio of <~100 (i.e. contain more than 1wt% nitrogen) and so it is probable that the 600°C peak represents the combustion of the graphitic component. Although single graphitic grains isolated from carbonaceous meteorites can be either more or less ^{13}C rich than terrestrial values, the average is >0‰ (*e.g.* Amari *et al.*, 1990). The oxidative acid treatment may destroy graphite from some sources and leave other populations untouched and so the $\delta^{13}C$ values recorded (>+300‰) could be biassed towards the more chemically stable populations of graphite. The heavy carbon peak at 600- 700°C seen in many meteorites may thus be from this source. In addition, isotopically "normal" graphite is observed in many meteorites with a $\delta^{13}C$ of between -10 and -20‰ (Grady, 1983). The carbon in Efremovka released at 600° to 800°C during stepped combustion with $\delta^{13}C$ = -10‰ could tentatively be ascribed to this source.

Other Carbides

SiC is not the only isotopically anomalous carbide observed in acid resistant residues of primitive meteorites. Bernatowicz *et al.* (1992) have observed, using TEM, TiC inside graphite grains and intertwined with SiC. Carbides such as this would undoubtedly contribute to the carbon release profile, possibly as sources of isotopically heavy carbon by analogy to the silicon carbide; but thus far the TiC quantities have been estimated as just 700 ppm of the concentration of SiC, and so would have a negligible effect on the release profile unless the $\delta^{13}C$ of TiC was very different to SiC. Similarly, the low abundance of the TiC suggests that this components cannot explain the second heavy carbon peak released at 1200°C from the CM2 Murchison and Cold Bokkeveld.

Carbynes

The only other carbonaceous phase that has been so far (tentatively) identified by TEM in residues of this type is chaoite (Gilkes *et al.*, 1992). The combustion temperature of this almost mythical component is not known but its sp bonding suggests affinities to alkynes which combust below 500°C. It can be assumed that the carbon release temperature of this component would be lower than ~600°C, and so it is hoped that carbyne combustion will not interfere with the combustion regime described in this chapter.

Carbon from the other minerals identified by electron microscopy

The other minerals known to exist in the residues studied from direct microscopy identification include hibonite, chromite, barytes and rutile. These components are present in very minor amounts (the most abundant is hibonite that made up 5.7% of the Cold Bokkeveld residue). The last two minerals are almost certainly terrestrial contaminants; barytes should dissolve in the acid treatment and rutile is not reported in the petrology of Cold Bokkeveld. Carbon is not a major element in any of these components and so will only be present in trace amounts if detectable at all. Thus the carbon contribution from these components is likely to be negligible compared to the silicon carbide release and possible release from spinel which makes up by far the greatest proportion of the residue.

Unidentified phases

The high resolution stepped combustion experiments performed on the perchloric acid-resistant residues at high (>550°C) temperatures have indicated the presence of several components in addition to the SiC which is found ubiquitously in low petrologic type chondrites. Ash *et al.* (1990) reported the presence of several isotopically anomalous carbonaceous components from a HF/HCl residue of the Allende meteorite by preparative precombustion, but these phases have not yet been positively identified. The presence of poorly crystalline graphite that they tentatively attributed to some of the carbonaceous components would have been destroyed during the oxidative treatments. There is some evidence that the silicon carbide may start to combust at temperatures as low as ~750°C from the NaOH experiment (section 6.8.1), and under some conditions the major heavy carbon fraction can combust at ~800°C (see section 6.8.2: the H_3PO_4 experiment). Thus the 800°C heavy carbon peak seen in the CM2 stepped combustion experiments has been attributed to SiC, although this identification is extremely tentative. As well as the phases listed above it is likely that other components, as yet unidentified, make up the carbonaceous component inventory. All the components for which there is some evidence in Murchison are listed in table 6.8.

	Comb. Temp. (°C)	$\delta^{13}C$	Found in:	Tentative identification
1	~600	>+300	M2	graphite
2	700-800	+900	M2	SiC? (*c.f.* 8)
3	900-1100	+1400	M2	SiC
4	1200	+1400	M2	SiC ("Indarch-type")
5	600	+ 550	M2B (NaOH)	Graphite cf. 1
6	750	+900	M2B (NaOH)	*c.f.* 2
7	800-1200	~0	M2B (NaOH)	C from spinel?
8	800-900	+1400	M2A (H_3PO_4)	SiC with poor thermal resistance
9	650	>+600	MIL (NH_3)	graphite, *c.f.* 1 and 5
10	700-800	~0	MIL (NH_3)	nanometre SiC

Table 6.8. Components found in the Murchison suite of residues: M2 is the parent perchloric residue.

There is evidence of additional components in almost every residue; although not an exhaustive list, the most abundant of these are listed in table 6.9.

Meteorite	Combust. Temp (°C)	$\delta^{13}C$	$\delta^{15}N$	C/N	Tentative ID
Efremovka	600-800	-10‰	-300‰	186	graphite?
Cold Bokkeveld	750 -800	+1160‰			SiC + graphite?
Orgueil	600-1000	+300‰			?
Inman	600-700	+60‰			graphite?
Adrar 003	1000-1200		+357‰*	13	nitride?
Inman	800-1000		+332‰*	4	nitride?
Tieschitz	800 -1000		+326‰*	3	Si_3N_4
Indarch	1200-1300		+12‰*	0*	Si_3N_4

Table 6.9. Components other than SiC in the perchloric resistant residues * calculated values after stripping away the SiC contribution.

Nitrogen within the three carbonaceous chondrites for which good data could be obtained had a mean $\delta^{15}N$ of -636±11‰ (blank corrected). This is somewhat lighter than the mean value of 28 grains after ashing treatments analysed using ion probe ($\delta^{15}N$ = -395‰) reported by Zinner *et al.*, (1989), although this could be explainable as a grain size effect; smaller grains have lower $\delta^{15}N$ values (Zinner, *pers. comm*). It is however interesting

that a similar discrepancy that is also seen in ion probe studies of diamond which report heavier $\delta^{15}N$ values (~-150‰; Virag *et al.*, 1989) than those obtained by stepped combustion (-351±8‰, this thesis).

The enstatite chondrite Indarch and the ordinary chondrites definitely contain high temperature nitrogen in a form other than SiC. The nitrogen in Indarch, with a $\delta^{15}N$ close to zero, may be carried by a Solar system condensate, such as Si_3N_4 that has been observed in similar residues by microscopy. In contrast, nitrogen within the ordinary chondrites seems to be anomalously heavy, and may represent an additional interstellar component. Alexander *et al.* (1990) suggested that the heavy nitrogen from Tieschitz may be associated with SiC, but the low C/N ratio recorded in this thesis indicates that this is unlikely to be the case; a nitride may be a more probable carrier. A recent TEM study by M. Lee has identified Si_3N_4 in the Tieschitz residue; work is now in progress to identify nitrogen bearing components in the Inman and Adrar 003 perchloric residues. A nitride can condense at any C/O; the ^{15}N enrichment suggests it may have condensed near a stellar environment in which hot CNO cycling occurs, such as a nova.

6.13. Implications for early Solar system history

There is evidence that the ubiquitous, isotopically heavy SiC, known to have diverse carbon isotopic values, was sufficiently mixed in the early Solar nebula to produce similar mean $\delta^{13}C$ values, if only the lowest petrologic types of each meteorite class are considered. The CV3s however, although poor in overall SiC abundance, may contain proportionally more silicon carbide that has a lower $\delta^{13}C$ value. Chapter 7 explores this observation and the distribution of SiC and diamond between meteorite classes further, and particularly in relation to parent body processes. The difference in combustion temperature between meteorite classes is more difficult to explain but suggests that parent body processing may affect the properties of the SiC in some way, *e.g.*, by partial oxidation of the grains. In addition to SiC, minor carbon and nitrogen bearing components are present in perchloric acid resistant residues that vary in abundance and type from meteorite to meteorite. The isotopic composition of these minor components indicate that many of them may be presolar in origin.

CHAPTER 7

OVERVIEW AND FUTURE WORK

The survival of SiC and diamond grains of apparently presolar origins within meteorites surely qualifies as an incredible feat of nature; although the origins and preservation of these interstellar grains are not yet well understood, they provide an excellent opportunity to study the material that formed our Solar system, as well as providing information about conditions that existed within the meteoritic parent bodies over the last 4.55×10^9 years since their condensation. This chapter attempts to recap the possible formation environment of these grains and goes on to discuss how the SiC and diamond abundances could be related to parent body processing. The final part of the chapter reviews the future research opportunities this study may provoke.

7.1 Origin of SiC and Diamond

Ion probe studies of SiC (*e.g.* Zinner *et al.*, 1989) have shown that this component has several sources; since the techniques described in this thesis do not involve the analysis of individual grains it is beyond the scope of this text to comment on these sources in depth. The $^{12}C/^{13}C$ ratio of the present day interstellar medium, at 45±3 (Hawkins and Jura, 1987), is lower than that of the Solar system as a whole but higher than the mean value for SiC ($^{12}C/^{13}C$ =36.6±0.5). Since the $^{12}C/^{13}C$ ratio is believed to evolve to lower values over time, then it can be assumed that the value for the interstellar medium at the time of the condensation of the Solar system was higher than 45, and so different from the value for SiC. This is unsurprising since the grains are believed to represent specific, evolved, stellar sources. Measurements of the mean values of SiC during stepped combustion are in broad agreement with both theoretical values (*e.g.* Obaravic *et al.*, 1992) and observational values of $^{12}C/^{13}C$ ratio of present day carbon stars in the AGB stage of their evolution (*e.g.* Lambert *et al.*, 1986), although the $\delta^{13}C$ values recorded for SiC are possibly more ^{13}C rich than mean values given for carbon stars in most studies. This could be because the SiC was dominated by a single source that had a lower $^{12}C/^{13}C$ ratio than the

mean value, or else the AGB stars that condense SiC are not typical of the population as a whole.

The chondritic diamond associated with isotopic anomalies is too fine for single grain analysis. The work described in chapter 3 however suggests that the differences in nitrogen content between meteorite groups can be most easily, although not exclusively, explained if a diversity in sources, similar to that proposed for SiC, is invoked. Furthermore, although the proposed site for the formation of Xe-HL is a supernova, the $\delta^{13}C$ and nitrogen isotopic composition of the diamond cannot easily be reconciled with a single supernova source (Clayton, 1989), and multiple sources thus seem likely. This would help explain the "normal" (*i.e.* Solar system) $\delta^{13}C$ values for the diamond if, like the Solar system as a whole, the diamond was made from carbon from a variety of different stellar sources. It is also likely that some diamond is a Solar system rather than presolar condensate. The carbon and nitrogen isotope studies discussed in chapter 3 indicate that one diamond component could have a $\delta^{13}C$ of -25‰ and a low nitrogen content and thus may be a Solar condensate.

The presence of both silicon carbide and diamond in Abee, apparently not associated with any isotopic anomalies, and containing trapped planetary noble gases, indicates that Solar system sources for these two components cannot be ignored; a portion of these minerals in the more primitive chondrites may be of an early Solar system, rather than presolar, origin.

7.2. Destruction and distribution of SiC and diamond in meteorites

The overall abundance of diamond and SiC in meteorites decreases with increasing petrologic type: the CM2s and CI1 are rich in interstellar grains, and the higher petrologic type ordinary chondrites are depleted. Except for the enstatite chondrites, the grains are absent in petrologic type > 3. This implies that both grain types are either destroyed by preaccretionary processing or metamorphic reactions, but since the hydrothermally altered CI1 Orgueil is a prolific source of both diamond and SiC it can be inferred that reactions involving water are unimportant in grain destruction.

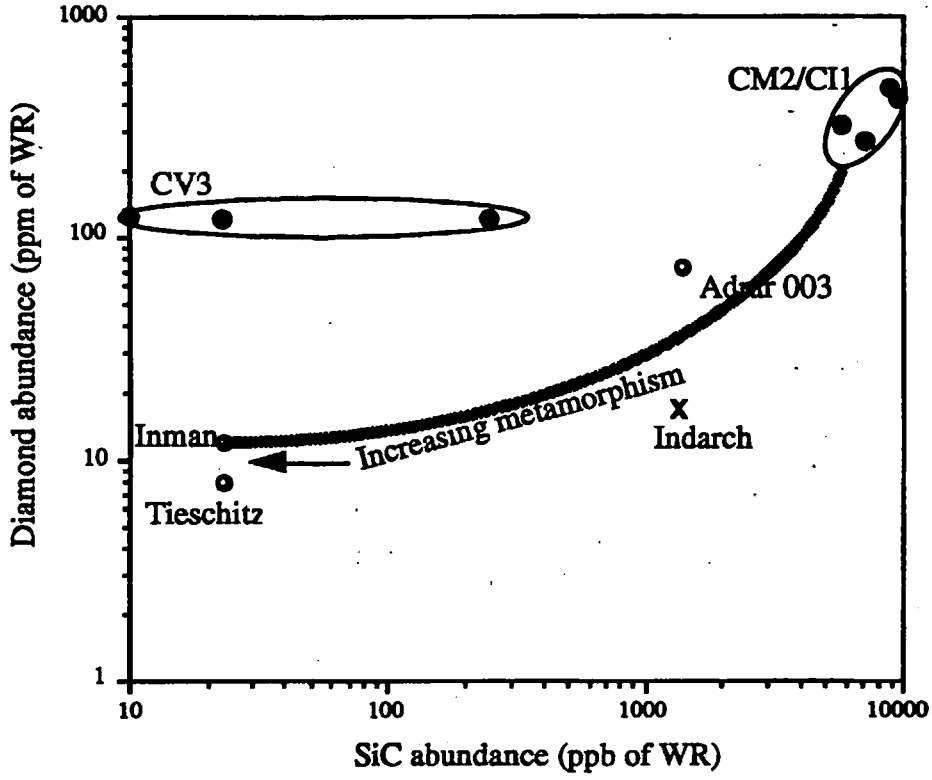

Figure 7.1. The abundances of "presolar" SiC and diamond in chondritic meteorites.

Figure 7.1 plots the abundance of SiC and diamond in the meteorites that have been discussed in this thesis. It can be seen that the CM2's, CI1 and ordinary chondrites fall on a line that could represent the progressive destruction of the grains, although admittedly more data is necessary from the more metamorphosed meteorites, to constrain this process better. The concentration of the grains within the matrix has been estimated by Huss (1990) by normalising the grain abundance. This assumes that the diamond and SiC are located only in the matrix of the meteorite. The normalised results from the abundance data given in this thesis are shown in table 7.1. After normalisation the abundances show significant differences that can be largely explained by metamorphic destruction of the grains in the parent body.

Meteorite	Matrix (%)	Diamond (ppm)	SiC (ppb)	Diamond (norm)	SiC (norm)	Diamond/ SiC
Orgueil	100	424	9640	424	9640	44
C. Bokkeveld	50	318	5733	636	3440	55
ALH 83100	50	272	7067	544	14134	38
Murchison	50	467	8763	934	17526	53
Allende	38.4	125	10	325	26	12500
Efremovka	?	120	23			5220
Vigarano	34.5	130	167	377	484	778
Adrar 003	4.1	57	1387	419	10192	41
Krymka	13.6	136		999		
Inman	20	12	23	60	172	333
Tieschitz	15.1	8	23	53	153	347
Indarch	10	17	1363	170	13630	12

Table 7.1. Abundances of diamond and SiC normalised to matrix abundance. Matrix % data from Huss, 1990

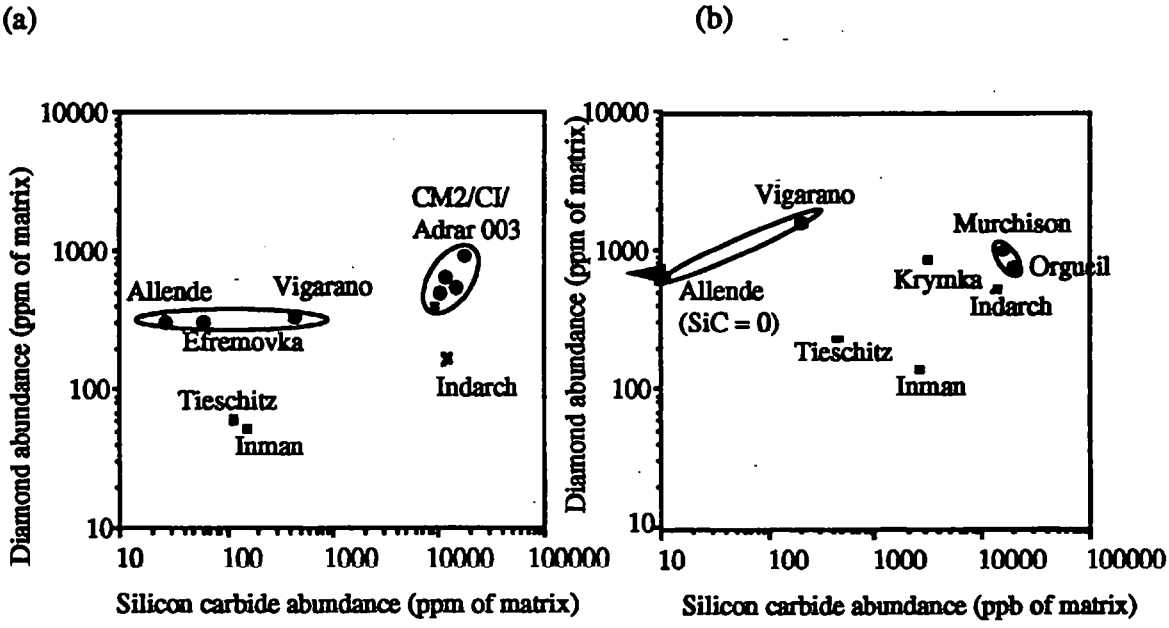

Figure 7.2. Matrix normalised diamond and silicon carbide ratios: (a) data from this thesis and (b) data from Huss, 1990.

After normalisation, the most primitive ordinary chondrite for which there is a full dataset (Adrar 003) has a similar diamond and SiC abundance to the most primitive carbonaceous chondrites (the CM2s) (table 7.1 and figure 7.2). The enstatite chondrite Indarch has a SiC content that matches that of the CM2s but is apparently depleted in diamond, possibly through metamorphic destruction (see below).

The normalised data given by Huss (1990) are similar in spirit to those in this thesis (figure 7.2): the primitive ordinary chondrites and primitive carbonaceous chondrites yield similar data whereas the CV3s are apparently depleted in silicon carbide. The enstatite chondrite Indarch is enriched in SiC relative to its diamond content although this is slightly less apparent using Huss's data. Overall, the SiC abundances are similar, but the diamond abundances given by Huss are consistently higher than those obtained in this thesis. It is probable that, as discussed in chapter 3, a small proportion of the diamond is lost during our oxidative acid treatments to give a low yield.

The diamond abundances are closely related to petrologic type; the SiC abundance also varies with petrologic type but is more sensitive to oxidation state. A good example of this is the CV3 group which have experienced similar metamorphic temperatures to each other but show intragroup variations in oxidation state. The diamond contents of the 3 meteorites studied are very similar (120 *vs.* 125 *vs.* 130) but their SiC contents are very low; in particular, the SiC abundance of Allende is low compared to that of Vigarano and Efremovka. The intraclass differences could be explained by the differences in oxidation state between the CV3 meteorites; McSween (1977) reported Allende to be more oxidised than Efremovka or Vigarano, and in addition the Allende meteorite appears to have suffered some thermal metamorphism. The metamorphic destruction of silicon carbide in the CV3s in general could be especially efficient, perhaps reflecting their very oxidised state. Also, the $\delta^{13}C$ of the SiC in CV3s is apparently less than for the other meteorites ($^{12}C/^{13}C$ for CV3= ~52; $^{12}C/^{13}C$ for CM2/EH4/Adrar 003 = 36.6). A possible explanation is that the CV3s, although low in total SiC are relatively enriched in Solar system SiC. All the meteorites are thought to contain a proportion of isotopically "normal" SiC. It is possible that on condensation all the chondrites contained the same proportions of Solar and presolar SiC, and that the presolar component is more unstable than the Solar one (Solar SiC appears to survive in the Abee meteorite where all the presolar may have been destroyed). As metamorphism progressed, the overall abundance

of SiC would decrease and the $\delta^{13}C$ of the residual silicon carbide would decrease. This process would be expected to be mirrored in the other chondrites that have experienced a small degree of thermal metamorphism (*e.g.* the H3.6 Tieschitz) but the $\delta^{13}C$ values of SiC in these meteorites are difficult to measure because their overall abundance of SiC is so low that combustion is affected by co-release of the relatively more important blank contribution, and carbon associated with indigenous minerals.

An alternative way to explain these residual variations is by invoking an abundance difference at the time of meteorite accretion. Huss (1990) suggested that the CV3s were diamond enriched, possibly because the diamond followed the refractory primitive Solar system dust in the early Solar nebula, which is highly abundant in the CV3s. This would not explain the paucity of SiC in these meteorites; also the nitrogen content of the CV3 diamond in in keeping with a original diamond abundance similar to the other meteorites (figure 3.22). A more likely explanation could be that the CV3s are SiC poor, possibly not containing the entire allocation of SiC found in the other meteorites. There is some evidence that the CV3s were among the first chondrites to condense: Vigarano gives the oldest reliable I-Xe date of any meteorite (Crabb *et al.*, 1982; Swindle and Podosek, 1988). Allende yields the oldest age using Rb/Sr dating (Tilton, 1988) and contains CAI inclusions which are apparently the first meteoritic condensates in the Solar system (Kirschbaum, 1985). Could it be possible that a new type of SiC grains was injected into the Solar nebula after CV3 condensation but before the accretion of the other meteorites? This would in addition account for the different $\delta^{13}C$ of SiC in CV3s.

The SiC to diamond ratio varies between meteorite classes, suggesting that the metamorphic processes involved in their destruction are not the same. The destruction of carbonaceous grains has not been widely discussed in the literature, but Alexander *et al.* (1990) suggested that, in analogy to the oxidation of iron in the ordinary chondrite mesostasis during equilibration, reactions of diamond and SiC with magnetite may be important:

$$\text{(a)}\quad C + 2Fe_3O_4 + 3SiO_2 \rightarrow 3Fe_2SiO_4 + CO_2$$

$$\Delta G_{700} = -32\text{kJ}$$

$$\text{and}\quad \text{(b)}\quad SiC + 4Fe_3O_4 + 5\,SiO_2 \rightarrow 6Fe_2SiO_4 + CO_2$$

$$\Delta G_{700} = -375\text{kJ}$$

It can be seen that this process is more favourable thermodynamically for the oxidation of SiC than for diamond. Alexander *et al.* expressed reservations about the kinetic feasibility of these reactions, but the high nitrogen content of both diamond and silicon carbide compared to terrestrial analogues, along with radiation damage that they must surely have suffered before meteorite accretion, may make the grains more susceptible to destruction.

The reaction with magnetite will not be an option in the more reduced meteorites particularly when it becomes a minor or absent phase (for example, there is no magnetite in the enstatite chondrite Indarch). Thus, an alternative candidate for the oxidation must be found. Of the oxidised minerals common in the EH4 chondrites, olivine is a more likely oxidant than pyroxene because the activity of FeO in olivine is greater than the activity of FeO in pigeonite (Berkeley *et al.*, 1976). Possible reactions are:

$$(c)\ 2C + Fe_2SiO_4 \rightarrow 2Fe + SiO_2 + 2CO$$

and:

$$(d)\ C + Fe_2SiO_4 \rightarrow 2Fe + SiO_2 + CO_2$$

$$\Delta G_{700} = -42kJ$$

and:

$$(e)\ SiC + 2Fe_2SiO_4 \rightarrow 4Fe + 3SiO_2 + CO_2$$

$$\Delta G_{700} = +215kJ$$

Berkley *et al.* (1976) suggested that metal reaction rims found around olivine grains in the ureilite meteorite Kenna have may been formed at <1000°C by oxidation of surrounding carbonaceous material in this way, but the same mechanism can apply equally well to the chondrites, especially those depleted in Fe_3O_4. The oxidation of diamond (c and d) would be thermodynamically favourable, but the reaction involving SiC (e) is endothermic and so would be less likely to occur. If these reactions were the dominant ones in the enstatite chondrites, this could explain the higher SiC to diamond ratio recorded in Indarch. The products of the suggested reaction, free iron and silica, are observed in the enstatite chondrites; although olivine is a minor or rare phase in

the enstatite chondrites, especially those of higher petrologic type, where it occurs it is typically associated with silica (Dodd, 1981).

The carbon oxides liberated by these oxidation reactions would degas from the parent body, although it is possible that some may have become trapped as gas bubbles within the olivine grains as a result of reactions a and b. A test of the reactions c, d and e would be to determine the carbon content and $\delta^{13}C$ of the silica and other product phases in the higher petrologic type meteorites.The overall effect of all the reactions (a to e) is therefore a depletion in overall carbon content and the reduction in oxidation state of iron. The iron might be expected to show some Fe_3C or C in solid solution. The system C- CO- CO_2 is extremely sensitive to pressure. The SiC -CO- CO_2 system has not been studied but it may depend on pressure to a different extent; the above reaction schemes can thus only be considered qualitatively.

The abundances of SiC and diamond can thus be partially explained by the petrologic type, degree of oxidation and matrix content of the host meteorite. Even after these considerations there are, however, some peculiarities in the diamond/SiC ratios. Most notably, the diamond/SiC ratios of the CV3s, especially Allende, is extremely high. This discrepancy would have to be explained by a primordial difference in the amount of SiC injected into the CV3s or by preferential metamorphic destruction of the crystals of more extreme carbon isotopic composition.

7.3. Future Work

Although in recent years it has become widely accepted that circumstellar grains are ubiquitous constituents of primitive chondrites, these components are still far from being fully understood. A protocol has been established for the isolation and analysis of meteoritic diamond that allows the accurate measurement of the carbon isotopes (using dynamic mass spectrometry) and conjoint nitrogen yield and isotope measurement with carbon yield determination. This system can now be used as a standard technique. In addition, the development of a highly sensitive carbon mass spectrometer (Prosser *et al.*, 1989) and analytical protocol (Yates *et al.*, 1992; Yates, 1992) has allowed high resolution stepped combustions to be performed on SiC rich residues.

7.3.1. Techniques

The current development of a nitrogen mass spectrometer will allow similar progress to that made using carbon mass spectrometry to be made in the analysis of low nitrogen samples. The development of a new technique for aliquotting standard gas, the capillary aliquotter, was too late for the research work in this thesis. However, the technique has been incorporated and is currently being tested on the new automated nitrogen static mass spectrometer, with promising preliminary results (I. Franchi, *pers comm*).

Conjoint carbon and nitrogen yield measurement was an important developmental technique for this work that allowed the "extra dimension" of C/N ratios to be determined, thus allowing a better characterisation of the carbon and nitrogen components during stepped combustion. It is imperative that this system be incorporated into any new nitrogen extraction line to allow this essential technique to be continued. All future work should remain aware of the "condensible nitrogen problem" that leads to low nitrogen yields. Since the production of condensible nitrogen appears to be related in some way to how the nitrogen is bonded within the sample, if more fully understood, this property of some nitrogen could be harnessed to become a useful technique allowing a better characterisation of nitrogen in samples analysed by stepped combustion techniques.

A natural progression of the C/N yield measurements would be the simultaneous measurements of dual $\delta^{13}C$ and $\delta^{15}N$ with respective abundances. For the work described herein, the carbon dioxide yielded during a stepped experiment was accumulated and measured as a bulk $\delta^{13}C$ for the experiment by dynamic mass spectrometry after the nitrogen analyses had been completed. However, $\delta^{13}C$ measurements for each step would be extremely useful in interpreting the nitrogen data and C/N ratio measurements. A system is currently being designed (Verchovsky, *pers. comm.*) that will allow the storage of CO_2 from each step separately for later measurement by dynamic mass spectrometry, but this system can clearly only be used for carbon rich samples utilising large step sizes so that the carbon yield is high enough for this type of measurement. More useful would be a "link-up" of a static carbon and static nitrogen machine, which would allow C and N isotope measurements on small steps, a system which would yield far more information than individual experiments for each element.

7.3.2. Diamond associated with isotope anomalies

The reason for the differences in nitrogen content of the diamond is still not fully understood. A project is in progress (Newton *et al.*, 1992) to measure nitrogen in a suite of CO carbonaceous chondrites that are believed to have originated at different depths (*i.e.* been heated to different degrees) in the same parent body. This study will reveal the importance of metamorphism to nitrogen loss in meteorites that probably contained the same interstellar grain inventory on accretion, and may also shed some light onto the diamond/SiC ratio problem. Further work on the nitrogen in diamond may focus on the metamorphic behaviour of nitrogen in these diamonds, both through experimental petrology and computer modelling.

The observation of large (~10nm crystallites) diamond in relatively unprocessed residues may make these enigmatic grains easier to study. For example, 10nm diamond crystals should be large enough to give meaningful results on analysis by EPR.

The metamorphic destruction of diamond in the higher petrologic types may have left bubbles of gas trapped within the olivine grains. The selection and analysis of these grains may reveal isotopically anomalous nitrogen and noble gases that would confirm that metamorphic destruction has taken place.

It is important to search for new ways of extracting the diamond from the meteorites without resorting to harsh acid treatments which may affect the characteristics of the diamond, and lead to low yields and possible isotopic fractionation. Preliminary work to this end has included gently crushing the meteorite and then extracting with water or dilute alkali solutions. If the diamond is not bonded within the matrix of the meteorite it may in this way be separable from the bulk meteorite. If a sample of diamond that has not been in contact with acids could be isolated then the relationship between diamond and other meteoritic minerals could be discerned as well as its exact grain size distribution. In addition, a reliable measurement of its D/H ratio could be made on samples that had not been acid treated, which would suggest if the grains had resided in the interstellar medium.

7.3.3. Acid resistant components in Abee

The discovery of diamond and SiC of apparently Solar system origin in the enstatite chondrite Abee provides much scope for future investigation. These grains appear to represent a primary Solar system condensate and as such may reveal information about the conditions within the Solar nebula. The grains could be studied further by ion probe techniques to determine if they are all identical or show isotopic diversity. An ion probe study of SiC would be especially useful as the combustion dynamics of SiC of this polytype is not known and it is possible that the stepped combustion to 1250°C did not achieve a full analysis of this mineral.

Diamond and SiC of the Abee type have so far been isolated from only one meteorite, which has a brecciated petrology (Rubin and Keil, 1983). A future study could prepare similar residues from other enstatite chondrites to determine if these components were ubiquitous in the enstatite chondrite forming region of the early Solar system or if they are unique to Abee. The higher petrologic type meteorites may be especially useful in this regard as, unlike the petrologic types lower than Abee, they will be uncontaminated with the thermally more fragile interstellar SiC and diamond.

The diamonds found in Abee may provide a link between the enstatite parent bodies and other meteorite groups. There is evidence that the carbon rich veins that run through ureilites may be related to enstatite parent bodies (Wasson, 1976) and if so the diamonds, which have apparently retained their primitive noble gas signatures, may provide a link between the two meteorite types. Similarly, extraterrestrial diamond (as opposed to diamonds produced in a terrestrial impact) has been isolated from an iron meteorite (Clarke *et al.*, 1981). The sophisticated isolation techniques that have been devised for the isolation of diamond from the primitive chondrites can now be used to acquire pure samples of the other meteoritic diamonds so that their origins can become better constrained.

7.3.4. Synthetic and terrestrial analogies to meteoritic diamond

The possible economic importance of diamond produced by CVD has provoked much research into its formation mechanisms. In this thesis, the primary interest in this diamond was inspired by its possible relationship to meteoritic diamond. The possibility of nitrogen doping to simulate the diamond with the attributes of nitrogen enriched "Cδ" diamond has still to be explored. In addition the carbon isotope fractionation involved in the CVD diamond formation process have not yet been established yet may throw some light on the exact mechanism by which the diamond condenses.

The carbon and nitrogen isotopic composition of carbonado diamond is a subject that has been apparently ignored by the scientific community. These fascinating diamonds could have had a low pressure synthesis that Ozima *et al.* (1991) suggested was due to irradiation of an organic precursor material; nitrogen isotope studies, if they reveal an abundance of nitrogen with a $\delta^{15}N$ reminiscent of organic material, may indicate if this interpretation is the correct one.

7.3.5. Silicon Carbide

High resolution stepped combustion experiments have been performed on SiC rich residues from a variety of meteorite groups, and demonstrated that the $\delta^{13}C$ of SiC from different primitive meteorite groups is indistinguishable. The development of an extremely sensitive nitrogen mass spectrometer could allow a similar project to be performed for high temperature nitrogen in these residues. This would be useful as the pathfinder work on nitrogen in these samples has demonstrated the apparent presence of nitride components, which may, in the case of the ordinary chondrites, be presolar. Thus, stepped combustion using small step sizes may allow the resolution of these components from nitrogen associated with SiC, and ensure that the mean $\delta^{15}N$ for SiC from non-carbonaceous samples be determined accurately, allowing any differences between meteorites due to poor mixing of SiC in the Solar nebula to be detected. This would be especially productive if conjoint $\delta^{13}C$ measurements could be made.

The analysis of acid resistant residues by TEM and SEM has proved very useful in characterising the residues and determining the carbon and nitrogen components contained within them. Future work should employ these techniques

more rigourously, and in particular, samples should be extracted at various stages of the stepped combustion experiment to ascertain which components combust over each temperature regime.

Many of the minor components in acid resistant residues appear to have a presolar isotopic signature and could be usefully characterised. The usual way that this is done is to treat the residues with a variety of reagents in an attempt to isolate the grains involved in sufficient purity to allow their identification. A complimentary technique could be to predict the identity of the grains and then experimentally determine the exact expected physical and chemical properties of the component. This technique was used to search for C_{60} in meteorites (Gilmour *et al.*, 1991); although this produced a null result it demonstrated the feasibility of this approach.

7.3.6. Other Work

In addition to the carbonaceous interstellar grains, silicate circumstellar grains may also be abundant in the less altered chondrites. A study of these components would reveal a wealth of information about interstellar dust from the oxygen rich stars, but the difficulties in isolating these components from the mostly silicate solar and secondary condensates in meteorites are immense. Ion probe studies may prove important here in detecting these grains *in situ*. Knowledge of the locality and associations of carbonaceous interstellar grains within meteorites may help to identify the probable site of potential silicate grains. Again a project is already underway (Ash, *pers comm*) to separate out parts of primitive chondrites (matrix, chondrule rims, chondrules, CAI's *etc.*) in an attempt to constrain the locality of their circumstellar dust.

To date the number of samples analysed for interstellar grains is small. If a full understanding is to be reached of the origins and preservation of interstellar grains in meteorites then a larger database must be obtained. For example, more ordinary chondrites from a suite of petrologic types should be studied so that the effects of metamorphism can be ascertained. CI meteorites other than Orgueil could be usefully studied to determine if Orgueil is typical of its class. In addition, the diamond and silicon carbide from CR meteorites has not yet been isolated and closely studied even though the CR Renazzo was the first meteorite from which Xe-HL was reported (Reynolds and Turner, 1964). To increase the number of low petrologic type samples available, it will be necessary to

undertake more meteorite collection programmes to hot and cold desert regions. The number of recently collected Antarctic meteorites does, however, pose some problems. Is the interstellar grains inventory of Antarctic samples the same as that of the non-Antarctic specimens? The Antarctic meteorite used in this study, ALH 83100 contain diamond that was typical for a CM2 meteorite but its silicon carbide had different combustion characteristics to that of non-Antarctic meteorites. Clearly, more samples are needed to determine if ALH 83100 is typical of Antarctic specimens or anomalous.

Many "oddball" meteorites contain as yet unexplained isotope anomalies (*e.g.* ALH 85085; Grady *et al.*, 1990; Bencubbin; Prombo and Clayton, 1985; Franchi *et al.*, 1986). It is hoped that our increased understanding of grains such as diamond and silicon carbide can be used in the future to isolate and characterise the putative interstellar grains in these meteorites.

In summary, recent research efforts into the interstellar grain inventory of meteorites has amply demonstrated the complexities involved in the formation and preservation of these enigmatic components. Many more years of work will be needed before a full understanding of these grains is reached.

APPENDIX 1: SAMPLE PREPARATION

An attempt was made to prepare samples for this thesis in a consistent way so that comparisons could be justifibly made between samples from different meteorites. The procedure used is described in the diagram below, adapted from that of Tang and Anders (1988). Carbon and nitrogen containing reagents are avoided at all stages in the sample preparation because they represent potential contamination sources, and stages such as H_3PO_4, which apparently affect the diamond or SiC grains (chapter 6) were also avoided. In addition, residues from two Russian meteorites, Krymka and Efremovka, were analysed. These samples were prepared by Luba Semjenova at the Vernadsky Institute, Moscow, and utilised a different preparation technique. Some of the differences resulting from this separate procedure are discussed in chapter 6.

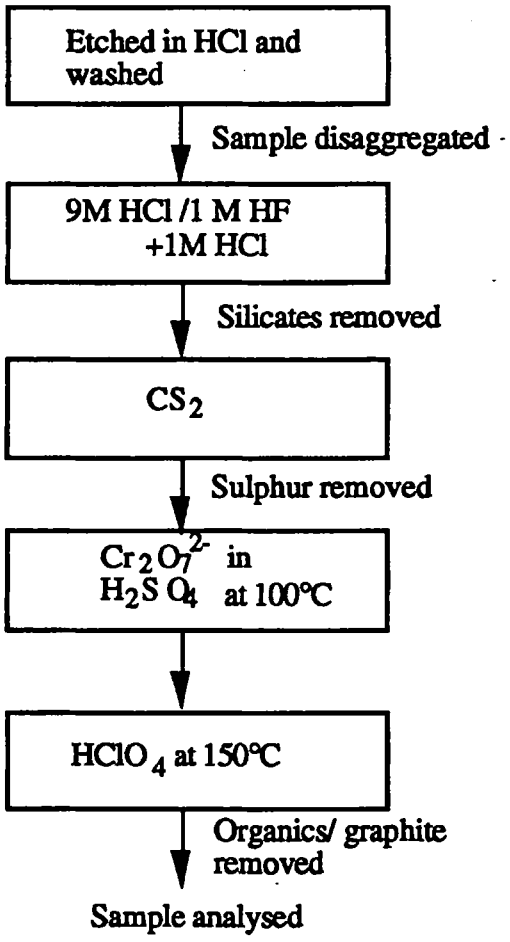

Names of meteorites studied and of acid resistant residues after the perchloric acid stage (pseudonyms in brackets):

Meteorite	Residue	ppmOP
Orgueil	OP1D	703
Murchison	M2	590
ALH83100,78	ALH3	436
Cold Bokkeveld	CB3B	1580
Allende	ARC IVDS (ARCIVD2)	495
Efremovka	DE2, DE5	~200
Vigarano	V2	1869
Krymka	KR4, KR6	
Adar 003	AD2	165
Inman	IN3	93
Tieschitz	TR2 (T3)	127
Indarch	I3	42
Abee	A2	135

APPENDIX 2: STEPPED COMBUSTION DATA

The stepped combustion data lists the temperatures of each step (measured using a chromel/ alumel thermocouple) that are accurate to ±5°C (Ash, 1990). The carbon yields were determined using a capacitance manometer, and nitrogen yields using the major intercept value of the M/Z = 28 beam in the mass spectrometer. Isotope values, and the 1σ errors on the isotope measurement, are also listed. "nm" indicates that the sample gas was either lost or too small to allow accurate measurement. To allow easy comparisons, the yield data for the acid resistant residues are listed wherever possible in parts per million (or billion) of the whole rock meteorite. This value is listed as OP. For the few residues that made up an unknown proportion of the whole rock (e.g. the Russian residues) the yields are listed as ppm of the residue.

Layout of this appendix.

The first experiments listed are the blanks that were discussed in the text. The terrestrial diamond data are then listed followed by data from the Abee samples. The carbon data for the rest of the acid resistant residues is reported next, beginning with the results of dynamic mass spectrometry over the diamond burning temperature regime, followed by the static mass spectrometry measurements. Finally, the nitrogen data for these residues are listed.

BLANKS DISCUSSED IN TEXT

Empty combustion section, CuO at 450°C overnight

Temp	ng N	ng C
300	0.57	7.56
400	0.69	11.34
600	0.61	11.79
800	0.58	15.7
1000	0.54	12.09
1200	0.54	12.7

Empty comb. section, CuO at 850°C overnight

Temp	ng N	ng C
200	0.5	7.56
400	0.42	6.04
600	0.42	7.56
900	0.42	6.05
1100	0.5	9.07

Pt bucket, baked with CuO, quenched from 1000°C

Temp	ng N	ng C
200	0.6	23.6
300	0.55	8.6
400	0.63	18.4
600	0.75	16.3
800	0.64	7.2
1000	0.96	
1200	0.67	13.3

25°C carbon blank

Temp	ngC	$\delta^{13}C$	Error
500	13.7	-25.8	0.7
550	1.59	-27.1	0.6
575	1.03	-30.2	0.7
600	0.84	-25.5	0.7
625	0.74	-24.5	0.7
650	0.92	-26.8	0.8
675	0.79	-28.2	1.0
700	0.55	-25.2	1.0
725	0.528	nm	
750	0.475	-27.4	0.9
775	0.462	-27	1.1
800	0.396	-25.1	1.1
825	0.396	-24.9	1.1
850	0.475	-27.6	1.0
875	0.422	-25.8	1.0
900	0.343	-25.7	0.9
925	0.369	-25.7	1.0
950	0.396	-29.9	0.9
975	0.356	-25.7	1.0
1000	0.383	-27.8	0.9
1025	0.369	-29.3	0.8
1050	0.475	-29.7	1.0
1075	0.469	-27.2	0.7
1100	0.475	-26.5	0.8
1125	0.528	-28.6	0.7
1150	0.533	-29.1	0.8
1175	0.528	-28.9	0.7
1200	0.541	-29.3	0.8

50°C carbon blank

Temp	ngC	$\delta^{13}C$	Error
500	9.72	-43.7	0.7
550	1	-43.1	0.7
600	1.11	-44.2	0.5
650	1.56	-32.8	0.6
700	0.87	-40.4	0.5
750	0.74	-40.7	0.6
800	0.73	-40.4	0.6
850	0.73	-40.3	0.6
900	0.85	-41	0.6
950	0.73	-38.8	0.6
1000	0.58	-37.9	0.6
1050	0.63	-38.8	0.5
1100	0.53	-41.9	0.6
1150	0.55	-37.5	0.5
1200	0.79	-40.5	0.5
1250	0.71	-35.6	0.5

TERRESTRIAL DIAMOND DATA

CVD 151

Temp	Yield (ppm)	$\delta^{13}C$	Error
200	1	-26.4	5.2
300	4	-32.1	3.0
400	4	-27.5	1.2
450	2	-36.1	3.8
500	3	-35.4	2.0
550	31	-56.4	1.2
600	248	-65.3	1.1
650	66	-52.7	1.0
750	21	-54.2	1.2
1000	1	-45.8	3.9
1250	1	-45.2	5.7

CVD diamond like after perchloric

Temp	Yield (ppm)	$\delta^{13}C$	Error
200	1226	-26.9	1.3
250	651	-15.5	1.2
300	728	-14.6	1.0
350	757	-14.9	0.9
375	1172	-10.4	1.1
400	2190	-8.3	1.2
450	4711	-7.0	1.0
425	12982	-6.1	1.1
475	14834	-5.1	1.4
500	27421	-4.5	1.1
525	74442	-4.9	1.0
550	245621	-3.2	0.9
575	245254	-4.1	1.0
600	468	-8.3	1.3
625	192	-8.2	1.2
700	88	-8.1	1.1
800	76	-14.0	2.0
1000	45	-13.2	3.8
1250	45	-12.9	3.5

CVD110

Temp	Yield (ppm)	$\delta^{13}C$	Error
200	1	-47.3	7.6
250	1	-36.7	8.3
300	1	-15.3	3.6
350	1	-23.3	3.0
400	1	-22.3	3.6
450	1	-36.2	2.3
500	7	-65.6	1.1
550	315	-71.1	1.3
575	965	-71.8	2.6
600	1222	-70.1	1.4
625	3	-58.4	1.2
650	1	-55.4	2.8
700	0	-38.9	9.7
800	1	-35.7	5.3
900	1	-28.0	6.4
1000	0	-22.7	7.2
1250	0	-49.0	7.8

CVD diamond like

Temp	Yield (ppm)	$\delta^{13}C$	Error
200	206	-29.0	1.0
250	273	-28.5	1.1
300	83	-24.2	2.0
325	70	-19.1	1.4
350	51	-13.3	1.2
375	98	-9.0	1.1
400	183	-5.4	2.1
425	270	-10.1	1.2
450	590	-3.9	1.1
475	1044	-4.4	1.6
500	2062	-4.5	1.3
525	3224	-2.6	1.5
550	1860	-4.8	1.1
575	753	-7.0	1.2
600	14	-7.4	3.0
650	7	-39.1	6.4
700	11	-22.9	3.8
800	28	-58.1	7.3
900	42	-52.1	9.5
1000	53	-70.4	8.9
1250	244	-74.1	10.7

CVD 125

Temp	Yield (ppm)	$\delta^{13}C$	Error
200	1	-30.7	5.5
250	1	-30.9	4.1
300	2	-33.7	1.5
400	20	-31.2	1.8
450	23	-31.8	1.8
475	17	-53.1	1.2
500	82	-58.3	1.7
525	316	-57.2	1.8
550	838	-59.9	1.3
575	1142	-59.2	2.3
600	57	-51.2	1.4
625	3	-16	1.3
650	1	-19.1	2.9
675	1	-9.7	6.4
700	1	-40.3	7.5
750	1	-23.3	6.0
800	1	-22.7	5.0
850	1	-22.7	6.4
900	0	-34.8	5.8
950	1	-24.2	4.9
1000	1	-24.5	8.3
1100	0	-41.2	7.6
1200	1	-25	6.2

Carbonado JWF 4

Temp	N (ppm)	$\delta^{15}N$	Error	C(ppm)
300	0.90	7.9	1.4	29
400	7.04	10.9	2.6	205
500	4.07	7.8	3.2	319
550	11.55			261
600	7.48	7.6	2.5	1904
650	0.11			4990
700	0.88	9.3	2.4	39417
750	3.96	-13.5	3.4	226358
800	1.87	-26.7	3.5	378026
850	0.44	-5.2	4.8	582
900	0.00			153

Carbonado JWF5

Temp	N (ppm)	$\delta^{15}N$	Error	C(ppm)
600	34.82	16.1	2.1	3673.6
750	7.14			109926
800	18.43			286528
900	25.73			400230

Carbonado JWF 11 27.4ug

Temp	N (ppm)	$\delta^{15}N$	Error	C(ppm)
600	65.70	16.8	1.8	5606.4
1000	73.37	8.7	2.1	959694

Carbonado JWF 1 67ug

Temp	N (ppm)	$\delta^{15}N$	Error	C(ppm)
600	14.40	-4.0	2.9	2223
800	18.00	-1.7	2.4	149685
1000	105.45	4.7	0.9	425610

Crater diamond

Temp	N (ppm)	$\delta^{15}N$	Error	C (ppm)
500	176.75	-3.3	0.9	2056
650	11.56	1.5	2.3	10793
700	114.25	10.6	1.0	131284
725	222.45	12.2	1.4	250733
750	85.35	10.9	1.0	167151
775	46.84	29.9	1.5	82715
800	36.96			84946
825	61.83	17.7	1.2	76613
850	27.42	24.2	1.8	65034
900	13.44			25605

ABEE RESIDUE DATA

CARBON COMBUSTION

Temp	Yield (ppmOP)	$\delta^{13}C$	Error
300	0.15	nm	
400	0.51	-19.9	0.1
450	0.81	-14.1	0.1
475	1.15	-9.3	0.1
500	2.12	-3.8	0.1
525	6.15	-2.1	0.0
550	16.60	-1.7	0.1
575	25.40	-2.3	0.1
600	18.60	-1.6	0.0
650	21.80	-1.7	0.1
750	18.00	-1.8	0.0

High temperature carbon

Temp	Yield (ppmOP)	$\delta^{13}C$	Error
700	0.406	-33.800	0.4
725	0.164	-3.800	0.4
750	0.236	-2.000	0.4
775	0.246	-2.0	0.4
800	0.274	-1.4	0.4
825	0.307	-1.9	0.4
850	0.303	-2.5	0.4
875	0.218	-4.6	0.4
900	0.197	-3.8	0.4
925	0.108	-4.9	0.4
950	0.0348	-15.9	0.3
975	0.0144	-22.3	0.4
1000	0.0144	-22.3	0.4
1050	0.0093	-23.4	0.3
1100	0.0083	-24.1	0.3
1150	0.0072	-24.5	0.4
1200	0.0071	-24.9	0.4
1250	0.0095	-25.1	0.4

Colloidal fraction F4

Temp	Yield (ppmOP)	$\delta^{13}C$	Error
400	4.12	-25.7	0.1
500	10.8	-23	0
550	39.5	-8.5	0
575	35.1	-2.6	0
600	13.7	-1.7	0.1
625	1.8	-4.4	0.1
650	0.97		

NITROGEN COMBUSTION

Temp	N (ppb OP)	$\delta^{15}N$	Error	C (ppm OP)
200	1.460	-1.4	-1.4	0.04
300	1.66	10.8	1.8	0.18
400	1.450	-3.8	2.1	0.79
500	0.730	NM	0.0	2.59
600	2.370	-24.0	2.1	52.60
700	3.810	-24.1	1.6	31.90
800	6.310	-21.6	1.3	7.66
900	3.22	-20.9	1.9	0.82

Colloidal fraction F1

Temp	Yield (ppmOP)	$\delta^{13}C$	Error
400	2.5	nm	
450	2.3	nm	
500	2.8	-25.9	0.1
525	2.4	-16.0	0.1
550	7.6	-4.3	0.0
575	12.9	-3.5	0.1
600	13.2	-3.0	0.0
625	32.5	-2.3	0.0
650	18.1	-2.6	0.1
675	1.8	nm	
700	1.4	nm	

HF/HCl residue (A1)

Temp	Yield (ppmOP)	$\delta^{13}C$	Error
250	12	nm	
300	20.7	nm	
350	166	nm	
400	253	nm	
450	235	nm	
500	47.2	nm	
550	115	-15.1	0.0
600	581	-1.8	0.0
650	1828	-2.6	0.0
700	1357	-1.4	0.0
900	8.85	nm	
1200	3.2	nm	

CARBON DATA OVER DIAMOND BURNING REGIME

ORGUEIL

Temp	Yield (ppmOP)	$\delta^{13}C$	Error
300	1.4	-26.7	0.1
400	4.2	-29.6	0.0
450	33.3	-29.4	0.0
475	49.3	-32.1	0.0
500	159.0	-37.1	0.0
525	168.0	-38.5	0.0
550	8.6	-26.3	0.2

MURCHISON

Temp	Yield (ppmOP)	$\delta^{13}C$	Error
300	1.4	-26.7	0.1
400	4.2	-29.6	0.0
450	33.3	-29.4	0.0
475	49.3	-32.1	0.0
500	159.0	-37.1	0.0
525	168.0	-38.5	0.0
550	8.6	-26.3	0.2

ALH 83100, 78

Temp	Yield (ppmOP)	$\delta^{13}C$	Error
300	3.8	-23.8	0.1
400	16.4	-28.0	0.1
450	62.4	-29.1	0.1
475	135.0	-34.1	0.0
500	51.8	-38.8	0.0
525	1.3	30.4	0.1
550	0.6	142.2	0.4

COLD BOKKEVELD

Temp	Yield (ppmOP)	$\delta^{13}C$	Error
300	5.1	-22.5	0.1
400	16.1	-27.3	0.0
450	50.2	-29.1	0.0
475	106.0	-30.7	0.1
500	128.5	-37.8	0.0
525	12.0	-24.0	0.0
550	2.6	-16.9	0.1

ALLENDE

Temp	Yield (ppmOP)	$\delta^{13}C$	Error
300	4.220	-28.6	0.1
400	8.64	-31.5	0.0
450	23.780	-33.8	0.0
475	47.260	-35.5	0.0
500	39.060	-30.8	0.0
525	1.720	-1.0	0.1
550	0.690	nm	

VIGRANO

Temp	Yield (ppmOP)	$\delta^{13}C$	Error
300	1.600	-24.7	0.1
400	7.52	-26.6	0
450	24.300	-27.1	0.1
475	45.500	-30.2	0.1
500	46.100	-35.1	0.1
525	5.570	-12.6	0
550	0.200	nm	

MURCHISON M2A

Temp	Yield (ppmOP)	$\delta^{13}C$	Error
250	1.42	nm	0.3
300	1.12	-27.1	
350	2.44	nm	0.1
400	6.31	-21.5	0.0
450	23.80	-28.7	0.0
475	36.00	-30.9	0.1
500	57.90	-32.1	0.0
525	71.40	-34.1	0.0
550	69.60	-37.1	0.0
575	33.80	-38.2	0.0

KRYMKA KR6

Temp	Yield (ppm)	$\delta^{13}C$	Error
300	8228	-24.9	0.1
400	7748	-29.5	0.1
450	19820	-32.9	0.1
475	72673	-13.1	0.0
500	28048	14.7	0.0
525	10270	-25.7	0.1
550	5345	-27.7	0.0

INMAN

Temp	Yield (ppmOP)	$\delta^{13}C$	Error
300	0.7	-26.7	0
400	1.3	-29.8	0.1
450	2.9	-32.5	0.1
475	2.2	-31.9	0
500	0.4	-18.4	0.1
525	0.2	-5.4	0.2
550	0.1	NM	

ADRAR 003

Temp	Yield (ppmOP)	$\delta^{13}C$	Error
300	6.7	-26.7	0
400	13.1	-29.8	0.1
450	28.6	-32.5	0.1
475	22.3	-31.9	0
500	4.3	-18.4	0.1
525	2.0	-5.4	0.2
550	0.7	NM	

ADRAR 003

Temp	Yield (ppmOP)	$\delta^{13}C$	Error
400	3.2	-24.5	0.1
450	8.4	-27.3	0.1
475	16.7	-30.9	0
500	24.4	-37.3	0
525	2.4	-22.4	0.1
550	0.3	nm	

KRYMKA KR4

Temp	Yield (ppmOP)	$\delta^{13}C$	Error
300	1.87	-29.2	0
400	1.62	-27.2	0
450	3.63	-28.8	0
475	5.35	-29.3	0
500	11.20	-30.2	0
525	16.40	-33.0	0
550	18.60	-37.2	0
575	9.37	-35.7	0
600	0.24	nm	

INDARCH

Temp	Yield (ppm OP	$\delta^{13}C$	Error
200	0.650	-25.4	0.4
250	0.491	-24.5	0.4
300	0.470	-24.9	0.4
350	0.728	-25.4	0.4
400	0.920	-26.3	0.4
425	1.129	-27.4	0.4
450	2.570	-32.7	0.4
475	4.662	-34.5	0.4
485	7.812	-37	0.5
495	5.292	-34.4	0.4
505	1.956	-4.4	0.4
515	0.610	32.4	0.4
525	0.413	34.2	0.4
550	0.461	24.2	0.4
575	0.332	23.5	0.5
600	0.150	23.3	0.4
650	0.143	46.6	0.5
700	0.193	82.5	0.4
800	0.273	89.2	0.3
900	0.178	44.6	0.4
1000	0.065	51.1	0.4
1100	0.040	29.1	0.4
1200	0.035	59.6	0.4

CARBON DATA OVER THE HIGH TEMPERARURE REGIME

ORGUEIL OP1D

Temp	Yield (ppmOP)	$\delta^{13}C$	Error
550	1.200	-14.7	0.5
575	0.694	-4.4	0.5
600	1.470	-2.7	0.5
625	1.710	8.9	0.4
650	1.160	60.3	0.4
675	0.584	139.8	0.5
700	0.629	192.7	0.4
725	0.898	206.7	0.4
750	0.819	258.2	0.3
775	1.020	328.1	0.3
800	1.070	343.3	0.4
825	0.824	329.2	0.4
850	0.942	276.6	0.3
875	1.120	316.3	0.4
900	0.681	469.3	0.4
925	0.603	583.7	0.4
950	0.672	683.3	0.4
975	0.685	787.2	0.4
1000	0.646	870.8	0.4
1025	0.672	963.1	0.4
1050	0.561	1073.8	0.3
1075	0.354	1259.8	0.4
1100	0.075	1344.8	0.4
1125	0.015	992.6	0.4
1150	0.009	518.3	0.8
1175	0.007	403.0	1.0
1250	0.010	nm	nm

ALH 83100,78 3

Temp	Yield (ppmOP)	$\delta^{13}C$	Error
450	0.603	-18.6	0.7
550	0.318	28.8	0.4
600	0.124	108.8	0.4
625	0.039	403.0	0.4
650	0.072	667.6	0.4
675	0.052	791.4	0.4
700	0.075	837.2	0.6
725	0.060	905.5	0.3
750	0.056	972.8	0.3
775	0.064	1063.7	0.3
800	0.054	1087.6	0.4
825	0.064	1134.1	0.4
850	0.058	1183.8	0.3
875	0.088	1238.8	0.3
900	0.192	1323.0	0.0
925	0.451	1371.7	0.4
950	0.524	1402.9	0.4
975	0.256	1396.1	0.4
1000	0.071	1330.8	0.3
1025	0.043	1250.8	0.3
1050	0.036	1149.3	0.4
1075	0.036	1208.7	0.4
1100	0.031	1140.7	0.4
1125	0.060	1187.9	0.4
1150	0.058	1274.4	0.4
1175	0.068	1200.3	0.4
1200	0.070	1100.9	0.4
1250	0.057	1001.4	0.3

MURCHISON M2

Temp	Yield (ppmOP)	$\delta^{13}C$	Error
500	0.287	-24.5	0.4
550	0.0426	113.3	1.1
575	0.036	323.7	0.9
600	0.037	430.4	1
625	0.031	423.9	0.9
650	0.038	477.9	0.8
675	0.055	514.5	0.4
700	0.070	599.4	0.4
725	0.076	707.0	0.4
750	0.079	884.1	0.3
775	0.068	873.4	0.3
800	0.054	810.8	0.4
825	0.071	870.9	0.3
850	0.082	946.7	0.3
875	0.079	992.4	0.3
900	0.099	1056.8	0.3
925	0.076	1137.1	0.4
950	0.153	1207.1	0.3
975	0.136	1260.0	0.4
1000	0.283	1303.9	0.4
1025	0.357	1389.6	0.3
1050	0.288	1425.0	0.3
1075	0.219	1429.4	0.3
1100	0.153	1418.4	0.4
1125	0.168	1405.3	0.4
1150	0.142	1417.8	0.4
1175	0.134	1412.8	0.3
1200	0.145	1427.0	0.4
1250	0.165	1421.2	0.4

MURCHISON MIL

Temp	Yield (ppm)	$\delta^{13}C$	Error
500	196.0	-25.6	0.5
550	8.0	68.0	0.6
600	8.9	306.5	0.6
650	27.7	629.5	0.5
675	35.8	701.6	0.4
700	40.1	674.9	0.5
725	41.8	547.5	0.5
750	57.7	273.4	0.5
775	70.0	104.1	0.5
800	68.8	64.0	0.5
825	82.4	38.5	0.5
850	77.0	23.6	0.5
875	45.0	26.3	0.5
900	8.1	23.5	0.8
950	3.0	43.6	1.1
1000	2.6	19.5	1.1
1100	3.5	-10.4	1.0
1250	4.4	-18.8	1.1

MURCHISON M2A

Temp	Yield (ppmOP)	$\delta^{13}C$	Error
500	1.570	-30.1	0.7
600	10.300	-24.7	0.3
625	3.890	4.7	0.8
650	2.260	60.4	0.7
675	1.410	182.6	0.7
700	1.090	377.3	0.6
725	0.548	517.9	0.6
750	0.263	1169.1	0.6
775	0.328	1352.4	0.5
800	0.358	1388.7	0.6
825	0.433	1122.4	0.5
850	0.219	1344.7	0.5
875	0.116	1324.4	0.4
900	0.076	1280.9	0.5
925	0.067	1279.3	0.5
950	0.058	1286.9	0.5
975	0.054	1283.2	0.5
1000	0.039	1243.7	0.5
1025	0.030	1122.1	0.6
1050	0.026	995.3	0.5
1075	0.019	937.5	0.5
1100	0.019	927.3	0.5
1150	0.026	925.7	0.5
1200	0.016	902.0	0.6
1250	0.013	759.5	0.6

MURCHISON M2B

Temp	Yield (ppmOP)	$\delta^{13}C$	Error
500	13.6	12.9	0.3
550	8.45	137.0	0.3
575	1.63	335.3	0.3
600	1.52	490.0	0.2
625	0.211	572.3	0.5
650	0.058	321.3	0.6
675	0.0666	303.4	0.6
700	0.0538	621.5	0.5
750	0.0776	981.1	0.5
800	0.0496	706.6	0.6
850	0.0212	135.3	0.5
900	0.0248	24.0	0.5
1000	0.033	6.0	0.6
1100	0.0522	-14.8	0.5
1200	0.0464	-26.5	0.6
1250	0.0476	-25.2	0.6

ALLENDE ARCIV

Temperature	Yield (ppmOP)	d13C	Error
500	0.135	-10.2	0.5
550	0.052	50.4	0.4
575	0.028	108.6	0.5
600	0.027	138.3	0.5
625	0.017	165.4	0.5
650	0.010	269.4	0.4
675	0.004	572.5	0.4
700	0.003	727.5	0.4
725	0.004	768.2	0.4
750	0.003	896.0	0.4
775	0.003	981.5	0.5
800	0.003	989.4	0.4
825	0.005	1036.1	0.4
850	0.006	1048.2	0.4
875	0.007	1073.2	0.4
900	0.008	1188.7	0.4
925	0.010	1187.6	0.4
950	0.010	1211.5	0.5
975	0.013	1232.6	0.4
1000	0.015	1252.4	0.4
1025	0.021	1275.6	0.4
1050	0.025	1300.7	0.4
1075	0.048	1351.3	0.4
1100	0.034	1375.9	0.4
1125	0.016	1363.4	0.4
1150	0.013	1350.4	0.4
1175	0.016	1375.2	0.4
1200	0.030	1406.6	0.4
1250	0.0855	1431.1	0.4
1285	0.0695	1416.2	0.4

VIGARANO V2

Temperature	Yield (ppmOP)	d13C	Error
500	1.040	nm	nm
550	0.087	-12.0	0.5
600	0.060	-6.9	0.5
650	0.042	-3.1	0.5
700	0.024	13.0	0.6
800	0.010	64.8	0.6
900	0.025	73.7	0.6
1000	0.024	322.2	0.6
1100	0.051	590.5	0.4
1200	0.050	540.0	0.5
1250	0.031	204.1	0.5

Efremovka DE-5

Temperature	Yield (ppmOP)	d13C	Error
300	1.270	-21.7	0.1
400	1.747	-24.8	0.0
450	3.454	-24.7	0.0
475	5.907	-28.5	0.0
500	13.054	-29.4	0.0
525	20.839	-29.4	0.0
550	25.478	-28.8	0.0
575	19.194	-25.9	0.0
600	36.367	-20.2	0.3
605	0.539	-8.3	0.8
625	0.863	-10.1	0.4
650	1.233	-10.2	0.8
675	1.808	-8.7	0.8
700	2.286	-8.7	0.8
725	2.142	-6.7	0.7
750	1.621	-5.8	0.8
775	1.079	-5.4	0.8
800	1.114	-3.4	0.8
825	0.747	2.1	0.8
850	0.333	11.3	0.8
875	0.058	-1.8	0.3
900	0.007	27.7	0.8
925	0.003	124.9	0.8
950	0.002	176.6	0.7
1000	0.002	229.4	0.7
1050	0.002	296.7	0.7
1100	0.003	491.7	0.8
1150	0.006	710.7	0.6
1200	0.007	362.5	0.7
1250	0.003	83.4	0.8

COLD BOKKEVELD CB3B

Temp	Yield (ppmOP)	$\delta^{13}C$	Error
500	0.52	-18.5	0.3
550	0.03	201.2	0.7
575	0.03	312.5	0.6
600	0.04	352.4	0.7
625	0.04	410.4	0.7
650	0.05	465.4	0.7
675	0.06	621.6	0.6
700	0.09	980.8	0.6
725	0.15	1176	0.5
750	0.14	1161.3	0.4
775	0.09	1080.8	0.5
800	0.07	1011.5	0.6
825	0.06	985	0.6
850	0.07	969.9	0.6
875	0.06	989.4	0.6
900	0.06	1010.7	0.6
925	0.07	1037.8	0.6
950	0.09	1109.6	0.5
975	0.11	1218.7	0.5
1000	0.19	1313.7	0.5
1025	0.23	1370.8	0.5
1050	0.23	1394.6	0.5
1075	0.18	1398.6	0.5
1100	0.13	1374.8	0.5
1125	0.10	1324.4	0.5
1150	0.09	1296.8	0.6
1175	0.10	1285.2	0.5
1200	0.10	1222.7	0.6
1250	0.10	959.6	0.6

COLD BOKKEVELD REPLICATE

Temp	Yield (ppmOP	$\delta^{13}C$	Error
450	0.60	-18.6	0.7
490	0.36	-8.3	0.7
550	0.48	38.6	0.7
575	0.16	111.2	0.7
600	4.89	260.2	0.7
625	0.09	413.3	0.6
650	0.08	706.9	0.6
675	0.12	952.2	0.5
700	0.13	998.4	0.5
725	0.08	948.8	0.6
750	0.07	890.4	0.6
775	0.06	887.7	0.5
800	0.06	908.7	0.5
825	0.06	949.3	0.5
850	0.07	985.9	0.6
875	0.07	1044.5	0.5
900	0.08	1107.6	0.6
925	0.09	1173.2	0.6
950	0.11	1235.2	0.5
975	0.12	1285.2	0.4
1000	0.13	1323.0	0.5
1025	0.16	1353.4	0.5
1050	0.20	1389.2	0.5
1075	0.20	1405.6	0.5
1100	0.15	1393.6	0.5
1125	0.11	1347.5	0.5
1150	0.11	1325.3	0.5
1175	0.10	1296.3	0.4
1200	0.12	1308.5	0.5
1250	0.16	1205.0	0.5

INDARCH 13

Temp	Yield (ppmOP)	$\delta^{13}C$	Error
500	0.046	-21.8	0.5
550	0.008	45.0	0.5
600	0.012	91.5	0.4
650	0.033	129.5	0.5
675	0.029	273.2	0.5
700	0.018	527.4	0.4
725	0.017	760.8	0.4
750	0.016	876.4	0.5
775	0.016	1074.5	0.4
800	0.015	1151.5	0.4
825	0.013	1160.9	0.4
850	0.013	1161.0	0.4
875	0.009	1136.4	0.4
900	0.011	1179.5	0.4
925	0.012	1187.5	0.4
950	0.010	1199.5	0.4
975	0.011	1206.7	0.4
1000	0.012	1215.6	0.4
1025	0.013	1226.5	0.4
1050	0.013	1241.5	0.4
1075	0.015	1253.5	0.4
1100	0.016	1263.1	0.4
1125	0.018	1271.3	0.4
1150	0.021	1288.8	0.4
1175	0.027	1318.7	0.4
1200	0.029	1330.9	0.4
1225	0.030	1368.1	0.4
1250	0.037	1390.7	0.4
1270	0.029	1395.5	0.4
1300	0.039	1419.5	0.4
1320	0.024	1432.8	0.4
1350	0.023	1420.0	1.0

Terrestrial SiC+spinel

Temp	Yield (ppmOP)	$\delta^{13}C$	Error
500	128	-25.8	0.7
550	29.7	-23.9	0.6
600	27.9	-24.3	0.6
650	11.7	nm	
700	16.5	-28.1	0.7
750	17.5	-28.0	0.6
800	13.8	-27.8	0.7
850	14.6	-29.9	0.7
900	17.6	-29.5	0.6
950	24.6	-28.7	0.6
1000	38.9	-29.0	0.6
1050	62.1	-29.3	0.7
1100	120	-30.4	0.7
1150	202	-30.7	0.7
1175	125	-30.7	0.6
1200	117	-31.0	0.7
1225	135	-30.8	0.7
1250	165	-31.1	0.7
1275	164	nm	
1300	97.5	-33.4	0.5

TIESCHITZ TR2

Temp	Yield (ppmOP)	$\delta^{13}C$	Error
550	0.198	-26.1	0.3
575	0.011	-16.2	0.7
600	0.007	-8.7	0.7
625	0.007	12.6	0.8
650	0.007	33.3	0.8
675	0.008	48.1	0.8
700	0.010	50.1	0.8
725	0.011	50.8	0.8
750	0.008	63.1	0.7
775	0.006	67.1	0.7
800	0.006	58.2	0.7
850	0.006	91.7	0.7
900	0.007	154.3	0.7
950	0.006	250.8	0.6
1000	0.006	252.7	0.6
1050	0.006	319.7	0.8
1100	0.007	292.5	0.7
1150	0.005	157.2	0.7
1200	0.005	81.9	0.7
1250	0.005	6.4	0.8

ADRAR 003 A2

Temp	Yield (ppmOP)	$\delta^{13}C$	Error
500	0.135	-10.2	0.5
550	0.052	50.4	0.4
575	0.028	108.6	0.5
600	0.027	138.3	0.5
625	0.017	165.4	0.5
650	0.010	269.4	0.4
675	0.004	572.5	0.4
700	0.003	727.5	0.4
725	0.004	768.2	0.4
750	0.003	896.0	0.4
775	0.003	981.5	0.5
800	0.003	989.4	0.4
825	0.005	1036.1	0.4
850	0.006	1048.2	0.4
875	0.007	1073.2	0.4
900	0.008	1188.7	0.4
925	0.010	1187.6	0.4
950	0.010	1211.5	0.5
975	0.013	1232.6	0.4
1000	0.015	1252.4	0.4
1025	0.021	1275.6	0.4
1050	0.025	1300.7	0.4
1075	0.048	1351.3	0.4
1100	0.034	1375.9	0.4
1125	0.016	1363.4	0.4
1150	0.013	1350.4	0.4
1175	0.016	1375.2	0.4
1200	0.030	1406.6	0.4
1250	0.0855	1431.1	0.4
1285	0.0695	1416.2	0.4

INMAN IN3

Temp	Yield (ppmOP	$\delta^{13}C$	Error
500	0.078	-22.0	0.5
575	0.023	33.7	0.4
600	0.040	-2.9	0.4
625	0.009	62.9	0.5
650	0.008	67.6	0.4
675	0.013	64.4	0.4
700	0.017	59.8	0.3
725	0.016	73.7	0.4
750	0.011	112.7	0.4
775	0.007	195.0	0.4
800	0.005	348.9	0.3
825	0.003	288.6	0.4
850	0.003	288.6	0.4
875	0.003	231.7	0.3
900	0.003	173.9	0.3
925	0.003	171.8	0.4
950	0.003	199.7	0.4
975	0.003	229.5	0.3
1000	0.004	272.3	0.3
1025	0.002	833.2	0.4
1050	0.002	993.7	0.4
1075	0.001	945.7	0.4
1100	0.001	825.1	0.7
1150	0.001	643.0	0.7
1200	0.001	351.5	0.5
1250	0.001	207.8	0.8

NITROGEN STEPPED COMBUSTION DATA

Orgueil 1

Temp	N (ppmOP)	$\delta^{15}N$	Error	C (ppm OP)
200	0.01	-10.0	5.0	0.2
300	0.01	-71.1	1.4	1.23
350	0.04	-46.4	0.8	2.28
400	0.03	-80.9	0.5	5.19
450	0.04	-231.5	0.6	17.3
460	0.09	-245.6	0.5	20.5
470	0.19	-303.1	0.9	27.7
480	0.26	-315.8	0.9	26.2
490	0.28	-327.3	0.8	39.1
500	0.30	-332.5	0.8	44.4
530	0.69	-322.2	0.8	79.5
560	0.47	nm		43.5
600	0.19	-277.8	0.6	17.5
650	0.03	nm		3.4

Cold Bokkeveld CB3B

Temp	N (ppmOP)	$\delta^{15}N$	Error	C (ppm OP)
200	0.034	11.5	0.8	0.16
300	0.043	-27.1	0.5	1.64
350	0.028	-64.6	1.0	1.92
400	0.039	-132.0	0.9	6.37
430	0.048	-186.6	0.7	10.28
450	0.073	-240.3	0.9	17.52
470	0.204	-288.1	0.6	35.07
480	0.294	-282.2	3.8	37.98
490	0.458	-325.4	0.9	49.31
500	0.959	-334.9	1.0	72.59
510	0.992	-346.9	1.0	72.59
520	0.531	-335.7	1.0	37.98
530	0.039	-289.6	1.2	8.32
550	0.006	-13.4	3.9	1.22
600	0.006	-9.4	1.7	0.25
700	0.041	-9.8	1.0	0.03
800	0.008	-156.1	7.4	0.19
900	0.007	-111.6	5.0	0.15
1000	0.017	-91.4	1.8	0.26
1100	0.023	-407.1	2.6	0.75
1200	0.040	-187.6	1.4	0.54
1250	0.073	-76.6	0.9	0.40

Orgueil 2

Temp	N (ppmOP)	$\delta^{15}N$	Error	C (ppm OP)
200	0.360	-1.3	0.6	0.4
300	0.021	-101.5	1.0	1.7
350	0.014	nm		2.4
400	0.018	-196.8	1.6	6.7
430	0.022	-216.0	1.4	8.7
450	0.023	-218.6	1.5	9.3
470	0.046	-279.4	1.0	17.0
480	0.092	-304.0	1.0	25.2
490	0.236	-324.9	1.0	35.4
500	nm			59.9
510	0.632	-340.5	1.1	64.8
520	0.737	-343.8	1.2	65.3
535	0.745	-341.3	1.2	78.1
600	0.086	-324.6	1.4	20.1
650	0.005	-4.7	3.2	0.2
700	nm			0.8
800	0.007	-292.9	1.9	2.3
900	0.010	-381.4	2.3	2.2
1000	0.016	-535.6	3.2	1.6
1100	0.035	-576.5	3.0	0.3
1200	0.048	-424.9	2.0	

Cold Bokkeveld CBJA

Temp	N (ppm)	$\delta^{15}N$	Error	C (ppm OP)
200	0.66	nm		278
250	4.32	-48.3	1.5	1951
300	4.14	-53.9	1.0	2527
350	6.23	-80.2	1.2	5169
400	10.64	-81.0	0.6	11217
430	14.84	-122.3	1.3	18389
450	19.23	-208.6	1.0	29178
460	16.15	-246.7	0.9	37514
470	26.50	-277.4	1.0	52920
480	32.26	-302.2	0.7	64771
490	40.91	-318.0	0.6	62319
500	58.28	-330.7	0.7	115239
510	64.59	-342.5	0.6	125046
520	45.87	-344.2	0.6	76213
530	91.20	-348.1	0.7	2493
540	2.37	-206.3	2.3	306
550	1.21	-130.5	3.8	286
600	nm	nm		286
800	1.52	-187.3	4.6	1179
1200	2.89	-497.4	3.8	1485

ALH 83100, 78 3

Temp	N (ppm)	$\delta^{15}N$	Error	C (ppm OP)
200	0.0052	-4.8	2.4	0.087
300	0.0198	-61.6	1.8	1.73
350	0.0159	-85.4	1.8	2.56
400	0.0269	-136.6	1.9	6.51
430	0.074	-195.0	1.2	15.21
450	0.176	-263.8	1.6	23.74
460	0.35	-281.0	0.8	37.89
470	0.55	-324.3	1.9	48.72
480	0.56	-323.7	2.3	46.05
490	0.43	-343.7	2.2	37.3
500	0.062	-320.5	2.0	11.1
530	0.0075	nm		2.77

Murchison M2

Temp	N (ppm)	$\delta^{15}N$	Error	C (ppm OP)
200	0.10	-18.0	7.7	0.59
250	0.10	-11.5	5.0	0.63
300	0.13	nm		1.38
350	0.07	-78.0	2.8	3.36
400	0.09	-112.5	1.9	9.27
430	0.06	-165.5	2.0	15.14
450	0.08	-222.2		37.91
460	0.17	-275.5	1.1	38.11
470	0.18	-299.1	1.3	39.44
480	0.35	-318.5	0.6	62.46
490	0.88	-334.0	1.2	91.60
500	0.55	-342.5	0.1	83.86
510	0.22	-328.9	0.8	40.03
525	0.22	-224.0	2.5	12.72
550	0.12	-269.1	0.9	4.93
600	0.02	-143.8	9.0	0.74
700	0.02	-37.1	8.1	0.45
800	0.02	-35.7	10.5	0.49
1000	0.02	-31.5	9.6	nm
1200	0.06	-365.7	2.1	nm

ALH 83100, 78 3

Temp	N (ppm)	δ^{15}	Error	C (ppm OP)
200	0.01	-31.8	3.5	0.1
250	0.01	-106.6	0.6	0.5
300	0.00	-157.3	2.2	1.3
350	0.01	-185.7	0.6	2.4
400	0.03	-205.4	0.7	6.3
430	0.03	-248.3	0.5	8.9
450	0.06	-289.3	0.8	15.9
460	0.12	-313.4	0.7	21.3
470	0.14	-323.4	0.5	23.5
480	0.32	-336.7	0.7	32.8
490	0.48	-338.0	1.0	52.6
500	0.42	-352.3	0.8	38.7
510	0.32	-358.5	0.7	28.4
520	0.18	-354.5	0.7	11.6
530	0.10	-363.1	0.7	3.0
540	0.21	-343.7	0.7	1.3
550	0.08	-317.7	0.7	0.6
570	0.01	-283.0	2.0	0.1
600	0.00	-214.8	2.0	0.1
750	0.01	-119.7	1.5	0.1
900	0.00	-261.8	2.6	0.2
1000	0.02	-544.2	2.8	0.5
1100	0.03	-594.6	2.7	1.0
1175	0.01	-363.1	2.0	0.4
1250	0.01	-197.2	1.6	0.2

Murchison M2B (NaOH)

Temp	N (ppm)	$\delta^{15}N$	Error	C (ppm OP)
300	0.13	-11.5	1.4	12.5
350	0.36	-289.9	1.0	88.5
400	1.01	-328.9	1.4	103.5
430	2.11	-338.7	1.6	262.0
450	0.07	-235.6	1.8	28.7
460	0.03	-119.5	2.9	10.3

Efremovka DE2

Temp	N (ppm)	$\delta^{15}N$	Error	C (ppm)
200	46	nm		7144
300	221	-3.3	3.0	17686
350	56	-10.8	1.8	10057
400	74	-17.0	2.1	14252
430	100	-51.4	1.9	28264
450	152	-97.1	1.8	44390
460	323	-173.5	2.3	81500
470	475	-234.4	2.3	106812
480	908	-276.4	1.5	123110
495	1270	-305.0	3.0	154321
510	80	-239.6	2.7	12867
520	24	-45.8	2.5	4856
550	19	-30.1	3.5	3399

Efremovka EF5

Temp	N (ppm)	$\delta^{15}N$	Error	C (ppm)
200	12.7	13.4	1.0	449
300	77.1	41.0	1.8	7890
350	322	11.6	0.7	14909
400	238	nm		13986
430	210	0.8	1.4	13668
450	206	-9.0	1.6	21532
460	168	-16.7	1.6	20054
470	215	-31.1	1.6	27073
480	290	-57.3	2.0	43012
490	352	-75.4	2.1	50981
500	476	-96.8	2.1	69927
525	752	-138.9	2.4	109244
550	842	-109.4	2.0	143812
575	94.4	54.7	5.0	41956

Efremovka DE5

Temp	N (ppm)	$\delta^{15}N$	Error	C (ppm OP)
300	169	11.2	0.5	6851
350	65	-1.8	0.5	6406
400	33	nm		8691
430	33	-11.6	1.5	8841
450	56	-31.5	1.4	14616
460	69	-44.5	1.7	16537
470	84	-72.7	1	19533
480	136	-100.8	0.9	32420
490	154	-122.9	0.9	33373
500	307	-150.8	1.1	47267
515	470	-171.5	1.2	60888
530	503	-179.9	1.3	60752
545	575	-181.1	1.7	77915
560	442	-165.8	1.4	69879
575	327	-132.8	1.3	50400
600	197	-73.2	0.8	55032
700	119	-11.5	1	80368
800	21	nm		8759
900	13	nm		316
1040	17	nm		24.1
1250	17	nm		21.8

Efremovka DE2 High T

Temp	N (ppm)	$\delta^{15}N$	Error	C (ppm OP)
500	3.56	14.2	2.5	193
550	1.21	-43.4	4.0	90.4
600	2.55	-60.5	3.7	1137
700	12.90	-234.4	1.8	5470
750	24.90	-260.4	2.2	6190
800	14.40	-280.0	3.3	3339
850	14.70	nm		3958
900	17.80	-304.4	4.0	2867
950	20.50	-271.6	2.2	1243
1000	6.98	-228.2	4.9	284
1100	0.87	-1.6	5.5	22.3
1200	1.31	16.4	4.9	20.3
1300	2.32	-7.2	6.5	25.9

Allende ARC4DS

Temp	N (ppmOP)	$\delta^{15}N$	Error	C (ppm OP)
200	0.058	-41.3	0.4	0.3
250	0.033	-22.7	0.8	0.2
300	0.007	-18.0	2.2	0.1
350	0.024	-11.1	0.7	0.7
400	0.005	-40.3	3.8	1.8
430	0.006	-70.7	4.1	2.5
450	0.007	-118.9	2.1	3.8
460	0.021	-89.2	1.2	4.7
470	0.009	-156.7	1.7	6.2
480	0.002	nm		8.9
490	0.021	-264.4	2.2	13.2
500	0.039	-290.9	1.0	15.9
510	0.051	-287.7	1.0	14.5
520	0.058	-337.4	0.9	19.4
530	0.232	-352.1	0.7	6.3
545	0.012	-33.1	1.0	0.5
560	0.003	-8.4	6.0	0.0

Allende ARC4DS

Temp	N (ppmOP)	$\delta^{15}N$	Error	C (ppm OP)
200	0.018	-26.4	1.1	0.1
300	0.020	-2.7	1.8	0.6
350	0.008	-11.4	3.0	1.4
400	0.007	nm		2.0
430	0.005	-49.5	2.6	3.5
450	0.026	-35.9	1.2	5.6
460	0.003	nm		6.0
470	0.012	198.1	2.2	7.8
480	0.026	-181.1	1.1	11.5
490	0.025	-296.7	1.7	13.9
500	0.060	-321.2	0.8	19.2
510	0.080	-341.1	0.8	11.6
520	0.049	-260.1	1.1	3.4
530	0.027	nm		0.3
540	0.014	25.4	1.9	0.2
550	0.014	14.7	1.5	0.1
560	0.011	16.9	1.7	0.1
580	0.003	1.6	5.2	

Allende ARC4DS

Temp	N (ppm OP)	$\delta^{15}N$	Error	C (ppm OP)
200	0.006	-1.6	1.6	0.1
250	0.009	-22.6	1.1	0.1
300	0.008	-29.8	1.5	0.4
350	0.011	-31.1	1.2	0.8
400	0.011	-39.1	1.1	2.1
430	0.016	-43.2	0.8	3.1
450	0.009	-153.4	1.2	4.3
460	0.005	-139.0	2.6	4.3
470	0.008	-145.6	2.6	6.2
480	0.012	-207.7	2.1	9.0
490	0.019	-269.8	0.6	9.9
500	0.037	-297.8	0.8	14.5
510	0.059	-297.6	0.7	16.0
520	0.081	-319.7	0.7	19.4
530	0.052	-325.4	0.6	15.3
540	0.029	-204.2	0.5	1.8
550	0.016	-312.2	1.0	0.5
560	0.053	-339.0	0.7	0.3
575	0.065	-318.9	0.4	0.2
590	0.017	-253.5	1.2	0.1

Allende ARC4DS

Temp	N (ppmOP)	$\delta^{15}N$	Error	C (ppm OP)
200	0.012	nm		0.1
300	0.016	-18.7	1.1	0.6
350	0.008	nm		0.7
400	0.007	nm		3.1
430	0.009	nm		5.1
450	0.013	-176.4	2.3	8.1
460	0.015	-230.5	2.4	8.4
470	0.026	-271.5	2.8	11.7
480	0.023	-311.0	0.8	16.0
490	0.060	-331.8	0.7	15.9
500	0.064	-342.0	0.8	17.3
510	0.060	-345.6	0.8	14.8
520	0.017	-274.9	1.4	4.7
530	0.005	-53.3	3.2	0.6
580	0.003	nm		

Allende ARC4DS

Temp	N (ppm)	$\delta^{15}N$	Error	C (ppm OP)
200	0.017	-30.0	1.3	0.22
250	0.008	-11.4	2.1	0.14
300	0.020	-21.3	1.1	0.54
350	0.009	-6.3	2.3	1.22
400	0.015	-7.2	2.1	2.97
430	0.016	-14.3	1.5	5.85
450	0.018	-95.1	2.0	7.64
460	0.029	-151.3	1.4	10.16
470	0.038	-210.1	0.5	13.70
480	0.052	-268.7	0.7	16.06
490	0.124	-303.7	0.9	23.87
500	0.189	-318.9	0.6	21.85
510	0.044	-303.9	1.1	2.64
540	0.138	-320.6	1.0	7.90
570	0.005	-117.5	4.6	0.39
600	0.003	nm		0.23
800	0.004	-24.1	4.3	0.06
1200	0.005	-22.4	3.8	0.08

Allende ARC4DS cryotrap experiment

Temp	N (ppm)	$\delta^{15}N$	Error
200	0.013	-4.3	1.4
250	0.012	-7.3	2.0
300	0.011	-2.1	1.5
350	0.008	-0.2	4.0
400	0.018	-13.0	0.3
430	0.006	-37.2	3.9
450	0.010	-83.8	2.2
460	0.009	-134.5	2.4
470	0.014	-180.3	2.0
480	0.019	-222.1	1.5
490	0.027	-241.5	1.2
500	0.046	-289.8	0.9
510	0.089	-191.7	0.4
520	0.063	-204.3	0.4
530	0.023	-152.7	1.2
560	0.003	nm	
600	0.003	nm	
cryotrap to -140°C			
	0.027	nm	
cryotrap to=+25°C			
	0.426	-330	

Tieschitz

Temp	N (ppmOP)	$\delta^{15}N$	Error	C (ppmOP)
200	0.003	-2.0	3.8	0.13
250	0.005	-2.0	1.8	0.07
300	0.012	-1.1	0.7	0.19
350	0.009	-5.2	1.0	0.27
400	0.005	-16.2	1.5	0.37
430	0.005	-45.4	2.5	0.68
450	0.003	-93.6	2.9	1.17
460	0.004	-159.7	1.2	1.50
470	0.006	-191.8	2.3	1.46
480	0.008	-169.8	1.8	0.92
490	0.010	-107.2	1.0	0.48
500	0.018	-168.4	0.7	0.25
510	0.006	-45.2	1.0	0.15
520	0.002	-35.2	3.8	0.11
550	0.003	-4.7	5.1	0.06
600	0.001	nm		0.05
800	0.002	214.5	3.3	0.05
1000	0.002	nm		0.01
1100	0.004	65.9	2.1	0.02
1250	0.002	1.5	6.3	0.03

Krymka KR4

Temp	N (ppm)	$\delta^{15}N$	Error	C (ppm OP)
200	9.31	-0.1	2.5	128
250	9.46	18.3	4.0	391
300	15.2	-31.6	2.8	1265
350	16.7	-56.2	2.4	2733
400	25.8	-114.6	2.1	10518
430	30.2	-191.5	2.2	17669
450	60.1	-264.9	2.5	30333
460	128	-298.4	2.0	40366
470	440	-328.8	2.6	79349
480	725	-337.2	2.7	81539
490	1201	-346.6	3.2	133323
500	1092	-347.4	2.8	96532
510	71.2	-293.9	3.5	8917
550	24.1	-226.1	6.4	2318

Adrar 003 A3

Temp	N (ppmOP)	$\delta^{15}N$	Error	C (ppm OP)
300	0.01	-13.3	1.0	1.01
350	0.00	-4.3	1.2	0.71
400	0.02	-19.2	1.8	0.40
430	0.02	-58.5	1.7	0.35
450	0.02	-135.2	2.2	3.57
475	0.06	-220.9	2.6	8.33
500	0.12	-264.5	3.3	13.20
510	0.13	-297.9	2.6	11.70
520	0.24	-308.3	3.0	15.30
530	0.24	-308.3	3.0	13.70
550	0.13	-293.6	3.3	5.61
560	0.01	nm		0.14

Inman

Temp	N (ppmOP)	$\delta^{15}N$	Error	C (ppmOP)
225	0.001	15.2	1.7	0.04
250	0.001	17.2	1.9	0.05
300	0.001	-10.2	2.6	0.10
350	0.001	-24.6	6.0	0.16
400	0.002	-42.3	2.3	0.33
430	0.001	-136.1	3.6	0.55
450	0.003	-201.4	1.5	1.24
460	0.003	-278.9	2.6	1.46
470	0.011	-292.1	0.7	2.43
480	0.010	-325.2	0.7	1.61
490	0.004	-309.5	1.2	0.43
500	0.004	nm		0.18
510	0.006	-293.8	0.9	0.10
520	0.001	-153.4	3.3	0.07
530	0.000	-110.4	8.4	0.04
540	0.000	-116.0	2.4	0.02
550	0.000	nm		0.02

Inman

Temp	N (ppmOP)	$\delta^{15}N$	Error	C (ppmOP)
200	0.004	6.6	4.7	0.07
250	0.003	0.3	3.3	0.10
300	0.004	-3.3	3.5	0.16
350	0.003	-14.3	3.9	0.22
400	0.007	-6.9	2.0	0.46
430	0.004	-130.2	2.6	1.11
450	0.005	-209.1	2.0	2.12
460	0.009	-268.9	1.5	2.93
470	0.003	-308.0	3.6	3.29
480	0.005	-244.0	3.0	0.61
490	0.012	-13.1	0.9	0.19
500	0.003	-89.3	3.5	0.07
510	0.004	-210.0	2.3	0.07
520	0.005	-236.7	2.5	0.08
530	0.013	-253.6	4.8	0.07
540	0.001	-7.1	4.3	0.02
550	0.001	nm		0.02
570	0.001	-20.6	4.8	nm
800	0.003	45.9	2.0	0.13
1000	0.008	204.5	1.2	0.03
1100	0.009	126.4	1.1	0.02
1250	0.002	62.0	4.3	0.01

Cold Bokkeveld Pyrolysis 84ug

Temp	N (ppmOP)	$\delta^{15}N$	Error	C (ppm OP)
200	0.013	4.9	7.2	0.03
300	0.122	nm		0.34
400	0.055	-122.2	1.0	0.82
435	0.022	-101.6	1.9	0.56
470	0.027	-156.9	4.9	0.82
500	0.030	-167.7	3.3	0.80
533	0.027	-170.9	3.6	0.48
567	0.035	-184.1	2.9	0.91
600	0.079	-68.9	3.5	0.62
700	0.213	-240.9	3.2	1.08
800	0.780	-267.5	0.7	0.69
850	1.045	-282.0	0.6	0.55
900	1.373	nm	0.6	1.11
925	1.051	-302.9	1.0	1.20
950	0.410	nm		1.09
975	0.418	-311.7	1.0	1.16
1050	1.345	-325.6	0.7	2.62
1125	1.076	-338.0	0.8	4.48
1200	1.123	-344.5	0.9	6.12
1200 ON	1.821	-350.3	0.7	18.30
Combustion after pyrolysis				
400	0.253	-340.1	1.0	0.07
450	0.013	-26.0	6.0	0.04
475	0.013	-26.4	5.7	0.03
500	0.049	-7.3	2.8	0.03
525	0.009	nm		0.12
550	0.016	-7.5	2.2	0.08
625	0.015	-3.2	5.4	3.06
700	0.020	nm		6.45
750	0.011	nm		0.02
800	0.008	nm		0.02
900	0.009	nm		0.01
1000	0.009	nm		0.01
1200	0.012	nm		0.02

Indarch Precombustion experiment

Temp	N (ng)	$\delta^{15}N$	Error	C (ng)
200	1.61	-3.1	2.7	47.17
300	4.54	-11.7	0.9	423.36
350	2.63	-29.8	1.4	1152
400	2.27	-35.1	1.3	2215
400	2.37	-70.5	2.0	1813
400	6.29	-114.2	0.4	3576
400	6.16	-171.6	0.7	3901
400	5.29	-184.6	0.9	2620
400	4.69	-182.0	0.6	1695
400	6.17	-205.5	0.6	2148
400	6.86	-192.3	0.6	1904
400	8.37	-229.3	0.7	2630
400	7.87	-235.7	1.6	2256
400	7.74	-242.1	0.7	2332
400	10.95	-226.7	0.6	2466
400	7.38	-234.6	0.6	1828
400	10.87	-257.5	0.5	2764
400	8.7	-256.9	0.6	2108
400	10.76	-256.3	0.5	2259
400	2.77	-247.8	1.5	2218
400	8.16	-278.3	0.8	2496
400	18.1	-302.3	0.7	4249
400	11.2	-287.0	0.7	3342
400	12.2	-291.2	0.8	3010
400	29.61	-294.5	0.7	5050
400	2.02	-220.5	1.6	842
400	9.88	-168.9	0.5	2586
400	5.95	-278.9	0.8	2218
400	5.57	-257.7	0.6	1557
400	7.86	-240.9	0.5	3039
400	20.7	-298.0	0.5	2462
400	9.66	-260.4	0.6	1349
400	9.17	-232.5	0.6	1270
400	6.33	-198.7	0.7	818
400	1.48	-75.4	2.5	194

COLD BOKKEVELD CB2C/B/2

Temp	Yield (ppbN OP	$\delta^{15}N$	Error	ppmC OP
500	75.9	-322	1.2	5.37
525	1240.0	-344.7	1.6	84.30
550	924.0	-341.3	1.9	92.60
575	589.0	-343.7	2.4	74.00
600	128.0	-354.8	1.9	22.60
625	21.5	-300.2	1.7	11.40
650	15.9	-141.1	1.3	7.74
675	10.0	-157.5	2.4	3.57
700	5.8	-245	3.1	1.76
750	5.5	-338.5	4.8	0.58
800	10.6	-436.7	5.1	0.57
850	5.1	-325.2	5.2	0.27
900	5.9	-384.3	6.7	0.34
950	9.9	-452.8	6.1	0.37
1000	11.0	-503	6.2	0.54
1050	52.6	-626.4	6	1.30
1100	27.4	-525.1	5	0.85
1150	28.2	-482.9	4.5	0.79
1200	25.0	-364.9	3.4	0.69
1250	18.2	-182.5	1.7	0.45

APPENDIX 3: NOBLE GAS DATA FROM THE ABEE METEORITE DIAMOND RESIDUE

This data was acquired by U. Ott, of the Max Planck Institut für Chemie, Saarstraße 23, Mainz, Federal Republic of Germany.

Temp. (°C)	comb. C (μg)	$^{20}Ne_t$[x]	^{36}Ar	^{84}Kr	^{132}Xe	$^{136}Xe/^{132}Xe$	$^{3}He_c$	$^{21}Ne_c$
510 P	—	< 0.3	13	< 0.06	< 0.07	—	—	< 0.03
400 C	< 9	< 0.6	2	< 0.04	< 0.02	—	< 0.5	< 0.02
600 P	—	< 0.3	5	< 0.04	< 0.03	—	< 0.05	< 0.02
500 C	130	3.3	267	1.46	1.08	0.325	7.3	< 0.75
700 P	—	< 0.2	7	< 0.04	< 0.02	—	< 0.5	< 0.03
600 C	123	1.6	79	0.41	0.68*	0.329*	5.9	0.74

Noble gas abundances are in units of 10^{-8} cm^3 STP/g. $P = pyrolysis, C = combustion step.
[x]Subscript t and c refer to the trapped and cosmogenic components, resp., of He and Ne.
*The original fraction for Xe analysis was lost due to a breakdown of the mass spectrometer. A split was stored in the extraction line and analysed 10 days later. Isotopic systematics suggest that some air Xe had accumulated during that time, but amounting to less than 50% of the analysed fraction.

REFERENCES

Adamsky R.F. (1959) Oxidation of silicon carbide in the temperature range 1200 to 1500°. *J. Phys. Chem.*, **63**, 305-307.

Addamiano A., Anderson G.W., Comas J., Hughes H.L. and Lucke W. (1972) Ion implantation effects of nitrogen, boron and aluminium in hexagonal silicon carbide. *J. Electrochem. Soc.*, **119**, 1355-1362.

Alaerts L., Lewis R.S., Matsuda J. and Anders E. (1980) Isotopic anomalies of noble gases in meteorites and their origin-VI. Presolar components in the Murchison C2 chondrite. *Geochim. Cosmochim. Acta*, **44**, 189-209.

Alexander C.M.O'D, Arden J.W., Ash R.D. and Pillinger C.T. (1990) Presolar components in the ordinary chondrites. *Earth Planet. Sci. Lett.*, **99**, 220 - 229.

Alexander, C.M. O.'D., Prombo C., Walker R.M., Zinner E., and Arden, J.W. (1990) Ion probe studies of SiC from different chondrite groups. *Meteoritics* **25**, 347.

Alexander C.M.O'D., Prombo C.A., Swan P.D. and Walker R.M. (1991) SiC and Si_3N_4 in Qingzhen (EH3). *Lunar Planet. Sci.*, **XXII**, 5-6.

Alexander C.M.O'D., Swan P.D. and Walker R.M.(1992) Continued in situ studies of interstellar grains in primitive meteorites. *Lunar Planet. Sci.*, **XXIII**, 9-10.

Alexander C.M.O.'D., Swan P.D. and Walker R. (1990) In situ measurement of interstellar SiC in two CM chondrite meteorites. *Nature*, **348**, 715-717.

Amari S. and Lewis R.S. (1989) Interstellar SiC and its noble gas components. *Meteoritics*, **24**, 247.

Amari S., Anders E., Virag A. and Zinner E. (1989) Interstellar amorphous carbon in the Murchison meteorite: Carrier of neon-E(L). *Meteoritics*, **24**, 248.

Amari S., Hoppe P., Zinner E. and Lewis R.S. (1992) Interstellar SiC with unusual isotopic compostions. *Lunar Planet. Sci.*, **XXIII**, 27-28.

Amari S., Lewis R.S. and Anders E. (1990) Interstellar graphite in meteorites: growing complexity, implied by its noble-gas components. *Lunar Planet. Sci.*, **XXI**, 19-20.

Amari S., Zinner E. and Lewis R.S. (1991) The C, N, Al and Si isotopic compositions of SiC grain size separates from Murchison: Indirect evidence for highly anomalous grains. *Lunar Planet. Sci.*, XXII, 19 - 20.

Amari S., Zinner E. and Lewis R.S. (1991) Ca, Ti and Sm isotopic compositions of fine grained interstellar SiC. *Meteoritics*, **26**, 314.

Anders E. (1981) Noble gases in meteorites: evidence for presolar matter and heavy elements. *Proc. R. Soc. Lond.*, **A374**, 207-238.

Anders E. (1987) Local and exotic components of primitive meteorites, and their origin. *Phil. Trans. R. Soc. Lond.*, **A323**, 287-304.

Anders E. (1988) Circumstellar material in meteorites: noble gases, carbon and nitrogen. *In: Meteorites and the Early Solar System. Kerridge J.F. and Matthews M.S. (Eds.). Univ. Arizona Press.*, 927-955.

Anders E. and Heymann D. (1969) Elements 112 to 119: were they present in meteorites? *Science*, **164**, 821-823.

Angus J.C. and Gradner N.C. (1969) U.S. Patent number 3661526.

Arden J.W., Ash R.D., Grady M.M., Wright I.P. and Pillinger C.T. (1989) Further studies on the isotopic composition of interstellar grains in Allende. *Lunar Planet. Sci.*, **XX**, 21-22.

Arrhenius G., Fitzgerald R., Markus S. and Simpson C. (1978) Isotope fractionation under simulated space conditions. *Astrophys. Space Sci.*, **55**, 285-297.

Ash R.D. (1990) A carbon and nitrogen isotope study of interstellar grains. *Unpublished Ph.D. Thesis, Open University.*

Ash R.D., Arden J.W. and Pillinger C.T. (1989) Light nitrogen associated with SiC in Cold Bokkeveld. *Meteoritics*, **24**, 248.

Ash R.D., Arden J.W., Grady M.M., Wright I.P. and Pillinger C.T. (1988) An interstellar dust component rich in ^{12}C. *Nature*, **336**, 228-230.

Ash R.D., Arden J.W., Grady M.M., Wright I.P. and Pillinger C.T. (1990) Recondite interstellar carbon revealed by preparative precombustion. *Geochim. Cosmochim. Acta*, **54**, 455-468.

Ash R.D., Russell S.S., Wright I.P. and Pillinger C.T. (1991) Minor high temperature carbon components confirmed by stepped combustion using a new sensitive mass spectrometer. *Lunar Planet. Sci.*, **XXII**, 35-36.

Ash R.D., Wright I.P., Grady M.M., Pillinger C.T., Lewis R.S. and Anders E. (1987) An investigation of C and N isotopes in Cδ and the effects of grain size on combustion temperature. *Meteoritics*, **22**, 319.

Atwood C.H. (1990) Supernova 1987A: What have we learnt about nucleosynthesis? *J. Chem. Educ.*, **67**, 731-735.

Badziag P., Verwoerd W.S., Ellis W.P. and Griener N.R. (1990) Nanometre-sized diamonds are more stable than graphite. *Nature*, **343**, 244-245.

Battey M.H. (1982) Mineralogy for students. *Longman Group, New York*, pp255.

Berkley J.L., Gassaway Brown H., Keil K., Carter N.L., Mercier J-C. C. and Huss G. (1976) The Kenna ureilite: An ultramafic rock with evidence for igneous, metamorphic, and shock origin.

Berman R. and Simon F. (1955) The graphite-diamond equilibrium. *Z. Eleckrochem.*, **59**, 333-345.

Bernatowicz T., Fraundorf G., Tang M., Anders E., Wopenka B., Zinner E. and Fraundorf P. (1987) Evidence for interstellar SiC in the Murray carbonaceous meteorite. *Nature*, **330**, 728-732.

Bernatowicz T.J., Amari S. and Lewis R.S. (1992) TEM studies of an interstellar rock. *Lunar Planet. Sci.* , **XXIII**, 91-92.

Bernatowicz T.J., Gibbons P.C. and Lewis R.S. (1990) Electron energy loss spectrometry of interstellar diamonds. *Astrophys. J.*, **359**, 246-255.

Bethe H.A. and Brown G. (1985) How a supernova explodes. *Scientific American*, **May, 1985.**

Bishop S.G., Freitas J.A., Kennedy T.A., Carlos W.E., Moore W.J., Nordquist P.E.R. and Gipe M.L. (1989) Donor identification in thin film cubic SiC. *In : Amorphous and crystalline SiC. Eds: G.L. Harris and C Y-W. Yang, Springer Verlag, New York.*

Blake D.F., Freund F., Krishnan K.F.M., Echer C.J., Shipp R., Bunch T.E., Tielens A.G., Lipari R.J., Hetherington C.J.D. and Chang S. (1988) The nature and origin of interstellar diamond. *Nature*, **332**, 611-613.

Bode M.F. (1988) Observations and modelling of circumstellar dust. *In: Dust in the Universe, Eds. M.E. Bailey and D.A. Williams, CUP, Cambridge*, 73-102.

Bode M.F. and Evans A. (1983) Dust in nova systems - thoughts in transition. *Q. Jl. R. astr. Soc.*, **24**, 83-105.

Bode M.F., and Evans A. (1988) Infrared observations of Novae. *In: Classical Novae, Eds: M.F. Bode and A. Evans, Wiley, NY.*

Boyd S.R. (1988) A study of carbon and nitrogen isotopes from the Earth's mantle. Unpublished PhD Thesis. Open University.

Boyd S.R. and Pillinger, C.T. (1990) Determination of the abundance and isotope composition of nitrogen within organic compounds: a sealed tube technique for use with static vacuum mass spectrometers. *Meas. Sci. Tech.* **1**, 1176-1183.

Boyd S.R. and Pillinger C.T. (1991) Rubidium sulphate-ammonium sulphate solid solution: a standard for use during the determination of the abundance and isotopic composition of nitrogen at the ppm level, by mass spectrometry. *Anal. Chem.*, **63**, 1332-1335.

Boyd S.R., Pillinger C.T., Milledge H.J. Mendelssohn M.J. and Seal M. (1988) Fractionation of nitrogen isotopes in a synthetic diamond of mixed crystal habit. *Nature*, **331**, 604-607.

Boyd S.R., Wright I.P., Franchi I.A. and Pillinger C.T. (1988) Preparation of sub-nanomole quantities of nitrogen gas for stable isotopic analysis. *J. Phys. E: Sci. Instrum.*, **21**, 876-885.

Breger J.A. (1964) Formation of uranium ore deposits. *Vienna*, **99**.

Brezina A. (1904) The arrangement of collections of meteorites. *Trans. American Phil. Soc.*, **43**, 211-247.

Burbidge E.M., Burbidge G.R., Fowler W.A. and Hoyle F. (1957) Synthesis of the elements in stars. *Rev. Mod. Phys.*, **29**, 547-651.

Burrows A. and Lattimer J. (1987) Neutrinos from SN1987A. *Astrophys. J. (Lett.)*, **318**, L63.

Cameron A.G.W. and Truran J.W. (1977) The supernova trigger for the formation of the Solar system. *Icarus*, **30**, 447-461.

Campbell A.B., Shewcun J., Thompson D.A., Danes J.A. and Mitchell J.B. (1975) Ion Implantation Semi Con.. *Sci. Technol. Proc. 4th Intern. Conf. Osaka, 1974*, 191-198.

Carr R.H., Gibson E.K.(Jr.), Rietmeijer F.J.M., Grady M.M., Wright I.P. and Pillinger C.T. (1986) Characterisation of carbonaceous materials in interplanetary dust particles. *Meteoritics*, **21**, 344-345.

Carr R.H., Wright I.P., Joines A.T. and Pillinger C.T. (1986) Measurement of carbon stable isotopes at the nanomole level; a static mass spectrometer and sample preparation technique. *J. Phys. E: Sci. Instrum.*, **19**, 798-808.

Clarke R.S.(Jr.), Appleman D.E. and Ross D.R. (1981) An Antarctic iron meteorite contains preterrestrial impact-produced diamond and lonsdaleite. *Nature*, **291**, 396-398.

Cartensen J.T., and Rodriguez-Hornedo, N. (1985) *J. Pharm. Sci.* **74** 1322-1326

Clausen M.J., Kleinmann S.G., Joyce R.R. and Jura M. (1987) A flux-limited sample of galactic carbon stars. *Astrophys. J. Suppl.*, **65**, 33-F1.

Clayton D.D. (1981) Some key issues in isotopic anomalies: astrophysical history and aggregation. *Proc. Lunar Planet. Sci. Conf.*, **12B**, 1781-1802.

Clayton D.D. (1982) Cosmic chemical memory- A new astronomy. *Quart. J. Roy. Astron. Soc.* **23**, 174-212.

Clayton D.D. (1989) Origin of Xe-HL and supernova 1987A. *Lunar Planet. Sci.*, **XX**, 165-166.

Clayton D.D. (1989) Origin of heavy xenon in meteoritic diamonds. *Astrophys J.*, **340**, 613-619.

Clayton D.D. and Brown L.E. (1992) New ideas for SiC: Mg burning in AGB shell flashes. *Lunar Planet. Sci.*, **XXIII**, 229-230.

Clayton D.D. and Hoyle F. (1976) Grains of anomalous isotopic composition from novae. *Astrophys. J.*, **203**, 490-496.

Clayton D.D. and Ward R.A. (1978) s-Process studies: xenon and krypton isotopic abundances. *Astrophys. J.*, **224**, 1000-1006.

Clayton R.N. and Mayeda T.K. (1984) The oxygen isotope record in Murchison and other carbonaceous chondrites. *Earth Planet. Sci. Lett.*, **67**, 151-161.

Clayton R.N. and Mayeda T.K. (1977) Anomalous anomalies in carbonaceous chondrites. *Lunar Planet. Sci.*, **VIII**, 193-195.

Clayton R.N. Onuma N. and Mayeda T.K. (1976) A classification of meteorites based on oxygen isotopes. *Earth Planet. Sci. Lett.*, **30**, 10.

Clayton R.N., Grossman L. and Mayeda T.K. (1973) A component of primitive nuclear composition in carbonaceous chondrites. *Science*, **182**, 485-488.

Climenaga J.L., Harns B.L., Holts J.T., and Smolinski J. (1982) The $^{12}C/^{13}C$ ratio of 18 cool carbon stars. *Astrophys. J.*, **215**, 836-844.

Collins A.T. (1978) Migration of nitrogen in electron irradiated type Ib diamond. *J. Phys.C:Solid State Phys.*, 11, L417-L422.

Collins A.T. (1980) Vacancy enhanced aggregation of nitrogen in diamond. *J.Phys.C.:Solid State Phys.*, 13, 2641-2650.

Cooper A. Stannard R. and Jones B.W. (1985) The Formation and Evolution of the Stars. Course unit, S256 Matter in the Universe. Open University Press.

Courtin R., Gautier D., Marten A., and Kunde V. (1983) The $^{12}C/^{13}C$ ratio in Jupiter from the voyager infrared investigation *Icarus* **53**, 121- 132.

Cowie L.L.(1978) Refractory grain destruction in low velocity shocks. *Astrophys. J.*, **225**, 887.

Crabb J., Lewis R.S., and Anders, E. (1982) Extinct ^{129}I in C3 chondrites. *Geochim. Cosmochim. Acta*, **46**, 2511-2526.

D'Anatona and Mazzitelli (1992) Stellar evolution: Low mass stars. *In: The Astronomy and Astrophysics Encyclopeadia. Ed: S. P. Maran, Cambridge University Press.*

Dakowski M. (1969) The possibility of extinct superheavy elements occuring in meteorites. *Earth Planet. Sci. Lett.*, **6**, 152-154.

Davies G. and Evans T. (1972) Graphitisation of diamond at zero pressure and at a high pressure. *Proc. R. Soc. Lond. A.*, **328**, 413-427.

Dawson K.R., Maxwell J.A. and Parsons (1960) A description of a meteorite that fell near Abee, Alberta, Canada. *Geochim. Cosmochim. Acta*, **21**, 127-144.

Deines P. and Wickman F.E.(1975) A contribution to the stable isotope geochemistry of iron meteorites. *Geochim. Cosmochim. Acta*, **39**, 547.

Deryaguin B.V. and Spitzyn B.V. (1956) USSR Authors certificate No 399134.

Des Marais D.J. (1978) Variable-temperature cryogenic trap for the separation of gas mixtures. *Anal. Chem.*, **50**, 1405-1406.

DeVries R.C.(1987) Synthesis of diamond under metastable conditions. *Ann. Rev. Mater. Sci.*, **17**, 161-187.

Dodd R.T. (1981) Meteorites: A petrologic-chemical synthesis. *Cambridge University Press, Cambridge*, pp368.

Dodd R.T. (1986) Thunderstones and Shooting stars. *Harvard University Press*, 196.

Dominy J.F., Walllerstein G. and Suntzeff N.B. (1986) Abundances of C, N, and O and their isotopes in the atmospheres of four SC stars. *Astrophys. J*, **317**, 810-818.

Draine B.T. and Salpeter E.E. (1979) Destruction mechanisms for interstellar dust. *Astrophys. J.*, **231**, 438.

Eberhardt P., Jungck M.H.A., Meier F.O. and Niederer F. (1979) Neon-E: new limits for isotopic composition. Two host phases? *Lunar Planet. Sci.*, **10**, 341-343.

Eberhardt P., Jungck M.H.A., Meier F.O. and Niederer F. (1979) Presolar grains in Orgueil: evidence from neon-E. *Astrophys. J. (Lett.)*, **234**, L169-171.

Edmond J.A., Withrow S.P., Wadlin W. and Davis R.F. (1987) High temperature implantation of single crystal beta silicon carbide thin films. *Proc. Mats. Res. Soc. Symp.*, **77**, 193-198.

Epstein S., and Taylor H.P., (1970) $^{18}O/^{16}O$, $^{30}Si/^{28}Si$, D/H, and $^{13}C/^{12}C$ studies of lunar rocks and minerals. *Science*, **167**, 533-535.

Ergun S., Donaldson W.F. and Breger I.A. (1974) Some physical and chemical properties of vitrains associated with uranium. *Fuel*, **39**, 71-77.

Ervin G. (1958) Oxidation behavior of silicon carbide. *J. Am. Ceram. Soc.*, **41**, 347-352.

Evans T. (1976) Diamond. *Contemp. Phys.*, 1745-1770.

Evans T. and Phaal (1962) The kinetics of the diamond-oxygen reaction. *Proceedings of the fifth conference on Carbon, Pergamon Press.*

Evans T. and Qi Z. (1982) The kinetics of aggregation of nitrogen atoms in diamond. *Proc. R. Soc. Lond.*, **A381**, 159-178.

Eversole W.G. (1958) US patent number 3030188.

Field G.B. (1974) Interstellar abundances: Gas and Dust. *Astrophys. J.*, **187**, 435-459.

Fishenko A.V., Kashkarov L.L. and Semjenova L.F. (1992) On the origin of the diamonds from the Efremovka chondrite by the thermoluminescence. *Lunar Planet. Sci.*, XXIII, 363-364.

Franchi I.A. (1988) Nitrogen Isotopic Variations in Irons and other Fe-Ni Metal Rich Meteorites. *Unpublished Ph.D. thesis, Open University.*

Franchi I.A., Wright I.P. and Pillinger C.T. (1986) Heavy nitrogen in Bencubbin - a light element isotopic anomaly in a stony-iron meteorite. *Nature*, **323**, 138-140.

Frenklach M., Kernatick R., Huang D., Howard W., Spear K.E., Phelps W. and Koba R. (1989) Homogeneous nucleation of diamond powder in the gas phase. *J. Appl. Phys.*, **66**, 395-398.

Fukunaga K., Matsuda J., Nagao K., Miyamoto M. and Ito K. (1987) Noble gas enrichment in vapour-growth diamonds and the origin of diamonds in ureilites. *Nature*, **328**, 141-143.

Galimov E.M. (1985) Some evidence of the reality of the cavitation synthesis of diamonds in nature. *Geokhimiya*, **4**, 456-471.

Galimov E.M. (1991) Isotope fractionation related to kimberlite magmatism and diamond formation. *Geochim. Cosmochim. Acta*, **55**, 1677-1708.

Gallino R., Busso M., Picchio G. and Raiteri C.M. (1990) On the astrophysical interpretation of isotope anomalies in meteoritic SiC grains. *Nature*, **348**, 298 - 302.

Ganapathy R. and Larimer J.W. (1980) A meteoritic component rich in volatile elements: its charaterisation and implications. *Science*, **207**, 57-59.

Geiss J. and Bochsler P. (1982) Nitrogen isotopes in the solar system. *Geochim. Cosmochim. Acta*, **46**, 529-548.

Gilkes K.W.R., Gaskell P.H., Russell S.S., Arden J.W., and Pillinger C.T. (1992) Do carbynes exist as interstellar material after all? *Meteoritics*, **27**, 224.

Gillman R.C. (1969) On the composition of circumstellar grains. *Astrophys. J. (Lett.)*, **155**, L185.

Gilmour I., Russell S.S., Newton J. and Pillinger C.T. (1991) A search for the presence of C60 as an interstellar grain in meteorites. *Lunar Plan. Sci.*, **XXII**, 445-446.

Glasgow P.A. (1989) 6H-SiC studies and developments at the Corporate Research Laboratory of Siemens AG and the Institute for Applied Physics at the University in Erlangen In: Amorphous and Crystalline SiC and Related Materials, Eds. G.L. Harris and C. Y-W. Yang. *Springer-Verlag.*

Göbel R., Ott U. and Begemann F. (1978) On trapped noble gases in ureilites. *J. Geophys. Res.*, **83**, 855-867.

Grady M.M. (1983) The content and isotopic composition of carbon in stony meteorites. *Unpublished PhD Thesis. University of Cambridge.*

Grady M.M., and Pillinger C.T. (1990) ALH 85085: nitrogen isotope anomalies of a highly unusual primitive chondrite. *Earth Plan. Sci. Lett.*, **97**, 29-40.

Grady M.M., Ash R.D., Morse A.D. and Pillinger C.T. (1991) Acfer 182: An unusual chondrite with affinities to ALH 85085. *Meteoritics*, **26**, 339-340.

Grady M.M., Wright I.P., Swart P.K. and Pillinger C.T. (1985) The carbon and nitrogen isotopic composition of ureilites: implications for their genesis. *Geochim. Cosmochim. Acta*, **49**, 903-916.

Grady M.M., Wright, I.P., Carr L.P., and Pillinger, C.T. (1985) . Compositional differences in enstatite chondrites based on carbon and nitrogen stable isotope measurements. *Geochim. Cosmochim. Acta* **50** 2799-2813.

Greenwood N.N. and Earnshaw A. (1984) Chemistry of the elements. *Pergamon Press, Oxford,* pp1543.

Grossman L. (1971) Condensation in the primitive Solar nebula. *Geochim. Cosmochim. Acta,* **36**, 597-619.

Gugel E. (1969) *Haus. Tech. Vortragsveroff,* **206**, 29-38.

Guimon R.K., Keck B.D., Weeks R.S., Dehart J. and Sears D.W.G. (1985) Chemical and physical studies of Type 3 chondrites IV. Annealing studies of a type 3.4 ordinary chondrite and the metamorphic history of meteorites. *Geochim. Cosmochim. Acta.*, **49**, 1515-1524.

Halstead R.E. and Nier, A.O. (1950) Gas flow through the mass spectrometer viscous leak. *Rev. Sci. Instrum.*, **21**, 1019-1021.

Hanneman R.E., Strong H.M. and Bundy F.P. (1967) Hexagonal diamonds in meteorites: implications. *Science,* 155, 995-997.

Hawkins I., and Jura M. (1987) The $^{12}C/^{13}C$ ratio of the interstellar medium in the neighborhood of the Sun. *Astrophys. J.*, **317**, 926-950.

Heymann D. and Dziczkaniec M. (1979) Xenon from intermediate zones of supernovae. *Proc. Lunar Planet. Sci. Conf.*, **10**, 1943-1959.

Hoefs J. (1987) Stable isotope geochemistry. *Springer-Verlag, New York,* 241pp.

Howard W., Huang D., Yuan J., Frenklach M., Spear K.E., Koba R. and Phelps A.W. (1990) Synthesis of diamond in acetylene oxygen plasma. *J. App. Phys.*, **68**, 1247-1251.

Howard W.M., Clayton D.D., and Meyer B.S. (1991) XeH and BaH from a weak neutrino burst. *Meteoritics,* **26**, 347.

Hoyle F. and Wickramasinghe N.C. (1970) Dust in supernova explosions. *Nature,* **226**, 62-63.

Huss G.R. (1990) Ubiquitous interstellar diamond and SiC in primitive chondrites: abundances reflect metamorphism. *Nature,* **347**, 159-162.

Huss G.R. and Lewis R.S. (1990) Interstellar diamonds and silicon carbide in enstatite chondrites. *Lunar Planet. Sci.*, **XXI**, 542-543.

Iben I. (1985) Nucleosynthesis in low and intermediate mass stars on the asymptotic giant branch. *In: Nucleosynthesis: Challenges and new developments. Eds: W.D. Arnett and J.W. Truran, University of Chicago Press,* 272-291.

Ierofeieff M.V. and Latchinoff P.A. (1888) Météorite diamantère tombé le 10/22 Septembre 1886, en Russie, à Nowo-Urei, gouvernemet de Penza. *Compt. Rend. Acad. Sci. Paris,* **106**, 1679-1682.

Ierofeieff M.V. and Latchinoff P.A. (1888) Description of Novo Urei meteorite. Petersberg.

Ireland T.R., Zinner E. and Amari S. (1991) Ti isotopic compositions of Murchison SiC. *Lunar Planet. Sci. Conf.*, **XXII**, 613-614.

Janssen G., Vollenberg W., Giling L.J., van Enckevort W.J.P.O., Schaminee J.J.D. and Seal M. (1990) Diamond deposition using an oxygen acetylene flame. *Proc. Diamond Conference, Reading,* page 2.

Javoy M., Pineau F. and Demaiffe D. (1984) Nitrogen and carbon isotopic composition in the diamonds of Mbuji Mayi (Zaire). *Earth Planet. Sci. Lett.*, **68**, 399-412.

Jorgensen P.J., Wadsworth M.E., Cutler I.B. (1959) Oxidation of silicon carbide. *J. Am. Ceram. Soc.*, **42**, 613-616.

Jørgensen U.G. (1988) Formation of Xe-HL-enriched diamond grains in stellar environments. *Nature*, **332**, 702-705.

Jura M. (1988) Astronomical Observations of Solid Phase Carbon *In: Carbon and the Galaxy: Studies from Earth and Space. NASA Conference Publication*, **3061**, 39-45.

Jura M. (1987) The Milky Way as a Galaxy. *In: Interstellar Processes Ed. D.J. Hollenbach and H.A. Thronson Jr. Reidel.*

Kalish R., Amir O., Brener R., Spits R.A. and Derry T.E. (1991) Incorporation of N into amorphous-hydrogenated carbon diamond like films. *Appl. Phys.*, **A52**, 48-51.

Kaminskiy F.V. (1987) Origin of polycrystalline carbonado diamond aggregates. *Dokl. Akad. Nauk. SSSR*, **294**, 439-440.

Karttunen H. Kroger P., Oja H., Poutanen M. and Donner K.J. (1987) Fundamental Astronomy, *Springer Verlag*, 478pp.

Kerridge J. F.(1980) Secular variations in the composition of the Solar wind: evidence and causes. *In: Proc. Conf. Ancient Sun*, Pergamon Press, 475-489.

Kim H.J. and Davis R.F. (1986) Theoretical and empirical studies of impurity incorporation into β-SiC thin films during epitaxial growth. *J. Electrochem, Soc.*, **133**, 2350.

Kirchstein G., Ed., (1984) Silicon, *Gmelin Handbook of Inorganic Chemistry*, suppl. vol. **B2**, Springer, New York.

Kirschbaum C. (1985) Iodine and chlorine in two fine grained inclusions from the Allende meteorite. *Meteoritics*, **20** 683-684.

Knapp G.R. and Chang K.M. (1985) Mass loss from evolved stars. V. Observations of the ^{12}CO and ^{13}CO J=1-0 lines in Mira variables and carbon stars. *Astrophys. J.*, **293**, 281-287.

Kuroda P.K. and Manuel O.K. (1970) Mass fractionation and isotopic anomalies in neon and xenon. *Nature*, **227**, 1113-1116.

Lambert D.L., Gustafsson B., Eriksson K. and Hinkle K.H. (1986) The chemical composition of carbon stars. I. Carbon, nitrogen, and oxygen in 30 cool carbon stars in the galactic disk. *Astrophys. J. Suppl. Ser.*, **62**, 373-425.

Lancet M. and Anders E. (1970) Carbon isotope fractionation in the Fischer-Tropsch synthesis and in meteorites. *Science*, **170**, 980-982.

Landau R. (1970) Diamonds and the interstellar extinction curve. *Nature*, **226**, 924.

Larimer J.W. (1988) The cosmochemical classification of the elements. *In: Meteorites and the Early Solar system. Eds: J.F. Kerridge and M.S. Matthews. University of Arizona Press*, 375-389.

Larimer J.W. and Bartholomay M. (1979) The role of carbon and oxygen in the chemistry in cosmic gases: some applications to the chemistry and mineralogy of enstatite chondrites. *Geochim. Cosmochim. Acta*, **43**, 1455-1466.

Laul J C, Ganapathy R., Anders E. and Morgan J.W. (1973) Chemical fractionations in meteorites VI. Accretion temperatures of H, LL and E chondrites from abundances of volatile trace elements. *Geochim. Cosmochim. Acta*, **37**, 329.

Lee T., Papanastrassiou D.A. and Wasserburg G.J. (1976) Demonstration of excess ^{26}Mg in Allende and evidence for ^{26}Al. *Geophys. Res. Lett.*, **3**, 109-112.

Lewis J.S. and Ney E.P. (1979) Iron and the formation of astrophysical dust grains. *Astrophys. J.*, **234**, 154-157.

Lewis R.S., Amari S. and Anders E. (1990) Meteoritic silicon carbide: pristine material from carbon stars. *Nature*, **348**, 293-298.

Lewis R.S., Anders E. and Draine B.T. (1989) Interstellar diamonds in meteorites: properties, detectability and origin. *Nature*, **339**, 117-121.

Lewis R.S., Anders E., Swart P.K., Grady M.M. and Pillinger C.T. (1983) Isotopically anomalous carbon in the Murchison meteorite and its association with noble gas components. *Lunar Planet. Sci.*, **XIV**, 438-439.

Lewis R.S., Anders E., Wright I.P., Norris S.J. and Pillinger C.T. (1983) Isotopically anomalous nitrogen in primitive meteorites. *Nature*, **305**, 767-771.

Lewis R.S., Grady M.M., Wright I.P., Pillinger C.T. and Fallick A.E. (1983) Isotopic composition of C and N in noble gas host phases in CI carbonaceous and Type 3 ordinary chondrites. *Meteoritics*, **18**, 340.

Lewis R.S., Gros J. and Anders E. (1977) Isotopic anomalies of noble gases in meteorites and their origins. 2. Separated minerals from Allende. *J. Geophys. Res.*, **82**, 779-792.

Lewis R.S., Huss G.R. and Lugmair G. (1991) Finally, Ba and Sr accompanying XeHL in diamonds from Allende. *Lunar Planet. Sci.*, **XXII**, 807-808.

Lewis R.S., Srinivasan B. and Anders E. (1975) Host phase of a strange xenon component in Allende. *Science*, **190**, 1251-1262.

Lewis R.S., Tang M., Wacker J.F., Anders E. and Steel E. (1987) Interstellar diamonds in meteorites. *Nature*, **326**, 160-162.

Lewis R.S., Huss G.R., Anders E., Lui Y.-G., and Schmitt R.A. (1991) Elemental abundance patterns in presolar diamonds. *Meteoritics* **26**, 363-364.

Lipschutz M.E. (1964) Origin of diamonds in the Ureilites. *Science*, **143**, 1431-1433.

Lipschutz M.E. and Anders E. (1961) The record in meteorites. IV. Origin of diamonds in iron meteorites. *Geochim. Cosmochim. Acta*, **24**, 83-105.

Luther L.C. and Moore W.J. (1964) Diffusion of He, Si and Ge in diamond. *J. Chem. Phys.*, **41**, 1018-1026.

Manuel O.K., Hennecke E.W. and Sabu D.D. (1972) Xenon in carbonaceous chondrites. *Nature Phys. Sci.*, **240**, 99-101.

Manuel O.K., Wright R.J., Miller D.K. and Kuroda P.K. (1972) Isotopic compositions of rare gases in the carbonaceous chondrites Mokoia and Allende. *Geochim. Cosmochim. Acta*, **36**, 961-983.

Matsunami H., Shibahara K., Kuroda N., Yoo W. and Nishinu S. (1989) VPE growth of SiC on step-controlled substrates. *In: Amorphous and Crystalline SiC and Related Materials. Eds. G.L. Harris and C.-Y.W. Yang. Springer-Verlag, New York.*

Matz S.M., Share G.H., Leising M.D., Chupp E.L., Vestrand W.T., Purcell W.R., Strickman M.S. and Reppin C. (1988) Gamma ray line emission from SN 1987A. *Nature*, **331**, 416-418.

McGarvie D.W., Wright I.P., Grady M.M., Pillinger C.T. and Gibson E.K.(Jr). (1987) A stable carbon isotopic study of Types 1 and 2 carbonaceous chondrites. *Mem. Natl. Inst. Polar Res., Spec. Issue*, **46**, 179-195.

McLaughlin D.B. (1935) Remarks on Nova Herculis. *Publs. Am. astr. Soc.*, **8**, 145-146.

McSween H.Y. (1986) Meteorites and their parent planets. *Cambridge University Press*, pp237.

Millman P.M. (1953) Meteor News. *J. Roy. Astron. Soc. Canada*, **47**, 29-33.

Minster J.F., Richard L-P., and Allegre C.J. (1979) ^{87}Rb-^{87}Sr chronology of enstatite meteorites. *Earth Plan. Sci. Lett.*, **44**, 420.

Moissan (1904) Nouvelles recherches sur la Météorite de Canyon Diablo. *Comptes Rendus, Paris*, **139** 773-780.

Moore E. (1985) The Formation and Evolution of the Stars. Course unit, S256 Matter in the Universe. Open University Press.

Moseley S.H., Dwek E., Glaccum W., Graham J.R., Loewenstein R.F. and Silverberg R.F. (1989) Far infrarod observations of thermal dust emission from supernova 1987A. *Nature*, **340**, 697-699.

Nakatogawa T. (1954) A study on the electrical resistance of SiC (2). The oxidation rate of SiC. *J. Chem. Soc. Japan: Ind. Chem. Sect*, **57**, 348-350.

Newton J., Arden J.W., and Pillinger C.T. (1992) Carbon and nitrogen isotope studies of a suite of type CO3 chondrites. *Lunar Planet. Sci.*, **XXIII**, 985-986.

Nichols R.H., Hohenberg C.M., Alexander C.M.O'D, Olinger C.T. and Arden J.W. (1991) Xe and Ne from acid-resistant residues of Inman and Tieschitz. *Geochim. Cosmochim Acta*, **55**, 2921-2936.

Nichols R.H., Hohenberg C.M., Hoppe P., Amari S., and Lewis R.S. (1992) ^{22}Ne and ^{4}He in single SiC grains and ^{22}Ne E(L) in single Cα grains of known carbon isotopic compositions. *Lunar Planet. Sci.*, **XXIII**, 989-990.

Nier A.O. (1940) A mass spectrometer for routine isotope abundance measurements. *Rev. Sci. Instrum.*, **11**, 212-216.

Nier A.O., McElroy M.B. and Yung Y.L. (1976) Isotopic composition of the Martian atmosphere. *Science*, **194**, 68-70.

Nishino S., Powell J.A. and Will H.A. (1983) Production of large-area single crystal wafers of cubic SiC for semiconductor devices. *Appl. Phys. Lett.*, **42**, 460.

Obradovic M., Brown L.E., Guha S. and Clayton D.D. (1991) Si, C and Ti isotopes: Are SiC particles from AGB stars? *Meteoritics*, **26**, 381.

Okumura (1989) Donor identification in thin film cubic SiC. *In: Amorphous and crystalline SiC. Eds: G.L. Harris and C Y-W. Yang., Springer Verlag, New York.*

Olsen E.J. and Bunch T.E. (1984) Equilibration temperatures of the ordinary chondrites. A new evaluation. *Geochim. Cosmochim. Acta.*, **48**, 1363-1365.

Onuma N., Clayton R.N. and Mayeda T.K. (1972) Oxygen isotope temperatures of "equilibrated" ordinary chondrites. *Geochim. Cosmochim. Acta*, **36**, 157-168.

Orlov Yu.L. (1977) The mineralogy of the diamond. *Wiley, N.Y.*

Ott U., and Begemann F. (1990) S-process material in Murchison: Sr and more on Ba. *Lunar Planet. Sci.*, **XXI**, 920-921.

Ott U., Begemann F., Yang J. and Epstein S. (1988) s-Process krypton of variable isotopic composition in the Murchison meteorite. *Nature*, **332**, 700-702.

Ott U., Lohr H.P. and Begemann F. (1991) NeE (H) and Kr-, Xe-S in Indarch and Krymka: Are they a measure of the SiC abundance? *Meteoritics*, **26**, 382.

Ott U., Yang J. and Epstein S. (1985) s-Process Xe and Kr and Ne-E in a ^{13}C rich Murchison sample; noble gas analysis by stepped combustion. *Meteoritics*, **20**, 722-723.

Ozima M. and Zashu S. (1991) Radiation induced diamond (carbonado): A possible mechanism for the origin of diamond in some meteorites. *Meteoritics*, **26**, 382-383.

Ozima M., Zashu S., Tomura K. and Matsuhisa Y. (1991) Constraints from noble gas contents on the origin of carbonado diamonds. *Nature*, **351**, 472-474.

Pillinger C.T. (1984) Light element stable isotopes in meteorites - from grams to picograms. *Geochim. Cosmochim. Acta*, **48**, 2739-2766.

Pillinger C.T., Russell S.S., Ash R.D., and Arden J.W. (1989) The role of CVD in the production of interstellar grains. *Meteoritics*, **24**, 316.

Powell J.A. and Matus L.G. (1989) Recent developments in SiC (USA). *In: Amorphous and Crystalline SiC and Related Materials, Eds. G.L. Harris and C. Y-W.Yang. Springer-Verlag.*

Prombo C.A. and Clayton R.N. (1985) A striking nitrogen isotopic anomaly in the Bencubbin and Weatherford meteorites. *Science*, **230**, 935-937.

Prombo C.A., Podosek F.A., Amari S., and Lewis R.S. (1992) S process Sr and Ba in SiC from Murchison series KJ *Lunar.Plan. Sci. Conf.* XXIII 1111-1112.

Prosser S.J., Wright I.P. and Pillinger C.T. (1990) A preliminary investigation into the isotopic measurement of carbon at the picomole level using static vacuum mass spectrometry. *Chem. Geol.*, **83**, In Press.

Ramadohr P. (1972) . *Meteoritics*, **7**, 565.

Reeves H. (1978) The Origin of the Solar system. *In: The origin of the Solar system. Ed. S.F. Dermott, Wiley.*

Reynolds J.H. (1967) Isotopic abundance anomalies in the solar system. *Ann. Rev. Nucl. Sci.*, **17**, 253-316.

Reynolds J.H. and Turner G. (1964) Rare gases in the chondrite Renazzo. *J. Geophys. Res.*, **69**, 3263-3281.

Richter S., Ott U., and Begemann F. (1992) S-process isotope anomalies: Nd, Sm and a bit more Sr. *Lunar Planet. Sci.*, **XXIII**, 1147-1148.

Ringwood A.E. (1960) The Novo Urei meteorite. *Geochim. Cosmochim. Acta*, **20**, 1-4.

Rubin A.E. (1984) The Blithfield meteorite and the origin of sulphide-rich, metal poor, clasts and inclusions in brecciated enstatite chondrites. *Earth Planet. Sci. Lett.*, **67**, 273-283.

Rubin A.E. and Keil K. (1983) Mineralogy and petrology of the Abee enstatite chondrite breccia and its dark inclusions. *Earth Planet. Sci. Lett.*, **62**, 118-131.

Russell H.N. (1928) Review of "The Internal Constitution of Stars" by A.S. Eddington. *Astrophys. J.*, **67**, 83-88.

Russell S.S., Ash R.D., Pillinger C.T. and Arden J.W. (1990) On the existence of occluded isotopically light carbon in Allende. *Lunar Planet. Sci.*, **XXI**, 1049-1050.

Russell S.S., Pillinger C.T. and Arden J.W. (1990) Nitrogen concentration of interstellar diamond. *Lunar Planet. Sci.*, **XXI**, 1051-1052.

Russell S.S., Pillinger C.T. Arden J.W., Lee M.R. and Ott U. (1992) A new type of meteoritic diamond in the enstatite diamond Abee. *Science*, In Press.

Sackmann and Boothroyd (1992) Carbon Stars. *In: The Astronomy and Astrophysics Encyclopeadia. Ed: S. P. Maran, Cambridge University Press.*

Safranov V.S. (1991) Kuiper Prize Lecture: Some problems in the formation of the Planets. *Icarus*, **94**, 260-271.

Saslaw W.C. and Gaustad J.E. (1969) Interstellar dust and diamonds. *Nature*, **221**, 160-162.

Schelhaas N., Ott U. and Begemann F. (1990) Trapped noble gases in unequilibrated ordinary chondrites. *Geochim. Cosmochim. Acta*, **54**, 2869.

Schultz L. and Kruse H. (1989) Helium, neon and argon in meteorites - A data compilation. *Meteoritics*, **24**, 155-172.

Schutte W.A. and Greenberg J.W. (1987) The evolution of organic refractory mantles on interstellar grains. *In: Dust in the Universe. Eds M.E. Bailey and D.A. Williams. C.U.P., Cambridge*, 403-406.

Seab C.G. (1987) Grain destruction, formation, and evolution. *In: Interstellar Processes. Hollenbach D.J. and Thronson H.A.(Jr.) (Eds.). Reidel Publ. Co., Dordrecht*, 491-512.

Sears D.W., Kallemeyn G.W. and Wasson J.T. (1983) Composition and origin of clasts and inclusions in the Abee enstatite chondrite breccia. *Earth Planet. Sci. Lett.*, **62**, 180-192.

Sears D.W.G. and Dodd R.T. (1988) Overview and classification of meteorites. *In: Meteorites and the early Solar system. Eds: J.F. Kerridge and M.S. Matthews, University of Arizona Press.*, 3-31.

Sonett C.P. (1971) The relationship of meteoritic parent body thermal histories and electromagnetic heating by a pre main sequence, T. Tauri Sun. *In Physical Studies of Minor Planets, ed. T. Gehrels*, **NASA SP-267**, 239-245.

Spitzer L. (1978) Physical processes in the interstellar medium. *John Wiley and Sons.*

Srinivasan B. and Anders E. (1978) Noble gases in the Murchison meteorite: possible relics of s-process nucleosynthesis. *Science*, **201**, 51-55.

Srinivasan B., Alexander E.C.(Jr.), Manuel O.K. and Troutner D.E. (1969) Xenon and krypton from the spontaneous fission of californium-252. *Phys. Rev.*, **179**, 1166-1169.

Srinivasan B., Gros J. and Anders E. (1977) Noble gases in separated meteoritic minerals: Murchison (C2), Ornans (C3), Karoonda (C5), and Abee (E4). *J. Geophys. Res.*, **82**, 762-778.

Starrfield S.G., Sparks W.M. and Truran J.W. (1985) Recurrent novae as a consequence of the accretion of solar material on to a 1.38 M⊙ white dwarf. *Astrophys. J.*, **291**, 136.

Stone J. Hutcheon I.D., Epstein S. and Wasserburg G.J. (1990) Si isotopes in SiC from carbonaceous chondrites. *Lunar Plan. Sci.*, **XXI**, 1212-1213.

Stone J., Hutcheon I.D., Epstein S., and Wasserburg G.J. (1991) Si, C, and N isotopes in SiC from Orgueil and Murchison: H and He burning components in presolar grains. *Lunar Planet. Sci.*, **XXII**, 1337-1338.

Stone J., Hutcheon I.D., Epstein S., and Wasserburg G.J. (1991) Correlated Si isotope anomalies and large ^{13}C enrichments in a family of exotic SiC grains. *Earth Planet. Sci. Lett.*, **107**, 570-581.

Sturgeon G. and Marti K. (1990) Nitrogen components and isotopic signatures in the Acapulco meteorite. *Lunar Planet. Sci.*, **XXI**, 1220-1221.

Sugiura N. and Strangeway D.W. (1983) A paleomagnetic test using the Abee E4 meteorite. *Earth Planet. Sci. Lett.*, **62**, 169-179.

Swart P.K., Grady M.M. and Pillinger C.T. (1983) A method for the identification and elimination of contamination during carbon isotopic analysis of extraterrestrial material. *Meteoritics*, **18**, 137-154.

Swart P.K., Grady M.M., Pillinger C.T., Lewis R.S. and Anders E. (1983) Interstellar carbon in meteorites. *Science*, **220**, 406-410.

Tang M. and Anders E. (1988) Isotopic anomalies of Ne, Xe, and C in meteorites. II. Interstellar diamond and SiC: carriers of exotic noble gases. *Geochim. Cosmochim. Acta*, **52**, 1235-1244.

Tang M. and Anders E. (1988) Isotopic anomalies of Ne, Xe, and C in meteorites. III. Local and exotic noble gas components and their interrelations. *Geochim. Cosmochim. Acta*, **52**, 1245-1254.

Tang M. and Anders E. (1988) Interstellar silicon carbide: how much older than the Solar System? *Astrophys. J. (Lett.)*, **335**, L31-34.

Tang M., Anders E. and Zinner E. (1988) Noble gases, C, N and Si isotopes in interstellar SiC from the Murchison carbonaceous chondrite. *Lunar Planet. Sci.*, **XIX**, 1177-1178.

Tang M., Anders E., Hoppe P. and Zinner E. (1989) Meteoritic silicon carbide and its stellar sources; implications for galactic chemical evolution. *Nature*, **339**, 351-354.

Tang M., Lewis R.S., Anders E., Grady M.M., Wright I.P. and Pillinger C.T. (1988) Isotopic anomalies of Ne, Xe and C in meteorites. I. Separation of carriers by density and chemical resistance. *Geochim. Cosmochim. Acta*, **52**, 1221-1234.

Tang M., Lewis, R.S., and Anders, E. (1987) Diamond and SiC: carriers of presolar noble gases in carbonaceous chondrites. *Meteoritics*, **22**, 462-463.

Thronson H.A., Latter W.B., Black J.H., Bally J. and Hacking P. (1987) Properties of evolved mass-losing stars in the Milky Way and variations in the interstellar dust composition. *Astrophys. J.*, **322**, 770.

Tielens A.G.G.M. (1988) Carbon stardust: from soot to diamonds. *In: Carbon in the Galaxy. Studies from Earth and Space NASA Conference Publ.*, **3061**, 59-111.

Tielens A.G.G.M. and Allamandola L.J. (1987) Composition, structure, and chemistry of interstellar dust.. *In: Interstellar Processes. Hollenbach D.J. and Thronson H.A.(Jr.) (Eds.). Reidel Publ. Co.*, 397-469.

Tielens A.G.G.M., Seab C.G., Hollenbach D.J. and McKee C.F. (1987) Shock processing of interstellar dust: diamonds in the sky. *Astrophys. J. Lett.*, **319**, L109-113.

Tilton G.R. (1988) Age of the Solar system. *In: Meteorites and the early Solar system. Eds: J.F. Kerridge and M.S. Matthews, University of Arizona Press*, 259-275.

Trumpler R.J. (1930) Preliminary results on the distances, dimensions and space distribution of open star clusters. *Lick Observatory Bull.*, **14**, 154-169.

Trumpler R.J. (1930) Absorption of light in the galactic system. *Publ. Astr. Soc. Pacific*, **42**, 214-227.

Van Schmus W.R. and Wood J.A. (1967) A chemical-petrologic classification for the chondritic meteorites. *Geochim. Cosmochim. Acta*, **31**, 747-765.

Vdovykin G.P. (1970) Ureilites. *Space Sci. Rev.*, **10**, 483-510.

Verchovsky A.B., Fisenko A.V., Semjenova L.F., Shukolyukov Yu.A., Ott U. and Begemann F. (1991) Multicomponent noble gas structure in diamond rich acid residues from Efremovka CV3 carbonaceous chondrite. *Lunar Planet. Sci.*, **XXII**, 1439-1440.

Virag A., Zinner E., Lewis R.S. and Amari S. (1989) Oxygen isotopic compositions of spinel grains from the Murchison carbonaceous chondrite. *Lunar Planet. Sci.*, **24**, 334.

Virag A., Zinner E., Lewis R.S. and Tang M. (1989) Isotopic compositions of H, C, and N in Cδ diamonds from the Allende and Murray carbonaceous chondrites. *Lunar Planet. Sci.*, **XX**, 1158-1159.

Virag A., Wopenka B., Amari S., Zinner E., Anders E., and Lewis R.S. (1992) Isotopic, optical, and trace element properties of large single SiC grains from the Murchison meteorite *Geochem. Cosmochem. Acta* **56**, 1715-1734.

Von Bolton W. (1911) Über die ausscheidung von kohlenstoff in form von diamant. *Z. Elektrochem.*, **17**, 971-973.

Wacker J.F. and Marti K. (1983) Noble gas components in clasts and separates of the Abee meteorite. *Earth Planet. Sci. Lett.*, **62**, 147.

Wasson J.T. (1974) Meteorites, Classification and Properties. *Springer-Verlag, New York*, 316pp.

Wasson J.T. Chou C-L., Bild R.W., Baedecker P.A. (1976) Classification of an elemental fractionation among ureilites. *Geochim. Cosmochim. Acta*, **40**, 1449.

Weibke G. (1960) Die oxydationvon siliziumkarbid. *Ber. Deut. Keram. Ges.*, **37**, 219-226.

Weidenschilling S.J. (1988) Formation processes and time scales for meteorite parent bodies. *In: Meteorites and the Early Solar system. Eds: J.F. Kerridge and M.S. Matthews. University of Arizona Press.*, 348-371.

Weinschenk E. (1889) Uber einige Bestandteile des meteoreisens von Magura, Arva, Ungarn. *Ann. des Naturhistorischen Hofmuseums, Wien*, **4**, 93-101.

Wetherill G.W. (1989) Origin of the Asteroid belt. *In: Asteroids II, Eds. R.P. Binzel, T. Gehrels and M.S Matthews. Univ. Arizona Press.* 666-700.

Wetherill G.W. and Chapman C.R. (1988) Asteroids and Meteorites. *In: Meteorites and the Early Solar System, Eds. J. Kerridge and M. Matthews. Univ. Arizona Press*, 35-67

Wetherill G.W. and Stewart G.R. (1986) The early stages of planetessimal accretion. *Lunar Planet. Sci.*, XVII, 939.

Wickramasinghe N.C. (1969) Interstellar dust and diamonds. *Nature*, **222**, 154.

Woodbury H.H., and Ludwig G.W. (1961) Electron spin resonance studies in SiC. *Phys. Rev.*, **124**, 1083-1089.

Woosley S.E. and Weaver T.A. (1986) The physics of supernova explosions. *Ann. Rev. Astron. Astroph.*, **24**, 205-253.

Wright I.P., Ash R.D., Grady M.M., Pillinger C.T., and Tang M. (1988) The carbon components in Murray residue CF. *Meteoritics*, **23**, 312-313.

Wright I.P., Boyd S.R., Franchi I.A. and Pillinger C.T. (1988) Determination of high precision nitrogen stable isotope ratios at the sub-nanomole level. *J. Phys. E: Sci. Instrum.*, **21**, 865-875.

Wright I.P., Carr R.H. and Pillinger C.T. (1988) Carbon stable isotope analysis of individual deep-sea spherules. *Meteoritics*, **23**, 339-348.

Wright I.P., McNaughton N.J., Fallick A.E., Gardiner L.R. and Pillinger C.T. (1983) A high precision mass spectrometer for stable carbon isotope analysis the nanogram level. *J. Phys. E: Sci. Instrum.*, **16**, 497-504.

Wright I.P., Norris S.J., Pillinger C.T., Lewis R.S. and Anders E. (1983) Light nitrogen, its composition, association and location in the Allende and Murchison meteorites. *Lunar Planet. Sci.*, XIV, 861-862.

Wright I.P., Russell S.S., Boyd S.R., Meyer C. and Pillinger C.T. (1992) Xylan: a potential contaminant for lunar samples and Antarctic meteorites. *Proc. Lunar Planet. Sci. Conf.*, **XXII**, 449-458.

Wyckoff S., Lindholm E., Wehinger P.A., Peterson B.A., Zucconi J-M and Festou M.C. (1989) The $^{12}C/^{13}C$ abundance ratio in Comet Halley. *Astrophys. J.* **339** 488-500

Yates P.D. (1992) The content and isotopic composition of carbon in spherical micrometeorites. *Ph.D. thesis, Open University.*

Yates P.D. ,Wright I.P. and Pillinger C.T. (1992) Application of high sensitivity carbon isotope techniques- a question of blanks. *Chem. Geol*, **101**, In press.

Zinner E. and Epstein S. (1987) Heavy carbon in individual oxide grains from the Murchison meteorite. *Earth Planet. Sci. Lett.*, **84**, 359-367.

Zinner E., Amari S. and Lewis R. (1991) S-process Ba and Nd in presolar Murchison SiC. *Lunar Planet. Sci.* , **XXII**, 1553-1554.

Zinner E., Amari S., Anders E. and Lewis R.S. (1991) Large amounts of extinct ^{26}Al in interstellar grains from the Murchison meteorite. *Nature*, **349**, 51-54.

Zinner E., Tang M. and Anders E. (1989) Interstellar SiC in the Murchison and Murray meteorites: Isotopic compositions of Ne, Xe, Si, C, and N. *Geochim. Cosmochim. Acta*, **53**, 3273-3290.

Zinner E., Tang M. and Anders E. (1987) Large isotopic anomalies of Si, C, N and noble gases in interstellar SiC from the Murray meteorite. *Nature*, **330**, 730-732.

Zinner E., Wopenka B., Amari S. and Anders E. (1990) Interstellar graphite and other carbonaceous grains from the Murchison meteorite: structure, composition and isotopes of C, N, and Ne. *Lunar Planet. Sci.*, **XXI**, 1379-1380.

Zuckerman B., Palmer, P., Morris, M., Turner, B.E., Gilra, D.P., Bowers, P.F. and Gilmore, W.S. (1977) Expanding molecular envelopes around evolved stars. *Astrophys. J. (Lett.)*, **211**, L97.